Site Restoration Programme

Winfrith End State Project:

CONCEPTUAL SITE MODEL TO UNDERPIN A HYDROGEOLOGICAL RISK ASSESSMENT AND RADIOLOGICAL PERFORMANCE ASSESSMENT OF THE STEAM GENERATING HEAVY WATER REACTOR AND DRAGON REACTOR COMPLEX END STATES

Project report – ES(21)P332 Issue 1, December 2024

TYPE OF DOCUMENT (VERSION) OFFICIAL

PROJECT NO. 20146580

OUR REF. NO. 20146580.606/A.3

DATE: DECEMBER 2024

WSP

WSP House
70 Chancery Lane
London
WC2A 1AF

Phone: +44 20 7314 5000

WSP.com

QUALITY CONTROL

Issue/revision	First issue	Revision 1	Revision 2
Remarks	This report has been authored by WSP UK Limited in collaboration with Galson Sciences Limited. Both companies have independently checked and reviewed their contributed text. This version of the report addresses comments made by the NRS appointed peer reviewer.	This report has been authored by WSP UK Limited in collaboration with Galson Sciences Limited. Both companies have independently checked and reviewed their contributed text. This version of the report addresses comments made by the NRS appointed peer reviewer.	This report has been authored by WSP UK Limited in collaboration with Galson Sciences Limited. Both companies have independently checked and reviewed their contributed text. This version of the report addresses comments made by NRS.
Date	25 March 2024	23 July 2024	11 December 2024
Project number	20146580	20146580	20146580
Report number	20146580.606	20146580.606	20146580.606
File reference	20146580.606/A.1	20146580.606/A.2	20146580.606/A.3

Glossary

Term	Explanation
ALES	Active Liquid Effluent System.
AOD	Above Ordnance Datum.
BAT	Best Available Technique.
BTEX	Benzene Toluene Ethylbenzene Xylene.
CCE	Cautious Central Estimate.
CSH	Calcium Silicate Hydrate.
CSM	Conceptual Site Model.
DfR	Deposit for Recovery.
DSRL	Dounreay Site Restoration Ltd.
EA	Environment Agency.
End State	The condition of the Winfrith Site that will be reached following completion of all physical decommissioning and clean-up activities.
EIA	Environmental Impact Assessment.
EPR 2016	Environmental Permitting (England and Wales) Regulations 2016 (as amended).
f_{oc}	Fraction of organic carbon.
FML	Flexible Membrane Liner.
GCL	Geosynthetic Clay Liner.
GRR	Regulatory guidance provided in “Management of radioactive waste from decommissioning of nuclear sites: Guidance on the Requirements for Release from Radioactive Substances Regulation” (Environment Agencies, 2018).
GTLD	Gas Tritium Luminescent Devices.
HRA	Hydrogeological Risk Assessment.
IES	Interim End State (synonymous with the End State for Winfrith).
IEP	Interim End Point. The point in time when the Winfrith Interim End State is achieved.
K_d	Partition coefficient.
K_{oc}	Coefficient of partition with organic carbon.
LCRM	Environment Agency guidance “Land Contamination Risk Management” (Environment Agency, 2020a).
LLWR	Low Level Waste Repository.
LOD	Limit Of Detection.
MTBE	Methyl Tert-Butyl Ether.
NDA	Nuclear Decommissioning Authority.

Term	Explanation
NRS	Nuclear Restoration Services (trading as Magnox Limited).
NVC	National Vegetation Classification.
ONDRAF /NIRAS	Belgian Agency for Radioactive Waste and Enriched Fissile Materials.
OoS	Out-of-scope of Radioactive Substances Regulation.
PA	Performance Assessment.
PAH	Polycyclic Aromatic Hydrocarbon.
PCB	Polychlorinated biphenyl.
PGPC	Purge Gas Pre-Cooler.
PIE	Post Irradiation Examination facility.
RMP	Restoration Management Plan
RSR	Radioactive Substances Regulation.
SGHWR	Steam Generating Heavy Water Reactor at Winfrith.
SI	Système International.
SFR	Repository for short-lived radioactive waste in Forsmark, Sweden.
SKB	Svensk Kärnbränslehantering Aktiebolag, a company formed to manage all the radioactive waste from nuclear power plants in Sweden.
SoLA	Substances of Low Activity.
SRS	Site Reference State. The condition of a site when it is fully compliant with the requirements for release of the site from radioactive substances regulation.
SWESC	Site-Wide Environmental Safety Case.
SWMMP	Site Wide Material Management Plan.
TPH	Total Petroleum Hydrocarbon.
UCL95	Upper 95th percent confidence level.
WAC	Waste Acceptance Criteria.
WHO	World Health Organisation.
WMP	Waste Management Plan.
WSDP	Winfrith Sea Discharge Pipeline.
WSP	WSP (UK) Limited.

CONTENTS

TABLES

FIGURES

1 INTRODUCTION

1.1 TERMS OF REFERENCE

This document has been prepared for Nuclear Restoration Services (NRS) by way of collaboration between WSP UK Limited (WSP) and Galson Sciences Limited (Galson).

1.2 REGULATORY CONTEXT FOR THE DEVELOPMENT OF A CONCEPTUAL SITE MODEL

The Nuclear Decommissioning Authority (NDA), under its duties set out in the Energy Act 2004, has assessed end state options through formal community consultation and determined that the Winfrith site will target land suitable for heathland with public access as its next use.

For nuclear sites, such as Winfrith, disposals of radioactive waste (solid, liquid or gaseous) on or from the site are regulated under the Environmental Permitting (England and Wales) Regulations 2016 (as amended) (EPR 2016). Release of a site from the radiological protection aspects of the regulations cannot take place until such disposals have ceased, and any radioactive wastes or radioactively contaminated ground remaining on the site have the necessary permission(s).

The condition of a site when it is fully compliant with the requirements for release from radioactive substances regulation is referred to as the Site Reference State (SRS). NRS defines an End State that is reached following completion of all physical decommissioning and clean-up activities required for the next planned use of the site.

According to Magnox (2019a) the Interim End State (IES) at Winfrith is the condition of the Winfrith site when all physical works have been completed, however a Permit will remain in place until the SRS is achieved. The Interim End Point (IEP) is the point in time at which the Winfrith IES is achieved.

The current configuration of the Winfrith Site and its envisaged End State is set out in the Site Description (NRS, 2024j) that is supported by an interpretation of present and future hydrogeological conditions (NRS, 2024f). Works are currently underway to configure the Winfrith site for its End State.

NRS has considered facility end state options to meet the agreed next planned land use whilst considering wider benefits and detriments of available options with input from stakeholders and representatives of the local community. The End State agreed through optimisation assessment and engagement with stakeholders includes on-site disposals of radioactive waste, and deposits of recovered non-radioactive wastes at the Steam Generating Heavy Water Reactor (SGHWR) and Dragon reactor complex (including the B78 Dragon fuel storage building and the mortuary holes structure it contains).

These disposals and deposits of wastes are currently envisaged by NRS as a combination of the following, using the terminology of the “Guidance on the Requirements for Release” (GRR, Environment Agencies, 2018) where applicable:

- Disposal in-situ of radioactive below ground structures (which are deemed to be radioactive waste);

- Disposal of radioactive waste (mainly blocks of concrete and broken concrete from demolition of the above ground building structures) for a purpose, namely infilling of unwanted below ground voids (for example in the SGHWR primary containment structure) as part of land restoration; and
- Use of non-radioactive waste (aged and newly formed broken concrete) in a 'deposit for recovery' (DfR) operation, also for the purpose of infilling unwanted below ground voids (for example in the SGHWR annexes) as part of delivering the next land use of heathland suitable for public access.

On-site disposal and recovery of wastes is considered optimised:

- The retention of the below ground structures under GRR is essential to the completion of site restoration and the implementation of the Site End State. This has created a defined need to carry out the backfilling of the below ground structures to produce a surface suitable for 'heathland with public access'. The work would therefore be completed using a non-waste material if the use of site-derived waste was not permitted;
- The engineering concept designs have been produced through a robust, iterative assessment process to national and international engineering standards and with input from key stakeholders to determine the preferred approach;
- No more waste than is required to fulfil the Engineering Concept Designs (as set out in NRS, 2024c) will be used during the works;
- The demolition arisings are suitable for their intended purpose and will meet the Engineering Functional Requirements and acceptance criteria for the voids;
- The proposed works are consistent with and supported by the Dorset Council Adopted Waste Plan;
- Restoration of the site will deliver Biodiversity Net Gain and amenity value for local communities; and
- Decommissioning, site restoration and recovery of site-derived materials directly support a number of the UK Governments objectives within the 25-year Environment Plan.

NRS is now required to prepare applications to the Environment Agency (EA) for the necessary permissions. The GRR requires the operator (NRS) to prepare a waste management plan (WMP) that documents the overall optimised approach to managing radioactive waste through to an acceptable SRS, and that is supported by a site-wide environmental safety case (SWESC). The SWESC will need to consider potential future site-wide radiological and non-radiological impacts, including potential impacts from radioactive waste disposals and radioactive land contamination, should any remain. The GRR also requires assessment of the risks from non-radiological properties associated with the radioactive wastes.

An application to vary the environmental permit to allow the 'on-site disposal of solid radioactive waste' in accordance with the GRR will be required. Furthermore, a permit for a DfR will be required. The applications are supported by assessment of non-radiological hazards associated with the disposals through a non-radiological hydrogeological risk assessment (HRA), and a radiological performance assessment (PA) for the reactor disposal concept designs. Both assessments are to be based on a conceptual site model (CSM). The CSM is a Tier 3 document within the Magnox Winfrith End State Permit Variation and DfR application documents hierarchy (Figure 606/1).

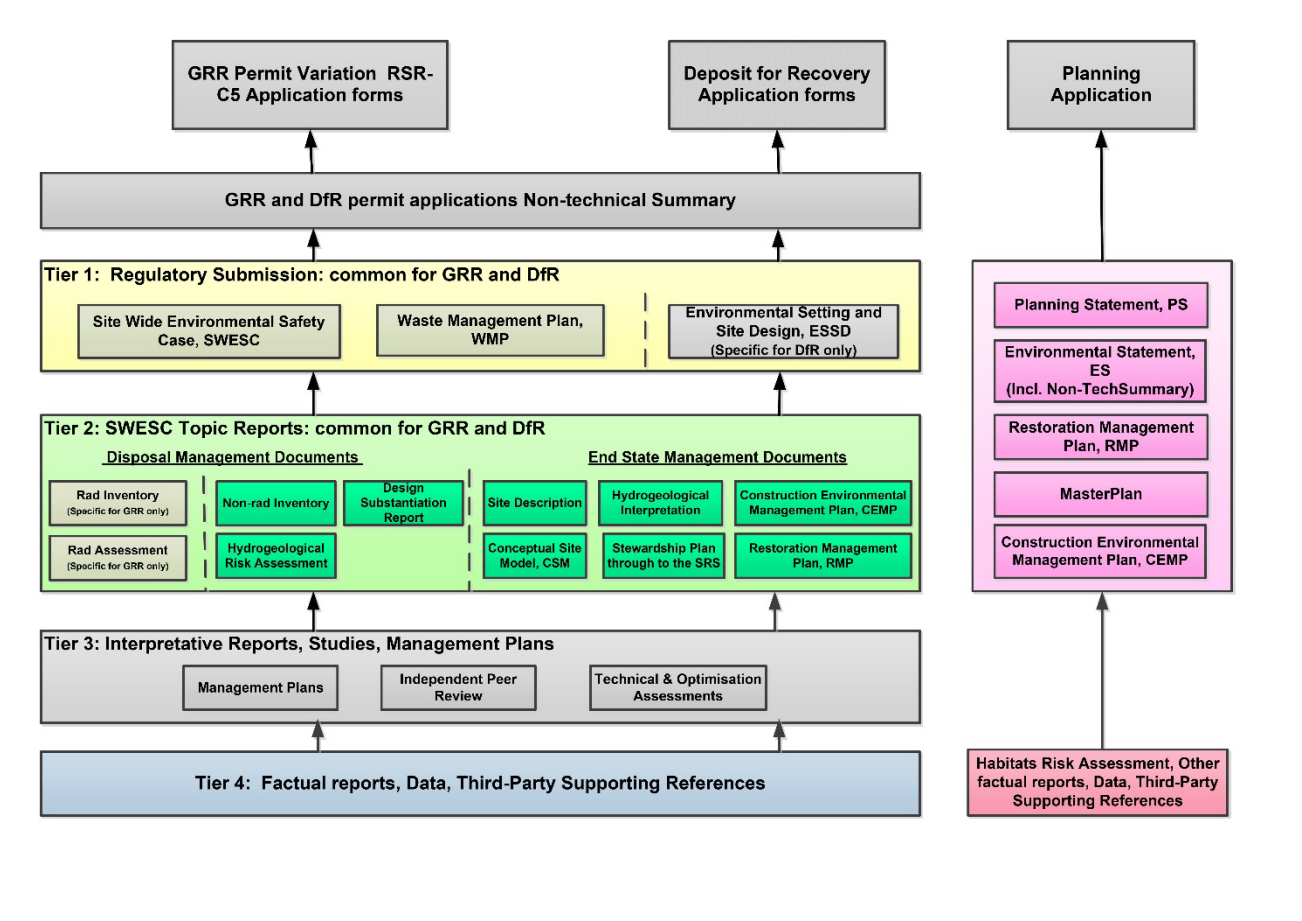

Figure 606/1: Winfrith End State GRR Permit Variation and DfR Application Documents Hierarchy

1.3 PURPOSE OF THIS REPORT

The purpose of this report is to present the CSM in the form of a narrative, supported by figures, describing the characteristics of the SGHWR and Dragon reactor complex End States in a manner suitable for mathematical model development.

The CSM considers the contamination sources, disposal system evolution, pathways for migrating contamination and potential receptors for that migrating contamination.

The CSM in this report is expected to be used to:

- Underpin non-radiological contaminant assessments for the SGHWR and Dragon reactor complex End States; and
- Underpin radiological assessments for on-site disposal at the SGHWR and Dragon reactor complex End States.

The assessments will be over timescales to ensure peak impacts are quantified. The timescales for the assessments could be different given the different behaviours, and the different receptors, of non-radiological and radiological contaminants. Nevertheless, both assessments will address processes described in this CSM that occur during the respective assessment periods.

This report satisfies many of the EA requirements (EA, 2020) for an Environmental Setting and Site Design report to support the DfR permit application.

1.4 SCOPE AND STRUCTURE OF THIS REPORT

The CSM will be developed and presented in accordance with ISO 21365:2019 “Conceptual Site Models for Potentially Contaminated Sites” and EA (2020a) ‘Land Contamination Risk Management’ (LCRM) guidance (part of Stage 1 Tier 1: Preliminary risk assessment).

The CSM describes both the SGHWR and Dragon reactor complex End States.

Decommissioning, characterisation and options assessments for features on the rest of the Winfrith site are ongoing. The overall activity remaining on the site will be described in the WMP and SWESC. The scope of the WMP and SWESC includes the Active Liquid Effluent System (ALES), the area of land at A59, and the Winfrith Sea Discharge Pipeline (WSDP) that runs from the site to the coast, as well as drains and ductwork. The non-radiological HRA is required to support the radioactive substances regulation (RSR) permit variation application and DfR permit application for the disposals/deposits. Therefore, this CSM only considers the SGHWR and Dragon reactor complex End States.

The CSM in this report is structured around sources (sections 2 to 5), pathways (section 6) and receptors (section 7).

- Section 2 describes the current configuration of the SGHWR and Dragon reactor complex and what will remain of the structures at the IEP following demolition. The volume of void in the remaining structures is quantified. The dimensions, volumes, and physical properties of materials that will be either deposited or disposed of within the structures to fill the voids are described.
- Sections 3 and 4 quantify the End State non-radiological and radiological inventory, respectively, associated with the structures, the deposits and the disposals.
- The purpose of section 5 is to provide a description of how the End State inventory from each component will be released to water within the structures - termed the near field - along with quantification of the changing rate of water inflow and outflow to the structures. The expected changes in water levels within the structures and how these changes in water level as well as changes to the degree of saturation within the structures affect aqueous release of the inventory is also described.
- Section 6 describes how water moves through the End State structures and through the geosphere (ground) beyond (‘pathways’). Pathway conditions are expected to be time variant, and the way flows might increase, for example because of structural concrete degradation, is explained.
- Section 7 describes the aqueous receptors potentially affected by both radiological and non-radiological contaminants. This includes a description of the biosphere to support the radiological PA. Aquifer classification and groundwater abstractions, and the identification of sensitive ecological communities, are included. The possible effects of climate change in the future on the receptors are discussed. To avoid repetition and as they are only relevant to the radiological assessment, the multiple scenarios required for the radiological PA are presented in the radiological assessment report.

The CSM is summarised in section 8. Naturally, the past, present and future evolution of the disposals/deposits cannot be described completely. Uncertainties with the narrative of the End State characteristics are listed in section 9.

1.5 CONVENTIONS AND DEFINITIONS

Within this report, all directions are referenced to Ordnance Survey Grid North. All elevations are referenced to Ordnance Datum (Newlyn).

All units are SI (Système International) base or derived units unless convention is to use alternative units (for example kilometres rather than metres for distances over 1 kilometre).

2 DESCRIPTION OF THE SGHWR AND DRAGON REACTOR END STATES

The purpose of this section is to:

- Describe the locations of the End States and their configurations;
- Quantify the volume of voids that will be subject to the disposals/deposits; and
- Describe the volume and other physical properties of the disposals/deposits.

This information is required to develop an inventory for the disposals/deposits (section 3 and section 4) and to underpin conceptualisation of near field evolution (section 5).

This section is structured as follows:

- Description of the locations of the SGHWR and Dragon reactor complex (section 2.1);
- Explanation of the terminology associated with the different parts of the SGHWR and Dragon reactor complex relevant to the description of the disposals/deposits in the End State configuration (section 2.2);
- Description of the geometry and configuration of the SGHWR and Dragon reactor complex including floor slab elevations and thicknesses (section 2.3);
- Calculation of the void volume of each region of the SGHWR and Dragon reactor complex in their End State configurations available for filling (section 2.4); and
- Description of the physical characteristics, including volume, of material the voids will be filled with (section 2.5).

A summary of the floor slab elevations and thicknesses and reconciliation of volumes of voids and disposals/deposits is presented in section 2.6.

Further detail on the features and layout of the SGHWR and Dragon reactor complex End States that are required for the purposes of developing the radiological inventory are described in section 4.

2.1 LOCATIONS OF THE SGHWR AND DRAGON REACTOR COMPLEX

The SGHWR and Dragon reactor complex are located towards the western boundary of the Winfrith site as shown in Figure 606/2. The B78 fuel storage building containing the Dragon reactor mortuary holes structure lies north-northeast of the Dragon reactor (Figure 606/3).

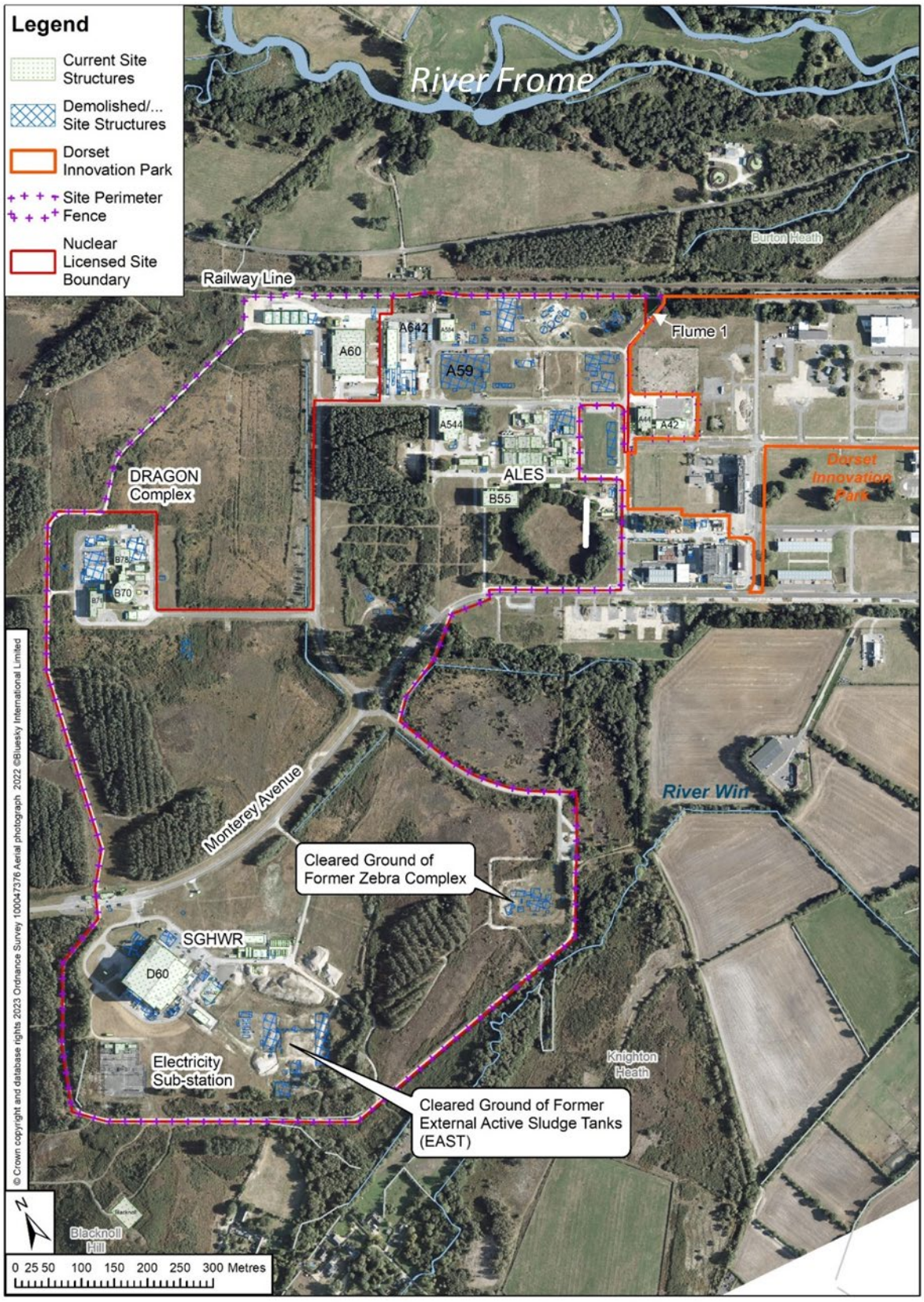

Figure 606/2: Principal features of the Winfrith Site and its surroundings including current and demolished Site structures.

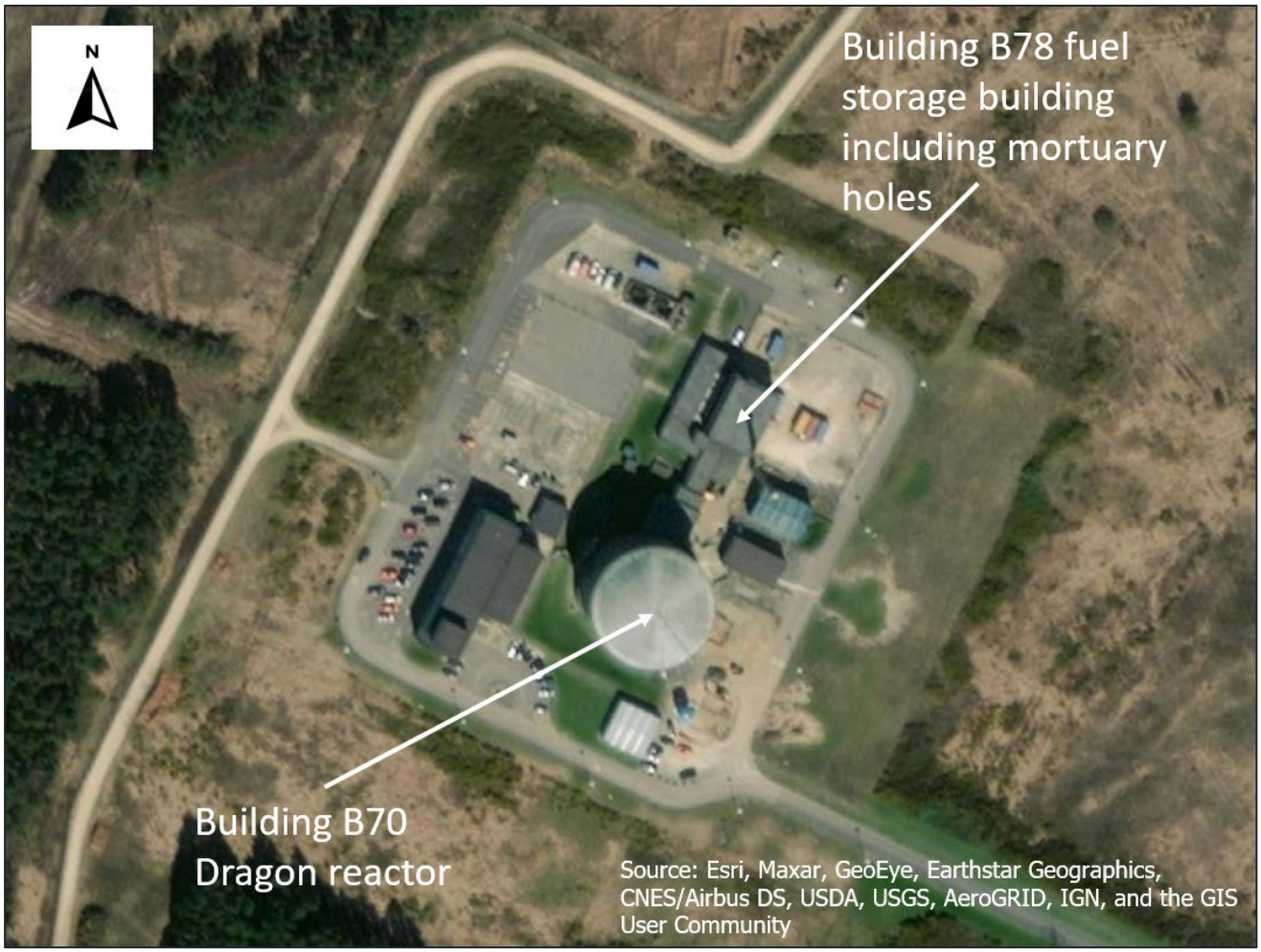

Figure 606/3 : Aerial photograph of the Dragon reactor complex showing location of the mortuary holes

2.2 LAYOUT AND TERMINOLOGY

2.2.1 SGHWR

The SGHWR building comprises 10 levels, three of which are below the level of the surrounding ground surface (below ground). The reactor has been defueled and ancillary equipment and facilities decommissioned. Above ground, the structure is a steel-clad metal frame with masonry (brick) and concrete internal structures. Below ground, the structure is mainly reinforced concrete. Although the SGHWR comprises many rooms, the below ground level elements of the SGHWR can be simplified into four regions based on the elevation of the top of the floor slab in each region:

- Region 1: The reactor bioshield, primary containment and immediate surrounds;
- Region 2: The steam labyrinth to the west of the primary containment, the delay tank room, and turbine hall;
- The South Annexe, including the pump pit to the north of the turbine hall; and
- The North Annexe.

A summary of the floor slab elevation and thickness of the floor in each region of the SGHWR is presented in Table 606/1.

Table 606/1: Summary of Floor Slab Elevation and Thickness of Each Region of the SGHWR

Component	Top of Floor Slab Elevation (m AOD)	Floor Slab Thickness / Description
SGHWR Region 1	28.8	2.74 m thick reinforced concrete
SGHWR Region 2	30.6 to 35.4	Turbine hall - 2.74 m reinforced concrete Delay tank room - 0.91 m reinforced concrete Steam labyrinth 0.69 m reinforced concrete
SGHWR North Annexe	37.8	Typically, 0.33 m reinforced concrete
SGHWR South Annexe	35.4 to 36.6	Variable – between 0.23 m and 0.53 m reinforced concrete

The four regions are shown in plan on Figure 606/4 and in section on Figure 606/5.

In preparation for the End State, the concept design is for the entire structure of the SGHWR to be demolished to 1 m below ground level (m bgl). Most internal walls in the subsurface structure will remain in-situ unless they need to be removed to gain access for deposition of the infill material. Accessible non-structural metal elements will be removed. The SGHWR void will be backfilled to 1 m bgl.

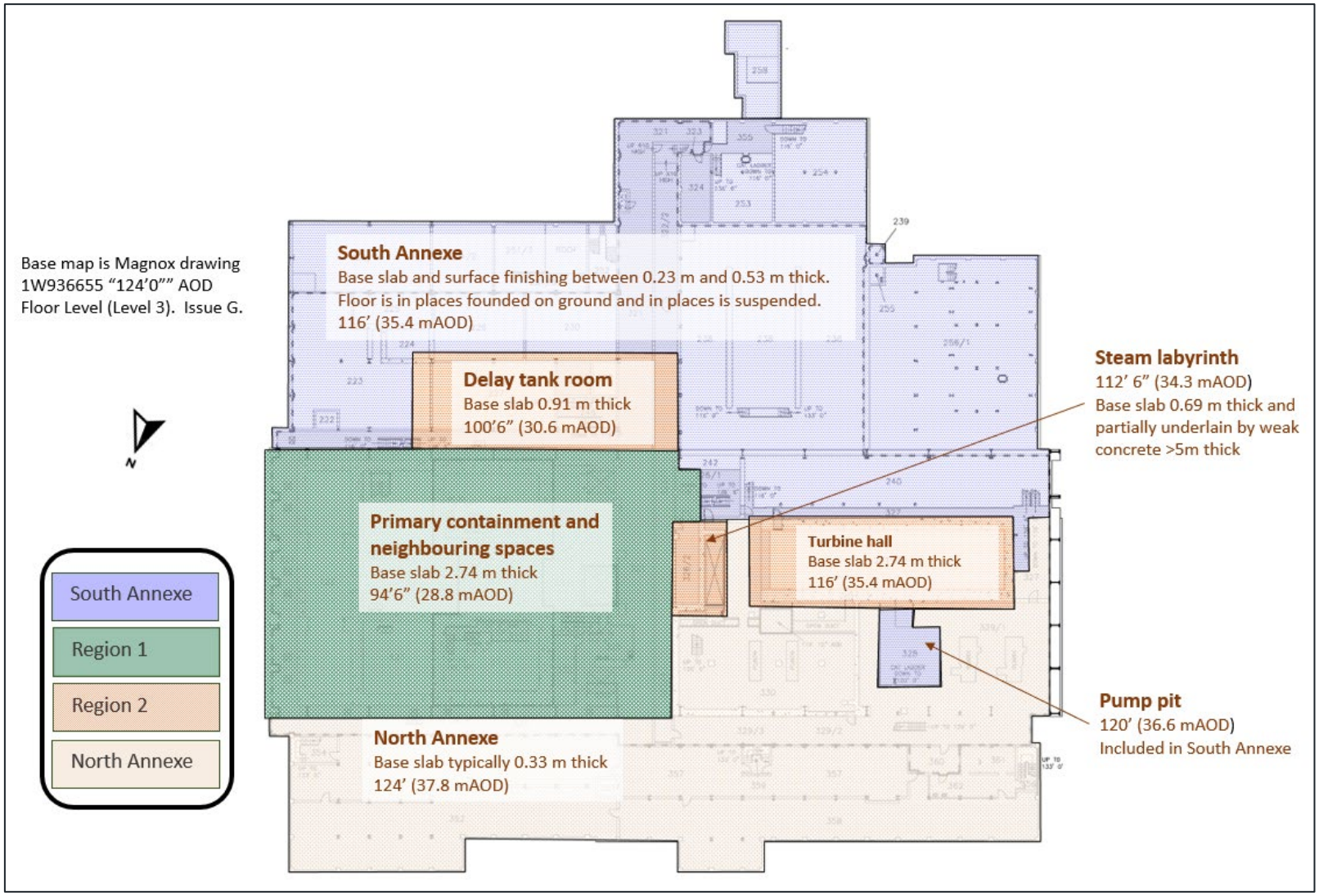

Figure 606/4: Plan showing the four regions of the SGHWR building

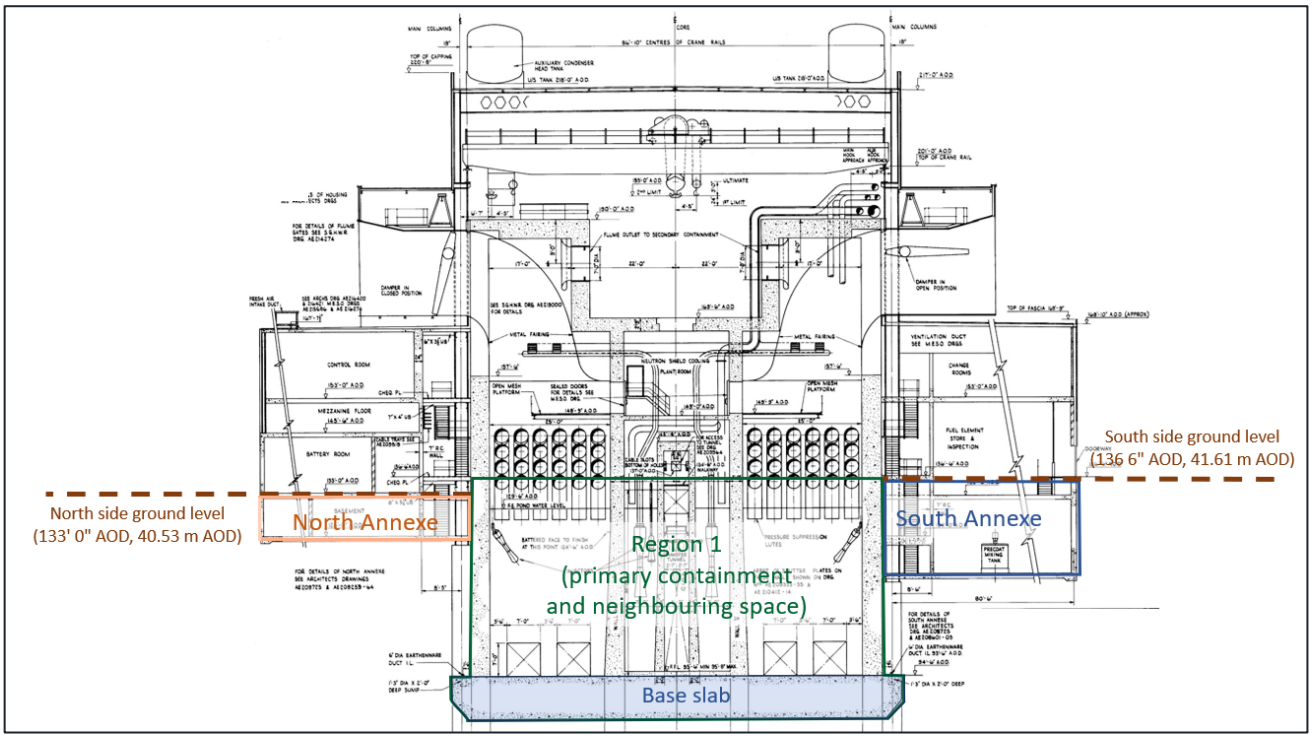

Figure 606/5: Cross section through the SGHWR building

2.2.2 DRAGON REACTOR

The elevation of the top of the floor slab of the Dragon reactor is 27.34 m AOD and its base slab is typically 3.7 m thick reinforced concrete.

The Dragon reactor is shown in plan on Figure 606/6 and in section on Figure 606/7. The Dragon reactor is circular in plan-view and has four concentric concrete walls referred to sequentially from the outside in as Wall A, Wall B, Wall C and Wall D. The aggregate in the concrete was observed to be flint during a WSP site visit on 27 July 2023. The reactor reinforced concrete bioshield is referred to as Wall D. A steel shell is located within a void between Wall B and Wall C. Wall B includes brick-filled apertures and Wall A has many penetrations into the services duct approximately 1 m above the -25' (27.43 m AOD) floor level.

The concept design is for the entire structure of the Dragon reactor and accessible non-structural metal elements to be demolished to ground level. As with the SGHWR, most internal walls in the subsurface structure will remain in-situ unless they need to be removed to gain access for deposition of the infill material.

The concept design for the demolition includes for conventional methods to demolish the Dragon reactor roof pre-cast concrete slabs and produce backfill (NRS, 2024c). The concept design for demolition of the primary containment is to use diamond wire cutting or similar techniques and to place concrete blocks within the below ground voids within Wall C. Reactor wall tops from outside Wall C will be demolished using a high reach machine. Arisings will be placed within Wall A and non-radioactive arisings in the services duct outside Wall A. Stockpiled material will be used to complete filling of the below ground voids (NRS, 2024c).

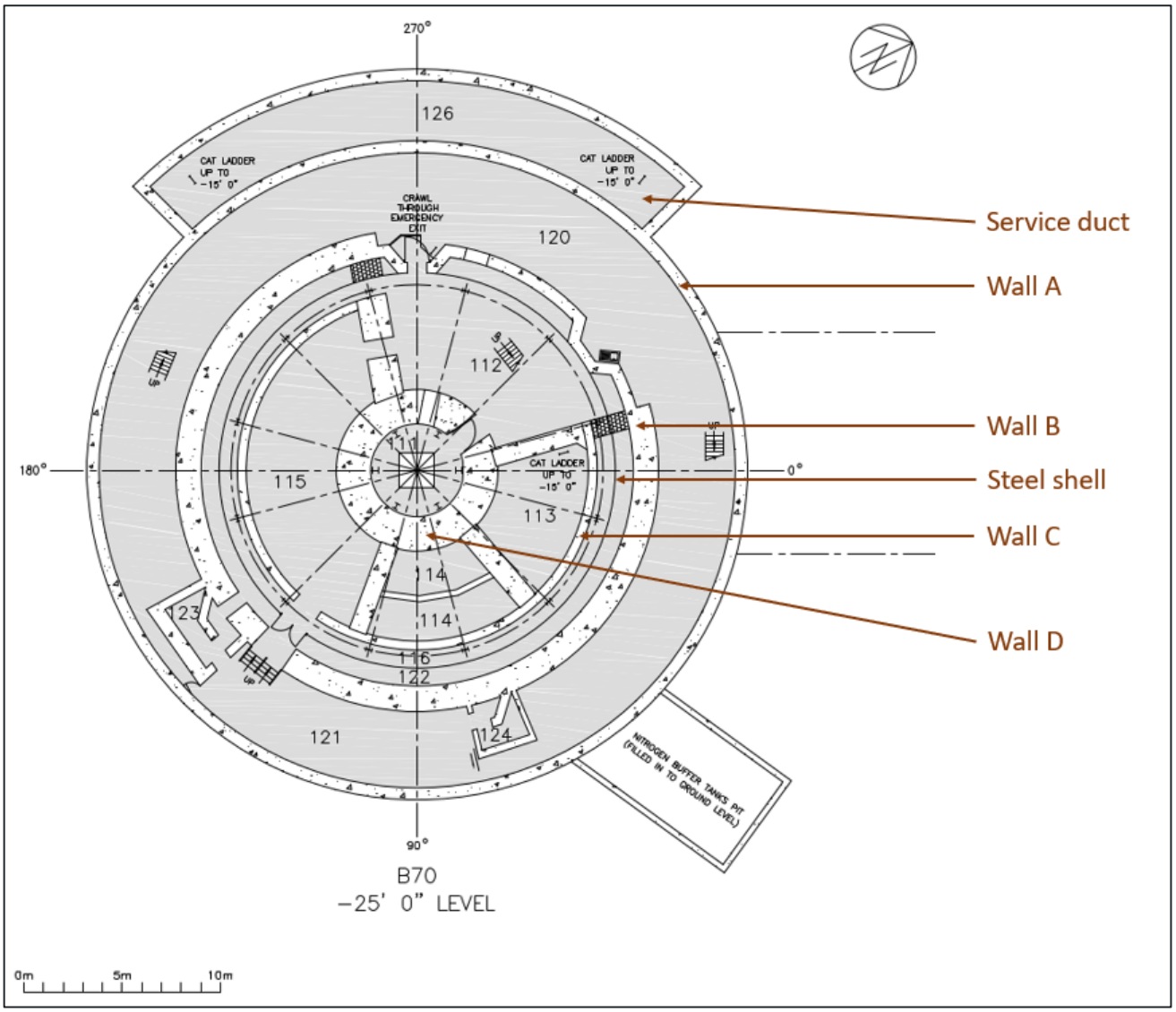

Figure 606/6: Plan view of the Dragon Reactor (from Magnox Drawing OW200403334 Rev C "29'0" to -15'0" (Level 1). B70 & B78 Combined", 08/12/2008)

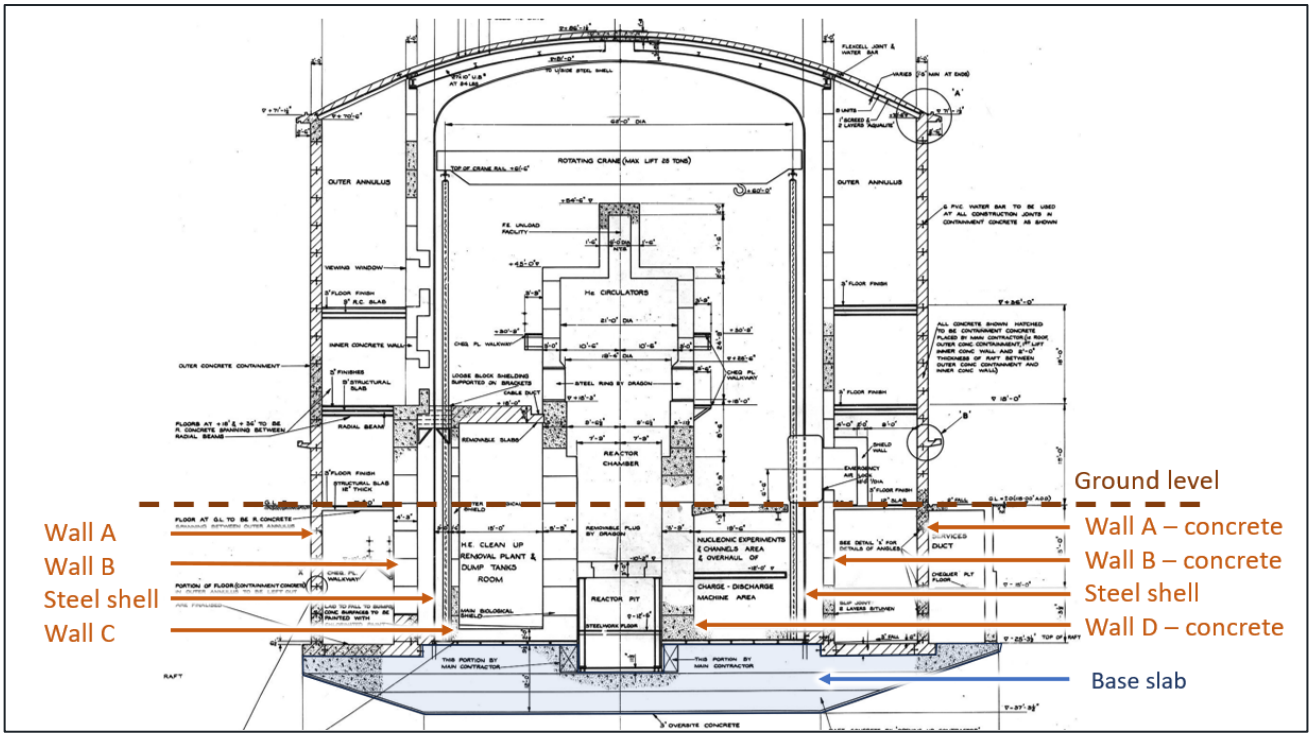

Figure 606/7: Cross section through the Dragon Reactor (from Magnox Drawing AE133370 Rev M "Dragon Reactor Project, Sectional elevation on A-A", 16/05/1962)

2.2.3 B78 FUEL STORAGE BUILDING

The B78 fuel storage building is connected to the Dragon reactor building by a vehicle access-way. The floor slab of the B78 building is contiguous with that of the reactor building vehicle airlock and there are steel rail tracks embedded in the floor slab running all the way from B78 to the reactor core. The mortuary holes structure is located within building B78 approximately 30 m north-north-east of the Dragon reactor (Figure 606/3), and comprises 50 mortuary holes that were built to store irradiated Dragon fuel elements (referred to herein as the 'primary mortuary holes structure') and 40 holes for fresh fuel. Constructed in a concrete lined and filled pit, the holes comprise galvanised mild steel tubes. The 50 mortuary holes that were used to store used Dragon fuel elements are planned to be filled with grout. The other 40 tubes can be relatively easily removed from their pit and are planned to be disposed of off-site. The concept design is to demolish the B78 building to ground surface, with the demolition arisings to be used as backfill in the Dragon reactor below ground voids (NRS, 2024c). The floor slab (into which the mortuary holes structure is set) will be left in-situ.

2.3 GEOMETRY AND CONFIGURATION

As shown in Figure 606/5 the ground elevation around the SGHWR is 40.53 m AOD on the north side and 41.61 m AOD on the south side. The ground elevation around the Dragon reactor and mortuary holes is 35.05 m AOD.

2.3.1 SGHWR REGION 1

Region 1 comprises the reactor bioshield, primary containment and immediate surrounds. The northern and southern external walls of Region 1 are 1.2 m thick where they interface with the North and South Annexes. The western wall is also 1.2 m thick from basal level up to ground level. The minimum thickness of the eastern wall is 1.2 m. The base slab of the primary containment area is 2.74 m thick. The elevation of the top of the base slab is 28.8 m AOD. The structure is constructed from reinforced concrete (NRS, 2024c).

2.3.2 SGHWR REGION 2

Region 2 comprises the turbine hall, the delay tank room, and the steam labyrinth to the west of the primary containment (as shown in Figure 606/4). The turbine hall has a concrete floor slab that is 2.74 m thick. The concrete floor slab in the delay tank room is 0.91 m thick. The thickness of the concrete floor slab in the steam labyrinth to the west of the primary containment is 0.69 m thick and is partially founded on weak concrete that is at least 5 m thick[1]. Wilson (construction era document) describes construction of mass concrete retaining walls allowing excavation of the enclosed soil to the required level for the turbine hall. The mass concrete was poured in via trenches and compacted by poker vibrators. It is assumed this is the weak concrete to which the drawing[1] refers and that it is unreinforced. The elevation of the top of the base slab is between 30.6 and 35.4 m AOD. The floor slab concrete is reinforced.

2.3.3 NORTH ANNEXE

The North Annexe comprises a central area with an east-west length of 81.3 m that is made up of numerous rooms. To the north and south of this central area are smaller ‘annexed’ areas with varying dimensions. The North Annexe has a minimum floor slab elevation of 37.8 m AOD. The base slab is 0.33 m to 0.46 m thick (according to Drawing AE208217 Mod H, 21/01/1964). Structures in the North Annexe are formed from reinforced concrete (NRS, 2024c).

2.3.4 SOUTH ANNEXE

The South Annexe comprises several rooms including a pump pit located to the north of the turbine hall that has a base slab elevation lower than the surrounding North Annexe. The South Annexe has a minimum floor slab elevation of 35.4 m AOD and the base slab ranges in thickness from 0.23 m to 0.53 m. Structures in the South Annexe are formed from reinforced concrete (NRS, 2024c).

2.3.5 DRAGON REACTOR

As shown in Figure 606/7 the Dragon reactor structure is founded on a 3.7 m thick steel reinforced concrete base slab and has an outer concrete wall that is 2’ (0.61 m) thick. The underside of the base slab is at 23.68 m AOD, and the top of the base slab is at 27.34 m AOD (UKAEA, 1962).

2.3.6 MORTUARY HOLES

The primary mortuary holes comprise a pit excavated below ground level and infilled with concrete, within which were housed galvanised mild steel tubes for storing spent fuel. The basal elevation is approximately 30.3 m AOD (Magnox, 2017).

[1] Magnox drawing AE208219 Rev G, SGHWR general arrangement sections through foundation sections 15-15 and 19-19.

2.4 VOID VOLUMES

The purpose of this section is to describe calculation of the volume of void within the different regions of the SGHWR and Dragon reactor complex.

Calculations of void volumes have been carried out by WSP (2023b). Assumptions underpinning these calculations are set out in Table 606/2.

Table 606/2: Assumptions underpinning Void Volumes and Volumes of Emplaced Waste

Assumption Number	Statement of Assumption
1	The ground surface elevation at the SGHWR is 41.61 m AOD[a].
2	The ground surface elevation at the Dragon reactor complex is 35.05 m AOD[b].
3	The SGHWR will be demolished to 1 m below ground surface (i.e. to 40.61 m AOD).
4	The Dragon reactor will be demolished to ground surface (i.e. to 35.05 m AOD)[c].
5	Building B78 will be demolished to ground surface.
6	The below ground voids of the SGHWR will be filled with waste to 1.0 m below ground surface (i.e., to 40.61 m AOD).
7	The below ground voids of Dragon reactor will be filled with waste to ground surface (i.e., to 35.05 m AOD).
8	Concrete blocks will be placed only in Region 1 of the SGHWR.
9	Concrete blocks will be placed only within Wall C of the Dragon reactor.
10	No future changes are made to the internal structures of the SGHWR and Dragon reactor that could affect the void volumes or volumes of emplaced waste prior to implementation of the End State.
11	The SGHWR and Dragon reactor cut and fill levels are horizontal.

Note a) This is taken from Drawing AE207421 Mod J dated 11 March 1965 that shows the south side ground level is at 136"6' AOD.

Note b) This is taken from Drawing AE133370 Mod M dated 16 May 1962 that shows ground level at 115' AOD.

Note c) The Dragon reactor complex will be demolished to ground surface as it is impractical to demolish it to 1 m bgl due to the level of rail line and surrounding hardstanding connecting Building B70 to Building B78.

2.4.1 SGHWR

Void volumes have been previously calculated and are reported in the Waste Recovery Plan (Magnox, 2021a). The SGHWR void is reported to have an estimated volume of 28,153 m^3. The SGHWR volume was calculated by a detailed assessment of the structure by UKAEA (UKAEA managed the site decommissioning at the time) in 2006 (UKAEA, 2006). The 2006 assessment is different to what is required to support the radiological and non-radiological assessments in two aspects:

1. It assumed the void extended to 40.04 m AOD. The volume is therefore an underestimate of the void to 40.61 m AOD (assumption 3 of Table 606/2).
2. It does not subdivide the void in the same manner as described in section 2.2.

Recalculations of the void volumes of the SGHWR regions in WSP (2023b) have adopted a proportionate but less sophisticated approach to that carried out in 2006 and are summarised in Table 606/4. The volume of each SGHWR region has been calculated as the product of its external plan area and the distance between the top of its base slab and the assumed top of the waste (Table 606/2). The plan areas have been calculated from the NRS engineering drawing (1W936655 "124'0"" AOD Floor Level (Level 3), Issue G), using Surfer™ software.

If internal structures within the subsurface structure remain, the void space calculated from the external dimensions will be an overestimate. The percentage of the volume calculated from external dimensions that is consumed by internal structures has been calculated using the detailed work of 2006. The 2006 work determined the volume of void below ground level and the volume of structural elements (walls, floors, etc) below ground level. It has been possible to extract from the calculations the volume of material left below ground level that is at, or below, the top of base slab. The volume of material left in the ground above the base slab can then be easily calculated as the difference between the total volume of material left below ground and the volume of material left at or below the slab. Table 606/3 presents a determination of the volume calculated from external dimensions that is consumed by internal structures.

Table 606/3: Calculation of the Percentage of the Void Calculated from External Dimensions that is Consumed by Internal Structures using UKAEA (2006) Assumptions

	Void volume below ground level[a] (m^3)	Volume of material left below ground level[a] (m^3)	Volume of material left below ground at or below the base slab[a] (m^3)	Volume of material left below ground level but above base slab[b] (m^3)	Volume of material left below ground above the base slab expressed as a percentage of void below ground level assuming no internal structure is left below ground level[c] (%) (used in Table 606/4)
Primary containment	10,431	6,662	3,760	2,902	22
Turbine block (condenser cell and feed heater cell, air pump cell etc.)	3,766	5,276	3,866	1,410	27
North Annexe	1,548	1,956	1,834	122	7
South Annexe	8,691	3,428	2,665	763	8

Note a) Extracted from UKAEA, 2006.

Note b) This is calculated as the difference between the values in the two columns to the left.

*Note c) This is calculated as the volume of internal structure as a percentage of void volume assuming no internal structure is present. E.g. the calculation for the primary containment is (2,902/(2,902+10,431))*100% = 22%. The percentage is required to be expressed in this way so it can be used to adjust the void volumes based on external plan dimensions, in Table 606/4, to account for the presence of internal structures.*

The final column of Table 606/4 is an estimate of the void volume available to be infilled by demolition arisings that takes account of internal structures.

Table 606/4: Estimate of the SGHWR Void Volumes

Sub-region	Plan Area (m^2)	Basal Floor Elevation (m AOD)	Void Volume based on External Plan Dimensions (m^3)	Estimate of Void Volume Accounting for Internal Structures (m^3)[a]
Region 1	1,265	28.8	14,935	11,649
Region 2:				
Delay tank room	294	30.6	2,941	2,147
Turbine hall	266	35.4	1,387	1,012
Steam labyrinth	58	34.3	365	266
Region 2 Sub-total	618		4,692	3,425
North Annexe	1,593	37.8	4,478	4,164
South Annexe:				
Pump pit	49	36.6	195	179
Remainder of south annexe	2,153	35.4	11,219	10,321
South Annexe Sub-total	2,202		11,414	10,501
Total	5,678		35,518	**29,739**

Note a) In-situ internal structures in Region 1 are calculated to take up 22% of the volume of the void derived using the external dimensions of the Primary containment (Table 606/3). In-situ internal structures in Region 2 are calculated to take up 27% of the volume of the void derived using external dimensions of the turbine block (Table 606/3). To illustrate how the final column is derived, the true void volume of Region 1 once internal structures are accounted for is 78% (i.e. 100% - 22%) of 14,935 m^3, i.e. 11,649 m^3.

Since the UKAEA calculations in 2006, concrete blocks have been removed from the main cooling water pump pit (Room 220) and the boiler feed pump area (Room 329/1) creating approximately 100 m^3 additional void available for demolition arisings. The additional void created since 2006 is small compared to the total estimated void volume and therefore is not considered to warrant an update to the void volume estimate presented in Table 606/4.

Estimates of void volumes presented here are for the purposes of conceptualisation to support mathematical model development and are not for underpinning detailed design; volumes to underpin detailed design will be calculated during the design phase of works. Had the calculations shown in Table 606/4 assumed the waste extended to 40.04 m AOD like UKAEA's calculations in 2006, then the void volume using this method would be calculated to be 26,921 m^3, less than 5% different to that calculated by UKAEA in 2006. There is therefore confidence that the void volume calculated for each region with the relatively unsophisticated method shown in Table 606/4 is

consistent with that used by UKAEA (2006). The SWMMP (NRS, 2024i) has been updated with the values calculated here.

2.4.2 DRAGON VOID VOLUMES

The Waste Recovery Plan (Appendix F, Magnox, 2021a) calculates the void volume in the below ground parts of the Dragon reactor to be 6,544 m^3. A value of 6,544 m^3 will be assumed for this assessment and is included in the updated SWMMP (NRS, 2024i).

The primary containment will be demolished using wireline cutting and the concrete blocks will be placed within Wall C. It is therefore important to understand the void within Wall C as well as the remaining void within Wall A. UKAEA (1962) shows the internal diameter of Wall A is 32.31 m and the diameter within Wall C is 17.37 m. If the geometry of the Dragon reactor void considered by the Waste Recovery Plan is simplified to a cylinder, it can be shown that approximately 29% of it (i.e., 1,891 m^3) lies within Wall C and approximately 71% (i.e., 4,653 m^3) outside of Wall C.

2.4.3 MORTUARY HOLES VOID VOLUMES

Fifty mortuary holes will be left in situ and filled with clean grout. The required volume of grout has been calculated by NRS (NRS, 2024h) to be 27.1 m^3.

2.5 PHYSICAL CHARACTERISTICS OF THE MATERIAL THAT WILL FILL THE SGHWR AND DRAGON REACTOR VOIDS

2.5.1 SGHWR REGION 1

The below ground voids in the primary containment area of Region 1 will be part-filled with placed concrete blocks (NRS, 2024c). These blocks will come from the demolition of the primary containment structure of Region 1 and the turbine hall of Region 2 (NRS, 2024c). It is assumed that the method by which any wall and floor slabs are removed to allow access to the previously obstructed parts of the basement void will be by wireline cutting. Wireline cutting will generate concrete blocks for disposal that can be expected to be cuboid in shape. Magnox (2020a) describes the block size as up to 2.4 m^3. Magnox (2020a) estimates the void space between the blocks to be 10% v/v. These and other physical properties of the blocks are set out in Table 606/5.

Table 606/5: Assumed Physical Properties of Concrete Blocks

Property	Value	Source
Shape of concrete block	Cube	Assumption
Size of concrete block	Up to 2.4 m^3	Assumption after Magnox (2020a)
Void space between concrete blocks	10% of the total volume occupied by blocks	Assumption after Magnox (2020a)
Porosity of concrete	15% v/v	SKB[2] (2001a)
Dry density of concrete block	2,400 kg/m^3	The value is uncertain. SKB (2001a) quotes a density of 2,343.5 kg/m^3 for structural concrete whereas SKB (2014) quotes a

[2] Svensk Kärnbränslehantering Aktiebolag, a company formed to manage all the radioactive waste from nuclear power plants in Sweden.

Property	Value	Source
		density of 2,450 kg/m^3. The value shown here is between those quoted in SKB (2001a) and SKB (2014) for structural concrete.

It is assumed that the entire volume of the blocks will be placed in the deepest basal areas of the subsurface structure in Region 1. It is assumed that after block emplacement, the remaining void will be filled with demolition arisings from the demolition of the SGHWR structure and from the existing D630 stockpiles (described in section 3.1.1). The stockpiled material will not be further processed by, for instance, crushing or segregation. Assumed physical properties of the demolition arisings are set out in Table 606/6.

Table 606/6: Assumed Physical Properties of the Demolition Arisings

Property	Value	Source
Shape of the particles	Sphere	Assumption
Porosity of emplaced demolition arisings	30% v/v	Assumption based on the minimum void space between spherical particles being 26% and random packing of equal spheres having a porosity of around 36%.
Dry density of concrete	2,400 kg/m^3	SKB (2001a) quotes a density of 2,343.5 kg/m^3 for structural concrete whereas SKB (2014) quotes a density of 2,450 kg/m^3. The value shown here is between those quoted in SKB (2001a) and SKB (2014) for structural concrete.

The particles of demolition arisings may not be spherical, and the porosity of the demolition arisings may differ from 30% v/v as shown in Table 606/6. Indeed, Magnox (2020b) assumes the volume occupied by arisings generated using conventional demolition techniques is 22% greater than the volume of the structures before they are demolished. On this basis the demolition arisings will have a porosity of 18% v/v and a dry bulk density of 1,967 kg/m^3.

The particle size distributions of ten samples of the D630 stockpiles have been determined and the results are presented in Figure 606/8. Based on this, particles of demolition arisings from the D630 stockpiles as well as the demolition arisings generated in situ are assumed to be less than 150 mm across and the median particle size (of the median distribution) is approximately 15 mm.

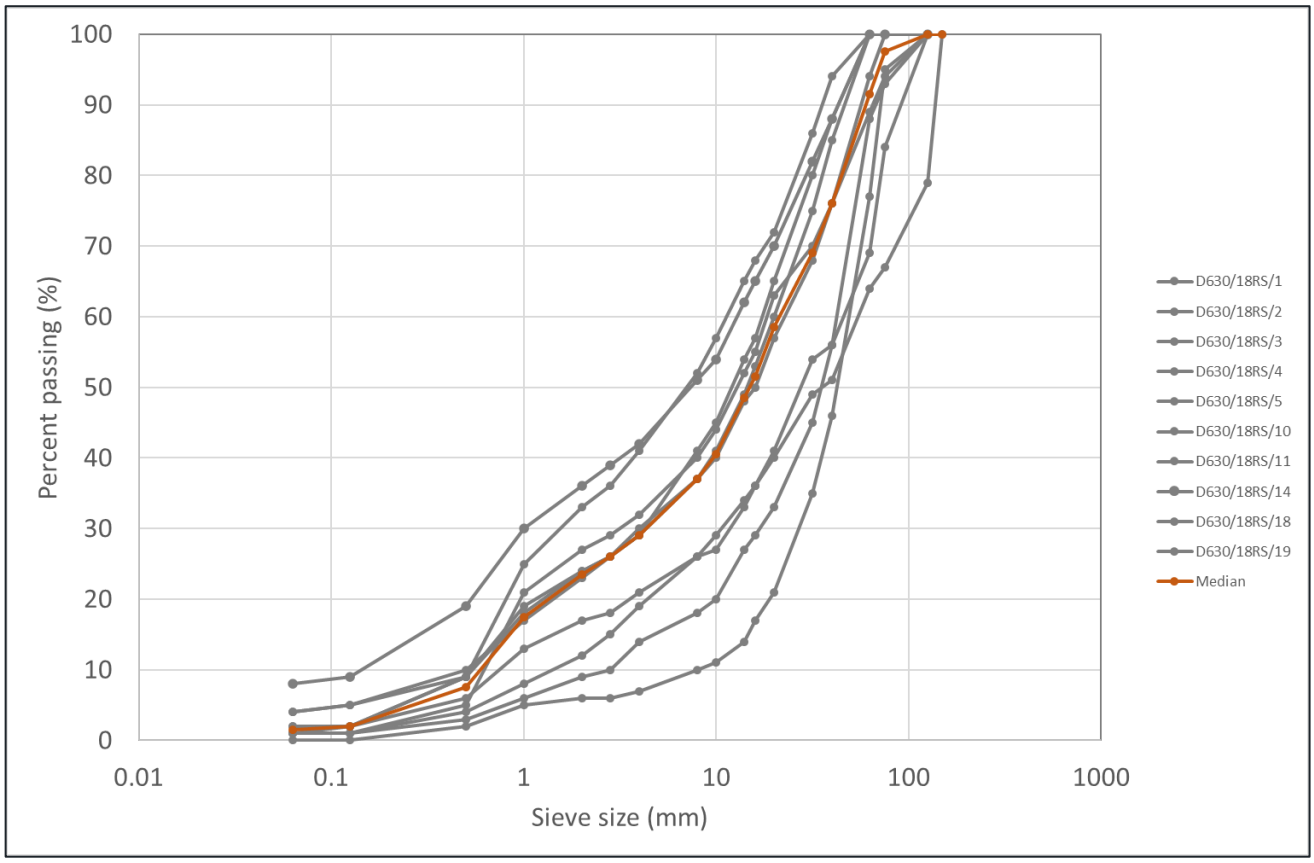

Figure 606/8: Particle size distribution of samples of the D630 stockpiles (Magnox, 2019d)

2.5.2 SGHWR REGION 2, NORTH ANNEXE AND SOUTH ANNEXE

The void space will be filled with a combination of demolition arisings from the D630 stockpiles and demolition arisings from the SGHWR Annexes and turbine hall (NRS, 2024c). The physical properties of the demolition arisings are described in section 2.5.1.

2.5.3 DRAGON REACTOR

The primary containment will be demolished using wireline cutting, and the below ground voids within Wall C will be filled with placed concrete blocks from the cutting. The assumed physical properties of the blocks to be placed in the Dragon reactor void are the same as those placed in the SGHWR and are set out in Table 606/5.

Above the blocks, arisings will be placed from conventional demolition techniques employed to demolish the remaining above ground concrete structure of the Dragon reactor and B78 fuel storage building. For example, the Dragon reactor roof will be demolished and the concrete in the roof will be pulverised and, along with the demolition arisings from Walls A and B, used to backfill the below ground voids (NRS, 2024c). The demolition arisings placed in the Dragon reactor structure are assumed to have the same physical properties as those placed in the SGHWR (Table 606/6).

2.6 RECONCILIATION OF THE SGHWR AND DRAGON REACTOR VOID SPACE AND VOLUMES OF MATERIAL FOR INFILL

Atkins used a 3D model[3] to determine that 6,300 m^3 of concrete blocks would be produced during demolition of the SGHWR and this volume is used in Magnox (2020b). The SWMMP (NRS, 2024i) uses this volume to describe the volume of the SGHWR below ground voids that will be filled with blocks instead of the volume of the blocks. Here, consistency with the SWMMP is retained.

Magnox (2020b) assumes the volume of blocks that will be placed in the Dragon reactor void is 350 m^3 and this was also calculated by Atkins[4]. The SWMMP (NRS, 2024i) states the volume that will be used to accommodate blocks in the Dragon reactor is 400 m^3.

A summary of void volumes and infill volumes developed in this section is provided in Table 606/7. The void volumes and volumes of demolition arisings cited in Table 606/7 are presented to the nearest cubic metre to retain traceability of values from cited sources. However, there is uncertainty with methods used to derive all the cited volumes and the error for each value is likely to be much greater than 1 m^3. Further, it is evident that the cited volumes that will be occupied by blocks are estimates to the nearest 50 m^3. Variation in the volume occupied by blocks will be accommodated by adjustment in the volume filled using material from the D630 stockpiles.

[3] Email from Atkins to Magnox dated 6 August 2019.

[4] An email from Atkins to Magnox dated 23 August 2019 states the volume is "~350 m^3".

Table 606/7: Summary of Void Space and Volumes of Material for Infill

Component	Void Volume (m^3)[a]	Volume Occupied by Blocks (m^3)	Volume Available for Demolition Arisings (m^3)[b]	Volume Available for Demolition Arisings (Total for the SGHWR/ Dragon reactor)	Volume of Demolition Arisings Generated In Situ (m^3)	Void Volume to be Filled using Material from the D630 Stockpiles (m^3)[e]
SGHWR Region 1	11,649	6,300	5,349	23,439	5,840[c]	17,599
SGHWR Region 2	3,425	None	3,425			
SGHWR North Annexe	4,164		4,164			
SGHWR South Annexe	10,501		10,501			
Dragon reactor – within Wall C	1,891	400	1,491	6,144	4,891[d]	1,253[f]
Dragon reactor – outside of Wall C	4,653	None	4,653			

Note a) Void space having taken account of remaining internal in-situ structures as they are presently understood, based on UKAEA, 2006, and rounded to the nearest whole number.

Note b) Based on subtraction of 'Volume Occupied by Blocks' from 'Void volume'. Demolition arisings to be sourced from arisings generated in-situ by demolition and imported from stockpiles.

Note c) Taken from Magnox (2020b) that assumes the volume occupied by arisings generated using conventional demolition techniques is 22% greater than the volume of the structures before they are demolished.

*Note d) The volume of the Dragon reactor structures to be demolished to ground level is 4,359 m^3 [5]. 350 m^3 will be demolished as blocks leaving 4,009 m^3 to be demolished using conventional demolition techniques. The demolition arisings generated by conventional demolition techniques are assumed to occupy a volume 22% greater than the volume of the structures before they are demolished: 4,009*1.22=4,891 m^3.*

Note e) Based on subtraction of 'volume of demolition arisings generated in situ' from 'volume available'.

Note f) The Dragon void volume to be filled using material from the D630 stockpiles may be reduced by 154 m^3 using arisings from demolition of building B78. This being the case, the volume to be filled using material from the D630 stockpiles would be reduced to 1,253-154=1,099 m^3.

[5] Email from Magnox Limited to WSP dated 11 October 2023.

3 DEVELOPMENT OF NON-RADIOLOGICAL ASSESSMENT INVENTORY

This section develops an 'assessment inventory' for the HRA.

In the context of hydrogeological risk assessment, the assessment inventory is not described by the total inventory but rather by the 'water available inventory'. The total non-radiological inventory of a substance in solid matter (for example concrete, brick or metal) is defined as the total mass of that substance that is present. NRS have developed a total non-radiological inventory for the Winfrith Site once the reactor buildings have been prepared for the End State (NRS, 2024g). The water available inventory of a contaminant is usually less than the total inventory because some of the contaminant is bound inextricably to, or within, solid material. Further, some components of the End State evidently pose no risk to groundwater quality, which could be because:

- The total inventory mass of contaminants that could contribute to the water available inventory is negligible; or
- There is compelling evidence that contaminants within the total inventory are of sufficiently low mobility or solubility that their contribution to the water available inventory will result in a negligible risk to groundwater quality.

This structure of this section is as follows:

- Description of the components of the structures and disposals/deposits and the available compositional data for each component (section 3.1);
- Derivation of a non-radiological assessment inventory from the available data for the demolition material that will be disposed/deposited within the structures (section 3.2);
- Derivation of a non-radiological assessment inventory for the End State structures, including the concrete, retained fibreglass and surface oil contamination on the concrete (section 3.3);
- Derivation of a non-radiological assessment inventory for the metals that will be deposited/disposed of or will remain in the structures (section 3.4); and
- Derivation of a non-radiological assessment inventory for emplaced non-waste materials (section 3.5).

3.1 NON-RADIOLOGICAL SOURCE COMPONENTS AND AVAILABLE DATA

A summary of the components of the End State of the reactor buildings, both retained in-situ and as infill materials, is presented in Table 606/8. For each component, the available inventory data are listed[6].

[6] Emplaced non-waste materials (grout and sealant) are products that will be specified during detailed design and are therefore excluded from the table.

Table 606/8: Summary of Available Compositional Information about Components Retained In-situ and Infill Materials

Reactor	Component (Structure/Infill)	Components Potentially Representing a Contaminant Source	Available Compositional Information
SGHWR	Demolition arisings (existing stockpiles from demolition activities at the site)	Concrete and brick Organic compounds	Non-radiological analysis of samples from the D630 stockpiles (Magnox, 2019d and Element, 2022)
	Demolition arisings (generated from demolition of remaining above ground SGHWR structures)	Concrete and brick	Non-radiological analysis of concrete cores from structures (Wood, 2020)
		Organic compounds	No direct data for SGHWR structures
	Concrete blocks (generated from demolition of remaining above ground SGHWR structures)	Concrete (with rebar)	Non-radiological analysis of concrete cores from structures (Wood, 2020) Study on the quantity and composition of rebar in SGHWR (Wood, 2020)
	Remaining in-situ structures	Standard concrete (with rebar)	Non-radiological analysis of concrete cores (Wood, 2020) Concrete core and bulk concrete analysis of Building D60[7] in GAU report 2938 (GAU, 2013) Summary of the quantity and composition of rebar in SGHWR (NRS, 2024h) Summary of the SGHWR oil-stained concrete (NRS, 2024d)
		Barytes concrete	Wilson (construction era document)
		Fibreglass liners	BAT report on pond liners (Magnox, 2018)
		Structural steel	Summary of the quantity and composition of structural steel (I-beams) in SGHWR (NRS, 2024h)
		Surface contamination by oils	BAT report on oils (Magnox, 2020c) Characterisation of Levels 1-3 (NRS, 2024d)
		Asbestos	Asbestos BAT (Magnox, 2019e)
Dragon Reactor	Demolition arisings (existing stockpiles from demolition activities at the site)	Concrete and brick Organic compounds	Non-radiological analysis of samples from the D630 stockpiles (Magnox, 2019d)

[7] Building D60 is the SGHWR.

Reactor	Component (Structure/Infill)	Components Potentially Representing a Contaminant Source	Available Compositional Information
	Demolition arisings (generated from demolition of remaining above ground Dragon reactor structures)	Concrete and brick	No direct data for Dragon reactor structures
		Potential surface contamination by oils	Dragon Oil Spill Survey Note for the Record (Magnox, 2021b)
	Concrete blocks (generated from demolition of remaining above ground Dragon reactor structures)	Concrete (with rebar)	No direct data for Dragon reactor structures
	Remaining in-situ structures	Standard concrete (with rebar)	No direct data for concrete from Dragon reactor. Summary of the quantity and composition of rebar in Dragon (NRS, 2024h)
		Barytes Concrete	Crawley (1960)
		Structural steel	Summary of the quantity and composition of structural steel in Dragon (NRS, 2024h)
		Potential surface contamination (organic compounds)	Dragon Oil Spill Survey Note for the Record (Magnox, 2021b)
		Asbestos	Email internal to Magnox dated 24 February 2022

3.1.1 DESCRIPTION OF COMPOSITIONAL DATA FOR THE EXISTING D630 STOCKPILES

Mechanically crushed site-derived brick and concrete demolition arisings are currently stockpiled approximately 100 m to the east of the SGHWR in four stockpiles (Figure 606/9). Collectively, the four stockpiles are referred to as the D630 stockpiles. NRS (2024a) describes the sources of the stockpiled material:

- The origin of material within Stockpiles #1 and #2, which has an estimated volume of 16,800 m^3, is from mixed locations across the Winfrith site. According to the SWMMP the first recorded rubble storage was approximately 250 tonnes of concrete debris from a 'streetlight replacement project' in 1997 and the last addition to the stockpile was 4,960 tonnes of rubble from the Zebra decommissioning project in 2010. It was consigned on the basis of satisfying the Radioactive Substances Act 1993 Substances of Low Activity (SoLA) Exemption Order values applicable at the time (the exemption values now applicable under Schedule 23 of EPR 2016 mean that some material in the stockpile may no longer meet the revised out-of-scope (OoS) values).
- Material in Stockpile #3 comprises approximately 3,500 m^3 crushed concrete and brick derived from the demolition of the A51 and A52 facilities.

- Material in Stockpile #4 was sourced from the D63/D64 Cooling Tower Basins and estimated to be around 1,400 m^3. It has been shown to meet OoS values (RSRL, 2012a and RSRL, 2012b).

The above volumes assume loose material with a density of the order of 1,500 kg/m^3 (NRS, 2024a). However, some element of compaction by settlement would be expected during emplacement of the material into the SGHWR and Dragon reactor voids, which would act to increase the density and decrease the material volume.

Figure 606/9: Aerial view of Winfrith D630 stockpiles 1 - 4 (NRS, 2024a).

NRS has determined that the percentage of brick in the stockpiles is more likely to be between 19% and 30% (Magnox internal email, 29 September 2020), and therefore, by extension, between 70% and 81% concrete.

Magnox carried out an investigation of the stockpiles in 2018. The investigation report (Magnox, 2019d) describes a visual inspection of foreign material within 21 samples collected from the stockpile. The samples were placed in 205 l drums as part of the investigation. The foreign material was plastic, tar/bitumen, wood, electrical cable, miscellaneous items and metal, and comprised less than 0.2% (w/w) of the investigated material. Following this, a further investigation for the purpose of solid phase analysis of samples for hydrocarbon species and total petroleum hydrocarbon (TPH) fractions in the stockpiles was conducted in 2022, with 20 samples collected from 10 locations at two depth intervals. As with the earlier investigation (Magnox, 2019d), the sampling locations were selected to provide a reasonable geographical coverage across the stockpiles.

Non-radiological laboratory analysis was completed on 10 samples taken from the D630 stockpiles during the initial 2018 investigation (Magnox, 2019d) comprising solid phase (metals and organic compounds) and leachate analysis. Solid phase non-radiological analysis of hydrocarbons was carried out on all 20 samples by Element (2022). Solid phase and leachable (single stage 10:1 liquid to solid ratio to BS EN 12457-2) concentrations are reproduced in Table 606/11 to Table 606/15. Whilst the concrete will not be sentenced for acceptance in an inert landfill, comparison of the emission values in Table 606/12 with criteria for the acceptance of waste at inert landfill sites (WAC) provides context to the results. The emission values of all parameters analysed are lower than the WAC limits in all ten samples.

Polychlorinated biphenyls (PCBs) were detected in half of the samples analysed from the 2018 investigation. Historical uses of PCBs include in cable sheaths, paints and anti-corrosion coatings, all of which have been identified, or are potentially present, in the stockpiled materials. PCBs could also be derived from their use as an additive in insulating oil and could be present as residual staining on concrete surfaces. Interpretation of the results of analysis of concrete cores described in section 3.1.6 finds that the dominant source of PCBs in demolition arisings is likely to be paint.

3.1.2 ANALYSIS OF CORED AND BULK CONCRETE SAMPLED FROM THE SGHWR

Analysis of concrete core and bulk concrete samples from Room 254 of Building D60 (the SGHWR) was carried out in 2013 and is summarised in a GAU laboratory report (GAU, 2013). WAC testing was carried out for the three samples described in Table 606/9.

Table 606/9: Description of Building D60 Room 254 Samples Scheduled for Waste Acceptance Criteria Analysis

GAU IDs	Customer ID	Sample Type	Required Fractions	Mass (g)	Observation	Preparation Prior to Analysis
GAU2955/1	D60/SEC/OGB/CON/Rm254/02/0-300mm	Floor Core	0-75mm	1,415	Core (275mm) in 3 sections. A (75mm), B (150mm), C (50mm). No paint	A) Crushed 378g, 112g removed for WAC test, 22g ground
GAU2955/2			75-225mm			B) Crushed 805g, 110g removed for WAC test, 20g ground
GAU2938/11	D60/SEC/OGB/CON/Rm254/FLOOR BULKED CONCRETE 2 OF 2	Concrete	-	550	-	109g removed for WAC test. 200g crushed and ground

The test results are summarised in Table 606/10. Comparison with WAC has been carried out to provide context to the results. The component emission values of all three samples analysed are lower than the WAC, other than cadmium which exceeded the WAC in a single sample and total dissolved solids which exceeded the WAC in all three samples. The values of the compositional analysis are lower than the WAC for all parameters analysed.

Table 606/10: Waste Acceptance Criteria Testing Results for Concrete from Building D60 Room 254 (all results mg/kg dry weight except where stated)

	Sample Lab Ref: GAU2938/11	Sample Lab Ref: GAU2955/1	Sample Lab Ref: GAU2955/2
Compositional Analysis (all results mg/kg dry weight except where stated)			
Mineral oil (C10 – C40)	< 50	94	< 50
Loss on ignition (%)	11 %	12 %	2.8 %
Total Organic Carbon (%)	1.9 %	< 1 %	< 1 %
BTEX[8]	< 5	< 5	< 5
PCBs (7 congeners)	< 1	< 1	< 1
PAH[9] compounds	< 10	< 10	< 10
% water (air drying)	< 1 %	< 1 %	< 1 %
Leach Test Analysis (all results mg leached per kg of dry material at a liquid to solid ratio of 10 l/kg)			
Arsenic	< 0.2	< 0.2	< 0.2
Antimony	0.05	0.05	< 0.05
Barium	0.4	2.7	0.70
Cadmium	< 0.03	0.06	< 0.03
Chromium (total)	0.42	0.38	< 0.3
Copper	< 0.3	< 0.3	< 0.3
Lead	< 0.2	< 0.2	< 0.2
Mercury	< 0.01	< 0.01	< 0.01
Molybdenum	< 0.2	< 0.2	< 0.2
Nickel	< 0.2	< 0.2	< 0.2
Selenium	< 0.1	< 0.1	< 0.1
Zinc	< 0.2	< 0.2	< 0.2
Sulphate	318	118	89
Fluoride	< 3	< 3	< 3

[8] Benzene Toluene Ethylbenzene Xylene.

[9] Polycyclic Aromatic Hydrocarbon.

	Sample Lab Ref: GAU2938/11	Sample Lab Ref: GAU2955/1	Sample Lab Ref: GAU2955/2
Chloride	80	43	39
Phenol index	< 1	< 1	< 1
pH (pH units)	11.95	12.00	11.99
Total dissolved solids	16500	18700	18400
Dissolved organic carbon	138	< 100	< 100

3.1.3 DESCRIPTION OF COMPOSITIONAL DATA FOR STRUCTURAL CONCRETE

Non-radiological analysis has been completed on eight core samples taken from concrete within the SGHWR. The results (as presented in Wood, 2020) are included in Table 606/16. Total concentrations are reported for five metals. It is unlikely that the five metals reported are all that are present and without the analysis of concrete cores in 2023 (see below), the composition of the structural concrete would be uncertain.

Consideration has been given as to whether any of the samples represent barytes concrete. The assumed density of cement in SGHWR is 1,440 kg/m^3. Wilson (construction era document) reports that the density of barytes concrete used in the construction of SGHWR was 218 lb / cu. ft, i.e., 3,492 kg/m^3 and implies that barytes was the only aggregate used in such concrete. Crawley (1960) reports the barytes concrete density used in the construction of the Dragon reactor was 3,650 kg/m^3. Based on a published baryte density of 4,500 kg/m^3 (Mindat, 2021), approximately 70% by volume barytes aggregate would have been required to achieve the barytes concrete densities reported by Crawley (1960) and Wilson (construction era document)[10]. Concentrations of barium significantly in excess of those reported in Table 606/16 would therefore be expected in barytes concrete, i.e. approximately 880,000 mg/kg barytes ($BaSO_4$) and therefore approximately 520,000 mg/kg barium. It is concluded that all the samples therefore are from standard concrete.

There is uncertainty, as previously summarised in Wood (2020), as to whether the relatively high iron and chromium concentrations in samples S1 to S3 are because of rebar in the sample. It is assumed that samples S1 to S3 contained rebar. The results of analysis of these samples will not be used to determine the composition of structural concrete.

In 2023 concrete core samples were taken from the floor of Levels 1-3 at 15 locations in SGHWR. The sampling approach and methodology is documented in NRS (2024d) and did not allow for inclusion of rebar. The samples were analysed for metals with the analytical results presented in Table 606/17. It is evident from the results that none of the sample were of barytes concrete as would be expected for floor samples.

[10] Wilson (construction era document) states, "*The size of the coarse aggregate was ¾" down with a specific gravity of 4.15, and the density of the concrete was specified as 215 lb/cu. ft*". This implies that the concrete contains only baryte and cement.

Table 606/11: Solid Concentrations (mg/kg) of Demolition Arisings in D630 Stockpiles (from Magnox, 2019d)

Contaminant	RS/1	RS/2	RS/3	RS/4	RS/5	RS/10	RS/11	RS/14	RS/18	RS/19	No. Samples	No. Results >LOD	Min. Detected Conc.	Max. Detected Conc.	Mean Conc.	UCL95 of Mean.
Antimony	<1	1	<1	<1	<1	<1	1	<1	2	<1	10	3	1	2	0.8	1.1
Arsenic	5	5	5	5	5	6	7	5	6	9	10	10	5	9	5.8	6.74
Barium	1300	390	250	390	250	410	130	150	130	42	10	10	42	1,300	344	601
Cadmium	<1	<1	<1	<1	<1	<1	<1	1	<1	<1	10	1	1	1	0.6	0.66
Chromium	15	18	12	16	12	14	18	34	14	20	10	10	12	34	17	22
Copper	14	18	11	8	11	9	22	42	18	24	10	10	8	42	18	25
Lead	390	220	54	25	48	180	100	100	120	64	10	10	25	390	130	208
Mercury	<1	<1	<1	<1	<1	<1	<1	<1	<1	<1	10	0	N/A	N/A	0.5	0.5
Molybdenum	<2	<2	<2	<2	<2	<2	<2	3	<2	<2	10	1	3	3	1.2	1.65
Nickel	10	11	10	10	10	12	14	32	11	7	10	10	7	32	13	17.71
Selenium	<3	<3	<3	<3	<3	<3	<3	<3	<3	<3	10	0	N/A	N/A	1.5	1.5
Zinc	160	160	78	41	71	50	79	110	120	62	10	10	41	160	93	123.65
Benzene	<0.001	<0.001	<0.001	<0.001	<0.001	<0.001	<0.001	<0.001	<0.001	0.002	10	1	0.002	0.002	0.0007	0.0010
Toluene	<0.001	<0.001	<0.001	<0.001	<0.001	<0.001	<0.001	<0.001	<0.001	0.001	10	1	0.001	0.001	0.0006	0.0007
Ethylbenzene	<0.001	<0.001	<0.001	<0.001	<0.001	<0.001	<0.001	<0.001	<0.001	<0.001	10	0	N/A	N/A	0.0005	0.0005
m/p Xylene	<0.001	<0.001	<0.001	<0.001	<0.001	<0.001	<0.001	<0.001	<0.001	<0.001	10	0	N/A	N/A	0.0005	0.0005
o - Xylene	<0.001	<0.001	<0.001	<0.001	<0.001	<0.001	<0.001	<0.001	<0.001	<0.001	10	0	N/A	N/A	0.0005	0.0005
PAH compounds	<1.6	<1.6	<1.6	<1.6	27	<1.6	1.8	<1.6	<1.6	<1.6	10	2	1.8	27	3.5	9.43
TPH	130	170	92	37	98	30	170	100	230	25	10	10	25	230	108	157
PCB-101	<0.01	0.039	<0.01	<0.01	<0.01	<0.01	0.26	0.067	0.017	0.019	10	5	0.017	0.26	0.043	0.099
PCB-118	<0.01	0.015	<0.01	<0.01	<0.01	<0.01	0.18	0.043	<0.01	0.012	10	4	0.012	0.18	0.028	0.067
PCB-138	<0.01	0.034	<0.01	<0.01	<0.01	<0.01	0.32	0.085	0.019	0.013	10	5	0.013	0.32	0.050	0.120
PCB-153	<0.01	0.021	<0.01	<0.01	<0.01	<0.01	0.24	0.057	0.014	<0.01	10	4	0.014	0.24	0.036	0.089
PCB-180	<0.01	<0.01	<0.01	<0.01	<0.01	<0.01	0.17	0.042	<0.01	<0.01	10	2	0.042	0.17	0.025	0.063
PCB-28	<0.01	0.012	<0.01	<0.01	<0.01	<0.01	<0.1	<0.01	<0.01	0.014	10	2	0.012	0.014	0.011	0.021
PCB-52	<0.01	0.021	<0.01	<0.01	<0.01	<0.01	<0.1	0.026	<0.01	0.012	10	3	0.012	0.026	0.014	0.025

Note a) Where concentration is reported as less than the laboratory limit of detection (LOD), the mean and UCL95 of the mean concentration has been calculated using a value of half the LOD. b) N/A signifies that the maximum and minimum cannot be presented as all results are <LOD.

Table 606/12: Water Leachable Concentrations (mg/kg) of Demolition Arisings in D630 Stockpiles (from Magnox, 2019d)

Contaminant	RS/1	RS/2	RS/3	RS/4	RS/5	RS/10	RS/11	RS/14	RS/18	RS/19	No. Samples	No. Results >LOD	Min. Detected Conc.	Max. Detected Conc.	Mean Conc	UCL95 of Mean
Antimony	<0.01	<0.01	<0.01	<0.01	<0.01	<0.01	<0.01	<0.01	0.03	<0.01	10	1	0.03	0.03	0.008	0.013
Arsenic	0.007	0.015	0.0082	0.009	0.011	0.0074	0.0075	0.028	0.0065	0.004	10	10	0.004	0.028	0.0104	0.015
Barium	1.5	0.22	0.3	0.5	0.21	0.39	0.14	0.1	0.27	1.2	10	10	0.1	1.5	0.48	0.82
Cadmium	<0.0002	<0.0002	<0.0002	<0.0002	<0.0002	<0.0002	<0.0002	<0.0002	<0.0002	<0.0002	10	0	N/A	N/A	0.0001	0.0001
Chloride	10	<10	<10	<10	<10	<10	18	<10	<10	28	10	3	10	28	9	14.72
Chromium	0.2	0.088	0.073	0.037	0.044	0.05	0.086	0.044	0.11	0.26	10	10	0.037	0.26	0.099	0.15
Copper	0.017	0.03	0.037	0.033	0.046	0.0071	0.006	0.021	0.042	0.063	10	10	0.006	0.063	0.0302	0.043
Fluoride	2	3.7	<0.5	0.55	<0.5	1	1.5	0.83	<0.5	1.4	10	7	0.55	3.7	1.17	1.94
Lead	0.0031	0.0071	0.0038	<0.003	0.0093	<0.003	<0.003	0.0034	0.0055	0.014	10	7	0.0031	0.014	0.0051	0.0080
Mercury	<0.0005	0.0006	<0.0005	<0.0005	<0.0005	<0.0005	<0.0005	0.00075	<0.0005	<0.0005	10	2	0.0006	0.00075	0.00034	0.00047
Molybdenum	0.017	0.018	0.014	<0.01	<0.01	<0.01	<0.01	0.012	0.018	0.014	10	6	0.012	0.018	0.011	0.015
Nickel	<0.01	<0.01	0.016	<0.01	0.013	<0.01	<0.01	<0.01	0.012	0.019	10	4	0.012	0.019	0.009	0.013
Selenium	<0.005	<0.005	<0.005	<0.005	<0.005	<0.005	<0.005	0.0051	<0.005	<0.005	10	1	0.0051	0.0051	0.0028	0.003
Sulphate	310	500	570	190	530	130	250	180	530	85	10	10	85	570	328	461
Zinc	0.039	0.034	0.04	0.052	0.039	0.053	0.029	0.31	0.03	0.026	10	10	0.026	0.31	0.065	0.13

Note a) Where concentration is reported as less than the laboratory limit of detection (LOD), the mean and UCL95 of the mean concentration has been calculated using a value of half the LOD. b) N/A signifies that the maximum and minimum cannot be presented as all results are <LOD.

Table 606/13: Speciated PAH Compound Concentrations (mg/kg) of Demolition Arisings from the 2022 Magnox Stockpiles Investigation (Element, 2022)

Sample	RS22		RS23		RS24		RS25		RS26		RS27		RS28		RS29		RS30		RS31		No. samples	No. samples >LOD	Min. Detected Conc	Max. Detected Conc	Mean Conc	UCL95 of Mean
Depth (m below surface)	0.5-0.6	1.7-1.8	0.8-0.9	1.8-1.9	0.6-0.7	1.7-1.8	0.6-0.7	1.6-1.7	0.5-0.6	1.6-1.7	0.6-0.7	1.6-1.7	0.6-0.7	1.4-1.5	0.5-0.6	1.6-1.7	0.5-0.6	1.4-1.5	0.6-0.7	1.6-1.7						
Naphthalene	<0.04	<0.04	<0.04	0.06	<0.04	<0.04	<0.04	<0.04	<0.04	<0.04	<0.04	<0.04	<0.04	<0.04	<0.04	<0.04	<0.04	<0.04	<0.04	<0.04	20	1	0.06	0.06	0.022	0.026
Acenaphthylene	<0.03	<0.03	<0.03	<0.03	<0.03	0.09	0.06	0.06	0.03	<0.03	0.09	0.14	<0.03	<0.03	<0.03	<0.03	<0.03	<0.03	<0.03	<0.03	20	6	0.03	0.14	0.034	0.051
Acenaphthene	<0.05	<0.05	<0.05	<0.05	<0.05	<0.05	<0.05	<0.05	<0.05	<0.05	<0.05	<0.05	<0.05	<0.05	<0.05	<0.05	<0.05	<0.05	<0.05	<0.05	20	0	N/A	N/A	0.025	0.025
Fluorene	<0.04	<0.04	<0.04	<0.04	<0.04	<0.04	<0.04	<0.04	<0.04	<0.04	<0.04	<0.04	<0.04	<0.04	<0.04	<0.04	<0.04	<0.04	<0.04	<0.04	20	0	N/A	N/A	0.020	0.020
Phenanthrene	<0.03	0.07	0.08	0.24	0.06	0.11	0.09	0.08	0.04	0.08	0.27	0.23	0.12	0.44	0.07	<0.03	0.32	0.09	0.07	0.03	20	18	0.03	0.44	0.13	0.18
Anthracene	<0.04	<0.04	<0.04	0.06	<0.04	0.14	0.06	0.07	<0.04	<0.04	0.15	0.21	<0.04	0.16	0.05	<0.04	0.09	<0.04	<0.04	<0.04	20	9	0.05	0.21	0.061	0.088
Fluoranthene	0.08	0.15	0.19	0.3	0.17	0.68	0.28	0.31	0.14	0.18	0.78	0.62	0.22	0.75	0.23	0.16	0.73	0.35	0.12	0.1	20	20	0.08	0.78	0.33	0.44
Pyrene	0.07	0.16	0.17	0.26	0.36	1.19	0.5	0.38	0.2	0.3	0.68	0.79	0.22	0.63	0.26	0.2	0.87	0.35	0.09	0.08	20	20	0.07	1.19	0.39	0.53
Benzo(a)anthracene	<0.06	0.1	0.13	0.16	0.18	0.77	0.29	0.22	0.12	0.16	0.4	0.42	0.12	0.39	0.19	0.13	0.42	0.27	0.08	<0.06	20	18	0.08	0.77	0.23	0.31
Chrysene	0.07	0.1	0.13	0.16	0.2	0.87	0.31	0.26	0.14	0.17	0.44	0.57	0.15	0.36	0.17	0.1	0.51	0.26	0.07	0.06	20	20	0.06	0.87	0.26	0.35
Benzo(bk)fluoranthene	0.16	0.23	0.21	0.3	0.38	1.56	0.62	0.55	0.39	0.36	0.93	2.1	0.28	0.65	0.36	0.15	0.89	0.45	<0.07	<0.07	20	18	0.15	2.1	0.53	0.77
Benzo(a)pyrene	0.1	0.12	0.12	0.17	0.2	0.75	0.33	0.33	0.24	0.2	0.56	1.7	0.15	0.37	0.27	0.09	0.6	0.26	<0.04	<0.04	20	18	0.09	1.7	0.33	0.51
Indeno(123cd)pyrene	0.09	0.09	0.1	0.15	0.15	0.56	0.26	0.27	0.21	0.17	0.5	1.64	0.14	0.29	0.21	0.06	0.39	0.2	<0.04	<0.04	20	18	0.06	1.64	0.28	0.44
Dibenzo(ah)anthracene	<0.04	<0.04	<0.04	<0.04	<0.04	0.11	0.06	0.06	<0.04	<0.04	0.09	0.27	<0.04	0.07	0.1	<0.04	0.19	0.07	<0.04	<0.04	20	9	0.06	0.27	0.062	0.093
Benzo(ghi)perylene	0.1	0.12	0.12	0.16	0.16	0.53	0.28	0.26	0.23	0.18	0.55	1.78	0.14	0.28	0.38	0.12	0.65	0.28	<0.04	<0.04	20	18	0.1	1.78	0.32	0.50
Benzo(b)fluoranthene	0.12	0.17	0.15	0.22	0.27	1.12	0.45	0.4	0.28	0.26	0.67	1.51	0.2	0.47	0.26	0.11	0.64	0.32	<0.05	<0.05	20	18	0.11	1.51	0.38	0.56
Benzo(k)fluoranthene	0.04	0.06	0.06	0.08	0.11	0.44	0.17	0.15	0.11	0.1	0.26	0.59	0.08	0.18	0.1	0.04	0.25	0.13	<0.02	<0.02	20	18	0.04	0.59	0.15	0.22

Note a) Where concentration is reported as less than the laboratory limit of detection (LOD), the mean and UCL95 of the mean concentration has been calculated using a value of half the LOD. b) N/A signifies that the maximum and minimum cannot be presented as all results are <LOD.

Table 606/14: TPH-CWG Aliphatic Fraction Concentrations (mg/kg) of Demolition Arisings from the 2022 Magnox Stockpiles Investigation (Element, 2022)

Sample	RS22		RS23		RS24		RS25		RS26		RS27		RS28		RS29		RS30		RS31		No. samples	No. samples >LOD	Min	Max	Mean	UCL95 of Mean
Depth (m below surface)	0.5-0.6	1.7-1.8	0.8-0.9	1.8-1.9	0.6-0.7	1.7-1.8	0.6-0.7	1.6-1.7	0.5-0.6	1.6-1.7	0.6-0.7	1.6-1.7	0.6-0.7	1.4-1.5	0.5-0.6	1.6-1.7	0.5-0.6	1.4-1.5	0.6-0.7	1.6-1.7						
>C5-C6 aliphatic	<0.1	<0.1	<0.1	<0.1	<0.1	<0.1	<0.1	<0.1	<0.1	<0.1	<0.1	<0.1	<0.1	<0.1	<0.1	0.2	<0.1	<0.1	<0.1	<0.1	20	1	0.2	0.2	0.058	0.073
>C6-C8 aliphatic	<0.1	<0.1	<0.1	<0.1	<0.1	<0.1	<0.1	<0.1	<0.1	<0.1	<0.1	<0.1	<0.1	<0.1	<0.1	<0.1	<0.1	<0.1	<0.1	<0.1	20	0	N/A	N/A	0.050	0.050
>C8-C10 aliphatic	<0.1	<0.1	<0.1	<0.1	<0.1	<0.1	<0.1	<0.1	<0.1	<0.1	<0.1	<0.1	<0.1	<0.1	<0.1	<0.1	<0.1	<0.1	<0.1	<0.1	20	0	N/A	N/A	0.050	0.050
>C10-C12 aliphatic	<0.2	<0.2	<0.2	<0.2	<0.2	<0.2	<0.2	<0.2	<0.2	<0.2	<0.2	<0.2	<0.2	<0.2	<0.2	1.5	<0.2	<0.2	<0.2	<0.2	20	1	1.5	1.5	0.17	0.32
>C12-C16 aliphatic	<4	<4	<4	<4	<4	<4	<4	<4	<4	<4	<4	<4	12	6	<4	6	<4	<4	<4	<4	20	3	6	12	2.9	4.1
>C16-C21 aliphatic	<7	<7	<7	<7	<7	<7	<7	<7	<7	<7	<7	<7	60	15	17	16	<7	<7	<7	<7	20	4	15	60	8.2	14
>C21-C35 aliphatic	<7	<7	<7	<7	<7	<7	<7	<7	81	34	<7	28	296	90	98	80	93	43	31	<7	20	10	28	296	45	78
>C35-C44 aliphatic	<7	<7	<7	<7	<7	<7	<7	<7	28	14	<7	9	67	16	21	20	19	128	<7	<7	20	9	9	128	18	32
>C5-EC7 aromatic	<0.1	<0.1	<0.1	<0.1	<0.1	<0.1	<0.1	<0.1	<0.1	<0.1	<0.1	<0.1	<0.1	<0.1	<0.1	<0.1	<0.1	<0.1	<0.1	<0.1	20	0	N/A	N/A	0.05	0.050
>EC7-EC8 aromatic	<0.1	<0.1	<0.1	<0.1	<0.1	<0.1	<0.1	<0.1	<0.1	<0.1	<0.1	<0.1	<0.1	<0.1	<0.1	<0.1	<0.1	<0.1	<0.1	<0.1	20	0	N/A	N/A	0.05	0.050
>EC8-EC10 aromatic	<0.1	<0.1	<0.1	<0.1	<0.1	<0.1	<0.1	<0.1	<0.1	<0.1	<0.1	<0.1	<0.1	<0.1	<0.1	<0.1	<0.1	<0.1	<0.1	<0.1	20	0	N/A	N/A	0.05	0.050
>EC10-EC12 aromatic	<0.2	<0.2	<0.2	<0.2	<0.2	<0.2	<0.2	<0.2	<0.2	<0.2	<0.2	<0.2	<0.2	<0.2	<0.2	<0.2	<0.2	<0.2	<0.2	<0.2	20	0	N/A	N/A	0.10	0.10
>EC12-EC16 aromatic	<4	<4	<4	<4	<4	<4	<4	<4	<4	<4	<4	<4	<4	<4	<4	<4	<4	<4	<4	<4	20	0	N/A	N/A	2	2
>EC16-EC21 aromatic	<7	<7	<7	<7	<7	<7	<7	<7	<7	<7	13	<7	8	<7	<7	<7	<7	<7	<7	<7	20	2	8	13	4.20	5.3
>EC21-EC35 aromatic	<7	<7	<7	<7	<7	<7	<7	<7	81	34	104	80	113	76	82	93	124	87	<7	<7	20	10	34	124	45.45	67
>EC35-EC44 aromatic	<7	<7	<7	<7	<7	<7	<7	<7	28	14	32	26	40	29	29	25	36	27	<7	<7	20	10	14	40	16.05	22
Total aliphatics C5-44	<26	<26	<26	<26	<26	<26	<26	<26	109	48	<26	37	435	127	136	124	112	171	31	<26	20	10	31	435	73	120
Total aromatics C5-44	<26	<26	<26	<26	<26	<26	<26	<26	109	48	149	106	161	105	111	118	160	114	<26	<26	20	10	48	161	66	93
Total aliphatics and aromatics(C5-44)	<52	<52	<52	64	99	71	77	88	295	189	149	143	596	232	247	242	272	285	<52	<52	20	15	64	596	159	225

Note a) Where concentration is reported as less than the laboratory limit of detection (LOD), the mean and UCL95 of the mean concentration has been calculated using a value of half the LOD. b) N/A signifies that the maximum and minimum cannot be presented as all results are <LOD.

Table 606/15: BTEX and MTBE[11] Concentrations (mg/kg) of Demolition Arisings in D630 Stockpiles from the 2022 Magnox Stockpiles Investigation (Element, 2022)

Sample	RS22		RS23		RS24		RS25		RS26		RS27		RS28		RS29		RS30		RS31		No. samples	No. samples >LOD	Min	Max	Mean	UCL95 of Mean
Depth (m below surface)	0.5-0.6	1.7-1.8	0.8-0.9	1.8-1.9	0.6-0.7	1.7-1.8	0.6-0.7	1.6-1.7	0.5-0.6	1.6-1.7	0.6-0.7	1.6-1.7	0.6-0.7	1.4-1.5	0.5-0.6	1.6-1.7	0.5-0.6	1.4-1.5	0.6-0.7	1.6-1.7						
MTBE	<0.005	<0.005	<0.005	<0.005	<0.005	<0.005	<0.005	<0.005	<0.005	<0.005	<0.005	0.011	<0.005	<0.005	<0.005	<0.005	<0.005	<0.005	<0.005	<0.005	20	1	0.011	0.011	0.0029	0.0038
Benzene	<0.005	<0.005	<0.005	<0.005	<0.005	<0.005	<0.005	<0.005	<0.005	<0.005	<0.005	<0.005	<0.005	<0.005	<0.005	<0.005	<0.005	<0.005	<0.005	<0.005	20	0	N/A	N/A	0.0025	0.0025
Toluene	<0.005	<0.005	<0.005	<0.005	<0.005	<0.005	<0.005	<0.005	<0.005	<0.005	<0.005	<0.005	<0.005	<0.005	<0.005	<0.005	<0.005	<0.005	<0.005	<0.005	20	0	N/A	N/A	0.0025	0.0025
Ethylbenzene	<0.005	<0.005	<0.005	<0.005	<0.005	<0.005	<0.005	<0.005	<0.005	<0.005	<0.005	<0.005	<0.005	<0.005	<0.005	<0.005	<0.005	<0.005	<0.005	<0.005	20	0	N/A	N/A	0.0025	0.0025
m/p-Xylene	<0.005	<0.005	<0.005	<0.005	<0.005	<0.005	<0.005	<0.005	<0.005	<0.005	<0.005	0.030	<0.005	<0.005	0.019	<0.005	<0.005	0.008	<0.005	<0.005	20	3	0.008	0.030	0.0050	0.0083
o-Xylene	<0.005	<0.005	<0.005	<0.005	<0.005	<0.005	<0.005	<0.005	<0.005	<0.005	<0.005	0.021	<0.005	<0.005	0.022	<0.005	<0.005	<0.005	<0.005	<0.005	20	2	0.021	0.022	0.0044	0.0071

Note a) Where concentration is reported as less than the laboratory limit of detection (LOD), the mean and the UCL95 of the mean concentration has been calculated using a value of half the LOD. b) N/A signifies that the maximum and minimum cannot be presented as all results are <LOD

Table 606/16: Solid Concentrations (mg/kg) in Concrete Cores from the SGHWR (from Wood, 2020)

Contaminant	S1	S2	S3	S4	S5	S6	S7	S8	No. samples	No. Results >LOD	Min. detected conc.	Max. detected conc.	Mean conc.
Arsenic	4	4	4	3.9	2.5	3.4	5.8	3.8	8	8	2.5	5.8	3.9
Barium	52	48	53	46	228	184	88	178	8	8	46	228	110
Beryllium	1	4	0.9	1	0.7	1	1	2	8	8	0.7	4	1.5
Chromium	152	152	136	16.4	16.6	14.5	14.4	16	8	8	14.4	152	64.7
Iron	24,900	32,100	26,100	7,000	2,880	3,730	4,700	6,010	8	8	2,880	32,100	13,428

[11] Methyl Tert-Butyl Ether.

Table 606/17: Solid Concentrations (mg/kg) in Concrete Cores from the SGHWR (from NRS, 2024d)

Lab Ref [Magnox Ref]	L220511-1 [D60/124/Oil/Floor Core/01]	L220511-3 [D60/124/Oil/Floor Core/02]	L220511-5 [D60/240/Oil/Floor Core/01]	L220511-7 [D60/240/Oil/Floor Core/02]	L220511-9 [D60/240/No Oil/Floor Core/03]	L220511-11 [D60/242/Oil/Floor Core/01]	L220511-13 [D60/242/Oil/Floor Core/02]	L220511-15 [D60/243/Oil/Floor Core/01]	L220511-17 [D60/243/Oil/Floor Core/02]	L220511-19 [D60/321/Oil/Floor Core/01]	L220511-21 [D60/321/Oil/Floor Core/02]	L220511-23 [D60/326/Oil/Floor Core/01]	L220511-25 [D60/326/Oil/Floor Core/02]	L220511-27 [D60/329/Oil/Floor Core/01]	L220511-29 [D60/329/Oil/Floor Core/02]	Min	Max	Mean	UCL95 of Mean
As	1.6	2.0	5.9	7.3	4.1	3.6	2.0	1.5	2.0	2.1	3.5	5.6	2.4	4.7	3.5	1.5	7.3	3.4	4.4
B	9.6	7.8	13.5	13.5	9.4	11.4	11.7	8.7	10.7	10.8	27.8	13.4	10.5	10.1	17.1	7.8	27.8	12.4	15.1
Ba	27.2	28.6	37.9	26.3	26.9	118.0	41.5	20.9	38.1	47.5	781.9	41.2	28.3	30.4	67.2	20.9	781.9	90.8	197.5
Be	<1	<1	<1	<1	<1	<1	<1	<1	<1	<1	<1	<1	<1	<1	<1	N/A	N/A	0.5	0.5
Ca	64488.9	59136.7	63898.8	62862.8	67022.1	75211.3	74081.6	49994.3	86372.3	60751.8	105773.0	75623.0	62709.2	66997.4	53022.0	49994.3	105773.0	68529.7	76180.7
Cd	<1	<1	<1	<1	<1	1.2	<1	<1	<1	<1	6.8	<1	<1	<1	<1	1.2	6.8	1.0	1.9
Co	4.9	12.3	10.8	11.2	7.3	5.7	6.4	5.4	7.2	9.6	14.9	13.5	8.1	10.5	10.0	4.9	14.9	9.2	10.9
Cr	9.3	8.4	10.4	10.5	7.3	11.0	9.1	8.1	12.9	14.8	23.0	15.7	11.6	9.9	23.4	7.3	23.4	12.4	15.1
Cr(VI)	0.45	0.086	0.064	0.040	0.054	0.040	0.094	0.070	0.056	0.068	0.034	0.054	0.070	0.034	0.034	0.03	0.45	0.1	0.1
Cu	4.4	2.1	4.6	5.4	6.8	5.7	4.0	3.6	4.6	9.1	24.4	21.6	4.4	2.9	9.6	2.1	24.4	7.6	11.2
Fe	5715.3	5003.1	11677.8	12050.8	5352.2	5629.8	4515.4	5802.9	6207.7	12255.4	9300.3	10139.7	7050.1	9089.3	13217.9	4515.4	13217.9	8200.5	9888.3
Hg	<1	<1	<1	<1	<1	<1	<1	<1	<1	<1	<1	<1	<1	<1	<1	N/A	N/A	0.5	0.5
K	635.3	769.3	1148.7	500.2	734.2	783.9	1048.7	527.5	832.8	828.0	707.9	1325.5	968.1	1061.3	1411.6	500.2	1411.6	885.5	1035.6
Li	<20	<20	<20	<20	<20	<20	<20	<20	<20	<20	<20	<20	<20	<20	<20	N/A	N/A	10.0	10.0
Mg	855.3	797.3	750.2	678.5	726.4	1246.5	901.9	762.8	1113.2	3659.7	1536.6	2363.4	1823.3	712.1	3837.8	678.5	3837.8	1451.0	2032.3
Mn	88.6	79.1	145.9	141.4	74.0	147.0	186.6	94.3	160.7	257.8	122.7	140.6	112.4	132.7	240.1	74.0	257.8	141.6	171.4
Mo	<1	<1	<1	<1	<1	<1	<1	<1	<1	<1	1.4	<1	<1	<1	<1	1.4	1.4	0.6	0.7
Na	166.5	200.5	208.4	127.8	206.6	232.5	236.6	196.2	275.5	495.0	393.7	254.5	213.5	216.3	412.1	127.8	495.0	255.7	311.3
Ni	4.7	4.1	8.2	8.2	6.2	6.6	5.5	4.2	7.0	11.8	11.6	10.6	6.6	6.6	15.0	4.1	15.0	7.8	9.5
Pb	<1	<1	4.4	27.1	<1	26.2	<1	<1	7.6	13.4	36.5	<1	<1	<1	4.1	4.1	36.5	8.2	14.9
Sb	<5	<5	<5	<5	<5	<5	<5	<5	<5	<5	<5	<5	<5	<5	<5	N/A	N/A	2.5	2.5
Sc	1.0	<1	1.4	1.3	<1	1.3	1.2	<1	1.3	2.6	1.4	1.8	1.3	1.2	2.9	1.0	2.9	1.3	1.7
Se	<5	<5	<5	<5	<5	<5	<5	<5	<5	<5	<5	<5	<5	<5	<5	N/A	N/A	2.5	2.5
Sr	190.0	192.4	225.8	146.6	145.3	171.0	128.3	127.7	272.6	201.1	254.4	138.7	120.4	201.1	228.5	120.4	272.6	182.9	209.7
Ti	206.2	191.8	234.6	191.0	178.5	247.4	224.0	146.2	236.9	717.6	304.9	437.1	292.1	210.7	813.2	146.2	813.2	308.8	418.7
V	12.9	11.7	17.0	17.0	11.2	12.8	11.1	10.7	16.7	26.7	20.6	19.6	14.2	14.1	29.5	10.7	29.5	16.4	19.5
Zn	22.0	16.4	27.0	26.8	18.0	75.5	18.0	18.3	27.1	34.7	46.8	24.4	18.5	43.6	58.7	16.4	75.5	31.7	41.3

Note a) Where concentration is reported as less than the laboratory limit of detection (LOD), the mean and the UCL95 of the mean concentration has been calculated using a value of half the LOD. b) N/A signifies that the maximum and minimum cannot be presented as all results are <LOD

3.1.4 DESCRIPTION OF AVAILABLE DATA RELATING TO SURFACE CONTAMINATION OF STRUCTURES IN THE SGHWR AND DRAGON REACTOR BY OILS

Oil was changed regularly during the operational phase of the SGHWR and minor spillages onto the concrete floor local to specific machinery could have occurred. Although spills would have been cleaned up, some residual oils could have penetrated the surface of the concrete. There are no records of the volumes of spills, but a visual survey of the condition of levels 1 to 3 of Regions 1 and 2 of the SGHWR building was carried out in August 2018 and samples of surface concrete were taken in 2013 for analysis, which included mineral oil (section 3.1.2, Table 606/10).

Magnox (2020c) states that the mineral oil used in SGHWR was Castrol Hyspin AWS 32™, and based on the extent of staining surveyed, the oil volume per unit area of oil stain reported in published literature and the density of oil, the following estimates have been made (Magnox, 2020c):

- Volume of oil remaining in the concrete = 78,840 ml; and
- Oil mass remaining in the concrete = 68.6 kg.

Magnox, 2020c states that it is assumed there is "*no significant oil contamination in the above ground part of the SGHWR that will be used as backfill for the below ground structure*". Any significant oil contamination in the above ground structure will be removed or segregated during demolition.

An additional investigation to characterise the oil staining was undertaken by Magnox in 2023. Concrete chips were taken from the floor of Levels 1-3 in SGHWR at 15 locations. The approach and methodology are outlined in NRS (2024d). Analysis of the concrete chips was undertaken and presented in NRS (2024d) and summarised in Table 606/18. As part of the 2023 Magnox investigation a visual inspection was undertaken for the presence of oil staining over the whole SGHWR structure. NRS (2024d) concluded that whilst surface oil staining was observed to be present in levels 1 to 3, the survey of levels 4 to 10 "*identified only very localised oil contamination on the floors and walls. This oil contamination is easily accessible, and it is assumed therefore that it will be removed prior to demolition"*.

A survey has been carried out to identify oil spills in Dragon Reactor (Magnox, 2021b). Only three small oil stains, each covering less than 1 m^2, were identified in the surveyed areas. Magnox (2021b) states that during future activity to decontaminate the Dragon reactor building prior to demolition, any identified oil surface contamination will be removed. Surface oil contamination will therefore not be included in the assessment inventory of the Dragon reactor.

Table 606/18: Organic Concentrations (mg/kg) in Concrete Chips from the SGHWR (from NRS, 2024d)

	Unit	L220511-2 D60/124/OIL/F LOOR CH	L220511-4 D60/124/OIL/F LOOR CH	L220511-6 D60/240/OIL/F LOOR CH	L220511-8 D60/240/OIL/F LOOR CH	L220511-10 D60/240/NO OIL/FLOO	L220511-12 D60/242/OIL/F LOOR C	L220511-14 D60/242/OIL/F LOOR C	L220511-16 D60/243/OIL/F LOOR C	L220511-18 D60/243/OIL/F LOOR C	L220511-20 D60/321/OIL/F LOOR C	L220511-22 D60/321/OIL/F LOOR C	L220511-24 D60/326/OIL/F LOOR C	L220511-26 D60/326/OIL/F LOOR C	L220511-28 D60/329/OIL/F LOOR C	L220511-31 D60/329/OIL/F LOOR C	Min	Max	Mean	UCL 95 of Mean
Benzene	µg/kg	<10	<10	<10	<10	<10	<10	<10	<10	<10	<10	<10	<10	<10	<10	<10	N/A	N/A	5.0	5.0
Ethylbenzene	µg/kg	<10	<10	<10	<10	<10	<10	<10	<10	<10	<10	<10	<10	<10	<10	<10	N/A	N/A	5.0	5.0
m/p-Xylene	µg/kg	<20	<20	<20	<20	<20	<20	<20	<20	<20	<20	26	26	<20	<20	<20	26	26	12.1	15.3
o-Xylene	µg/kg	<10	<10	<10	18	<10	11	<10	<10	<10	13	110	<10	23	<10	<10	11	110	15.0	29.9
Toluene	µg/kg	<10	<10	<10	<10	<10	<10	<10	<10	<10	<10	<10	<10	<10	<10	<10	N/A	N/A	5.0	5.0
>C6-C10	mg/kg	9.28	1.81	<0.200	3.75	<0.200	4.23	2.85	0.712	<0.200	6.34	14.5	3.01	4.86	1.61	4.45	0.71	14.5	3.8	6.0
>C6-C8 Aliphatic	mg/kg	<0.200	<0.200	<0.200	<0.200	<0.200	<0.200	<0.200	<0.200	<0.200	<0.200	<0.200	<0.200	<0.200	<0.200	<0.200	N/A	N/A	0.1	0.1
>C7-C8 Aromatic	mg/kg	<0.010	<0.010	<0.010	<0.010	<0.010	<0.010	<0.010	<0.010	<0.010	<0.010	<0.010	<0.010	<0.010	<0.010	<0.010	N/A	N/A	0.01	0.01
>C8-C10 Aliphatic	mg/kg	9.17	1.77	<0.200	3.7	<0.200	4.17	2.81	0.689	<0.200	6.3	14.2	2.86	4.8	1.59	4.43	0.689	14.2	3.8	5.9
>C8-C10 Aromatic	mg/kg	<0.040	<0.040	<0.040	0.048	<0.040	0.041	<0.040	<0.040	<0.040	0.043	0.146	0.046	0.053	<0.040	<0.040	0.041	0.146	0.04	0.1
C5-C6 Aliphatic	mg/kg	<0.200	<0.200	<0.200	<0.200	<0.200	<0.200	<0.200	<0.200	<0.200	<0.200	<0.200	<0.200	<0.200	<0.200	<0.200	N/A	N/A	0.1	0.1
C5-C7 Aromatic	mg/kg	<0.010	<0.010	<0.010	<0.010	<0.010	<0.010	<0.010	<0.010	<0.010	<0.010	<0.010	<0.010	<0.010	<0.010	<0.010	N/A	N/A	0.0	0.01
Total GRO C5-C10	mg/kg	9.32	1.83	<0.200	3.78	<0.200	4.26	2.88	0.733	<0.200	6.36	14.5	3.06	4.89	1.63	4.48	0.733	14.5	3.9	6.0
Acenaphthene	mg/kg	<0.08	<0.08	<0.08	<0.08	<0.08	<0.08	<0.08	<0.08	<0.08	<0.08	<0.08	<0.08	<0.08	<0.08	<0.08	N/A	N/A	0.04	0.04
Acenaphthylene	mg/kg	<0.08	<0.08	<0.08	<0.08	<0.08	<0.08	<0.08	<0.08	<0.08	<0.08	<0.08	<0.08	<0.08	<0.08	<0.08	N/A	N/A	0.04	0.04
Anthracene	mg/kg	<0.08	<0.08	<0.08	<0.08	<0.08	<0.08	<0.08	<0.08	<0.08	<0.08	<0.08	<0.08	<0.08	<0.08	<0.08	N/A	N/A	0.04	0.04
Benzo[a]anthracene	mg/kg	<0.08	<0.08	<0.08	<0.08	<0.08	<0.08	<0.08	<0.08	<0.08	<0.08	<0.08	<0.08	<0.08	<0.08	<0.08	N/A	N/A	0.04	0.04
Benzo[a]pyrene	mg/kg	<0.08	<0.08	<0.08	<0.08	<0.08	<0.08	<0.08	<0.08	<0.08	<0.08	<0.08	<0.08	<0.08	<0.08	<0.08	N/A	N/A	0.04	0.04
Benzo[b]fluoranthene	mg/kg	<0.08	<0.08	<0.08	<0.08	<0.08	<0.08	<0.08	<0.08	<0.08	<0.08	<0.08	<0.08	<0.08	<0.08	<0.08	N/A	N/A	0.04	0.04
Benzo[g,h,i]perylene	mg/kg	<0.08	<0.08	<0.08	<0.08	<0.08	<0.08	<0.08	<0.08	<0.08	<0.08	<0.08	<0.08	<0.08	<0.08	<0.08	N/A	N/A	0.04	0.04
Benzo[k]fluoranthene	mg/kg	<0.08	<0.08	<0.08	<0.08	<0.08	<0.08	<0.08	<0.08	<0.08	<0.08	<0.08	<0.08	<0.08	<0.08	<0.08	N/A	N/A	0.04	0.04
Chrysene	mg/kg	<0.08	<0.08	<0.08	<0.08	<0.08	<0.08	<0.08	<0.08	<0.08	<0.08	<0.08	<0.08	<0.08	<0.08	<0.08	N/A	N/A	0.04	0.04
Dibenzo[a,h]anthracene	mg/kg	<0.08	<0.08	<0.08	<0.08	<0.08	<0.08	<0.08	<0.08	<0.08	<0.08	<0.08	<0.08	<0.08	<0.08	<0.08	N/A	N/A	0.04	0.04
Fluoranthene	mg/kg	<0.08	<0.08	0.12	<0.08	<0.08	<0.08	<0.08	<0.08	<0.08	<0.08	<0.08	<0.08	<0.08	0.27	0.09	0.09	0.27	0.1	0.1
Fluorene	mg/kg	<0.08	<0.08	<0.08	<0.08	<0.08	<0.08	<0.08	<0.08	<0.08	<0.08	<0.08	<0.08	<0.08	<0.08	<0.08	N/A	N/A	0.04	0.04

	Unit	L220511-2 D60/124/OIL/F LOOR CH	L220511-4 D60/124/OIL/F LOOR CH	L220511-6 D60/240/OIL/F LOOR CH	L220511-8 D60/240/OIL/F LOOR CH	L220511-10 D60/240/NO OIL/FLOO	L220511-12 D60/242/OIL/F LOOR C	L220511-14 D60/242/OIL/F LOOR C	L220511-16 D60/243/OIL/F LOOR C	L220511-18 D60/243/OIL/F LOOR C	L220511-20 D60/321/OIL/F LOOR C	L220511-22 D60/321/OIL/F LOOR C	L220511-24 D60/326/OIL/F LOOR C	L220511-26 D60/326/OIL/F LOOR C	L220511-28 D60/329/OIL/F LOOR C	L220511-31 D60/329/OIL/F LOOR C	Min	Max	Mean	UCL 95 of Mean
Indeno[1,2,3-cd]pyrene	mg/kg	<0.08	<0.08	<0.08	<0.08	<0.08	<0.08	<0.08	<0.08	<0.08	<0.08	<0.08	<0.08	<0.08	<0.08	<0.08	N/A	N/A	0.04	0.04
Naphthalene	mg/kg	0.66	0.14	<0.08	0.23	<0.08	0.27	0.16	<0.08	0.12	<0.08	0.11	0.23	0.25	0.21	0.22	0.11	0.7	0.2	0.3
Phenanthrene	mg/kg	0.14	0.08	0.36	0.1	<0.08	0.09	0.11	<0.08	0.19	<0.08	0.1	0.09	0.13	0.24	0.12	0.1	0.36	0.1	0.2
Pyrene	mg/kg	<0.08	<0.08	<0.08	<0.08	<0.08	<0.08	<0.08	<0.08	<0.08	<0.08	<0.08	<0.08	<0.08	0.18	<0.08	0.18	0.18	0.05	0.1
Total PAH 16	mg/kg	1.92	1.34	1.6	1.45	1.28	1.48	1.39	1.28	1.42	1.28	1.33	1.44	1.5	1.86	1.48	1.28	1.92	1.5	1.6
>C10-C12 (Aliphatic)	mg/kg	5.28	6.56	15.1	7.73	<4.00	<4.00	<4.00	<4.00	11.5	<4.00	15	6.8	7.09	9.44	5.5	5.28	15.1	6.7	9.2
>C12-C16 (Aliphatic)	mg/kg	25.5	31.1	9.57	16.2	<4.00	10.4	7.03	8.4	29.3	4.3	35.4	20.2	25.1	<4.00	<4.00	4.3	35.4	15.2	21.7
>C16-C21 (Aliphatic)	mg/kg	36	31.9	79.7	142	<4.00	133	98.5	13.9	31.6	4.99	98.5	208	251	22.6	9.75	4.99	251	77.6	120.4
>C21-C35 (Aliphatic)	mg/kg	400	799	2890	3650	125	4250	3130	73.9	680	15.6	1210	4910	5770	604	208	15.6	5770.0	1914.4	3013.2
>C35-C44 (Aliphatic)	mg/kg	220	332	643	433	26.4	956	673	17.4	142	<6.00	210	951	1110	93.1	37.5	17.4	1110.0	417.5	638.1
Total TPH >C8-C40 (Aliphatic)	mg/kg	627	1110	3460	4140	150	5090	3730	114	858	29	1510	5850	6880	712	252	29	6880	2300.8	3593.9
>C10-C12 (Aromatic)	mg/kg	53.3	14	6.21	23.1	<4.00	23.7	8.61	9.67	45.9	7.16	358	14.1	28.7	29.2	25.6	6.2	358	43.3	92.2
>C12-C16 (Aromatic)	mg/kg	5.03	4.66	8.69	28.1	<4.00	17.8	<4.00	15.4	41.7	10.6	78.1	26.3	14.2	9.12	5.17	4.66	78.1	17.9	29.0
>C16-C21 (Aromatic)	mg/kg	17.3	15.4	34	35.3	<4.00	45.2	21.6	24.3	21.7	12.2	271	44.7	41.5	84.3	55.4	12.2	271	48.4	84.3
>C21-C35 (Aromatic)	mg/kg	366	298	1190	673	38.9	1110	853	332	369	708	84900	928	1350	1030	218	38.9	84900	6290.9	18335.8
>C35-C44 (Aromatic)	mg/kg	88.7	139	327	168	12.8	476	318	473	375	23.5	505	377	451	1740	153	12.8	1740	375.1	604.2
Total TPH >C8-C40 (Aromatic)	mg/kg	550	439	1460	893	59.5	1530	1110	635	691	757	86500	1270	1760	2110	391	59.5	86500	6677.0	18909.8

Note a) Where concentration is reported as less than the laboratory limit of detection (LOD), the mean and the UCL95 of the mean concentration has been calculated using a value of half the LOD. b) N/A signifies that the maximum and minimum cannot be presented as all results are <LOD

3.1.5 DESCRIPTION OF AVAILABLE DATA RELATING TO ASBESTOS WITHIN THE SGHWR AND DRAGON REACTOR COMPLEX STRUCTURES

Magnox (2019e) describes the characteristics of asbestos in the structural components to be retained in-situ in the SGHWR End State. Magnox plans to remove all traces of asbestos from the Dragon reactor complex prior to demolition.

It is long established that the process of filtration prevents migration of asbestos fibres in porous media such as soils (for example Gronow, 1986). A measure of the low risk to groundwater posed by asbestos is the absence of an asbestos drinking water standard in the UK. Likewise, the World Health Organisation (WHO) has not set a guideline value for asbestos in drinking water (WHO, 2017). It is therefore concluded that there is no requirement to develop an assessment inventory for asbestos.

3.1.6 DESCRIPTION OF AVAILABLE DATA RELATING TO PAINT WITHIN THE SGHWR STRUCTURE

Paint has been used to protect structural steel from corrosion and surfaces such as floors are painted. Paint has been, and will continue to be, removed from surfaces, but it is inevitable that a small mass of paint will be present in the disposals.

A sample of paint scrapings from the secondary containment of the SGHWR has been analysed. Results of analysis for metals and hydrocarbon compounds are presented in Table 606/19 and the results of a leach test are presented in Table 606/20. Whilst the material will not be sentenced for acceptance in an inert landfill, comparison of the results in Table 606/20 with WAC has been carried out to provide context to the results. The component emission values exceed the WAC for antimony, cadmium, lead, selenium, zinc and sulphate. The phenol index, dissolved organic carbon and total dissolved solids results, also exceed the WAC.

Table 606/19: Results of Analysis of a Sample of Paint Scrapings from the SGHWR (GAU, 2022)

Analyte	Conc. (mg/kg dry weight)[a]	Analyte	Conc. (mg/kg dry weight)[a]	Analyte	Conc. (mg/kg dry weight)[a]
Arsenic	<4.0	PAH (total)	2.4	TPH (total C10-C40)	4710
Antimony	3	Naphthalene	<0.10	TPH aromatic (C8-C10)	5400
Barium	2510	Acenaphthylene	<0.10	TPH aromatic (C10-C12)	196
Cadmium	1.8	Acenaphthene	<0.10	TPH aromatic (C12-C16)	198
Chromium (total)	6	Fluorene	<0.10	TPH aromatic (C16-C21)	1020
Cobalt	208	Phenanthrene	0.67	TPH aromatic (C21-C40)	1310
Copper	15	Anthracene	0.61	TPH aliphatic (C8-C10)	825
Mercury	<0.2	Fluoranthene	0.44	TPH aliphatic (C10-C12)	71.4
Molybdenum	<1	Pyrene	0.19	TPH aliphatic (C12-C16)	138

Analyte	Conc. (mg/kg dry weight)[a]	Analyte	Conc. (mg/kg dry weight)[a]	Analyte	Conc. (mg/kg dry weight)[a]
Nickel	4	Benz(a)anthracene	<0.10	TPH aliphatic (C16-C21)	561
Lead	3180	Chrysene	0.13	TPH aliphatic (C21-C40)	1210
Selenium	<1	Benzo(b)fluoranthene	<0.10		
Thallium	<0.5	Benzo(k)fluoranthene	<0.10		
Vanadium	<5	Benzo(a)pyrene	<0.10		
Zinc	1090	Dibenz(a,h)anthracene	0.13		
		Benzo(g.h.i)perylene	<0.10		
		Ideno(1,2,3-c,d)pyrene	<0.10		

Note a) 17.8% of the sample >2mm was not digested before analysis

Table 606/20: Results of Leach Testing of a Sample of Paint Scrapings from the SGHWR (GAU, 2022)

Analyte	Concentration (mg/kg dry weight unless stated) from whole sample analysis	Analyte	Concentration (mg/kg dry weight unless stated) in leachate following one stage batch leaching at a liquid to solid ratio of 10 l/kg
Mineral oil (C10-C40)	4710	Arsenic	<0.1
Loss on ignition (%)	30.9	Antimony	0.35
Total organic carbon (%)	23.7	Barium	<2.0
BTEX	<1.0	Cadmium	0.30
PCBs (7 congeners)	<1.0	Chromium (total)	<0.5
PAH compounds	2.4	Copper	<0.5
%water (105 °C)	13.0	Lead	20.9
% of material >4mm	3.2	Mercury	<0.01
		Molybdenum	<0.5
		Nickel	0.2
		Selenium	0.2
		Zinc	126
		Sulphate	3150
		Fluoride	<3.0
		Chloride	249

Analyte	Concentration (mg/kg dry weight unless stated) from whole sample analysis	Analyte	Concentration (mg/kg dry weight unless stated) in leachate following one stage batch leaching at a liquid to solid ratio of 10 l/kg
		Phenol index	204
		pH (pH units)	5.07
		Total dissolved solids	7960
		Dissolved organic carbon	94600

Samples of ten concrete cores of floors of Levels 1 to 3 of the SGHWR were analysed for PCB congeners and the results are reported in NRS (2024d). Since PCB congeners were identified in samples with and without oil staining and in some samples no PCB congeners were detected, it has been deduced that the PCB congeners are part of the floor paint on the samples. The analysis was not of the paint alone, but of each concrete core remaining following radiological analysis. The laboratory reported concentrations do not therefore relate to paint, but the range of concentrations summarised in Table 606/21 indicate the relative concentrations of analysed PCB congeners.

Table 606/21: Summary of Results of Analysis of Concrete Cores from the SGHWR for PCB Congeners of Leach Testing of a Sample of Paint Scrapings from the SGHWR (GAU, 2022)

Analyte	Minimum Concentration (µg/kg dry weight)[a]	Median Concentration (µg/kg dry weight)[b]	Maximum Concentration (µg/kg dry weight)[b]
PCB 28	<1	9.4	50
PCB 52	<1	15	57
PCB 101	<1	42	670
PCB 118	<1	16	160
PCB 138	<1	50	4400
PCB 153	<1	50	4900
PCB 180	<1	53	6700

Note a) The sample in which the minimum concentration was reported is interpreted to have not been painted.

Note b) Median and maximum concentrations have been calculated by halving the laboratory reported concentrations below the limit of detection.

Table 606/21 shows a bias towards the heavier PCB congeners in the paint.

3.1.7 DESCRIPTION OF AVAILABLE DATA RELATING TO FIBREGLASS WITHIN THE SGHWR STRUCTURE

The six fuel ponds located towards the eastern end of the turbine hall of the SGHWR are constructed from concrete and were lined with fibreglass in the 1960s. A Best Available Technique (BAT) report about disposal of the fibreglass has been prepared (Magnox, 2018) and forms the basis for all information in this sub-section.

Fibreglass comprises a fibre-reinforced polymer composite material, in which silica glass fibres are encapsulated within a thermosetting plastic such as epoxy/phenolic resin[12]. The fibreglass in the fuel ponds was primarily applied to provide containment of the water used for storage of the nuclear fuel. The pond liners will be disposed of in-situ within the SGHWR in line with the outcome of Magnox (2018).

The base of the ponds is at 29 m AOD and the ground level at the east end of the turbine hall is approximately 41 m AOD. The lining of the ponds covers an area of 2,477 m^2. The lining is up to 3 mm thick (email from Magnox, 12 April 2021) in places and has been removed in some areas during the pond decontamination process. If the lining is 3 mm thick on average, then the total fibreglass lining volume is 7.43 m^3. This is equivalent to approximately 14.5 tonnes of the glass-polymer composite material if the material is assumed to have a specific gravity of approximately 1,950 kg/m^3.

Epoxy resin is commonly prepared from epichlorohydrin and bisphenol-A, in the presence of a sodium hydroxide catalyst, to produce the diglycidyl ether of bisphenol-A. Di-amines are frequently used as the curing agents. The resins are manufactured with a wide range of molecular weights, but the use of epoxy resins in the production of fibreglass usually requires a low molecular weight, low-viscosity resin to ensure complete penetration of the woven fibre component.

The glass fibre component is expected to be a silica-based glass with additional calcium, magnesium and sodium, and possibly boron.

3.1.8 DESCRIPTION OF AVAILABLE DATA RELATING TO REBAR QUANTITIES AND COMPOSITION

Magnox completed a study of the quantities and composition of the rebar that is likely to remain in the SGHWR and Dragon reactor buildings, either in the structure or in the concrete blocks derived from the above ground demolition of each facility. The volume, surface area, mass and composition of the rebar is presented in NRS (2024h) for the SGHWR and Dragon reactor and are reproduced in Table 606/22.

[12] Magnox drawing AE224250_F 'General Arrangement of External Active Sludge Holding Tanks' states, 'The inside of all sludge tanks to be lined with Epoxide/Phenolic type resin similar to that used on the ponds'.

Table 606/22: Properties of Rebar at the SGHWR and Dragon Reactor

Property	Unit	SGHWR Rebar Values	Dragon Reactor Rebar Values
Total volume	m^3	287	267
Total mass	kg	2,239,000	2,080,000
Total surface area	m^2	57,407	53,332
Proportion of iron	kg/kg	0.979	0.979
Proportion of carbon	kg/kg	0.004	0.004
Proportion of manganese	kg/kg	0.007	0.007
Proportion of copper	kg/kg	0.003	0.003
Proportion of nickel	kg/kg	0.002	0.002
Proportion of silicon	kg/kg	0.003	0.003
Proportion of chromium	kg/kg	0.002	0.002
Proportion of phosphorus	kg/kg	0.0004	0.0004
Proportion of sulphur	kg/kg	0.0005	0.0005

3.1.9 DESCRIPTION OF AVAILABLE DATA RELATING TO STRUCTURAL STEEL QUANTITIES AND COMPOSITION

Magnox completed studies of the quantities and composition of the structural steel that is likely to remain in the SGHWR and Dragon reactor End States. The volume, surface area, mass and composition of the steel is presented in NRS (2024h) for the SGHWR and Dragon reactor buildings and are reproduced in Table 606/23.

Table 606/23: Properties of Structural Steel at the SGHWR and Dragon Reactor

Property	Unit	SGHWR I-Beam Values	Dragon Reactor Structural Steel Values[a]
Total volume	m^3	127	40
Total mass	kg	993,000	312,000
Total surface area	m^2	5,100	1,641
Proportion of iron	kg/kg	0.99	0.99
Proportion of carbon	kg/kg	0.0025	0.0025
Proportion of manganese	kg/kg	0.006	0.006
Proportion of copper	kg/kg	Reported as 0	Reported as 0
Proportion of nickel	kg/kg	Reported as 0	Reported as 0

Property	Unit	SGHWR I-Beam Values	Dragon Reactor Structural Steel Values[a]
Proportion of silicon	kg/kg	0.0005	0.0005
Proportion of chromium	kg/kg	Reported as 0	Reported as 0
Proportion of phosphorus	kg/kg	0.0004	0.0004
Proportion of sulphur	kg/kg	0.0005	0.0005

Note a) Assumed to include the steel shell of the Dragon reactor adjacent to Wall C.

3.2 DEVELOPMENT OF AN ASSESSMENT INVENTORY FOR DISPOSALS/DEPOSITS

3.2.1 DEMOLITION ARISINGS

Arisings generated by the demolition of the above ground SGHWR and Dragon reactor structures will be deposited/disposed of in the voids in the below ground structures supplemented with stockpiled arisings from previous demolition activities elsewhere on the Winfrith site.

The above ground structure at the SGHWR includes a steel-clad metal frame, and masonry and concrete internal structures. The metal frame and cladding will be removed, and the masonry and concrete will be mechanically broken. It is assumed that the rebar will be removed and will not form part of the disposals/deposits.

The D630 stockpiles analysis will be used to derive an assessment inventory for the disposals/deposits for both the SGHWR and Dragon reactor End States. The D630 stockpiles and the above ground SGHWR and Dragon structures contain both concrete and brick in differing proportions.

There is a higher proportion of concrete in the SGHWR and Dragon demolition material than the D630 stockpiles, as set out below taken from an email from Magnox dated 29 September 2020:

- The estimated proportion of brick in the existing D630 stockpiles is 19-30%. The concrete content is therefore, by extension, 70-81%;
- The proportion of brick in the above ground SGHWR structure is about 13%. The concrete content is therefore approximately 87%; and
- The only brickwork present in the Dragon reactor structure is in a few small infill panels that are insignificant in volume compared to the rest of the structure to be demolished. After the non-structural steel has been removed, the demolition arisings from the Dragon reactor will, therefore, comprise mainly concrete. It will be assumed that the demolition material derived from the Dragon reactor above ground structure will be 100% concrete.

The degree to which the concrete and the brick components contribute to the inorganic contaminant concentrations reported for the D630 stockpiles is uncertain. Brick is chemically stable. In using the D630 stockpiles analysis to derive an inorganic contaminant assessment inventory for components of the End States other than stockpiled material, account must be taken of the possibility that the inorganic contaminants are present predominantly within the stockpiled concrete and not the brick. Because the arisings generated by demolition of the above ground parts of the SGHWR and Dragon

reactor buildings will contain a higher proportion of concrete than the stockpiled material, it is conservative to assume the brick does not contribute to the inorganic contaminant concentrations in the stockpile. The reported inorganic contaminants in the stockpiles analysis are assumed to be associated solely with the concrete. The reported concentrations of inorganic contaminants in the stockpiled material will therefore be increased to account for the proportion of brick before they are used to represent the concentrations of inorganic contaminants in the demolition arisings generated in-situ.

According to the proportions set out above, the proportion by mass of concrete in the SGHWR demolition material will be up to 24% higher[13] than in the D630 stockpiles. Therefore, conservatively assuming the entire inventory in the D630 stockpiles is contained in the concrete, the concentrations of inorganic contaminants in demolition arisings from the SGHWR could be up to 24% higher than those reported in Table 606/11 for the D630 stockpiles material.

Likewise, the proportion by mass of concrete in the Dragon reactor demolition material will be up to 43% higher[14] than in the D630 stockpiles. Therefore, conservatively assuming the entire inventory in the D630 stockpiles is contained in the concrete, the concentration of inorganic contaminants in demolition arisings from the Dragon reactor could be up to 43% higher than those reported in Table 606/11 for the D630 stockpiles material.

For the purposes of simplicity, the inorganic contaminant concentrations in the stockpiles will be increased by 24% to describe the inorganic contaminant concentrations in the demolition arisings derived from a mix of the above ground SGHWR structure and from the D630 stockpiles used to fill SGHWR. Likewise, for the Dragon reactor, the inorganic contaminant concentrations in the stockpiles will be increased by 43% to describe the inorganic contaminant concentrations in the infill (both demolition arisings derived from the above ground Dragon reactor structure and from the D630 stockpiles). These are the theoretical highest inorganic contaminant concentrations that could occur due to the increased proportion of concrete and are therefore conservative. Adopting this approach negates the need to make an assumption about the degree to which brick contributes to the inorganic contaminant concentrations reported for the D630 stockpiles, and the amount of the D630 stockpiles material that will need to be used in both the SGHWR and Dragon reactor disposals/deposits.

With respect to organic contaminants, it is assumed that the same amount of foreign material containing PCB compounds, PAH compounds and TPH compounds in the D630 stockpiles could be generated in the demolition material of the above ground structures at the SGHWR and the Dragon reactor. The concentrations of PCBs and hydrocarbons from the stockpiles analysis will be applied without adjustment to derive a total inventory for the demolition arisings deposited in the SGHWR and Dragon reactor, whether they are derived from the above ground structure or the D630 stockpiles.

[13] If the proportion of concrete in the D630 stockpiles is 70% and in the above ground SGHWR structure is 87%, the proportion by mass of concrete in demolition arisings from the SGHWR will be 100*(87-70)/70 = 24% higher than in the D630 stockpiles material.

[14] If the proportion of concrete in the D630 stockpiles is 70% and in the above ground Dragon reactor structure is 100%, the proportion by mass of concrete in demolition arisings from Dragon reactor will be 100*(100-70)/70 = 43% higher than in the D630 stockpiles material.

Table 606/24 presents derived solid phase contaminant concentrations for the demolition material in the SGHWR and the Dragon reactor End States based on the existing stockpiles composition (with a 24% and 43% increase in inorganic contaminant concentrations, respectively).

The estimated volumes of demolition arisings that are presented in Table 606/7 and the leach test data from Table 606/12 allows calculation of a leachable (water available) inorganic contaminant mass for the SGHWR and Dragon reactor disposals/deposits once a liquid to solid ratio of 10:1 has been achieved. Table 606/25 presents the stockpiles leach test data with a 24% and 43% increase in leached inorganic contaminant concentrations for the SGHWR and the Dragon reactor, respectively.

There are no leach test data for the organic substances. The concentrations and masses of PCB congeners, hydrocarbon species and TPH fractions in Table 606/24 therefore represent the assessment inventory for organic substances. The following approach has been taken to develop the assessment inventory for organic substances:

- Organic substances which were not detected in the samples of stockpiled materials have been excluded from the assessment inventory. Examples of this are acenaphthene and >C5-C6 aliphatic compounds; and
- Laboratory error is highest where the concentration of a determinant in a sample is close to the method detection limit. Organic substances detected only on a single occasion and where the concentration was within an order of magnitude of the detection limit have been excluded from the assessment. Examples of these are benzene and toluene.

The calculated inventories of organic substances and metals rely on several assumptions, and they are therefore uncertain. Where calculated inventories are not demonstrably conservative (overestimates), the uncertainty is judged to be such that the inventory could not be more than a factor of two higher.

Table 606/24: Derived Solid Phase Contaminant Concentrations in Demolition Arisings to be Emplaced in the SGHWR and Dragon Reactor Basement Voids

Contaminant	UCL95 of Mean Total Concentration from D630 Stockpiles Analysis (mg/kg)	UCL95 of Mean Total Concentration Assumed for SGHWR Infill (24% Increase for Inorganic Contaminants) (mg/kg)	UCL95 of Mean Total Concentration Assumed for Dragon Reactor Infill (43% Increase for Inorganic Contaminants) (mg/kg)
Antimony	1.1	1.4	1.6
Arsenic	6.7	8.4	9.6
Barium	601	747	859
Cadmium	0.7	0.8	0.9
Chromium	22	27	31
Copper	25	31	36
Lead	208	259	298
Mercury	0.5	0.6	0.7

Contaminant	UCL95 of Mean Total Concentration from D630 Stockpiles Analysis (mg/kg)	UCL95 of Mean Total Concentration Assumed for SGHWR Infill (24% Increase for Inorganic Contaminants) (mg/kg)	UCL95 of Mean Total Concentration Assumed for Dragon Reactor Infill (43% Increase for Inorganic Contaminants) (mg/kg)
Molybdenum	1.7	2.1	2.4
Nickel	18	22	25
Selenium	1.5	1.9	2.1
Zinc	124	154	177
PCB-101	0.10	0.10	0.10
PCB-118	0.07	0.07	0.07
PCB-138	0.12	0.12	0.12
PCB-153	0.09	0.09	0.09
PCB-180	0.06	0.06	0.06
PCB-28	0.02	0.02	0.02
PCB-52	0.02	0.02	0.02
Acenaphthylene	0.05	0.05	0.05
Phenanthrene	0.18	0.18	0.18
Anthracene	0.09	0.09	0.09
Fluoranthene	0.44	0.44	0.44
Pyrene	0.53	0.53	0.53
Benzo(a)anthracene	0.31	0.31	0.31
Chrysene	0.35	0.35	0.35
Benzo(bk)fluoranthene	0.77	0.77	0.77
Benzo(a)pyrene	0.51	0.51	0.51
Indeno(123cd)pyrene	0.44	0.44	0.44
Dibenzo(ah)anthracene	0.09	0.09	0.09
Benzo(ghi)perylene	0.5	0.5	0.5
Benzo(b)fluoranthene	0.56	0.56	0.56
Benzo(k)fluoranthene	0.22	0.22	0.22

Contaminant	UCL95 of Mean Total Concentration from D630 Stockpiles Analysis (mg/kg)	UCL95 of Mean Total Concentration Assumed for SGHWR Infill (24% Increase for Inorganic Contaminants) (mg/kg)	UCL95 of Mean Total Concentration Assumed for Dragon Reactor Infill (43% Increase for Inorganic Contaminants) (mg/kg)
>C12-C16 aliphatic	4.06	4.06	4.06
>C16-C21 aliphatic	14.29	14.29	14.29
>C21-C35 aliphatic	77.75	77.75	77.75
>C35-C44 aliphatic	32.04	32.04	32.04
>EC16-EC21 aromatic	5.28	5.28	5.28
>EC21-EC35 aromatic	67.09	67.09	67.09
>EC35-EC44 aromatic	22.48	22.48	22.48
MTBE	0.0038	0.0038	0.0038
m/p-Xylene	0.0083	0.0083	0.0083
o-Xylene	0.0071	0.0071	0.0071

Table 606/25: Derived Leachable Contaminant Concentrations for Demolition Arisings to be Deposited in the SGHWR and Dragon Reactor Basement Voids, assuming L:S Ratio of 10:1

Contaminant	UCL95 of Mean Leachable Concentration from D630 Stockpiles Analysis at LS10 (mg/kg)	UCL95 of Mean Leachable Concentration Assumed for SGHWR Infill (24% Increase) (mg/kg)	UCL95 of Mean Leachable Concentration Assumed for Dragon Reactor Infill (43% Increase) (mg/kg)
Antimony	0.01	0.016	0.0188
Arsenic	0.02	0.019	0.022
Barium	0.82	1.02	1.18
Cadmium	0.00010	0.00012	0.00014
Chromium	0.15	0.19	0.22
Copper	0.04	0.05	0.06
Lead	0.008	0.010	0.011
Mercury	0.00047	0.00058	0.00067
Molybdenum	0.015	0.019	0.022

Contaminant	UCL95 of Mean Leachable Concentration from D630 Stockpiles Analysis at LS10 (mg/kg)	UCL95 of Mean Leachable Concentration Assumed for SGHWR Infill (24% Increase) (mg/kg)	UCL95 of Mean Leachable Concentration Assumed for Dragon Reactor Infill (43% Increase) (mg/kg)
Nickel	0.01	0.016	0.018
Selenium	0.0033	0.0042	0.0048
Zinc	0.13	0.16	0.18
Fluoride	1.9	2.4	2.8
Chloride	14.7	18.3	21.0
Sulphate	461	573	659

3.2.2 CONCRETE BLOCKS

It is assumed that the inorganic contaminants (excluding hydroxide) within the fabric of the concrete blocks are of sufficiently low mobility and/or they are released so slowly as the cement of the blocks dissolves over millennia (section 5.1.3) that they do not pose a risk to groundwater quality. This assumption will be tested by the HRA. On this basis an assessment inventory associated with inorganic contaminants in the concrete blocks is not developed.

3.3 ASSESSMENT INVENTORY ASSOCIATED WITH THE REMAINING STRUCTURES

3.3.1 FIBREGLASS

It is assumed that potential contaminants within the fibreglass have sufficiently low mobility that they do not pose a risk to groundwater quality. This assumption will be tested by the HRA. On this basis there is no water available inventory present in the fibreglass and an assessment inventory is not developed.

3.3.2 CONCRETE STRUCTURE

It is assumed that the inorganic contaminants (including hydroxide) within the fabric of the concrete structure have sufficiently low mobility and/or they are released so slowly as the cement of the structural concrete dissolves over millennia (section 5.1.3) that they do not pose a risk to groundwater quality. This assumption will be tested by the HRA. On this basis there is no water available inventory associated with inorganic contaminants in the concrete structure and therefore no assessment inventory is developed.

3.3.3 OIL CONTAMINATION ON SURFACES

Table 606/26 presents derived total mass of each organic contaminant detected on one or more occasions in oil-stained concrete as presented in Table 606/18. This assessment inventory only applies to SGHWR Regions 1 and 2 levels 1-3 as these are the levels where the oil staining is observed.

Magnox (2020c) states that the oil penetration depth is uncertain, and NRS (2024d) assumes it is 10 mm. A scoping calculation of the degree of saturation of the pore space with oil has been prepared to assess the validity of this assumption:

- Magnox (2020c) describes an experimental oil spread of 40 ml of oil on concrete. After one and a half days the surface area of the oil spread was measured to be 1,370 cm^2. This is equivalent to 0.03 ml/cm^2 of oil.
- On the basis the assumed porosity of the concrete is 15% v/v, the total pore volume of a 1 cm^2 area and 10 mm thick portion of the structural concrete in the SGHWR End State is 0.15 ml.
- Therefore, assuming a 10 mm penetration depth, the 0.03 ml/cm^2 of oil derived by the experiment would occupy 20% of the pore space in the concrete.

Saturation of 20% of the pore space with oil is credible and the 10 mm penetration depth assumption is therefore considered reasonable.

The estimated mass in Table 606/26 assumes a surface area of oil of 270 m^2 (Magnox, 2020c), a penetration depth of 0.01 m (cautious estimate based on Magnox, 2020c) and a concrete density of 2,400 kg/m^3 (between that of SKB, 2001a and SKB, 2014).

Table 606/26: Assessment Inventory for Oils in the SGHWR Structure

Contaminant	UCL 95 of Mean (mg/kg)	Derived Inventory Mass (Kg)
m/p-Xylene	0.015	0.00010
o-Xylene	0.030	0.00019
>C8-C10 Aliphatic	5.91	0.038
>C8-C10 Aromatic	0.055	0.00036
Fluoranthene	0.10	0.00064
Naphthalene	0.27	0.0018
Phenanthrene	0.17	0.0011
Pyrene	0.069	0.00045
>C10-C12 (Aliphatic)	9.2	0.059
>C12-C16 (Aliphatic)	22	0.14
>C16-C21 (Aliphatic)	120	0.78
>C21-C35 (Aliphatic)	3013	20
>C35-C44 (Aliphatic)	638	4.1
>C10-C12 (Aromatic)	92	0.60
>C12-C16 (Aromatic)	29	0.19
>C16-C21 (Aromatic)	84	0.55
>C21-C35 (Aromatic)	18336	119
>C35-C44 (Aromatic)	604	3.9

3.4 ASSESSMENT INVENTORY FOR METALS

The assessment inventory for metals refers to all metal, either as rebar or a separate structural element that will be left in the structures at the End State.

3.4.1 REBAR

The mass of rebar and the relative proportions of different constituents in the rebar are presented in section 3.1.8. Values are available for both the SGHWR and the Dragon reactor structures. The derived assessment inventory expressed as a total contaminant mass is presented in Table 606/27 and is based on multiplication of the total mass of rebar by the relative proportion of the constituents within the rebar. The contaminants and masses in Table 606/27 represent the assessment inventory for rebar with the exception of silicon and carbon. Carbon and silicon are not groundwater contaminants, and they are therefore not part of the assessment inventory.

Table 606/27: Assessment Inventory of Rebar in Concrete in the Remaining SGHWR and Dragon Reactor Structures

Contaminant	Mass of Contaminant in SGHWR Rebar (kg)	Mass of Contaminant in Dragon Reactor Rebar (kg)
Iron	2,196,864	2,036,320
Carbon[a]	8,956	8,320
Manganese	15,672	14,560
Copper	6,717	6,240
Nickel	4,478	4,160
Silicon[a]	6,717	6,240
Chromium	4,478	4,160
Phosphorus[b]	896	832
Sulphur[b]	1,119	1,040

Note a) Carbon and silicon are not groundwater contaminants and they are therefore not part of the assessment inventory.

Note b) Phosphorus and sulphur will be assumed to be in the form of phosphate and sulphate in the assessment inventory.

3.4.2 STRUCTURAL STEEL

The mass of structural steel and the relative proportions of different constituents in the structural steel are presented in section 3.1.9 for both the SGHWR and Dragon reactor structures. The derived assessment inventory is presented in Table 606/28 and is based on multiplication of the total mass of structural steel by the relative proportion of the constituents within the structural steel. These values represent the total contaminant masses. The contaminants and masses in Table 606/28 represent the assessment inventory for structural steel except for silicon and carbon.

Table 606/28: Assessment Inventory of Structural Steel in the Remaining SGHWR and Dragon Reactor Structures

Contaminant	Total Inventory Mass for I-beam in SGHWR (kg)	Total Inventory Mass for Structural Steel in Dragon Reactor (kg)
Iron	982,818	308,880
Carbon[a]	2,482	780
Manganese	5,956	1,872
Copper	0 (Relative Proportion Reported to be 0)	0 (Relative Proportion Reported to be 0)
Nickel	0 (Relative Proportion Reported to be 0)	0 (Relative Proportion Reported to be 0)
Silicon[a]	496	156
Chromium	0 (Relative Proportion Reported to be 0)	0 (Relative Proportion Reported to be 0)
Phosphorus[b]	397	125
Sulphur[b]	496	156

Note a) Carbon and silicon are not groundwater contaminants and they are therefore not part of the assessment inventory.

Note b) Phosphorus and sulphur will be assumed to be in the form of phosphate and sulphate in the assessment inventory.

3.5 NON-RADIOLOGICAL INVENTORY ASSOCIATED WITH EMPLACED NON-WASTE MATERIALS

Other emplaced material that will be used in the infilling of the subsurface structures is expected to be predominantly grout used to backfill the Dragon reactor mortuary holes. Other sealants may also be used to fill cracks and small subsurface voids in both reactor structures. The grout and any sealants used will be commercially available products that are commonly used for subsurface work (for example decommissioning groundwater boreholes). On this basis there is no water available inventory associated with these materials and therefore no assessment inventory.

3.6 SUMMARY OF THE NON-RADIOLOGICAL ASSESSMENT INVENTORY

Table 606/29 summarises the contaminants in the non-radiological assessment inventory.

Table 606/29: Summary of the Contaminants in the Non-radiological Assessment Inventory for the SGHWR and Dragon Reactor End States

Contaminant	Demolition Arisings Generated In-situ and Imported from the Stockpile	Concrete Blocks Generated In-situ	Oil Staining of Concrete in Structures Remaining In-situ	Rebar in Structures Remaining In-situ	Structural Steel Remaining In-situ
Hydroxide (pH)	✓	✓			
Antimony	✓				
Arsenic	✓				
Barium	✓				
Cadmium	✓				
Chromium	✓			✓	
Copper	✓			✓	
Lead	✓				
Mercury	✓				
Molybdenum	✓				
Nickel	✓			✓	
Selenium	✓				
Zinc	✓				
Sulphate	✓			✓	✓
Fluoride	✓				
Chloride	✓				
Iron				✓	✓
Manganese				✓	✓
Phosphate				✓	✓
Naphthalene			✓		
Acenaphthylene	✓				

Contaminant	Demolition Arisings Generated In-situ and Imported from the Stockpile	Concrete Blocks Generated In-situ	Oil Staining of Concrete in Structures Remaining In-situ	Rebar in Structures Remaining In-situ	Structural Steel Remaining In-situ
Phenanthrene	✓		✓		
Anthracene	✓				
Fluoranthene	✓		✓		
Pyrene	✓		✓		
Benzo(a)anthracene	✓				
Chrysene	✓				
Benzo(bk)fluoranthene	✓				
Benzo(a)pyrene	✓				
Indeno(123cd)pyrene	✓				
Dibenzo(ah)anthracene	✓				
Benzo(ghi)perylene	✓				
Benzo(b)fluoranthene	✓				
Benzo(k)fluoranthene	✓				
>C8-C10 aliphatic			✓		
>C10-C12aliphatic	✓		✓		
>C12-C16 aliphatic	✓		✓		
>C16-C21 aliphatic	✓		✓		
>C21-C35 aliphatic	✓		✓		
>C35-C44 aliphatic	✓		✓		
>C8-C10 aromatic			✓		
>C10-C12 aromatic			✓		
>EC16-EC21 aromatic	✓		✓		
>EC21-EC35 aromatic	✓		✓		
>EC35-EC44 aromatic	✓		✓		

Contaminant	Demolition Arisings Generated In-situ and Imported from the Stockpile	Concrete Blocks Generated In-situ	Oil Staining of Concrete in Structures Remaining In-situ	Rebar in Structures Remaining In-situ	Structural Steel Remaining In-situ
MTBE	✓				
m/p-Xylene	✓		✓		
o-Xylene	✓		✓		
PCB-101	✓				
PCB-118	✓				
PCB-138	✓				
PCB-153	✓				
PCB-180	✓				
PCB-28	✓				
PCB-52	✓				

4 SUMMARY OF RADIOLOGICAL ASSESSMENT INVENTORY

This section develops an assessment inventory for the radiological PA.

The Winfrith End State radiological inventory report ('the radiological inventory report', NRS, 2024a) presents an estimate of the potential radiological inventory remaining on the Winfrith site at 2027, and has been used as the basis for the information presented in this section.

In the PA, the inventory will be used to assess the potential dose resulting from releases due to the natural evolution of the on-site disposals, and inadvertent human intrusion into such features. The inventory will also provide inputs to the optimisation process. Both uses require separate consideration of parts of the on-site disposal features. Therefore, in deriving the inventory, separate estimates have been made for components of the in-situ features that are distinctly different in radiological fingerprint, amount, or spatial extent of contamination or activation. For the SGHWR, features include the bioshield, mortuary tubes, primary containment, secondary containment, ponds and ancillary areas. For the Dragon reactor complex, features include the bioshield, reactor building, B78 floor slab and primary mortuary holes structure.

In the radiological inventory report, the reference activity estimate was built through detailed consideration of the operational history of the facilities, the mechanisms by which facility components may have become radioactive (i.e. neutron activation and/or radiological contamination), and review of the available characterisation and neutron activation modelling data. Where necessary, the inventory estimates have been developed using a number of assumptions, making use of other experience at Winfrith or elsewhere as appropriate.

There is limited information for some components and access limitations prevent sampling and characterisation at this time. It is anticipated that the End State radiological inventory report will be revised as necessary as additional characterisation and sampling data become available.

In addition, in order to account for current inventory uncertainties and to consider their potential impact on doses, alternative (more conservative) inventory estimates have been derived for each feature. The alternative inventory estimates consider the potential for higher activity (for example, using maximum, rather than average, characterisation data) but also aspects such as different contamination volumes and fingerprints, as appropriate based on the key feature-specific uncertainties.

The structure of this section is as follows:

- Section 4.1 describes the key radiological features of the SGHWR structure End State (including the basis for both reference and alternative inventory estimates), describes how the inventory associated with each component has been allocated to the four SGHWR regions (Regions 1 and 2, and the South and North Annexes) and presents the resulting radiological assessment inventory.
- Section 4.2 describes the key radiological features of the Dragon reactor complex End State (including the basis for both reference and alternative inventory estimates) and presents the radiological assessment inventory for each.
- Section 4.3 summarises the estimated radiological assessment inventory, and the key uncertainties and assumptions associated with the estimated inventory (these are reported in detail in NRS (2024a)).

4.1 SGHWR RADIOLOGICAL ASSESSMENT INVENTORY

A number of sources contributing to the SGHWR radioactive inventory remaining at the IEP have been identified, including activity derived from neutron activation of the reactor bioshield during reactor operation and activity resulting from surface contamination. The radiological inventory report (NRS, 2024a, §2.3) summarises the three main sources of contamination in the SGHWR:

- The reactor primary circuit was directly in contact with the fuel and was the primary heat transfer medium. The primary circuit was contaminated due to activation (^{60}Co and ^{63}Ni form the majority of the total fingerprint) and corrosion of the metal core components and transport through the circuit. The primary circuit also held a significant inventory of ^{137}Cs and tritium from fission products and activation of the light (ordinary) water coolant.
- The moderator circuit contained deuterated water (D_2O) during operation. Exposure to high neutron fluxes led to significant tritium and ^{14}C activities in the circuit during operations. Operational tritium levels were known to be in the region of 4 TBq/l.
- The ponds and fuel route had greater contact with spent fuel and therefore elevated alpha and ^{137}Cs contamination levels compared to other areas of the facility.

All contamination within the SGHWR facility originates from these areas. The contamination of any particular room in the SGHWR structure is dependent on the relative influence of the three contaminant sources and the processes undertaken. The rooms and features associated with the SGHWR radiological inventory were grouped in the radiological inventory report as follows:

- Bioshield;
- Mortuary tubes;
- Primary containment;
- Secondary containment;
- Ponds;
- Ancillary areas;
- SGHWR bulk structure; and
- Backfill.

No inventory associated with external areas of the SGHWR and SGHWR land contamination is captured in the radiological inventory report, which assumes that any such contamination, if present, will be removed or confirmed as OoS.

4.1.1 BIOSHIELD

The SGHWR bioshield is a reinforced concrete structure located on levels 1 to 3 (below ground) at the centre of the primary containment that enclosed the reactor core during reactor operation. The bioshield is 7.0 m high and its walls vary in thickness, from 4' (1.22 m) adjacent to the fuel storage ponds to 9’ 3” (2.82 m) adjacent to the liquid shut down plant room (where the bioshield combines with the primary containment wall (radiological inventory report, Table 2.7).

Characterisation data for the bioshield comprises data from two cores analysed in 2005 (including limited rebar samples) supported by neutron activation modelling (radiological inventory report, §2.10). The data for some radionuclides, particularly ^{60}Co, ^{14}C, ^{41}Ca, ^{152}Eu and ^{154}Eu, indicate a clear decreasing trend in activity in concrete away from the inside surface of the bioshield, consistent with a source from neutron activation. Beyond around 1 m from the inside bioshield surface, a clear activation trend in concrete becomes difficult to discern (NRS, 2024a, §2.10). Further into the core sample at just over 1.5 m, a rise in activity occurs for some determinands that

would not be expected due to activation, which corresponds to the location of a 1 inch 'flexcell' joint that essentially separates the bioshield from the surrounding primary containment structure.

Tritium also follows a decreasing trend outwards from the inside surface of the bioshield, albeit with a differing slope. However, ^{3}H is known to be mobile in concrete and to have deeply penetrated the SGHWR structure from contamination sources and so its presence may not therefore be solely attributable to in-situ activation.

The radiological inventory report (NRS, 2024a, §2.10) calculated the bioshield reference inventory assuming a uniform 1.55 m thick full-height cylindrical layer of activated concrete close to the core, contained within a simplified outer cuboid of contaminated concrete. Paint is assumed to cover all surfaces of the simplified geometry except the east and west faces, where the bioshield joins with the primary containment. Vertically the full bioshield height was assumed to be activated, although in practice the top and bottom received significant shielding and somewhat lower activities may be expected in these areas.

The alternative inventory for the bioshield was derived by scaling the activation inventory by a factor of 14.9 to bring it into line with activation modelling.

4.1.2 MORTUARY TUBES

Ten storage locations for irradiated items were provided in the construction phase of the SGHWR primary containment, referred to as the mortuary tubes. Each tube consists of a 'cast-in' liner approximately 0.2 m in diameter and runs from the top of the bioshield to 2.7 m below the bioshield into the east wall of the primary containment, where a 90° bend exits into Room 111. Although the items currently in the tubes will be removed during decommissioning and the tubes cleaned, it is expected that residual radioactivity will remain within the tube structures.

There is currently no characterisation data from the mortuary tubes as it is not possible to access them. However, the radiological inventory report (NRS, 2024a, §2.11) developed a high-level conservative estimate based on five potential sources for the residual activity in the mortuary tubes based on the items stored and the location of the tubes:

- contamination carried over from items that came from the reactor core;
- contamination carried over from items that may have been in contact with the moderator circuit;
- contamination carried over from items that came from the ponds;
- contamination arising from the degradation of activated stored items; and
- activation of the metal tubes themselves due to reactor neutron flux in the bioshield.

The potential activity from each source was considered separately and the total reference inventory is derived from the sum of all potential sources of activity. Each of the contamination activities was derived by scaling a suitable fingerprint to an activity which is expected to be limiting of the contamination present in the mortuary tubes.

The alternative inventory for the mortuary tubes was derived by applying an alternative fingerprint based on average modelled activation of Zircaloy fuel channel tubes.

4.1.3 PRIMARY CONTAINMENT

The SGHWR primary containment comprises a massive concrete structure with walls 1.2 to 1.5 m thick extending from level 1 to level 6 (NRS, 2024a, §2.12). It housed the reactor core and numerous support operations and processes, including steam drums, clean-up plant and electrical control. The bioshield and mortuary tubes lie within the primary containment, but due to their

differing radioactive characteristics (mainly activated rather than contaminated) they are described separately.

The primary containment was exposed to contamination due to operational leaks from liquid circuits. An octagonal sump in the basement of Room 111 (below ground level) that collected active effluent to feed to active drainage is a known area of contamination (NRS, 2024a, §2.12). Wall penetrations also provide potential pathways for the spread of contamination.

Analytical results from two primary containment characterisation campaigns in 2005 and 2019 were used in the radiological inventory report (NRS, 2024a, §2.12.2) to inform development of the reference inventory estimate. The primary containment contamination is assumed to penetrate 0.15 m into the concrete and 1 mm into paint layers. Using the calculated volumes of the differing height sections of the primary containment, the proportion of the contaminated structure remaining in-situ below ground is estimated to be 67%, with the remaining 33% contributing to the above ground demolition material (demolition arisings and concrete blocks) to be emplaced in the below ground void (NRS, 2024a, §2.12.3).

The alternative inventory for the primary containment was derived by using maximum activity concentration values to calculate the inventory, rather than average values as in the reference inventory.

4.1.4 SECONDARY CONTAINMENT

The secondary containment comprises a concrete structure extending from level 1 to level 9 that housed the turbine / alternator, emergency water supplies, additional circuit supplies, plantrooms, ponds complex, effluent facilities, waste processing areas, and workshop areas (NRS, 2024a, §2.13). Circuits / systems in the primary containment fed into the secondary containment, allowing the transfer of contamination to some areas.

General and ancillary areas within the secondary containment include the turbine floor, walkways, high level structures, vehicle loading areas, access and exit points, cable basements, steam labyrinth and significant parts of the North and South Annexes.

The SGHWR secondary containment comprises dozens of rooms and features, from contaminated waste processing rooms to stairwells and inactive stores. As a consequence, the SGHWR characterisation programme ranges from ‘no characterisation’ to ‘extensive characterisation’. The radiological inventory report (NRS, 2024a, §2.13.2) notes that data for level 4 and above is incomplete with many rooms uncharacterised; however, many of these are deemed to have low contamination significance.

The secondary containment reference inventory estimated in the radiological inventory report (NRS, 2024a, §2.13.3) was based on the materials and dimensions for each room, the available characterisation data and radionuclide fingerprints, and assumed depths of penetration into the building fabric, details of which are provided in the radiological inventory report. Secondary containment activity on levels 1 to 3 of the existing structure was assigned to the inventory of the contaminated structure remaining in-situ below ground, with the remainder assigned to the above ground demolition material (rubble and blocks) to be emplaced in the below ground void.

The alternative inventory for the secondary containment was derived by using maximum activity concentration values to calculate the inventory, rather than average values as in the reference inventory.

4.1.5 PONDS

There are three distinct types of ponds within the SGHWR reactor complex, which are adjacent to the primary containment:

- Fuel element ponds for the storage of spent fuel prior to off-site transport;
- Dump ponds; and
- Suppression ponds.

The ponds were emptied after transfer of fuel ceased and were drained between 2003 and 2005 (NRS, 2024a, §2.14). A limited cleaning operation was completed using water jetting and decontamination agents prior to fixing remaining contamination using a waterproof paint. A significant characterisation programme for the SGHWR ponds was completed in 2016 comprising 17 cores from pond floor areas and 126 wall cores with associated health physics monitoring (NRS, 2024a, §2.14.2). The aims of the programme were to determine the distribution of contamination between the fibreglass liner and underlying bulk material, to determine the depth and type of contamination ingress into the bulk material, and to assess the variability in contamination levels at varying elevations above the pond floor.

Results for the fuel element pond show that most of the contamination was held within the 3 mm thick fibreglass liner, with activity orders of magnitude higher than that in the concrete beneath the liner. Across the fuel element pond, activities varied suggesting contamination was distributed heterogeneously. Other pond floors had much lower total activities than the fuel element pond. Tritium had a different distribution with relatively constant activity measured through the core depth and a slightly lower activity in the fibreglass; this was observed across the different pond types.

The floor beta/gamma activity fingerprint varied from pond to pond, with ^{90}Sr, ^{137}Cs and ^{241}Pu dominating in the fuel element pond, ^{137}Cs, ^{60}Co and ^{63}Ni dominating in the fuel transfer tunnel and dump ponds, and ^{137}Cs, ^{63}Ni and ^{90}Sr dominating in the suppression ponds (NRS, 2024a, §2.14.2). Alpha contamination (principally ^{241}Am and ^{239}Pu/^{240}Pu) was largely restricted to the fibreglass layer, with the highest specific activities in the fuel element pond floor. On the pond walls contamination was again located primarily in the fibreglass liner with the highest beta/gamma activities (dominated by ^{137}Cs) found in the fuel element pond and lowest the activities in the suppression ponds.

Several wall cracks are visible on the external walls of the fuel element and suppression ponds. Cores targeting these cracks indicated that most of the contamination was attributable to ^{137}Cs, with activities between 14.5 and 64 Bq/g on level 2 and 3.2 Bq/g on the external wall of the fuel element pond on level 3 (all pond types had liquor heights maintained at 10.7 m (radiological inventory report, §2.14)). All other beta/gamma and alpha emitting radionuclides were OoS. Tritium was uniformly distributed. The radiological inventory report (§2.14) notes that the extent of cracking was difficult to assess due to the fibreglass liner on the pond internal walls and a lack of access to many of the ponds' external walls.

The volumes of contaminated pond wall and floor materials were calculated using engineering plans to determine the surface area, in conjunction with an assumption that the fibreglass layer was 3 mm thick, and the remaining activity was held within the top 0.2 m of underlying concrete (NRS, 2024a, §2.14.3). The derived reference inventory also included an estimate for activity within the wall construction joints and observed cracks, which assumed the spread of contamination was limited to 2.2 mm each side of the joint/crack (4.4 mm total) – this assumption is explained in the radiological inventory report (NRS, 2024a, §2.14.3).

As the ponds are believed to be well-characterised, the main uncertainty is the volume of material assumed to be contaminated. Therefore, the alternative inventory for the ponds was derived by using average activity concentrations as in the reference inventory but applying more pessimistic dimensional assumptions.

4.1.6 ANCILLARY AREAS

A considerable number of rooms in the SGHWR exist outside the secondary containment structure. Some of these rooms supported active process operations: the active workshops, the boiler house basement, the fuel oil tank room, the active cooling water pump house basement and the cable basement.

The radiological inventory report (NRS, 2024a, §2.15) states that the highest levels of contamination measured in the ancillary areas are from the active workshops. Characterisation of this area was completed in 2012 and identified a fingerprint consisting primarily of ^{137}Cs, ^{3}H, ^{14}C and ^{60}Co. Contamination was removed to a level that would be consistent with the rooms being OoS and IAEA requirements (by sum of fractions) by 2021, in accordance with the requirements for the End State as defined at the time.

Many of rooms in the ancillary areas did not support active process operations and are uncharacterised. These are typically on level 4 and above and are dealt with in the SGHWR backfill section (section 4.1.8). These include rooms such as offices, stores and electrical facilities. The approach to reference inventory derivation for these rooms was considered on an individual basis.

The alternative inventory for the ancillary areas was derived by using maximum activity concentration values to calculate the inventory, rather than average values as in the reference inventory.

4.1.7 SGHWR BULK STRUCTURE

It is observed that the core depths for many features in the SGHWR do not bound the tritium content as it is highly mobile in concrete. It is also observed that measurable tritium contamination is present in areas with no history of processes or activity that would lead to contamination. These observations suggest tritium has diffused throughout the SGHWR structure through the operational period. The radiological inventory report (NRS, 2024a, §2.16) therefore derived an inventory for the bulk volume of concrete in the SGHWR structure to account for tritium contamination that was not otherwise captured. This included both uncharacterised rooms (mostly in the ancillary areas) and deeper intervals of structural materials not captured by core data in characterised rooms across the SGHWR.

The reference inventory was calculated assuming that the tritium contamination of the bulk structure is equal to the median tritium activity for characterised rooms. This approach avoids the strong bias that would be introduced to a mean by the small number of very active rooms, but also includes all the source data in the derived value. The volume of bulk concrete to which this applies was determined by subtracting the total volume of all other inventory entries from the estimated total volume of all SGHWR structural materials.

The alternative inventory for the SGHWR bulk structure accounts for the possibility of contamination pathways other than tritium diffusion and was derived by applying the average measured activity concentrations (for all radionuclides) for the ancillary areas to all uncharacterised structures.

4.1.8 BACKFILL

The on-site sources of materials considered for disposal in the SGHWR voids are concrete blocks and brick / concrete arisings from demolition of the above ground (levels 4 to 10) SGHWR structure, and demolition arisings from stockpiles already on site (section 3.1.1).

The above-ground SGHWR structure includes some of the primary containment, secondary containment and ancillary areas. The SGHWR ponds structures are primarily located below ground level, except for some minor associated rooms on higher levels that are uncharacterised. As such, for the purposes of the backfill inventory calculations, the ponds are excluded from the backfill inventory and are assumed to be fully below ground level. The bioshield structure is located entirely below ground and therefore does not contribute to the backfill inventory.

As discussed in section 3.1.1, the stockpiled material on site consists of broken concrete and brick demolition arisings, the majority of which was consigned using the now-obsolete SoLA Exemption Order levels. Any stockpiled material not satisfying the final version of the Emplacement Acceptance Criteria will be removed before its use as backfill material. A programme of characterisation of the stockpiles is planned prior to final disposal. However, between May and June 2018 a preliminary programme of characterisation was undertaken in support of ongoing technical and optioneering studies, and to support preparation of the disposal Permit application. The radiological inventory report (NRS, 2024a, §2.17.2) concludes that the radiological analysis showed very low levels of artificial activity in all samples with a likely additional component from naturally occurring radionuclides (for example ^{228}Ac, ^{226}Ra, ^{235}U). The results indicate that the bulk material is OoS of EPR 2016. While the sampling undertaken to date is not sufficient to be statistically representative of all the stockpiled demolition arisings, it is expected that the majority of the material will continue to meet the OoS levels. Therefore, for the purposes of the SGHWR disposal inventory, it was assumed that the demolition arisings contained within the stockpiles are at OoS levels, using the A59 fingerprint FP-004 (as building A59 is a significant source of the potentially active material in the main rubble mounds).

Maximum activity concentrations of the demolished above ground SGHWR structure were derived by taking a maximum value from data for the stockpiled material and SGHWR levels 4 to 10 (NRS, 2024a, §2.17.3). Average activities were calculated by dividing the total inventory by the estimated material mass.

The radiological inventory report used the estimates of material volumes that are presented in section 2.

It is likely that backfill material options (e.g. placement of concrete blocks and/or rubble) may be reviewed on an area-by-area basis during backfilling although concrete blocks are expected to be emplaced in SGHWR Region 1. The exact details of the backfilling process are not yet confirmed and given the uncertainties in volumetric estimates of void and backfill, and the packing efficiency and degree of compaction, it is unlikely that a precise understanding of the material balance will be achieved until implementation of demolition and disposal. Therefore, for the purposes of the inventory calculations, the radiological inventory report (NRS, 2024a §2.17.3) assumed that all the above-ground structure and stockpiled material can be disposed of in the SGHWR voids. This conservatively maximises the estimated backfill radiological inventory for the SGHWR End State.

The alternative inventory estimate for the backfill was derived by: i) applying the approaches described in the preceding sections for each contributing feature; ii) using an alternative inventory for the rubble stockpiles derived using maximum activity concentration values, rather than average

values as in the reference inventory; and iii) assuming that each feature contributes an extra 10% contaminated material volume.

4.1.9 INVENTORY ESTIMATE

The radiological inventory report (NRS, 2024a, §2.18) presents estimates for the maximum and average activity concentrations and total activity for the different SGHWR End State components on 1 January 2027.

The total estimated radionuclide reference inventory for the SGHWR End State at 01/01/2027 is 6.12 x 10^5 MBq. This increases by a factor of 9.7 to 5.91 x 10^6 MBq when accounting for uncertainties in the alternative inventory estimates for each feature. In the reference inventory, the bioshield contributes the highest proportion (59%) of the total radionuclide inventory. The bioshield dominates the inventory due to its high average activity concentrations, despite a fairly small overall mass (Table 606/30). The next two largest contributions are from the primary containment (9.9%) and the secondary containment (11.4%), which both have moderate average activities (~10 Bq/g) and masses. The large masses of the backfill and bulk SGHWR structure result in fairly significant respective contributions (13.5% and 3.0%) to the disposal inventory despite their low average activity concentrations. Conversely, the high average activity of the mortuary tubes is offset by their very low overall mass, resulting in a small overall contribution to the inventory (1.3%). The remaining contributions are from the ponds (1.8%) and the ancillary areas (0.5%), which couple low masses with moderate to low average activities. A summary of both the reference and alternative inventories for the SGHWR features is presented in Table 606/30.

The inventory of the in-situ features (excluding backfill) is illustrated in Figure 606/10, demonstrating that the majority of the inventory is located in a relatively small volume of the structure.

Table 606/30: SGHWR features, with activity concentration and total activity for the reference and alternative inventories, presented at a date of 1 January 2027.

Feature	Contam. Mass (kg)	Contam. Vol. (m^3)	Activity Concentration (Bq/g)		Feature Total Activity				
					Reference Inventory		Alternative Inventory		
			Average	Maximum	MBq	%	MBq	%	Increased by factor
Bioshield	7.65E+05	3.14E+02	4.69E+02	8.91E+03	3.58E+05	58.6	5.22E+06	88.3	14.6
Mortuary Tubes	2.75E+03	3.50E-01	2.95E+03	9.37E+03	8.11E+03	1.3	2.56E+04	0.4	3.2
Primary Containment	4.96E+06	2.07E+03	1.22E+01	1.55E+03	6.05E+04	9.9	2.55E+05	4.3	4.2
Secondary Containment	4.21E+06	1.75E+03	1.65E+01	5.62E+03	6.97E+04	11.4	1.35E+05	2.3	1.9
Ponds	1.17E+06	4.87E+02	9.32E+00	7.01E+03	1.09E+04	1.8	2.01E+04	0.3	1.9
Ancillary Areas	1.89E+06	7.89E+02	1.76E+00	7.81E+01	3.33E+03	0.5	1.66E+04	0.3	5.0
Bulk Structure	2.86E+07	1.19E+04	6.50E-01	6.50E-01	1.86E+04	3.0	3.54E+04	0.6	1.9

Feature	Contam. Mass (kg)	Contam. Vol. (m^3)	Activity Concentration (Bq/g)		Feature Total Activity				
					Reference Inventory		Alternative Inventory		
			Average	Maximum	MBq	%	MBq	%	Increased by factor
Backfill	6.12E+07	2.97E+04	1.35E+00	2.74E+03	8.23E+04	13.5	2.04E+05	3.4	2.5
SGHWR Total	**1.03E+08**	**4.71E+04**	**5.95E+00**	**9.37E+03**	**6.12E+05**	**100**	**5.91E+06**	**100**	**9.7**

The secondary containment, ancillary areas and bulk structure contamination each coincide with at least three of the four model regions. Therefore, the estimated inventory for these features needs to be appropriately split across the model regions. The inventory allocation has been derived by mapping the inventory of each room directly to a model region based on the SGHWR building plan. The above ground material for each component has been assigned to the backfill inventory for the same component. Table 606/31 summarises how the radiological inventory information has been allocated to the four SGHWR model regions described in section 2.2 and Table 606/32 presents a summary of the SGHWR radiological assessment inventory by region.

Table 606/31: SGHWR Radiological Inventory allocation to the SGHWR CSM Regions.

SGHWR Inventory Component	Features Contributing to SGHWR In-situ (Below Ground) Inventory			Features Contributing to SGHWR Backfill Inventory		
	All of Feature	Some of Feature	None of Feature	All of Feature	Some of Feature	None of Feature
SGHWR Region 1						
Bioshield	✓					✓
Mortuary tubes	✓					✓
Primary containment		✓			✓	
Ponds	✓					✓
Secondary containment		✓			✓	
Ancillary areas			✓			✓
Bulk structure		✓			✓	
Stockpiled Material					✓	
SGHWR Region 2						
Bioshield			✓			✓
Mortuary tubes			✓			✓
Primary containment			✓		✓	
Ponds			✓			✓

SGHWR Inventory Component	Features Contributing to SGHWR In-situ (Below Ground) Inventory			Features Contributing to SGHWR Backfill Inventory		
	All of Feature	Some of Feature	None of Feature	All of Feature	Some of Feature	None of Feature
Secondary containment		✓			✓	
Ancillary areas		✓			✓	
Bulk structure		✓			✓	
Stockpiled Material					✓	
SGHWR North and South Annexes						
Bioshield			✓			✓
Mortuary tubes			✓			✓
Primary containment			✓			✓
Ponds			✓			✓
Secondary containment		✓			✓	
Ancillary areas		✓			✓	
Bulk structure		✓			✓	
Stockpiled Material					✓	

Table 606/32: Summary of the SGHWR Radiological Assessment Inventory on 1 January 2027 by region.

Region	Reference Inventory				Alternative Inventory			
	Total activity (MBq)			Top 3 radionuclides	Total activity (MBq)			Top 3 radionuclides
	Total	In-situ	Backfill		Total	In-situ	Backfill	
Region 1	5.59E+05	5.05E+05	5.45E+04	H-3 (83%) Cs-137 (5%) Eu-152 (3%)	5.78E+06	5.62E+06	1.59E+05	H-3 (86%) Eu-152 (5%) Ni-63 (2%)
Region 2	1.31E+04	7.08E+03	6.02E+03	Cs-137 (48%) H-3 (33%) Ni-63 (7%)	3.87E+04	2.45E+04	1.42E+04	Cs-137 (68%) H-3 (15%) Ni-63 (5%)
North Annexe	9.96E+03	2.99E+03	6.98E+03	H-3 (54%) Cs-137 (19%) Sr-90 (6%)	1.81E+04	6.47E+03	1.16E+04	H-3 (35%) Cs-137 (21%) C-14 (14%)
South Annexe	2.98E+04	1.49E+04	1.49E+04	H-3 (51%) Cs-137 (22%) Ni-63 (8%)	7.12E+04	5.23E+04	1.90E+04	H-3 (39%) Cs-137 (30% Ni-63 (7%)
SGHWR Total	**6.12E+05**	**5.30E+05**	**8.23E+04**	**H-3 (80%) Cs-137 (7%) Eu-152 (3%)**	**5.91E+06**	**5.71E+06**	**2.04E+05**	**H-3 (85%) Eu-152 (5%) Cs-137 (3%)**

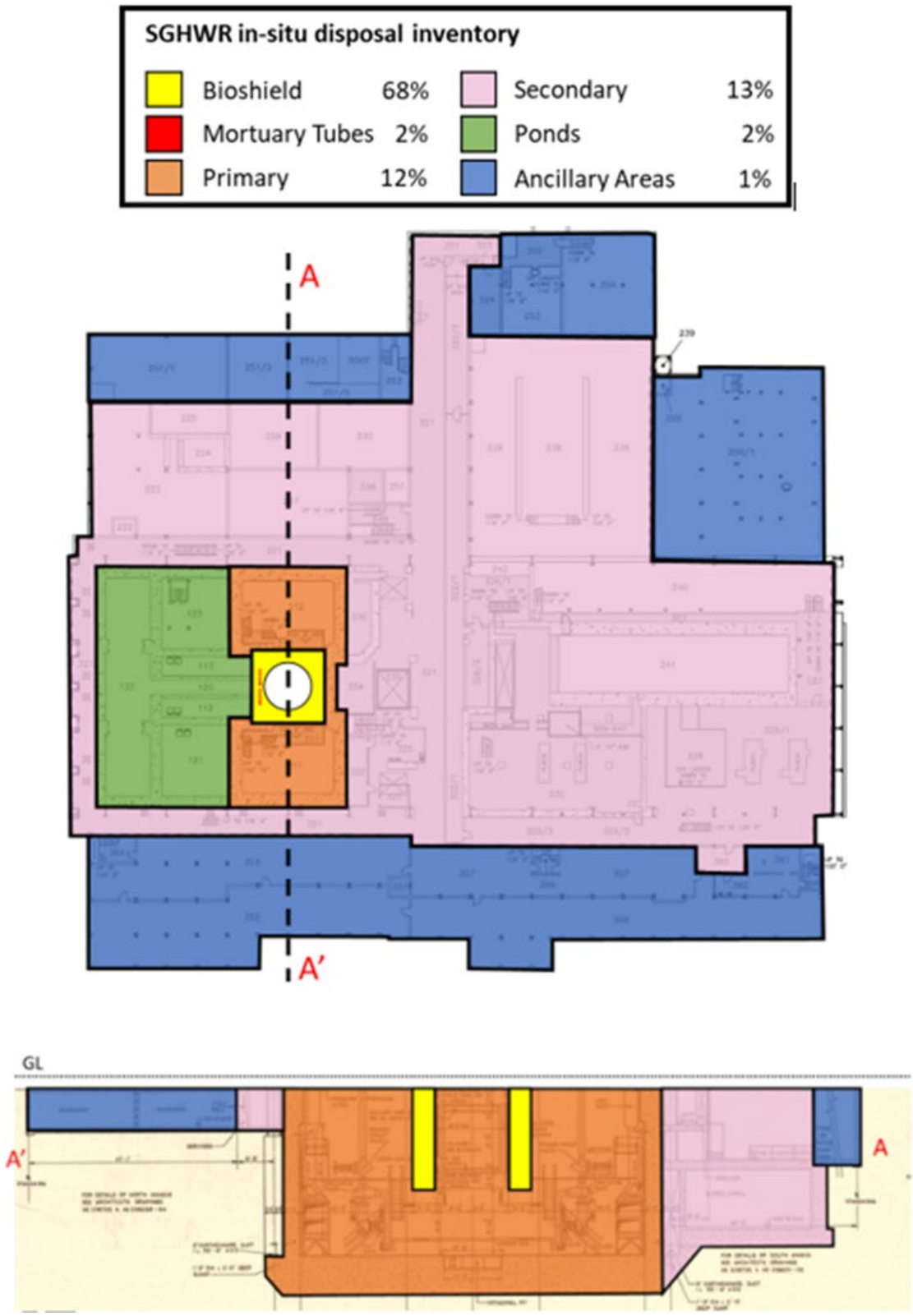

Figure 606/10: Plan and cross-sectional views of the SGHWR in-situ disposal inventory by component. Percentage total activity figures exclude the backfill and bulk SGHWR structure tritium contamination contributions (radiological inventory report, Figure 2.34).

4.2 DRAGON REACTOR RADIOLOGICAL ASSESSMENT INVENTORY

The majority of the radiological inventory present in the Dragon reactor complex in-situ disposal is expected to be concentrated in the bioshield, which is mildly activated. The remaining inventory is associated with low-level contamination in the building paint, walls and floors of the B70 and B78 building structures. In the B70 reactor building the inventory derives from a number of sources (NRS, 2024a, §3.3):

- Operational activities during the lifetime of the facility; ^{137}Cs is a common contamination product.
- Historically, ^{3}H dials were stored at -25' (-7.62 m) below ground floor level in the outer annulus, the leaking of which led to some contamination.
- There is patchy contamination (^{3}H, ^{137}Cs and ^{60}Co) elsewhere in the facility from decommissioning, found primarily in the paint layer. The radionuclides ^{137}Cs and ^{60}Co are not believed to have penetrated into the concrete, but there is some evidence of ^{3}H migration into the concrete in higher activity areas. Some fission product contamination is also expected.
- Historical decommissioning activities, and those remaining, have the potential to redistribute some contamination within the facility since they involve remote drilling, sawing and laser cutting. The degree of contamination cannot be predicted, but it is assumed that this will be decontaminated as appropriate.
- During a lifting operation in the cathedral area of B70 on the 22 March 2021 to transfer the Purge Gas Pre-Cooler (PGPC) into a bespoke shielded container, contaminated water spilled onto the concrete floor. Characterisation and clean-up of the spill is currently ongoing and it is expected to be largely decontaminated.

There is the potential for some low-level actinide contamination beneath the fuel carousel and fission product contamination in the steel-lined sump beneath the reactor. These areas will be characterised once they are accessible. These areas would be expected to have a different contamination fingerprint to that of the general building structure. It is assumed that they will be decontaminated prior to demolition and so they are not included in the End State inventory estimate (NRS, 2024a, §3.3).

As well as containing the spent and fresh fuel stores, the B78 building has been used more generally for decommissioning activities and waste packaging prior to dispatch off site. General contamination in the B78 building is assumed to have a similar source to those listed above for B70 (with the exception of the ^{3}H dial storage and the PGPC spill in B70).

The mortuary holes structure was used to store spent fuel and is therefore expected to be contaminated with actinide and fission product nuclides. Following defueling of the Dragon reactor, the mortuary holes structure (section 2.2.3 and Figure 606/3) was also used to house various items from the on-site Post Irradiation Examination (PIE) facility (A59), which gives the potential for increased contamination, particularly of alpha emitters not normally associated with the Dragon reactor in significant quantities (NRS, 2024a, §3.3). The PIE facility examined a variety of fuel assemblies and their structural components, including fuel from both on-site and off-site facilities.

It is assumed that the remaining plant and structures comprising the Dragon reactor complex are either radiologically uncontaminated, OoS, or will be decontaminated prior to their demolition and removal from site. There is no expectation that any other radiologically contaminated Dragon reactor complex below-ground concrete structures will be left in-situ at the IEP. Similarly, no inventory associated with external areas of the Dragon reactor complex or contaminated land is

captured in the radiological inventory report. It is assumed that any such contamination, if present, will be removed or is OoS.

For the purposes of developing the Dragon reactor complex radiological inventory, the features associated with the disposal inventory were grouped in the radiological inventory report as follows:

- Dragon reactor bioshield;
- Dragon reactor building (B70) general surface contamination and additional ^{3}H ingress into the structure;
- Residual contamination from the Dragon Reactor building PGPC contaminated water spill;
- Dragon fuel storage (B78) building general surface contamination and additional ^{3}H ingress into the structure;
- Backfill emplaced in the below-ground voids in the Dragon reactor building; and
- Primary mortuary holes structure.

4.2.1 DRAGON REACTOR BIOSHIELD

The bioshield is composed of reinforced concrete extending from the steel base plate. As of 2024, the bioshield had been removed down to the +18' level (NRS, 2024a, §3.4). The majority of the bioshield was shielded from significant activation by the thermal shields, but mild activation within the bioshield concrete and rebar has occurred. Higher levels of activation are expected in the region where the PGPC unit extended out from the reactor into the cathedral, penetrating the thermal shields and potentially creating a pathway for neutrons.

The bioshield, which forms a cylinder around the reactor pressure vessel and thermal shield tanks, is 5'9" (1.75 m) thick at its widest point and then narrows slightly (with a larger inner diameter) towards the top of the reactor chamber. The inner diameter is 4.7 m and the height in 2024 was 12.6 m (NRS, 2024a, Table 3.1).

The Dragon reactor bioshield inventory estimate was developed in the radiological inventory report (NRS, 2024a, §3.4.2) based on three main sources:

- Radiological characterisation data of six cores taken through the bioshield in 2005, 2013 and 2017;
- Fingerprints derived for Dragon reactor concrete blocks and the mild steel baseplate; and
- Analogy with the neutron activation modelling of the concrete and rebar in the SGHWR bioshield (activation modelling of the Dragon reactor bioshield has not been undertaken).

Based on analysis of the available sample data, the radiological inventory report (NRS, 2024a, §3.4.2) assumed that the outer section of the bioshield is not activated and that the derived Dragon reactor bioshield concrete activation fingerprint applies only to the first 750 mm from the inner bioshield surface.

Reinforced barytes concrete has been identified in the Dragon reactor, with technical drawings (for example AE149323) indicating it is generally located around penetrations. The significantly higher Ba content in barytes concrete will result in different activation proportions, as Ba is only a small constituent of ordinary concrete. It has not been possible to identify what barytes concrete composition was used when the Dragon reactor was constructed and no samples of barytes concrete from the Dragon reactor have been analysed. Indicative composition information on barytes concrete is presented in the radiological inventory report (NRS, 2024a, §3.4.2) and an approximate inventory estimate produced by scaling the bioshield concrete activation inventory to an average proportion reduction in Ca content and an increase in Ba content between ordinary and

barytes concretes. The ^{41}Ca content in the concrete fingerprint is reduced from 12.4 wt% to 7.8 wt%, and the ^{133}Ba content is increased from 0.5 wt% to 40.2 wt%. The barytes concrete volume was estimated by scaling from drawing AE149323 and conservatively assuming that the barytes concrete region extends through the full height of the bioshield. No attempt was made to account for the neutron absorption characteristics of Ba versus Ca.

The characterisation of the bioshield rebar is limited, with only three rebar samples taken and only two of these providing a few above LOD results (NRS, 2024a, §3.4.2). Steel reinforcing bar typically has a wide range of trace contaminants, and this can lead to substantial differences in activation models – review of the SGHWR activation model showed a two order of magnitude difference between the assumed Co content for mild steel and rebar. Therefore, in the absence of any further information, the more conservative of two separately derived possible fingerprints (a mild steel baseplate fingerprint and one based on the SGHWR activation analysis) was used for the Dragon bioshield rebar. A minimum of 1.5% steel within the bioshield was planned prior to construction, which equates to a minimum of ~36 kg/m^3 (NRS, 2024a, §3.4.3). However, 150 kg/m^3 (~6% steel) was pessimistically assumed in the inventory, which then includes some allowance for any additional steel above the specified minimum and for any steel activation past the 750 mm depth demonstrated for the bioshield concrete.

The height of the bioshield extends above ground level by 5.4 m and therefore the top portion of the bioshield will be demolished and used as part of the backfill for the Dragon reactor voids. Based on this height and assuming constant cross-sectional area and uniform activation contamination, 43% of the calculated bioshield inventory will contribute to the backfill inventory.

The alternative inventory for the bioshield was derived by using maximum activity concentration values to calculate the inventory, rather than average values as in the reference inventory.

4.2.2 REACTOR BUILDING CONTAMINATION AND ^3H INGRESS TO THE STRUCTURE

There are two main sources of radiological contamination within the Dragon reactor building structure itself (NRS, 2024a, §3.5.1):

- Surface contamination of the walls, floors and ceilings being exposed to the general Dragon reactor area atmosphere throughout operation and decommissioning, where contaminants may have been in the airflow or generated as a result of operations/decommissioning; and
- Tritium ingress to the concrete structures from the storage of millions of Gas Tritium Luminescent Devices (GTLDs, also known as Betalites), which were recovered from old Trimphones pending the completion of a safe recovery process for the tritium and were stored on the -25' below ground floor level of the Dragon reactor building in the late 1980s.

The Dragon reactor building general surface contamination inventory developed in the radiological inventory report (NRS, 2024a, §3.5.2) is based on three main sources:

- Radiological characterisation data from ten sampling datasets taken at various locations throughout the Dragon reactor complex between 1999 and 2016, upon which a contamination fingerprint was derived;
- An in-situ sampling campaign by ViridiScope of the Dragon reactor building in March 2018, leading to identification of a hotspot activity of 100 cps upon which to scale the fingerprint; and
- A probe response calibration and activity conversion using a standardised NRS procedure.

In the development of the general building surface contamination fingerprint, two aspects are noted in the radiological inventory report (NRS, 2024a, §3.5.2). Firstly, for many radionuclides in the

characterisation dataset, the measured activities are very low and could be considered to be at the level of noise in the results rather than being statistically meaningful. Secondly, other than for ^{3}H, ^{137}Cs and ^{60}Co, there are insufficient results for the identified radionuclides (both due to limited numbers of above-LOD results and because radionuclides were not analysed for) to draw statistically meaningful conclusions (regarding activity or distribution across the facility), particularly for application of a general fingerprint across the whole Dragon reactor facility. Further characterisation to reduce this uncertainty may be undertaken as decommissioning proceeds. Nonetheless, the approach taken in developing the fingerprint and assumptions made regarding its application to the entire building are generally conservative.

The approach applied to calculating the Dragon reactor surface contamination reference inventory has been to use the fingerprints derived from the sample data with the highest activity patch measured in the ViridiScope survey, which was assumed to apply to a proportion of the entire building surface. This is an extremely pessimistic approach as it applies the highest measured 100 cps localised hotspot surface contamination to the entire Dragon reactor building. Therefore, in the reference inventory, an assumption was made that only 5% of the surface activity is present – this assumption was made on the basis that the building does not have any significant contamination (§3.5.3).

The ^{3}H ingress reference inventory was based on two sampling datasets from the ten used for the surface contamination fingerprint, which were for concrete cores sub-sampled along their length, giving rise to 165 sub-surface concrete samples at various depths (NRS, 2024a, §3.5.2). Data review showed that the most appropriate approach was to split the sub-surface ^{3}H data into two groups, combining the inner wall, outer wall and B78 results into one set and separately considering the Betalite results to avoid substantial over-estimation of the ^{3}H activity.

The calculation applied in the reference inventory assessment is approximate, taking the calculated contaminated building surface area and multiplying this by the depth of contamination, without accounting for the actual surface thickness. As ^{3}H LOD values begin to be reported for thicknesses greater than 30 cm (for the Betalite area) and most structural walls are assumed to be this thick, the calculation of ^{3}H ingress into Dragon reactor surfaces assumes ingress to 30 cm deep (NRS, 2024a, §3.5.2).

The alternative inventory for the reactor building general contamination was derived: i) assuming that 100% of surface contamination is present (rather than 5% as in the reference inventory); ii) including a single anomalously high ^{3}H result in the Betalite area fingerprint (this was excluded from the reference inventory as very likely to be erroneous); and iii) using maximum activity concentrations for the ^{3}H ingress component (rather than average as in the reference inventory). A separate alternative inventory, applying an alternative Pu-containing fingerprint in addition to the approaches used for the main alternative inventory, has also been derived to account for the possibility of Pu isotopes being present within the building contamination, although there are no Pu sample measurements in the characterisation dataset for residual contamination.

4.2.3 RESIDUAL CONTAMINATION FROM THE PGPC SPILL

The PGPC's function was to cool the purge gases from the reactor core to approximately 100°C. It was removed from its in-situ position (connecting the lower section of the reactor pressure vessel and the cathedral area at the -16' level) in January 2018. It was stored within the Dragon reactor building after removal, pending processing. During a lifting operation in the cathedral area to transfer the PGPC into a bespoke shielded container, contaminated water spilled from it onto the

concrete floor at the base of the B70 reactor building (-25' level). Characterisation and clean-up of the spill is currently ongoing.

It is currently intended that the entire volume of contaminated concrete resulting from the spill will be decontaminated to 200 Bq/g, a level consistent with the optimisation threshold in the end state Emplacement Acceptance Criteria. However, it is not clear whether this will be possible and so, to bound the impact of incomplete removal, an estimate has been derived for residual contamination that could remain on site.

The derived reference inventory was based on a total activity for the spill estimated using dose rate measurements combined with MicroShield modelling (NRS, 2024a, §3.6). A smear sample taken from the PGPC shows contamination results that are closely correlated with the Dragon primary coolant fingerprint, and this fingerprint (dominated by ^{137}Cs) was applied to the estimated total activity. As NRS does not intend to dispose of ILW on the site, it was assumed that, as a minimum, sufficient decontamination will be undertaken to reduce the activity concentration to the upper limit of LLW. This corresponds to the removal of 95.5% of the contamination currently estimated to be present. Because of this assumption, no alternative inventory was calculated for residual contamination from the PGPC spill.

4.2.4 FUEL STORAGE BUILDING (B78) CONTAMINATION AND ^{3}H INGRESS TO THE STRUCTURE

As previously described, the B78 building is connected to the B70 building by the reactor building vehicle airlock, including a contiguous floor slab into which steel rail tracks are set and which will remain in-situ. As well as containing the spent and fresh fuel stores, the B78 building has been used more generally for decommissioning activities and waste packaging prior to dispatch off site. Although some rooms in B78 are believed to be clean, there is limited evidence to support this, and it is conservatively assumed (NRS, 2024a, §3.7) that the entire building is contaminated. Surface areas for the floor slab (which will remain in-situ) and the above-ground walls and ceilings (which will be used as backfill in the Dragon reactor voids) were calculated from building plans.

No additional data relating to the fingerprint or contamination level in B78 are available. The existing dataset for general Dragon reactor building contamination already includes samples from B78, and ratios between ^{3}H, ^{137}Cs and ^{60}Co suggest that there is little difference between sample groups from B78, inner B70, outer B70 and the vehicle airlock. Therefore, it was considered appropriate to use the same fingerprint for B78 as for the B70 general building contamination. Similarly, owing to a lack of recent sample data from B78, the same approach to scaling the fingerprint was used as for B70, that is, using a hotspot activity of 100 cps from the ViridiScope survey and assuming (for the reference inventory) that only 5% of surface contamination is present. The B78 sample data that do exist suggest that this is conservative.

As for B70, it is assumed that tritium has ingressed into the concrete structures of B78. No additional B78-specific information is available; therefore, the tritium ingress profile for the B70 general building (excluding the Betalite store area) was applied. This includes some samples from B78. Engineering drawings suggest that walls in B78 are no more than 30 cm thick. To avoid double counting (as the majority of the walls were assumed to be contaminated from both sides), only ingress up to 15 cm depth was considered.

The alternative inventory for the fuel storage building general contamination was derived: i) assuming that 100% of surface contamination is present (rather than 5% as in the reference

inventory); and ii) using maximum activity concentrations for the ^{3}H ingress component (rather than average as in the reference inventory). A separate alternative inventory, applying an alternative Pu-containing fingerprint in addition to the approaches used for the main alternative inventory, has also been derived to account for the possibility of Pu isotopes being present within the building contamination.

4.2.5 DRAGON REACTOR BUILDING BACKFILL

The contaminated backfill inventory comprises the above-ground portion of the Dragon reactor bioshield (43% of the total activity) and the inventory associated with surface contamination and ^{3}H ingress into the above-ground portion of the reactor building structure (56% of the surface contamination) and the fuel storage building structure (83% of the surface contamination), as discussed in the previous sub-sections.

The above ground part of the bioshield inventory assigned to the backfill includes the inventory associated with the rebar. Whilst the emplacement requirements mean that accessible metal will be excluded from the backfill, if the building is demolished by cutting into separate blocks the rebar will be retained. If the above ground building were broken into rubble, then accessible metal would be removed. As the exact demolition plans are still evolving and it is conservative to include the rebar inventory, it is included in the backfill inventory in the radiological inventory report (NRS, 2024a, §3.8).

Any below ground voids within the structure resulting from the demolition of the Dragon reactor building will be filled with material originating from the Winfrith site. In the radiological inventory report (NRS, 2024a, §3.8.1) it was assumed that the Dragon voids will be large enough to accommodate all of the above ground concrete structure of the Dragon reactor and fuel storage buildings in the form of concrete blocks and/or rubble, with a shortfall that will be met using material from the existing rubble stockpiles. Since it is also assumed that the entirety of the stockpiled material will be emplaced into the SGHWR voids, this represents deliberate double counting for the purpose of inventory derivation; however, only a small volume is estimated to be needed to fill the Dragon shortfall. In the event that not enough stockpile material is available to fill the shortfall in both the SGHWR and Dragon voids, additional clean material will be used. Assuming that rubble stockpile material will make up the entire shortfall is therefore conservative.

The alternative inventory estimate for the backfill was derived by: i) applying the approaches described in the preceding sections for each contributing feature; and ii) using an alternative inventory for the rubble stockpiles derived using maximum activity concentration values, rather than average values as in the reference inventory.

4.2.6 MORTUARY HOLES STRUCTURE

The primary mortuary holes system comprises 50 vertical mild steel storage tubes, with external diameter 0.27 m, wall thickness 13 mm and depth 4.2 m (radiological inventory report, Table 3.38). For the inventory estimate it is assumed that all storage hole lids and any detachable parts of the mortuary holes structure will be removed, and that the main ventilation ducts will be removed to ground level, the point at which they are embedded in concrete (radiological inventory report, §3.9). It is assumed that the metal lining of the storage pit will be removed, and the area cleaned. Given that the mortuary holes, sump and storage pit are metal lined, it is anticipated that there has been negligible radionuclide migration into the bulk system concrete. Therefore, all that is included in the End State inventory estimate is contamination associated with the steel structure of the primary

holes and the ventilation and sump system. To achieve the End State, the remaining structure will be infilled with clean grout.

The mortuary holes structure inventory is principally based on the results of a systematic sampling campaign undertaken in 2023. This campaign was driven by a lack of existing characterisation that was identified as a key uncertainty. The inventory estimate was developed using the following sources (radiological inventory report, §3.9):

- Count rate surveys and smear samples taken at top, cross vent and full height positions for all holes;
- Radioisotope analysis on samples with the highest counts per second (cps) readings at each of the three locations;
- A probe response calibration and activity conversion using a standardised NRS procedure; and
- A previous (2016) inventory estimate based on a smear sample from the outlet ventilation stacks.

An inventory for the mortuary holes component was derived from the fingerprint and probe response value from the analysed top smear and full-height samples, applied to the relevant cps reading for each individual hole. The average value (of the top smear and full-height values) was adopted for each radionuclide. The reference inventory for the cross vents was derived from the fingerprint and probe response value from the analysed cross vent sample, applied to the average cross vent cps reading for each group of five holes connected by each of the ten cross vents. The inventory for the main ventilation ducts and sump components was based on the 2016 inventory estimate which used a smear from the ventilation stack outlet (assumed to still be most representative sample for these components). The reference inventory for the overall structure is the sum of the mortuary holes, cross vents, main ducts and sump components.

For the assessment inventory the activity concentration has been calculated assuming that all the contamination is located in the first 1 mm thickness of the mild steel structure (equivalent to 0.32 m^3). The entire inventory is assumed to form a below ground level in-situ disposal.

The alternative inventory was derived using i) for the mortuary holes, the maximum rather than average value of full-height and top smear count rates for each radionuclide, and ii) for the cross vents, the maximum rather than average cross vent smear count rate for each group of five holes connected by each of the ten cross vents.

4.2.7 INVENTORY ESTIMATE

The radiological inventory report (NRS, 2024a, §3.10) presents estimates for the maximum and average activity concentrations and total activity for the different Dragon reactor components on 1 January 2027.

The total estimated radionuclide reference inventory for the Dragon reactor complex End State at 01/01/2027 is 7.23 x 10^3 MBq. This increases by a factor of 3.5 to 2.55 x 10^4 MBq when accounting for uncertainties in the alternative inventory estimates for each feature. The majority of the Dragon reactor complex inventory is associated with the B70 below-ground disposal. The backfill contributes the highest proportion (54%) of the total radionuclide inventory, followed by the below-ground bioshield (21%). The backfill dominates the inventory due to its high average activity concentrations and the large volume over which it is applied. The low average activity concentrations and low volume of the mortuary holes disposal results in a small contribution to the total inventory (0.5%). A summary of both the reference and alternative inventories for the Dragon features is presented in Table 606/33.

Table 606/33: Summary of the Dragon Reactor Complex Radiological Assessment Inventory at 1 January 2027.

Feature	Contam. Mass (kg)	Contam. Vol. (m^3)	Activity Concentration (Bq/g)		Feature Total Activity					Top 3 radionuclides (reference inventory)
			Average	Maximum	Reference Inventory		Alternative Inventory			
					MBq	%	MBq	%	Increased by factor	
Bioshield	2.57E+05	9.25E+01	5.86E+00	2.84E+01	1.51E+03	20.9	6.41E+03	25.2	4.2	H-3 (83%), Eu-152 (8%), Ba-133 (4%)
Reactor building contamination	4.58E+06	1.91E+03	1.52E+01	1.61E+02	8.12E+02	11.2	6.30E+03	24.7	7.8	H-3 (98%), Sr-90 (1%), Cs-137 (1%)
PGPC Spill	7.92E+01	3.30E-02	1.20E+04	1.20E+04	9.50E+02	13.1	9.50E+02	3.7	1.0	Cs-137 (99%), H-3 (1%), Sr-90 (1%)
Backfill	1.29E+07	6.54E+03	3.02E-01	1.61E+02	3.88E+03	53.7	1.16E+04	45.4	3.0	H-3 (56%), Cs-137 (24%), Sr-90 (9%)
Mortuary holes structure	2.51E+03	3.20E-01	5.18E-01	1.34E+01	3.37E+01	0.5	4.76E+01	0.2	1.4	Cs-137 (55%), Sr-90 (25%), Pu-241 (8%)
B78 floor slab	2.56E+05	1.07E+02	1.52E+01	1.61E+02	4.01E+01	0.6	2.20E+02	0.9	5.5	H-3 (95%), Sr-90 (2%), Cs-137 (1%)
Dragon Total	**1.80E+07**	**8.66E+03**	**4.02E-01**	**1.20E+04**	**7.23E+03**	**100**	**2.55E+04**	**100**	**3.5**	**H-3 (59%), Cs-137 (26%), Sr-90 (5%)**

In Figure 606/11 a plan view and cross-section of the Dragon reactor in-situ disposal structure is illustrated along with the inventory of the in-situ features (the figure excludes the inventory contribution from the backfill). The figure shows that the majority of the in-situ inventory is located in a relatively small volume of the structure.

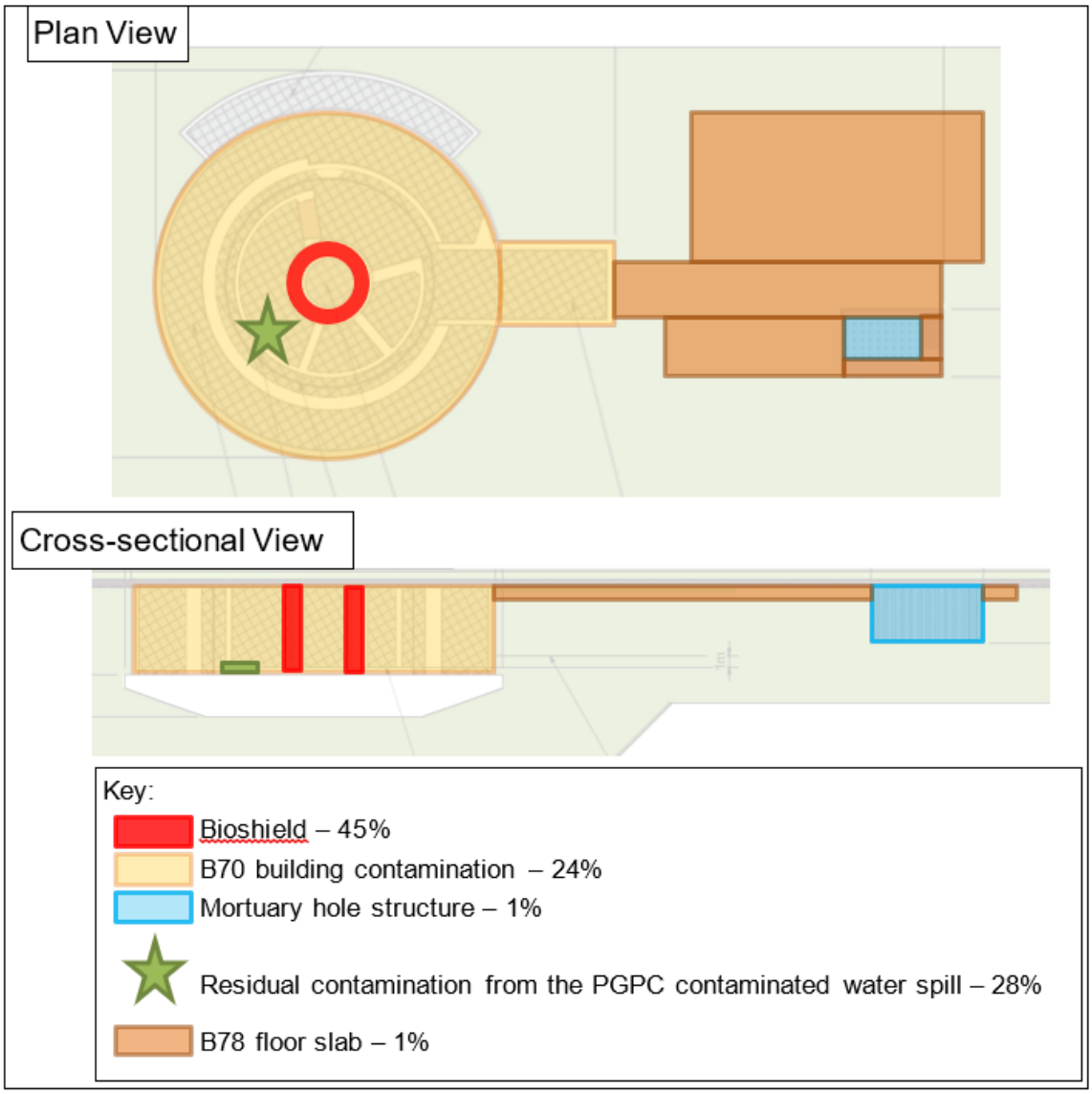

Figure 606/11: Plan and cross-sectional views of the Dragon reactor in-situ disposal inventory by feature. The unshaded hatched area outside of the main Dragon reactor building outline is the services duct, which is assumed to be uncontaminated. Position of the PGPC contaminated water spill is indicative. Percentage activity figures exclude the backfill inventory contribution (NRS, 2024a, Figure 3.21).

As for the SGHWR, the below-ground level elements of the Dragon reactor complex can be grouped into six features for the radiological conceptual model based on their location and inventory characteristics. These are summarised in Table 606/34.

Table 606/34: Summary of Dragon radiological PA model features.

Assessment feature	Inventory features and components included
Dragon bioshield	Bioshield, including Portland concrete, barytes concrete and rebar.
Dragon reactor building – inside Wall C	Reactor building contamination inside of Wall C, comprising surface contamination and tritium ingress. All backfill derived from above-ground bioshield.
Dragon reactor building – Walls A-C (up-gradient)	Half of general reactor building contamination covering Walls A-C, comprising surface contamination and tritium ingress. Betalite store area, comprising surface contamination and tritium ingress. Residual contamination from the Purge Gas Pre-Cooler (PGPC) spill. Half of the total backfill derived from above-ground B70 and B78 buildings plus stockpiled rubble.
Dragon reactor building – Walls A-C (down-gradient)	Half of general reactor building contamination covering Walls A-C, comprising surface contamination and tritium ingress. Half of the total backfill derived from above-ground B70 and B78 buildings plus stockpiled rubble.
Dragon Mortuary Holes	Primary mortuary holes structure.
Dragon B78 floor slab	Fuel storage building (B78) floor slab, excluding primary mortuary holes structure.

4.3 SUMMARY OF THE RADIOLOGICAL ASSESSMENT INVENTORY

The radiological inventory report (NRS, 2024a) is considered to present a cautious but credible estimate of the reference inventory that could be left on the Winfrith site, together with more conservative alternative inventories derived to explore the impact of the key inventory uncertainties for each feature. The radiological inventory report clearly indicates the dominance of the SGHWR inventory (98% of the total radioactivity) over that of the Dragon reactor complex, with the most significant SGHWR components being the bioshield and the secondary containment.

The radiological inventory estimates are presented in Table 606/32 and Table 606/33 for the SGHWR and Dragon reactor complex End States, respectively. The inventory estimates were developed in the radiological inventory report using a number of assumptions, as there is limited information for some components and access limitations prevent sampling and characterisation at this time. The radiological inventory uncertainties and assumptions are summarised in the Uncertainty Management Plan table in the radiological inventory report (Appendix A) and are categorised as follows:

- Potential for additional plant, structures and any contaminated land associated with the SGHWR and Dragon reactor structures to be included in the inventory scope.
- Uncertainties associated with comprehensiveness, scope, and applicability of waste radiological fingerprints.
- Use of generic material compositions and densities due to lack of site-specific data.
- Adequateness and statistical robustness of the available characterisation data.
- Impact of changes to current outline demolition and backfill plans.

Where possible, conservative assumptions have been made to manage uncertainties and data gaps. The end state inventory estimate will be revised as decommissioning proceeds and increased accessibility means further characterisation can be undertaken.

The radiological inventory report estimates activity data for 60 radionuclides expected to be present in the SGHWR and Dragon reactor complex End States. Augmenting the reported list of radionuclides with decay chain progeny radionuclides produces a long list of 117 radionuclides. However, many of these radionuclides are present with low activities and/or have short half-lives, such that they cannot contribute significantly to future radiological impacts. It is good practice and efficient to screen out radionuclides of lesser importance, enabling effort to be targeted at obtaining data for a sub-set of potentially significant radionuclides. The screening methodology applied is set out in the radiological PA report (NRS, 2024b), with 51 radionuclides retained and explicitly included in the natural evolution model. The screened-in radionuclides account for 99.5% of the estimated SGHWR reference inventory at 1/01/2027 and effectively 100% of the Dragon reactor complex End State reference inventory.

5 NEAR FIELD EVOLUTION

This section describes how the integrity of the structures remaining in-situ and the engineered cap will evolve with time to gradually allow greater passage of water into, through and out of the disposals/deposits. This, combined with the chemical properties of the disposals/deposits (such as contaminant sorption and solubility), is used to describe how the assessment inventory is released to water in the near field.

The following are described in this section:

- The integrity of the structures, as this will affect the rate of water ingress and leakage, which has the potential to affect the rate at which the water-available inventory is released from each End State component (section 5.1);
- The relationship between the structures and groundwater elevation, both currently (early 2020s) and in the future, as the potential interaction of groundwater with the structures and disposals/deposits will affect the rate of release of the water-available inventory (section 5.2);
- The rate of infiltration of water through the engineered cap to be constructed over the structures and disposals/deposits, as this has the potential to affect the rate of release of the water-available inventory (section 5.3);
- A water balance between infiltration and leakage, which describes how water will interact with the structures and the disposals/deposits through time (section 5.4);
- A description of the mechanisms by which the water-available non-radiological and radiological inventory of each component of the structures and the disposals/deposits will be released to the water (sections 5.5 and 5.6, respectively); and
- The influence on pH of water in the near field from demolition arisings (section 5.7).

This section goes beyond describing concepts and explains how the hydraulic conductivity of structural concrete, cement dissolution and cap integrity will be represented in numerical models supporting the non-radiological HRA and radiological PA. This has been done as a matter of practicality to ensure alignment of the models authored by different parties.

5.1 INTEGRITY OF THE SGHWR AND DRAGON REACTOR STRUCTURES

The integrity of the structures influences the rate of ingress and/or leakage of water from the disposals/deposits and therefore the rate at which the water-available inventory is released.

The concept for concrete degradation is that:

- Of cracking caused by rebar corrosion that increases the bulk hydraulic conductivity of the concrete over a few centuries until it provides no hydraulic resistance to the flow of water; and
- Of dissolution of the cement until all that remains is the concrete aggregate. This changes the density, porosity and tortuosity of the concrete over millennia.

For the purposes of the non-radiological HRA and the radiological PA no claims are made on the hydraulic integrity of the concrete structures of the SGHWR annexes and the Dragon reactor and the reasons for this are set out in section 5.1.1. Consideration of concrete cracking, described in section 5.1.2, is therefore only relevant to SGHWR Regions 1 and 2. The concept of cement dissolution is described in section 5.1.3.

With loss of integrity the gross hydraulic conductivity of the structures increases. The current integrity of the structures and the potential for changes in the integrity of the structures in the future

is described in section 5.1.4 and this leads to a description of how the gross or effective hydraulic conductivity of the structures changes with time. The numerical representation of cement dissolution is described in section 5.1.5.

5.1.1 CLAIMED INTEGRITY OF THE CONCRETE STRUCTURES

SGHWR Annexes

Magnox (2019b) describes the construction joints in the floor slab as leaky and the integrity of the floor slab is further compromised by manholes that access cofferdam voids beneath the suspended floor slab.

The Annexes are to be demolished using conventional demolition techniques that minimise operational safety risk but are "*inherently destructive*" and there is a risk of damaging the base slab and walls. Further, Magnox (2019b) concludes that the loading of the base slabs by demolition arisings "*will cause cracking to these slabs*". The integrity of the basement slabs in the annexes cannot therefore be guaranteed following demolition and filling with demolition arisings. It is assumed that, due to the damage sustained during demolition and placement of arisings as well as leak paths present at the moment, the North Annexe and South Annexe End States will not retain water from the outset. Further consideration of how the gross or effective hydraulic conductivity of the Annexes changes with time is not therefore required.

SGHWR Regions 1 and 2

NRS (2024e) discusses the integrity of the below ground reinforced concrete structure of the SGHWR during and following demolition of the above ground structure.

The entire above ground structure of the SGHWR will be demolished. The primary containment is to be demolished using wireline cutting and the below ground voids will be filled with placed concrete blocks from the cutting. The report concludes:

- "*the risk of causing damage to the primary containment walls (and creating new leak paths below groundwater level) during the cutting/lifting process is low*"; and
- "*damage to the primary containment foundation slab due to backfilling is not expected*".

Magnox (2019b) states that there is a preference for demolishing the turbine hall, steam labyrinth and the delay tank room using wireline cutting. These features all have thick floor slabs, and it is assumed that their demolition and backfilling, as with the primary containment, will not damage their structure.

Works have been commenced in the SGHWR to prepare it for decommissioning. The works are not expected to, and are assumed not to, damage or provide additional reinforcement to the SGHWR structure.

Dragon Reactor

Atkins (2020) discusses the applicability of the SGHWR study (Magnox, 2019b) to the Dragon reactor building structure and concludes that Wall B and the base of the Dragon reactor can be expected to behave like the structures in Regions 1 and 2 of the SGHWR. Regardless of their integrity, the walls of the Dragon reactor are discontinuous structures (Figure 606/6) and therefore do not provide an internal barrier to flow. Wall A of the Dragon reactor is a conventional concrete structure and Atkins (2020) concludes that it offers no barrier to groundwater flow, like the bases of the SGHWR Annexes.

5.1.2 CONCEPT OF CONCRETE CRACKING

Magnox (2019b) considers a range of physical and chemical factors which could affect the integrity of the SGHWR primary containment, including abrasion/erosion, cavitation, frost, exfoliation, fire, sulphate attack and acid attack. These processes are considered by Magnox (2019b) to have a low risk of compromising the integrity of the structure. Carbonation, decalcification and corrosion of steel reinforcement are also considered, and it is concluded by Magnox (2019b) that these effects may have some potential to reduce the integrity of the structure, although the timescales of these long-term degradation effects (over hundreds to thousands of years) are acknowledged as uncertain.

Carbonation, cracking and surface spalling of concrete in Regions 1 and 2 was investigated in 1985 by testing of concrete samples (Wexham Developments Limited, 1985). Carbonation of the structure was identified to 150 mm depth and is concluded by Wexham Developments Limited (1985) to have removed the corrosion inhibitive properties of the alkaline cement paste allowing corrosion of steel reinforcement. The radius of the steel reinforcement bars in the concrete was demonstrated to have increased due to corrosion and this is interpreted to have caused concrete surface spalling. Figure 606/12 illustrates the conjectured six stages of concrete cracking and spalling:

- Stage 1: As constructed. The horizontal steel reinforcement is 75 mm from the internal face of the structure and is 25 mm thick. The vertical steel reinforcement is further from the internal face of the structure and abuts the horizontal steel reinforcement.
- Stage 2: Carbonation of concrete interpreted to have reached 150 mm after approximately 20 years. This destroys the corrosion inhibitive properties of the alkaline cement paste. 2% anhydrous calcium chloride is found in most concrete samples and was probably added to the cement mix to facilitate winter concreting. It likely increased the rate of corrosion.
- Stage 3: Increase in the radius of horizontal steel reinforcement causes the first fracture plane.
- Stage 4: The first fracture plane allows the operating environment to permeate the structure and increases the depth of carbonation.
- Stage 5: A second fracture plane is caused by the increase in radius of the vertical steel reinforcement by corrosion.
- Stage 6: Concrete spalls from the internal face of the structure giving the impression that the horizontal steel reinforcement has “sprung” away from the surface.

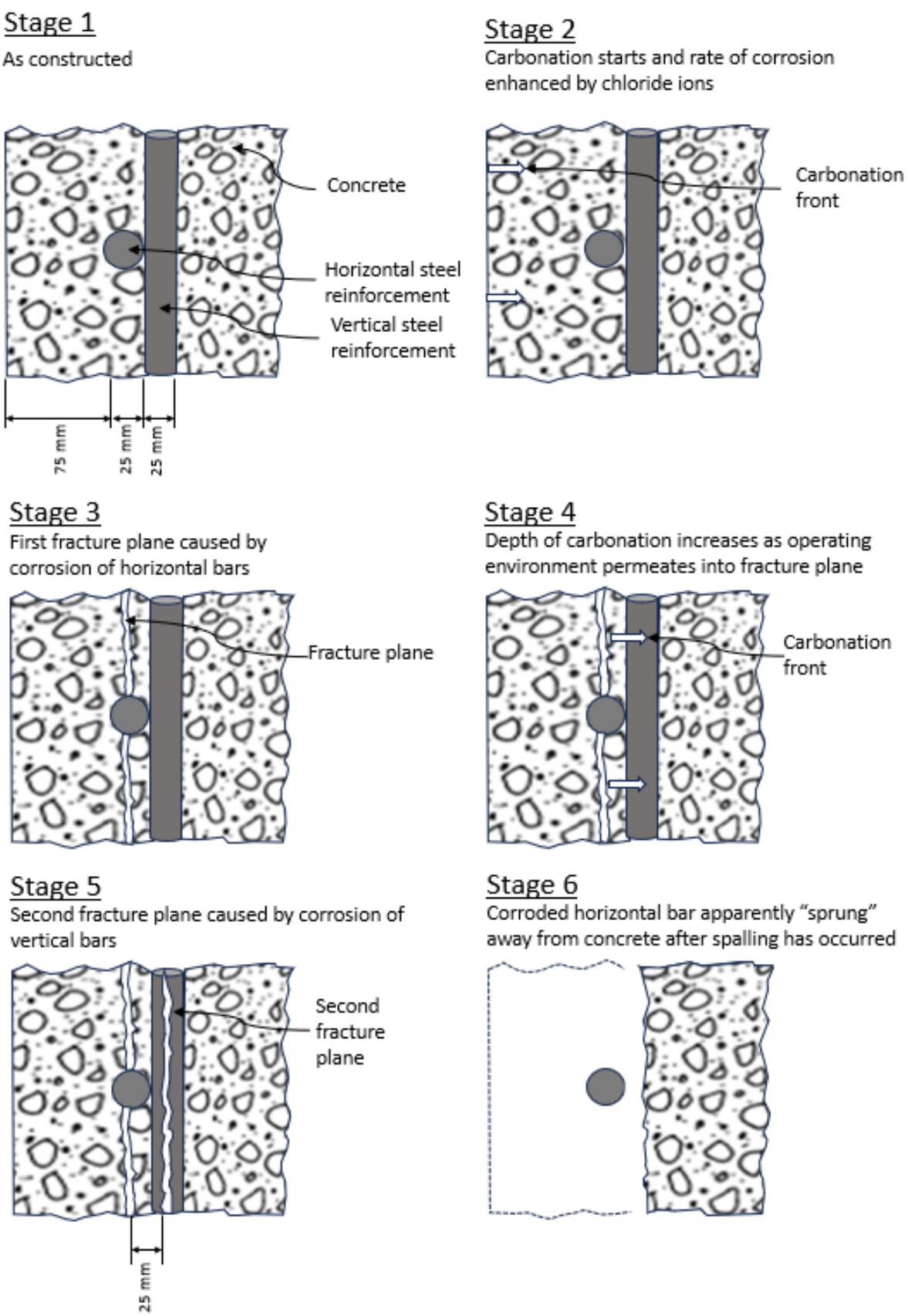

Figure 606/12: Conjectured model of concrete cracking and spalling (after Wexham Developments Limited, 1985).

5.1.3 CONCEPT OF CONCRETE DISSOLUTION

The passage of water through cementitious material, such as concrete, leaches mineral components, with four states being identified as generally controlling the process. The four states of cement leaching can be summarised as follows (Jacques et al, 2013) and are shown schematically in Figure 606/13.

- State 1: This state has a porewater pH >12.5 with a high concentration of sodium and potassium ions, resulting from the dissolution of sodium and potassium oxides. It typically requires less than one volume of water per volume of concrete to leach out all the highly soluble sodium and potassium oxides. This state may therefore only last for a short time if the flow rate of water percolating through the concrete-based demolition arisings is high. However, if water is stagnant then this highly alkaline pH may persist in the interstitial porewater for a long time.
- State 2: A pH of ~12.5 controlled by the dissolution of portlandite at its solubility limit of approximately 900 mg/l of Ca. It typically takes in the order of tens to a few hundred volumes of water exchange per volume of concrete to dissolve all the portlandite.
- State 3: This state begins when the portlandite has been leached out of the cement and the pH is between 12.5 and 10. The interstitial porewater composition at this time may be buffered by AFm phases[15], AFt phases[16] and calcium silicate-hydrate (CSH) cement phases. The end of this state is defined when these phases have leached out, typically after several thousand volumes of water exchange per volume of concrete have occurred.
- State 4: A pH <10 with aggregate mineral being present. The interstitial porewater composition is mainly influenced by the dissolution of calcite (from previous carbonation of the cement phase and from calcareous aggregate if present) and by the composition of the infiltrating water. As the solubility of calcite is much lower than that of the minerals controlling states 1 to 3, this state may persist for a very long time as large volumes of water are required for calcite dissolution.

The durations of the different states and the stoichiometric coefficients of the different dissolution/precipitation reactions depend strongly on the composition of the cement, the aggregate mineralogy and the composition of the infiltrating water.

[15] AFm is a group of cement minerals, the most common of which is monosulphate, $C_3A.CaSO_4.12H_20$.

[16] AFt is a group of cement minerals, the most common of which is ettringite, a hydrous calcium aluminium sulphate mineral with formula: $Ca_6Al_2(SO_4)_3(OH)_{12}\cdot 26H_2O$ ($C_3A.3CaSO_4.32H_2O$).

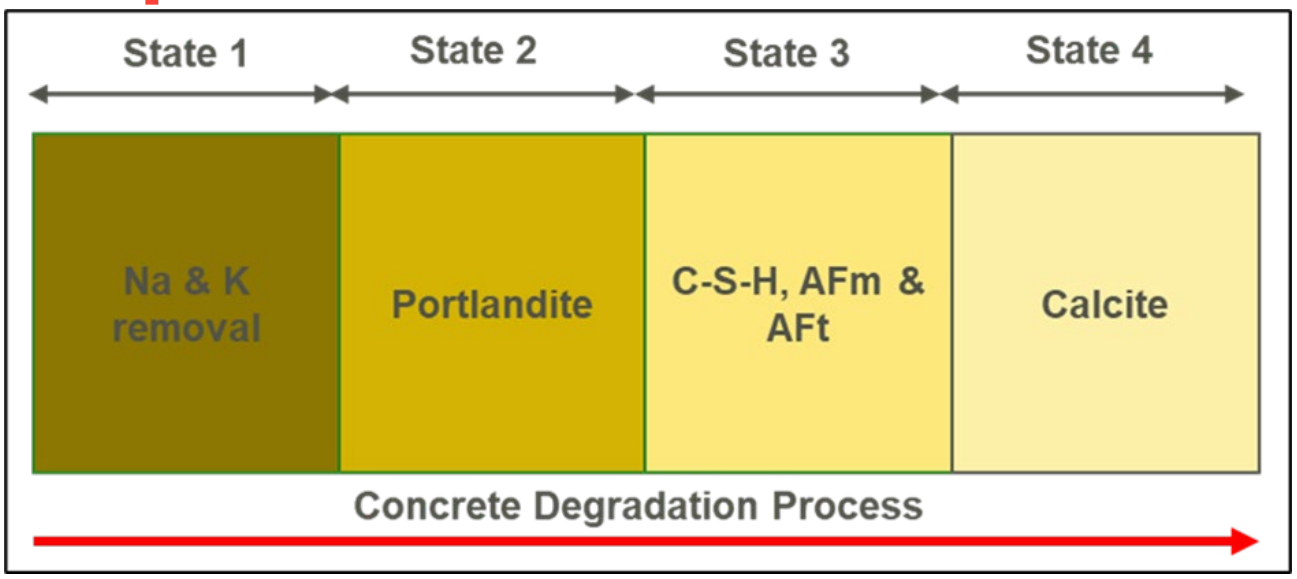

Figure 606/13: Concrete leaching (based on Jacques et al, 2013).

5.1.4 NUMERICAL REPRESENTATION OF THE EVOLUTION OF THE HYDRAULIC CONDUCTIVITY OF STRUCTURAL CONCRETE

Explanation of 'Effective Hydraulic Conductivity'

Hydraulic conductivity is the constant of proportionality between hydraulic gradient and flow per unit area. It is a useful concept when flow is evenly distributed through a porous medium. When it is used for media in which flow is through discontinuities (for example cracks in concrete) it describes the constant of proportionality between hydraulic gradient and flow, were that flow evenly distributed. Concrete degradation will change the effective hydraulic conductivity of the structure which will affect the rate of flow of water into and out of it.

Reference Case Effective Hydraulic Conductivity of the SGHWR Regions 1 and 2

Magnox (2019b) calculates the current effective hydraulic conductivity of the SGHWR Regions 1 and 2 structure to be 4.4×10^{-11} m/s based on the then reported current rate of water ingress to it (of the order of 5 m^3/year). There has been uncertainty about the provenance of water entering the SGHWR Regions 1 and 2. If not all the reported inflow is from groundwater, then the calculated current effective hydraulic conductivity of the structure would be an overestimate (i.e., the current effective hydraulic conductivity would be lower than 4.4×10^{-11} m/s).

Regions 1 and 2 of the SGHWR (and Wall B of the Dragon reactor) are not expected to be adversely affected by demolition, and minor defects and penetrations will be sealed before backfilling commences. On this basis the current effective hydraulic conductivity is assumed to remain appropriate at the point in time that the End States are created.

It is assumed that the hydraulic degradation of the concrete structure will mean that ultimately, over 100's to 1000's of years, the concrete structure provides no resistance to water flow and that the effective hydraulic conductivity will become that of the Poole Formation. NRS (2024f) summarises hydraulic conductivity information for the geological strata beneath the site. The mid-point of the range of results of large-scale tests for hydraulic conductivity is 2.7×10^{-4} m/s. This is also approximately the hydraulic conductivity required for the Poole Formation if rainfall infiltration upgradient of the SGHWR is to flow under the measured hydraulic gradient in the vicinity of the

SGHWR. It is therefore judged a reasonable estimate of the large-scale hydraulic conductivity of the Poole Formation. The effective hydraulic conductivity of the concrete when it provides no resistance to water flow will therefore be taken to be that of the Poole Formation, 2.7×10^{-4} m/s[17].

NRS has commissioned a review of the structural integrity of the basements of Region 1 and Region 2 of the SGHWR and the Dragon reactor basements (NRS, 2024e). It concludes that the basements are robust structures that will maintain their structural integrity both during demolition and backfilling operations and in their End State configurations. The assessment does not identify mechanisms that could give rise to structural defects. On this basis the concrete could take hundreds, if not thousands, of years, to hydraulically degrade. There is limited evidence to support the longevity of reinforced concrete. Complementary considerations for the safety case for the disposal of spent nuclear fuel at Olkiluoto (Posiva, 2012) point to the durability of ancient (e.g. Roman) concrete but these materials were not steel reinforced. The durability of steel reinforced concrete radioactive waste containers has been modelled for Radioactive Waste Management Ltd (AMEC Foster Wheeler, 2016). The study concludes that rebar corrosion and concrete degradation could take place within tens to hundreds of years depending on environmental conditions. Indeed, concrete carbonation, cracking and surface spalling of concrete has been observed in the SGHWR (Wexham Developments, 1985) but there are no measurements or observations of concrete degradation at Winfrith that can be used to reliably estimate the time it will take for full concrete degradation. There is therefore considerable uncertainty about the timescales over which hydraulic degradation of the Winfrith reinforced concrete structures could take place.

Safety assessments for near-surface disposal facilities assume hydraulic degradation. The time assumed for the concrete to hydraulically degrade by the safety assessments of the proposed Winfrith disposals/deposits has therefore been assessed by reference to hydraulic degradation rates assumed for concrete barriers in safety assessments for near-surface disposal facilities (Table 606/35). There are many differences between the designs and environments for the near-surface disposal facilities considered here (hence leading to the differences in degradation periods assumed), and between these purpose-built facilities and the extant SGHWR and Dragon reactor structures, but the safety assessments are generally associated with pessimistic modelling assumptions, rather than attempted realism, and provide a benchmark to support development of the Winfrith assessments.

Table 606/35: Assumed Hydraulic Degradation Rates for Concrete Barriers in Safety Assessments for Near-surface Disposal Facilities

Assessment	Material	Hydraulic Degradation Rate	Reference
Centre de l'Aube (France)	Concrete	Instantaneous change – Assumed failure and not modelled after 300 years.	Dounreay Site Restoration Limited (DSRL) (2010)
Low Level Waste	Concrete base	Linear change – Initial reduction in hydraulic performance after 1,000 years	BNFL (2002)

[17] As no claims will be made on the hydraulic integrity of the concrete structure of the SGHWR annexes or the walls of the Dragon reactor building for the purposes of non-radiological hydrogeological risk assessment or the radiological PA, these will be assumed to present no barrier to flow and the effective hydraulic conductivity will be conservatively assumed to be that of the Poole Formation (2.7×10^{-4} m/s) from the start of the modelling (the IEP).

Assessment	Material	Hydraulic Degradation Rate	Reference
Repository (LLWR) (UK)	Concrete walls	followed by gradual degradation to geosphere values over 10,000 years.	
	Grouted LLW[18]		
	Concrete base (future vaults)	Linear change – Initial reduction in hydraulic performance after 100 years followed by a further reduction after 5,000 years.	LLWR (2011a) & LLWR (2011c)
	Concrete walls (future vaults)		
D3100 (UK)	Concrete barriers	Linear change – Reductions in hydraulic performance over 200 and 500 years, complete degradation after 1,000 years.	DSRL (2021)
	Grouted LLW	Linear change – Reductions in hydraulic performance over 300 years and 1,000 years, with complete degradation by 10,000 years.	
	Cementitious backfill		
	Unencapsulated (demolition) LLW	Linear change – High initial conductivity decreases by an order of magnitude over 600 years due to clogging and settlement. At 1,600 years conductivity increases as the concrete completely degrades.	
El Cabril (Spain)	Concrete	Instantaneous change – Degradation to a porous sand after 300 years.	DSRL (2010)
Savannah River (US)	Concrete floor	Degradation after 1,050 years.	DSRL (2010)
SFR[19] (Sweden)	Concrete	Intact for 10,000 years or degraded after 1,000 years.	SKB (2001b) & SKB (2001c)
	Waste		
SFR (Sweden)	Concrete barriers	Intact concrete hydraulic conductivity is ≤1x10^{-9} m/s. Depending on its use,	SKB (2023)

[18] Low Level Waste.

[19] Repository for short-lived radioactive waste in Forsmark, Sweden.

Assessment	Material	Hydraulic Degradation Rate	Reference
		concrete degrades to a hydraulic conductivity of: ■ $1x10^{-7}$ m/s in 2,000-3,000 years ■ $1x10^{-5}$ m/s in 2,000-22,000 years ■ $1x10^{-3}$ m/s in 12,000-52,000 years.	
Dessel (Belgium)	Walls	Degradation implemented using an "S-shaped" function – fully degraded after 816 years.	ONDRAF/NIRAS (2011)
	Base		
	Roof		
	Grouted waste monolith		

Complete hydraulic degradation of the concrete structures of the studies in Table 606/35 varies between a few hundred years and a few thousand years. The middle of the range is around 1,000 years and this is what was assumed by the most recent UK study in Table 606/35 (that for DSRL's D3100 facility). Based on the studies listed in Table 606/35 a period of 1,000 years is judged to be a reasonable modelling assumption for complete hydraulic degradation of the structure.

It also necessary to describe how the effective hydraulic conductivity will evolve from its current value to that representative of complete degradation. Some studies in Table 606/35 assume that hydraulic properties are lost instantaneously at some point in the facility evolution, and some assume that the properties degrade gradually. Here it is considered reasonable to assume that degradation of the structure will accelerate with time. The effective hydraulic conductivity will therefore be modelled to change from its current value to that representative of complete degradation in an exponential (log K – linear time) fashion.

The effective hydraulic conductivity at time t (k_t) between 0 and 1,000 years from the IEP is described mathematically as follows:

$$k_t = 10^{[logK_0 - ((logK_0 - logK_{1000})\frac{t}{1000})]}$$

where:

K_0: effective hydraulic conductivity at the IEP (m/s);

K_{1000}: effective hydraulic conductivity 1,000 years after the IEP when it is assumed no further increases in effective hydraulic conductivity will occur (m/s); and

t: is time from the IEP (years).

The reference case evolution of effective hydraulic conductivity is shown in Figure 606/14.

Assessment of Uncertainty in Effective Hydraulic Conductivity of SGHWR Regions 1 and 2

There is uncertainty about the current effective hydraulic conductivity of the concrete and the period over which degradation takes place.

The current effective hydraulic conductivity could be lower than estimated. The performance assessment for the LLWR used an initial concrete hydraulic conductivity for its concrete vault walls above the water table of $1x10^{-12}$ m/s. The Belgian ONDRAF/NIRAS (2011) reference case used the same value for concrete initial hydraulic conductivity. The concrete of these facilities is newly constructed and the hydraulic conductivity values are therefore judged to be the minimum possible effective hydraulic conductivity for the aged Winfrith concrete. It is possible that the initial effective hydraulic conductivity could be higher than calculated. It is arbitrarily assumed here that the initial effective hydraulic conductivity could be as high as $1x10^{-9}$ m/s.

The period for complete hydraulic degradation of the concrete could be shorter than 1,000 years. Reference to Table 606/35 indicates that complete degradation in 300 years has been assumed in other assessments.

The range in initial effective hydraulic conductivity and a shorter period for complete degradation have been used to establish variant evolutions of effective hydraulic conductivity (Figure 606/14) that bound the reference case.

Complete hydraulic degradation of the concrete could take longer than 1,000 years. The low hydraulic conductivity variant (the green line in Figure 606/14) could be defined so that full degradation takes place over, say, 2,000 years. In these circumstances, it is evident that the performance of the disposals would be no worse than that of the selected low hydraulic conductivity variant calculation.

There is also uncertainty about how the rate of degradation of concrete changes between its initial state and complete degradation (i.e., whether the rate varies linearly or exponentially, for example, or is assumed to occur instantaneously). Instantaneous degradation is judged unrealistic. Alternative ways by which the effective hydraulic conductivity could evolve from the initial value to the value representative of complete degradation are assumed to be bounded by the variant cases shown in Figure 606/14.

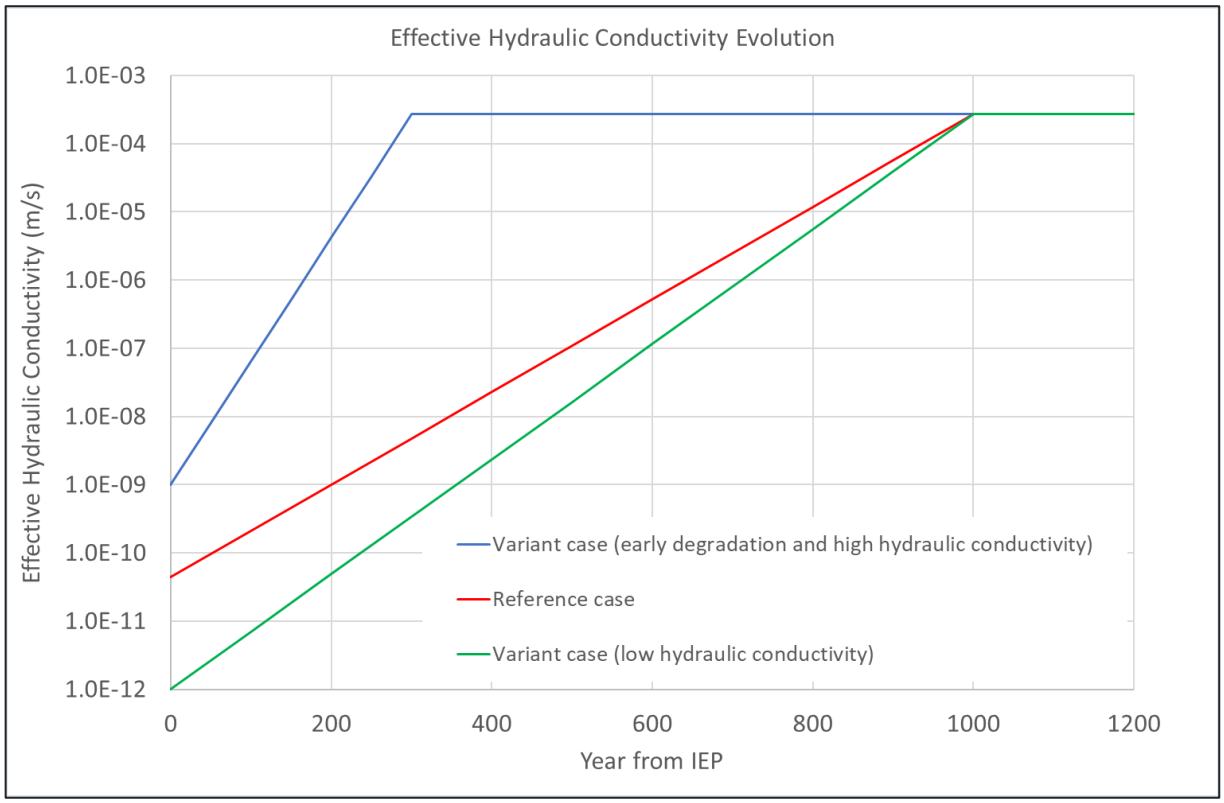

Figure 606/14: Reference and variant cases developed to represent the evolution of effective hydraulic conductivity of SGHWR Regions 1 and 2 structures

5.1.5 NUMERICAL REPRESENTATION OF CEMENT DISSOLUTION

As cement is leached from the concrete, the porosity, bulk density and tortuosity of the concrete will change from that of intact concrete to that of the aggregate which will in turn affect the release of radionuclides[20] from the contaminated parts of the structure. Table 606/36 presents the undegraded values of these parameters and the values that will apply to fully degraded structural concrete (i.e. aggregate). The porosity and density of undegraded concrete is uncertain and reference to other literature sources reveals slightly different values. For instance, SKB (2014) quotes a porosity of 0.099 (v/v) and a density of 2450 kg/m^3. The modelled undegraded concrete porosity and density will be subject to sensitivity analysis in the radiological PA. For reasons of simplicity the change from undegraded to degraded values because of cement leaching is assumed to be linear with time.

There is much uncertainty about how long it will take for complete cement dissolution. Jacques et al (2013) estimate that the third state of cement leaching ends after approximately 1766 kg of water has passed through each litre of concrete. Following a period of deterioration in the performance of the SGHWR engineered cap (1,000 years for the reference case), a maximum infiltration rate of 43 mm/year is estimated. The mass of concrete in Region 1 and Region 2 has been estimated

[20] The non-radiological hydrogeological risk assessment does not model the release of pollutants from structural concrete but instead conservatively assumes pollutants associated with the structural concrete (hydrocarbon fractions associated with oil stains in the SGHWR) are immediately available to water. The non-radiological hydrogeological risk assessment therefore does not need to be concerned with cement dissolution.

using Magnox (2024h) to be approximately 8000 tonnes. Degradation of structural concrete is expected to be, at least initially, by cracking. Water will preferentially flow through the concrete in cracks and much of the cement will be exposed to little, if any, water flow. However, if all the infiltrating water is cautiously assumed to contact all the cement of the concrete as it flows into the ground surrounding the structure (and not pass only through cracks in the concrete) it can be calculated that the cement will take over 50,000 years to dissolve. This is of the same order of magnitude as the 45,000 years assumed for chemical degradation of the Dounreay D3100 facility cement.

Given the uncertainties over evolution of the cap over such long timescales, the reference case will, for the purposes of simplicity, conservatively assume a chemical degradation duration of 50,000 years. Sensitivity analysis in the radiological PA will cautiously assume chemical degradation takes place on the same timescale as the reference hydraulic degradation case (1,000 years).

Table 606/36: Physical Properties of Undegraded and Degraded Structural Concrete

Parameter	Undegraded Concrete Value	Fully Degraded (aggregate) value	Justification
Porosity (v/v)	0.15	0.26	The undegraded value is that quoted by SKB (2001a) for structural concrete. Wexham Developments Limited (1985) found the average cement content of samples of concrete from the SGHWR to be around 250 kg/m^3. If the cement is assumed to be comprised of portlandite and using a bulk density for portlandite of 2230 kg/m^3 (e.g. Mindat, 2023) it can be calculated that the cement has a volume of 0.11 m^3/m^3 concrete. The fully degraded value is therefore 0.15+0.11=0.26 v/v.
Dry bulk density (kg/m^3)	2400	2150	The undegraded value is between those quoted in SKB (2001a) and SKB (2014) for structural concrete. Wexham Developments Limited (1985) found the average cement content of samples of concrete from the SGHWR to be around 250 kg/m^3. The fully degraded dry bulk density is therefore 2400-250=2150 kg/m^3.

Parameter	Undegraded Concrete Value	Fully Degraded (aggregate) value	Justification
Tortuosity[21] (m/m)	0.01	0.1	The undegraded value is chosen to give an effective diffusion coefficient consistent with saturated structurally intact concrete of around 10^{-11} m^2/s (SKB, 2001a). The degraded value is based on Dounreay "Demolition LLW" (DSRL, 2021), a porous broken concrete, similar to what intact concrete is expected to be like when the cement components have been removed and it has become sufficiently cracked, and is chosen to give an effective diffusion coefficient of around 10^{-10} m^2/s.

5.2 POTENTIAL FOR GROUNDWATER INGRESS TO THE DISPOSALS/DEPOSITS

Basal elevations and construction details for the SGHWR and Dragon reactor structures have been compared with current and potential future groundwater elevations for the purpose of assessing whether there is potential for groundwater to interact with the disposals/deposits and the structures. Whilst this section summarises work that has been completed, greater detail is provided in NRS (2024f).

5.2.1 THE SGHWR

Magnox (2021c) has considered the relationship between current (early 2020s) and potential future groundwater elevations and the elevation of the SGHWR structure. Figure 606/15 shows historical groundwater elevations measured in boreholes around the SGHWR. The screened sections of the boreholes extend from around 27 to 31 m AOD and across the water table. Some of the measured groundwater elevations are judged erroneous when considered in the context of other measurements (Golder, 2021) and the assumed erroneous data points are labelled on Figure 606/15.

Superimposed on the graph is a schematic of the elevation of the top of the base slab in three areas of the SGHWR (Regions 1 and 2, the South Annexe and the North Annexe). The groundwater elevation around the South Annexe is of particular interest and the measurements from borehole OW18 have been greyed out because this borehole is some distance upgradient of the South Annexe.

[21] Tortuosity, as defined in GoldSim (which differs to other definitions), is the ratio of the straight distance between the ends of the flow path to the actual flow path length. Thus, values are always less than or equal to one, with one representing a straight flow path. Here, the tortuosity value is assumed to increase (i.e., the flow path becomes less convoluted) as intact concrete degrades.

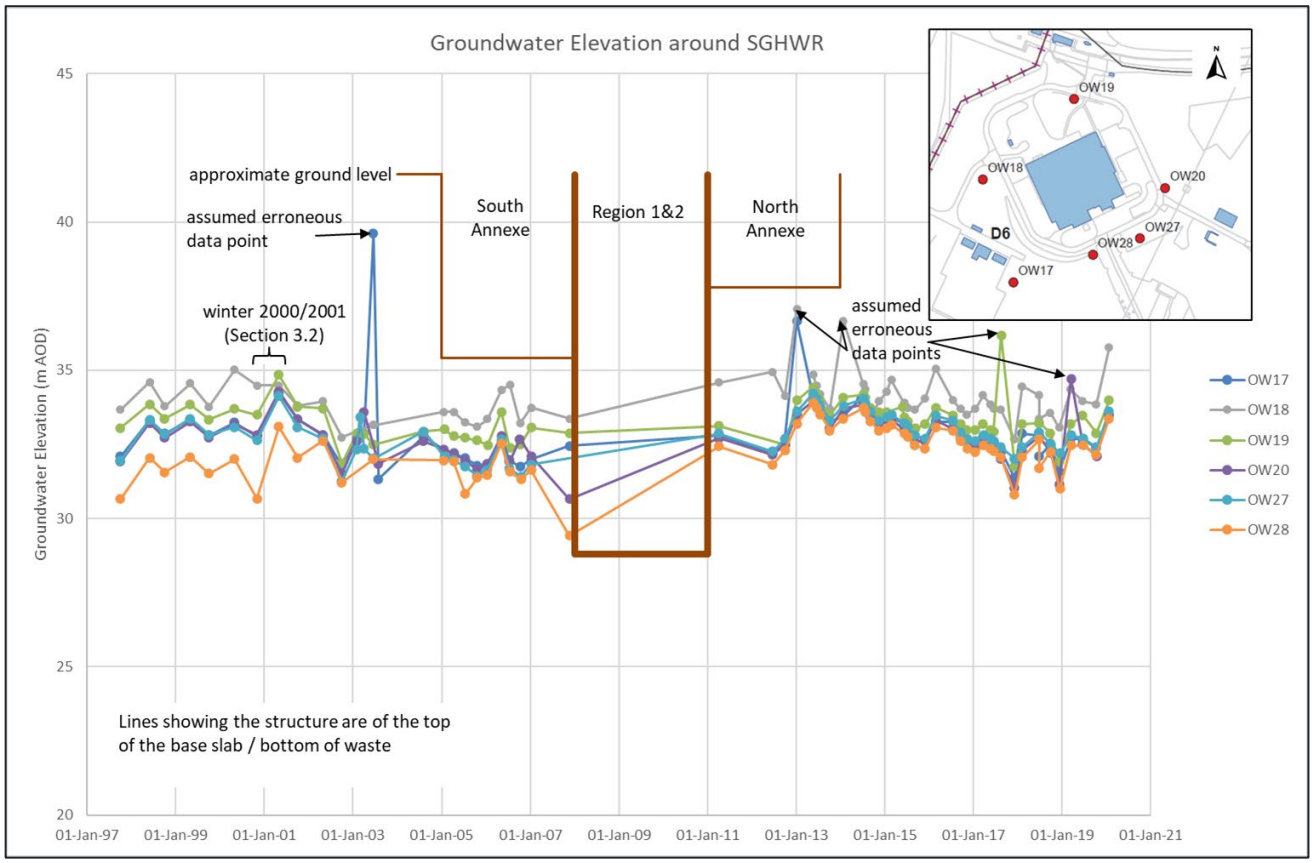

Figure 606/15: Historical groundwater elevations around the SGHWR

Figure 606/15 shows that historical and current groundwater elevations around the SGHWR are below the top of the base slabs of the Annexes, and there is no potential for saturation of the disposals/deposits by groundwater under current conditions.

As summarised in Magnox (2021c) changes to the site surface on implementation of the IES and consequential increases in infiltration may result in an average rise in groundwater elevation of approximately 0.4 m at the SGHWR. Reference to Figure 606/15 shows that with a rise of 0.4 m groundwater levels would remain below the top of the base slabs of the Annexes.

Magnox (2021d) explains that rainfall in the autumn and winter of 2000/1 was greater than is predicted under intermediate scenarios of climate change to 2100 and it followed a summer that was drier than is predicted under the same conditions. Measured groundwater elevations in 2000/1 indicate that under intermediate scenarios of climate change to 2100 groundwater will probably remain below the top of the base slab of the South Annexe even allowing for an average 0.4 m rise in groundwater level brought about by implementation of the End State.

The combined effects of the implementation of the IES and intermediate climate change scenarios are illustrated on Figure 606/16.

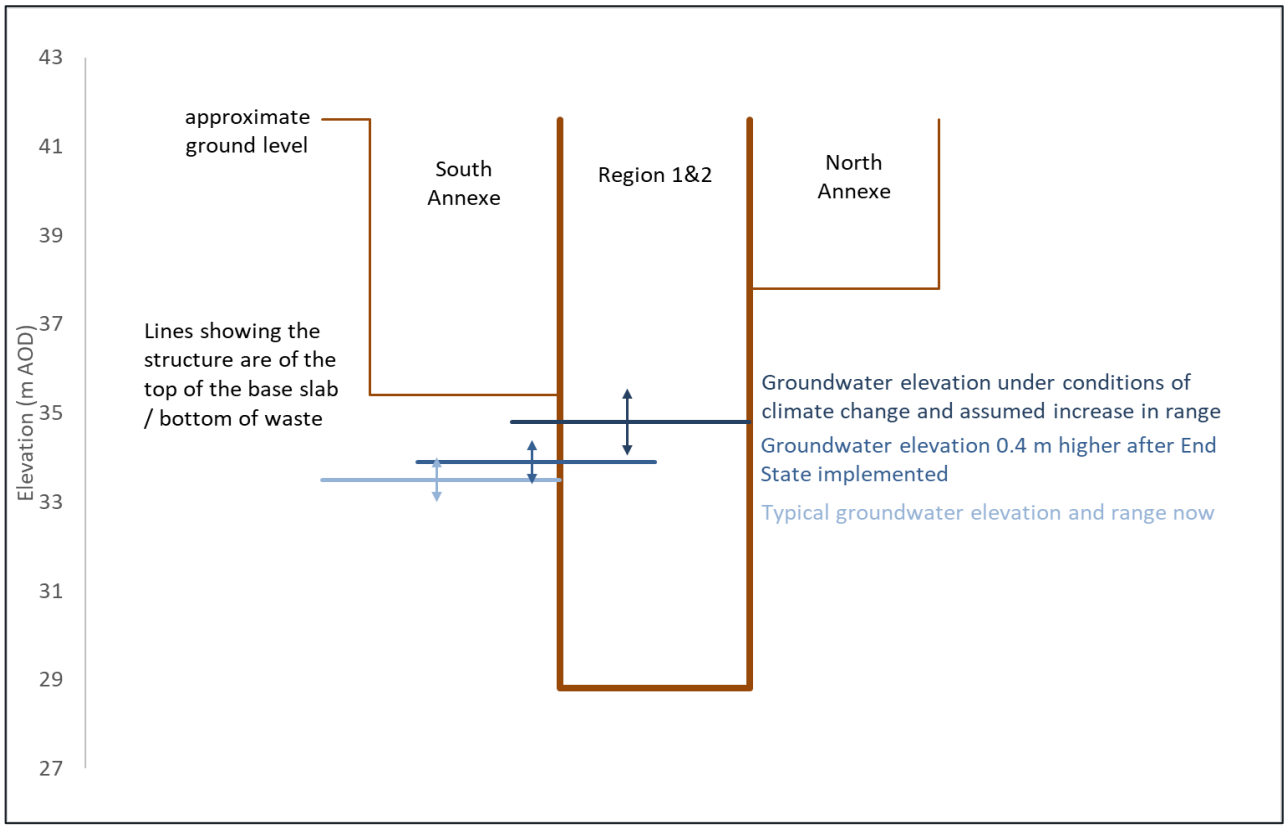

Figure 606/16: Illustration of current and future (to 2100) groundwater elevations and range at the SGHWR

Figure 606/15 and Figure 606/16 demonstrate that under current conditions the deeper parts of Regions 1 and 2 are below the water table. Following implementation of the IES and under a cautious central estimate (CCE) of the effect of climate change, as summarised in Magnox (2021c) and Golder (2022), more of Regions 1 and 2 will be below the water table, the North Annexe will remain above the water table, as will the South Annexe except for short periods only in extreme conditions totalling 4% of the time in the 2050s[22] and 4% of the time in the 2080s[23]. Conditions beyond the 2080s are assumed to be similar to the 2080s as discussed in section 7.1.4. There is therefore potential for groundwater ingress to Regions 1 and 2 of the SGHWR and, infrequently, for short periods of time to the South Annexe. The base of the SGHWR structure sits in a stiff clay the top of which was recorded during construction at approximately the same elevation as the top of the base slab (NRS, 2024f). Groundwater can be expected to be transmitted at only a very low rate through the stiff clay and groundwater ingress to Regions 1 and 2 is therefore assumed to be through the walls of the structures only.

As groundwater ingresses the SGHWR structure, precipitation of carbonate minerals and secondary aluminosilicates might occur and lead to 'healing' of the fractures in the concrete through which the flow occurs. Such processes have been observed and modelled at the Long-Term Cement Studies project in Grimsel in Switzerland (Watson et al, 2018). Given the uncertainties with cement solid

[22] Defined as 2040 to 2069.

[23] Defined as 2070 to 2099.

dissolution rates and rates of secondary mineral formation, such fracture 'healing' is cautiously not included in the concept of groundwater ingress to the SGHWR structure.

5.2.2 THE DRAGON REACTOR COMPLEX

Magnox (2021c) and Golder (2022) have considered the relationship between current (2020) and potential future groundwater elevations and the elevations of the Dragon reactor structure. Historical groundwater elevations measured in boreholes around the Dragon reactor are shown in Figure 606/17. The screened sections of the boreholes cross the water table. One of the measured groundwater elevations in BH411 is judged erroneous when considered in the context of other measurements from this borehole (Golder, 2021) and is labelled. Superimposed on the graph is a schematic of the elevation of the top of the base slab of the Dragon reactor.

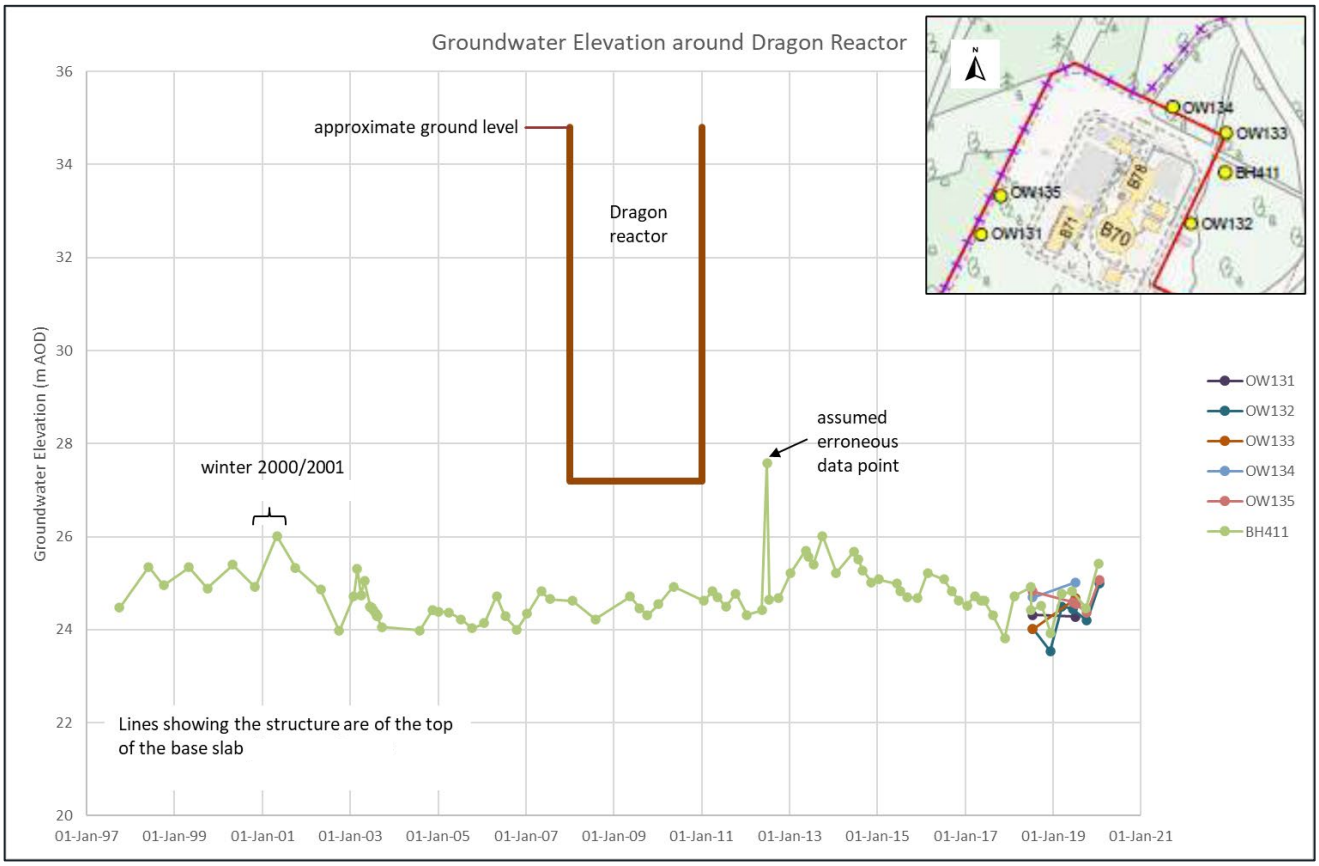

Figure 606/17: Historical groundwater elevations around the Dragon reactor structure

Figure 606/17 shows that historical and current groundwater elevations around the Dragon reactor structure are below the top of the base slab by at least 1 m.

Groundwater modelling summarised in Magnox (2021c) and Golder (2022) finds that average groundwater levels are likely to rise by 0.3 m at the Dragon reactor due to changes to the site surface in preparation for the End State, so groundwater will remain below the top of the base slab. The modelled CCE of groundwater level under conditions of climate change to 2100 is below the top of the base slab of the Dragon reactor (Figure 606/18). This is except for short periods only in extreme conditions totalling 5% of the time in the 2050s and 2% of the time in the 2080s. The modelled CCE of groundwater level under conditions of climate change to 2100 is below the base of the mortuary holes (and the B78 floor slab) to 2100.

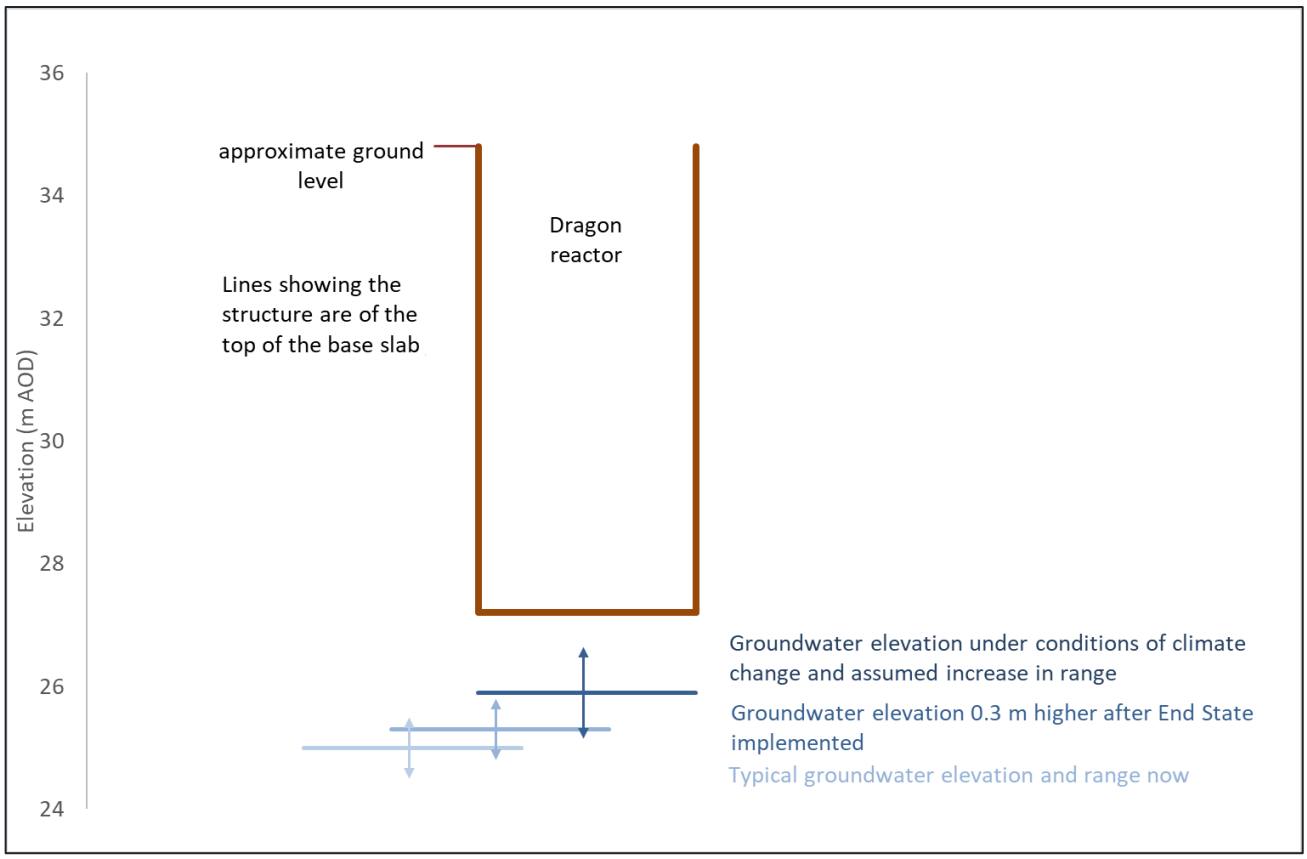

Figure 606/18: Illustration of current and future (to 2100) groundwater elevations and range at the Dragon reactor structure

5.3 INFILTRATION OF RAINWATER THROUGH THE CAPPING SYSTEM

The SGHWR and Dragon reactor complex End States will be covered by an engineered cap, designed to hinder intrusion into the disposals/deposits and to limit rainwater infiltration. Magnox (2019c) describes a concept cap design, approximately 3 m thick and summarised in Table 606/37, that would meet these functional requirements. Further, it is assumed the cap will be designed to include a layer or layers that, in the unlikely event that the disposals/deposits became saturated, would divert water from within the disposals/deposits into the unsaturated zone thereby preventing water from breaking out at the surface. Whilst the concept cap design will be subject to future optimisation, it is assumed for the purpose of developing a time variant profile of infiltration through the capping system for mathematical model development that the optimised cap design will include a composite flexible membrane liner (FML)/clay layer overlain by drainage.

Table 606/37: Summary Concept Design for Cap for the SGHWR and Dragon Reactor Complex (from Magnox, 2019c)

Cap Component	Description
Top	
Topsoil and subsoil	A layer of at least 0.40 m of subsoil and 0.40 m of topsoil
Geotextile	A dense geotextile should be applied atop the anti-intrusion barrier to minimise particle migration into the underlying anti-intrusion and drainage layers
Anti-intrusion barrier	The layer should be constructed of compacted cobbles in the range 0.10-0.15 m with a thickness of 0.30-0.60 m
Drainage layer	A minimum 0.30-0.45 m thick drainage layer, typically of a coarse (grain size between 16 mm and 32 mm) non-calcareous gravel
Geotextile	A dense geotextile (typically less than 5 mm thick) to minimise the potential for damage to the FML during emplacement of overlying drainage and restoration materials
Geomembrane	High density polyethylene or linear low density polyethylene flexible membrane liner
Geosynthetic Clay Liner	A thin (approximately 5 mm) layer of bentonite embedded between two needle punched layers of geotextile
Mineral Liner	For the purpose of concept design this is assumed to comprise a clay mineral liner of at least 0.50 m thickness, formed by reworking and compacting imported clays or mudstone in defined layers
Regulating layer	A regulating layer consisting of a coarse gravel (grain size between 16 mm and 32 mm) between 0.30 and 0.60 m thick will be placed directly on top of the geotextile
Geotextile	A dense geotextile (typically less than 5 mm thick) should be laid over the emplaced material prior to capping to provide separation and prevent loss of capping materials during installation
Bottom	

Schematic representation of the restoration is shown in Figure 606/19 and Figure 606/20 for the SGHWR and Dragon reactor End States, respectively. The extent of the cap will be subject to future optimisation.

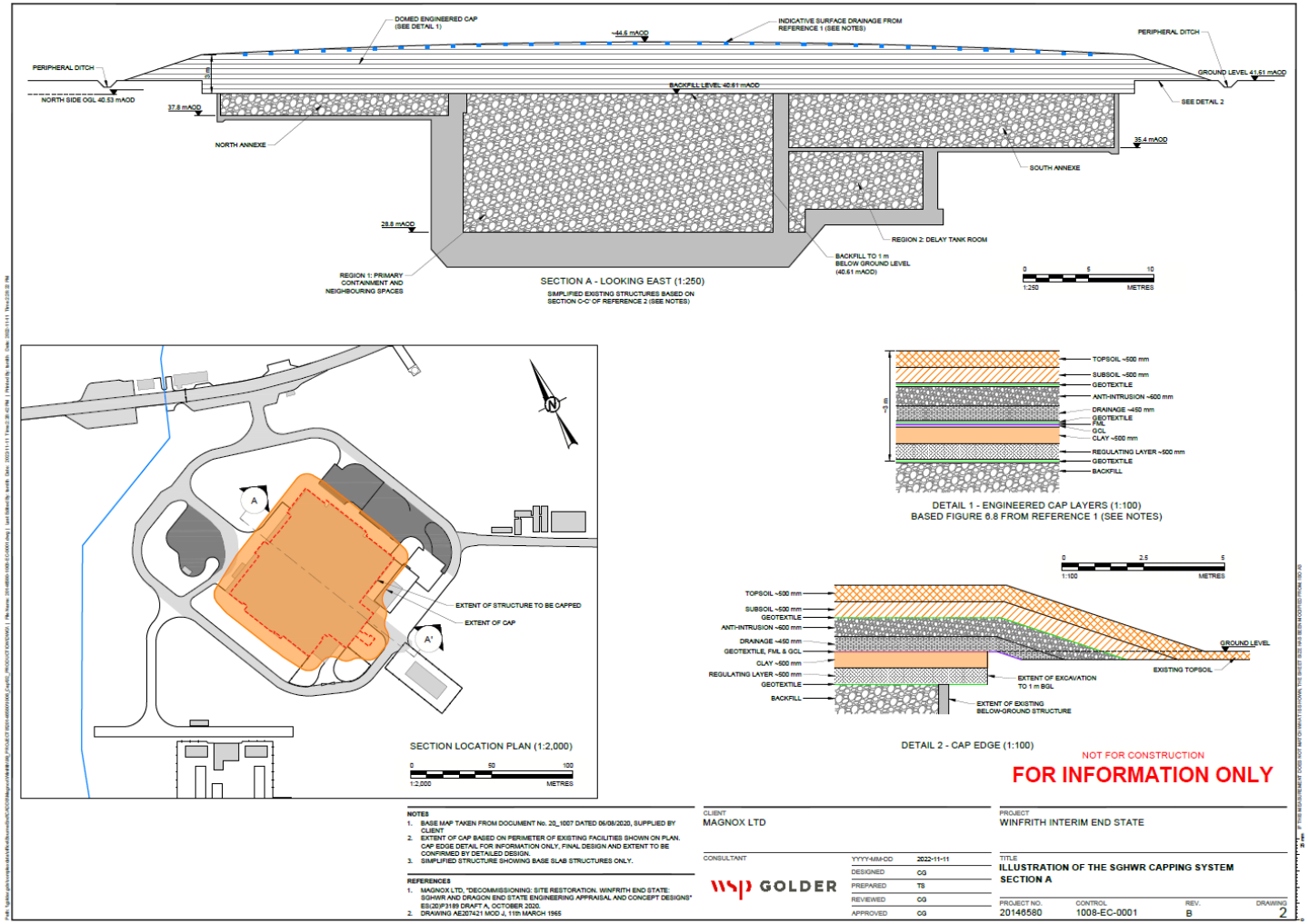

Figure 606/19: Schematic representation of the SGHWR restoration

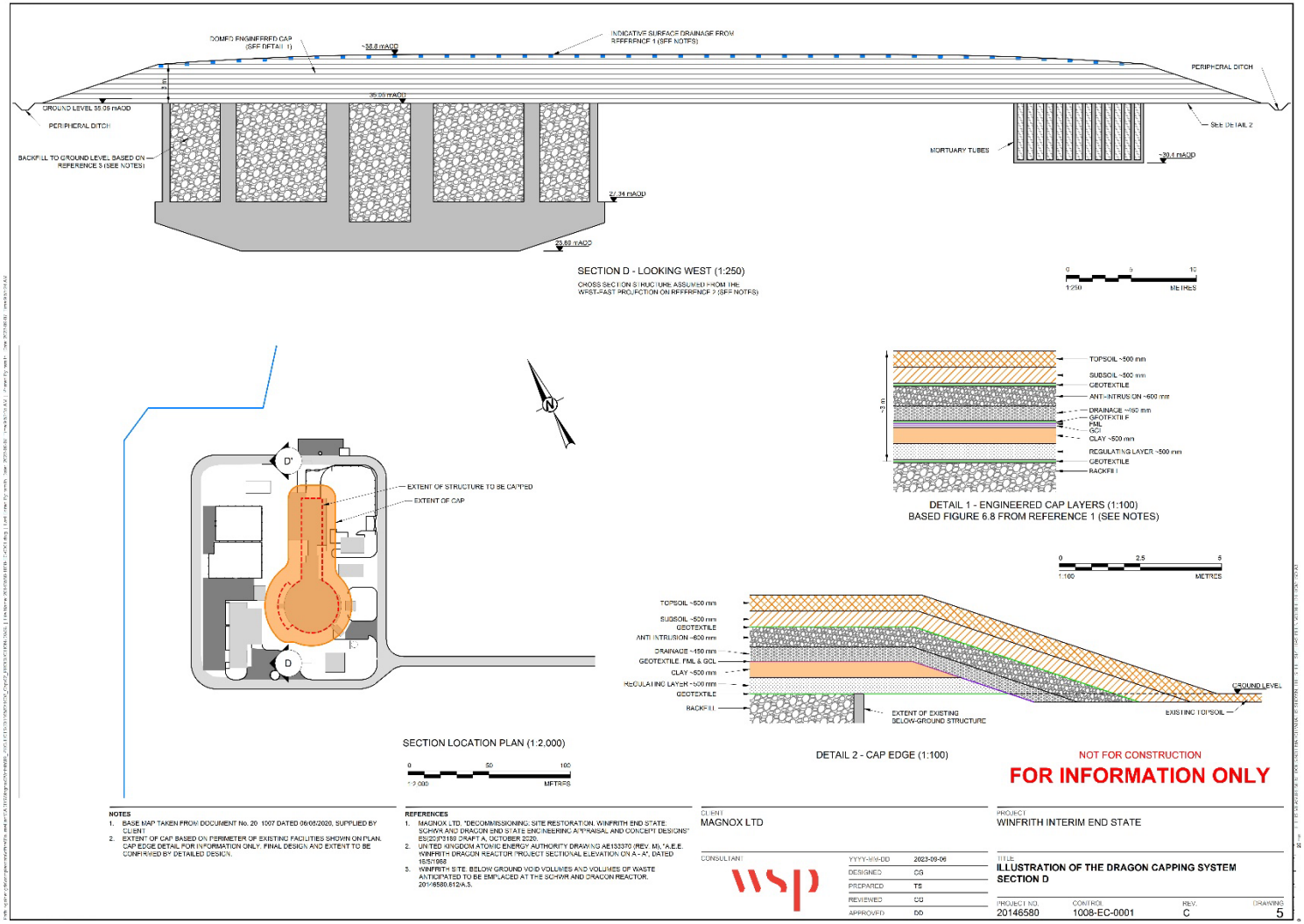

Figure 606/20: Schematic representation of Dragon reactor restoration

Magnox (2019c) quantifies the expected rate of infiltration through the cap, including consideration of how this will change through time as components of the cap naturally degrade.

Magnox (2019c) concludes that the initial infiltration rate of the cap will be controlled by the geomembrane. The geomembrane infiltration rate will depend on the quality of the installation. Magnox (2019c) calculates that the best case to worst case range of initial infiltration is in the order of 0.02 mm/year to 0.2 mm/year. The calculations have been carried out using the equations of Giroud (1997) and do not account for the effect of reduced drainage performance due to clogging that might be expected in the early decades following installation, which may increase the head gradient across the cap. In addition, WSP experience suggests that in practice FMLs installed in caps do not typically perform to such a high specification. WSP (2023a) provides an assessment of the short-term potential effects on the geosynthetic clay liner (GCL) and FML and concludes an infiltration rate of a few millimetres per year should be cautiously applied in the years shortly after emplacement. Therefore an initial infiltration rate of 5 mm/year is assumed.

Magnox (2019c) explains that the installed geomembrane will start to chemically degrade after a period. The onset of degradation is assumed to be 250 years following installation, in line with EA (2003a). An infiltration rate of 5 mm/year will be assumed through the cap for the first 250 years.

Magnox (2019c) explains that the rate of infiltration will increase linearly until 1,000 years following installation, when it is then controlled by the GCL. The design infiltration rate for the GCL is calculated by Magnox (2019c) to be 8 mm/year. However, Magnox (2019c) explains that if the GCL fails the infiltration rate will be 43 mm/year. This is the calculated infiltration rate for the mineral liner component of the cap which would control the infiltration rate if the GCL fails once the geomembrane has degraded.

Here, the GCL, as well as the FML, is assumed to allow the passage of progressively more water such that following the complete degradation of the geomembrane the infiltration rate is 43 mm/year. In line with the recommendations of Magnox (2019c) that draws on EA (2003a), a linear increase in infiltration rate will be assumed for the period between the initial infiltration rate and the long-term infiltration rate (250 years to 1,000 years following installation). The time to the onset of degradation and the rate of degradation of the FML is uncertain. WSP (2023a) assess the long-term effects on the capping system including consideration of climate change. WSP (2023a) concludes there is uncertainty as to the extent degradation of the polyethylene geomembrane in the proposed Winfrith capping system will be affected by an increase in average annual temperature caused by climate change. To account for this uncertainty, the timescales to onset of degradation and to complete degradation of polyethylene proposed by EA (2003a) are assumed for a reference scenario for hydrogeological risk assessment, but sensitivity will be assessed of the risk to a variant scenario of an increased degradation rate. A variant scenario will be considered in which the time to the onset of degradation is halved and the rate of degradation is doubled compared to that of the assumed reference scenario. The evolution of infiltration rate through the cap for reference and variant scenarios is summarised in Figure 606/21.

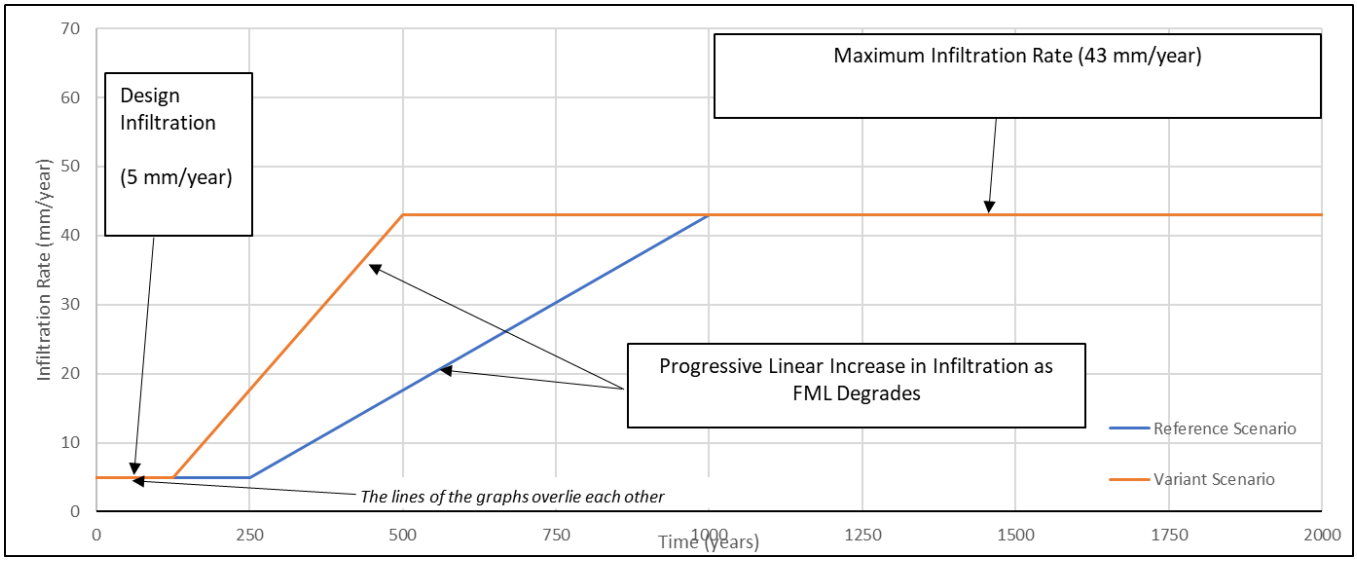

Figure 606/21: Infiltration profile of the engineered cap through time (reference and variant scenarios)

5.4 NEAR FIELD WATER BALANCE

The evolution of infiltration and leakage rate has been used to describe the near field water balance for the SGHWR structure. This is summarised for four key points in time in Figure 606/22 to Figure 606/25. Initially, the water level will rise within Regions 1 and 2 of the SGHWR because of infiltration of water through the cap. From 250 years the rate of infiltration will increase as the cap progressively degrades. The water level within Regions 1 and 2 of the SGHWR could potentially reach the 1 m bgl level of the tops of walls and thereafter any overtopping water could migrate into the Annexes. Whether the water level reaches the 1 m bgl level is dependent on the relative magnitude of the rate of water inflow through the progressively degrading cap and the rate of water outflow through the progressively degrading structure. It is assumed that the basements of the Annexes will not impede the vertical downward flow of water. Therefore, the leakage rate from the Annexes will be equal to (balanced with) the inflow rate through the cap over their surface (plus any water that overtops from Regions 1 and 2). The leakage rate from the South Annexe will also include any outflow as a result of groundwater that may have inundated the South Annexe basement.

The internal and external walls of the Dragon reactor may retain water, but, cautiously, no claims are made on their hydraulic integrity in the non-radiological HRA or radiological PA. The water balance of the Dragon Reactor (Figure 606/26) is therefore assumed to evolve in a similar way as for the South Annexe of the SGHWR but with leakage to groundwater also assumed to occur through the external walls. Water may also leak through the base as it progressively degrades. Like the South Annexe, the leakage rate is assumed to be equal to infiltration and leakage following occasional groundwater inundation.

The design of the capping system for the SGHWR and the Dragon reactor complex End States includes a drainage layer to prevent breakout of water at the ground surface.

The water balance for the mortuary holes structure will evolve similarly to the Dragon reactor (Figure 606/27), however there is considered no potential for groundwater levels to rise above the base.

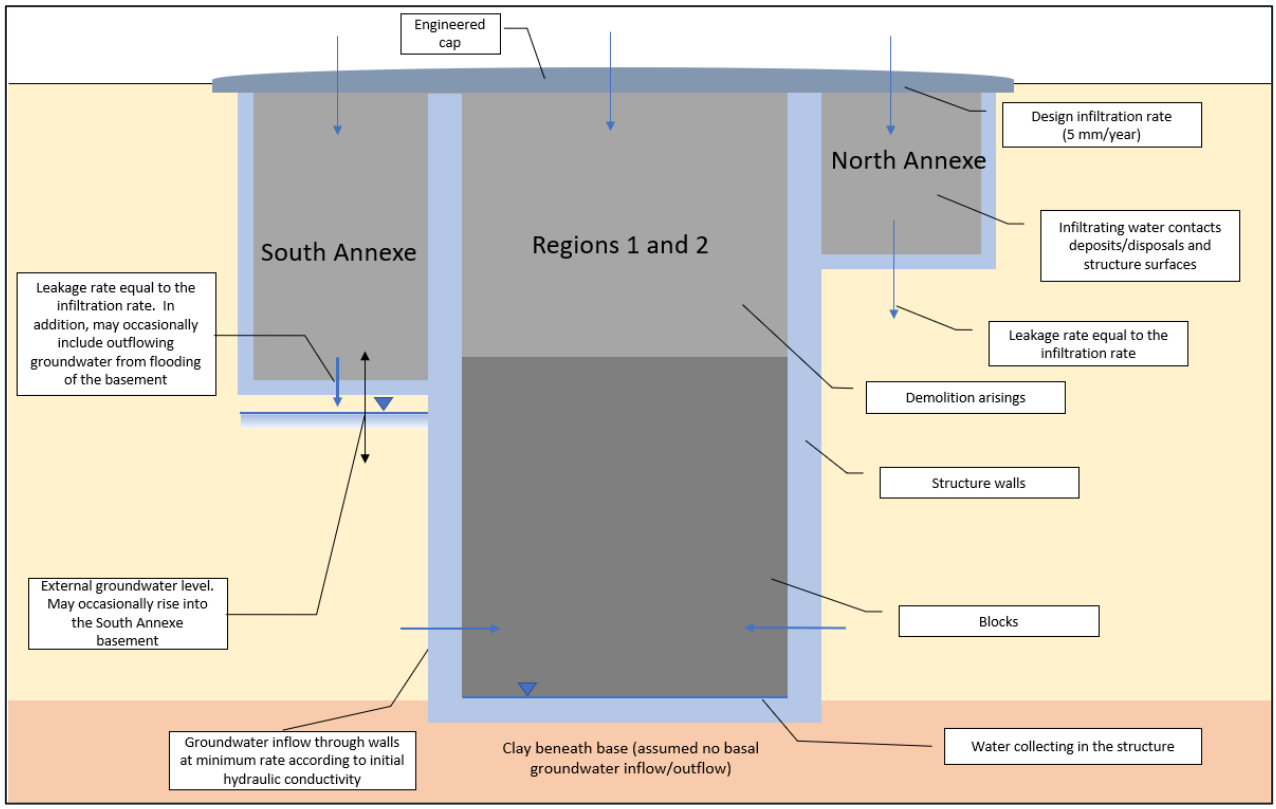

Figure 606/22: SGHWR End State water balance immediately following implementation of the End State

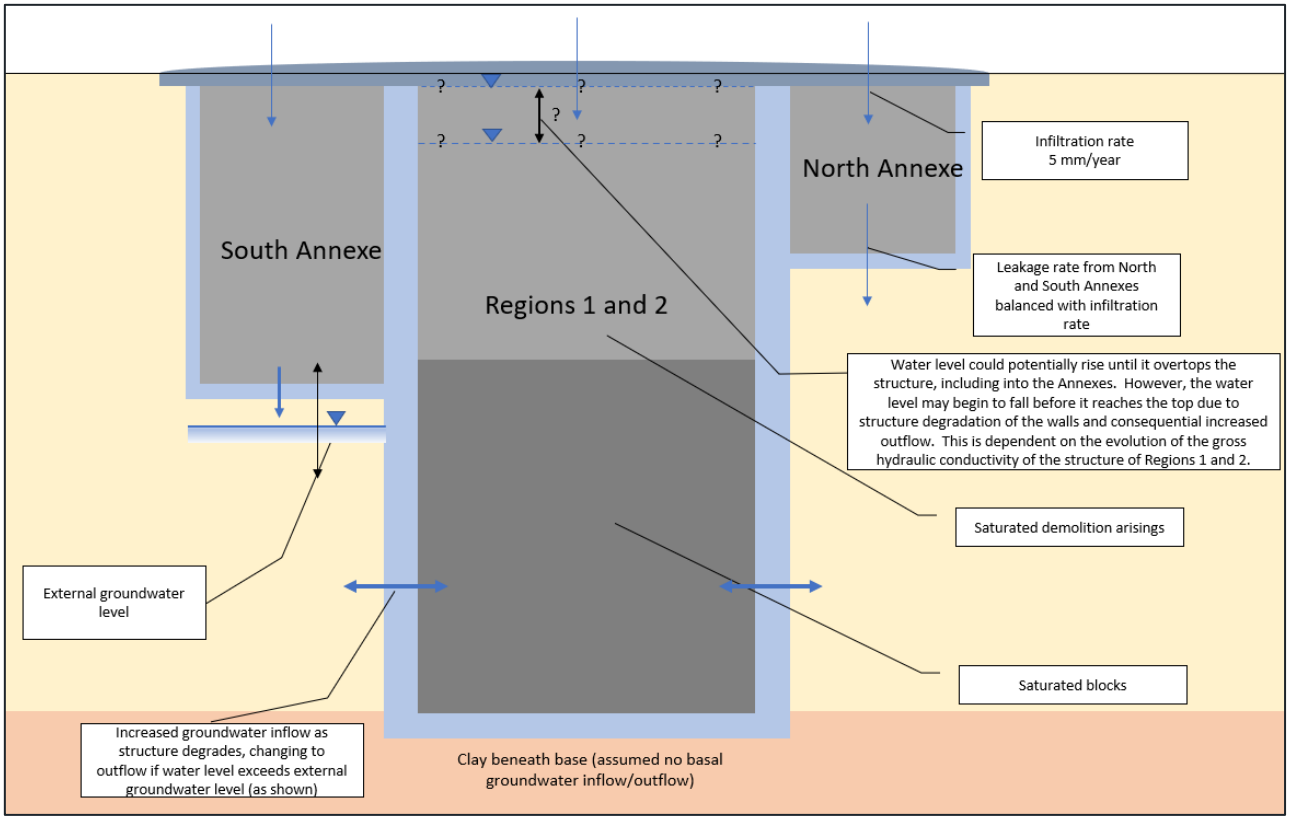

Figure 606/23: SGHWR End State water balance after approximately 100 Years

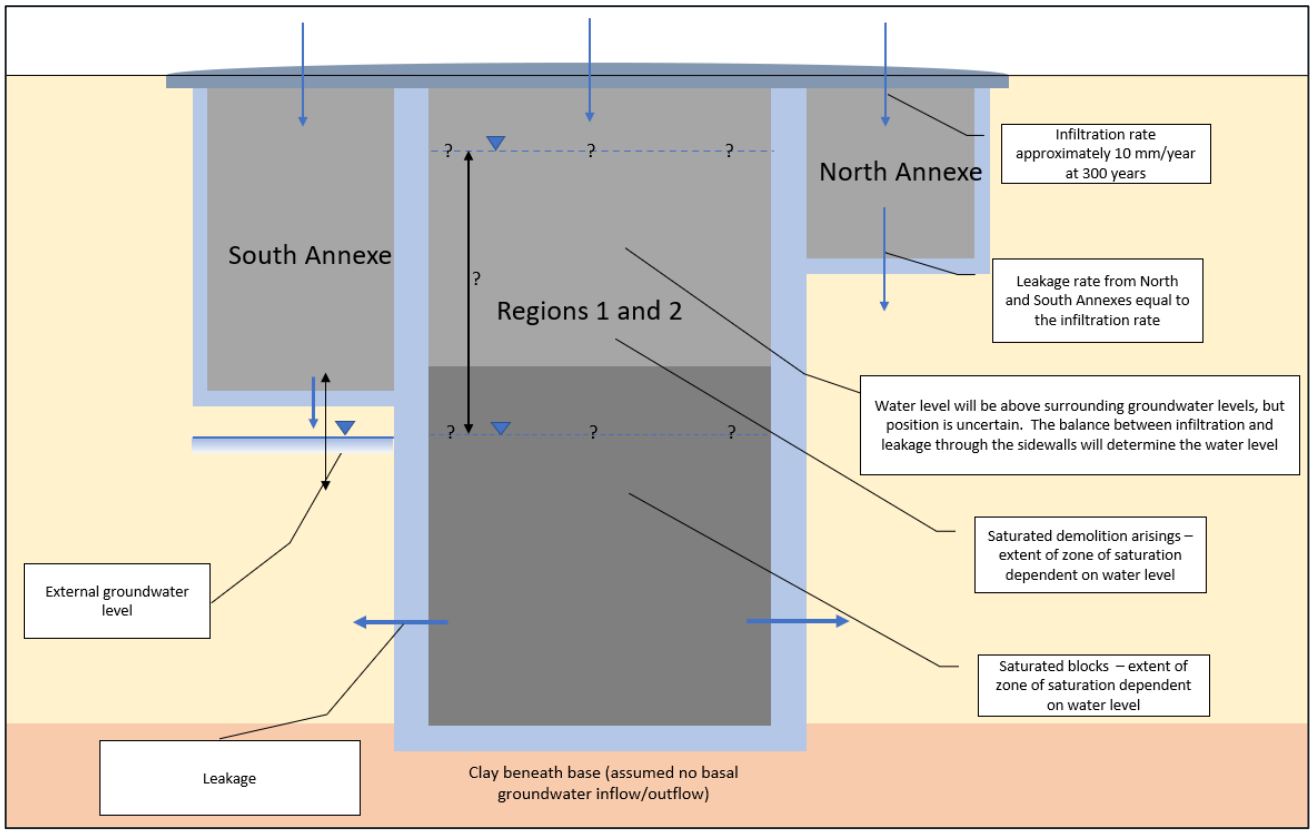

Figure 606/24: SGHWR End State water balance after approximately 300 years

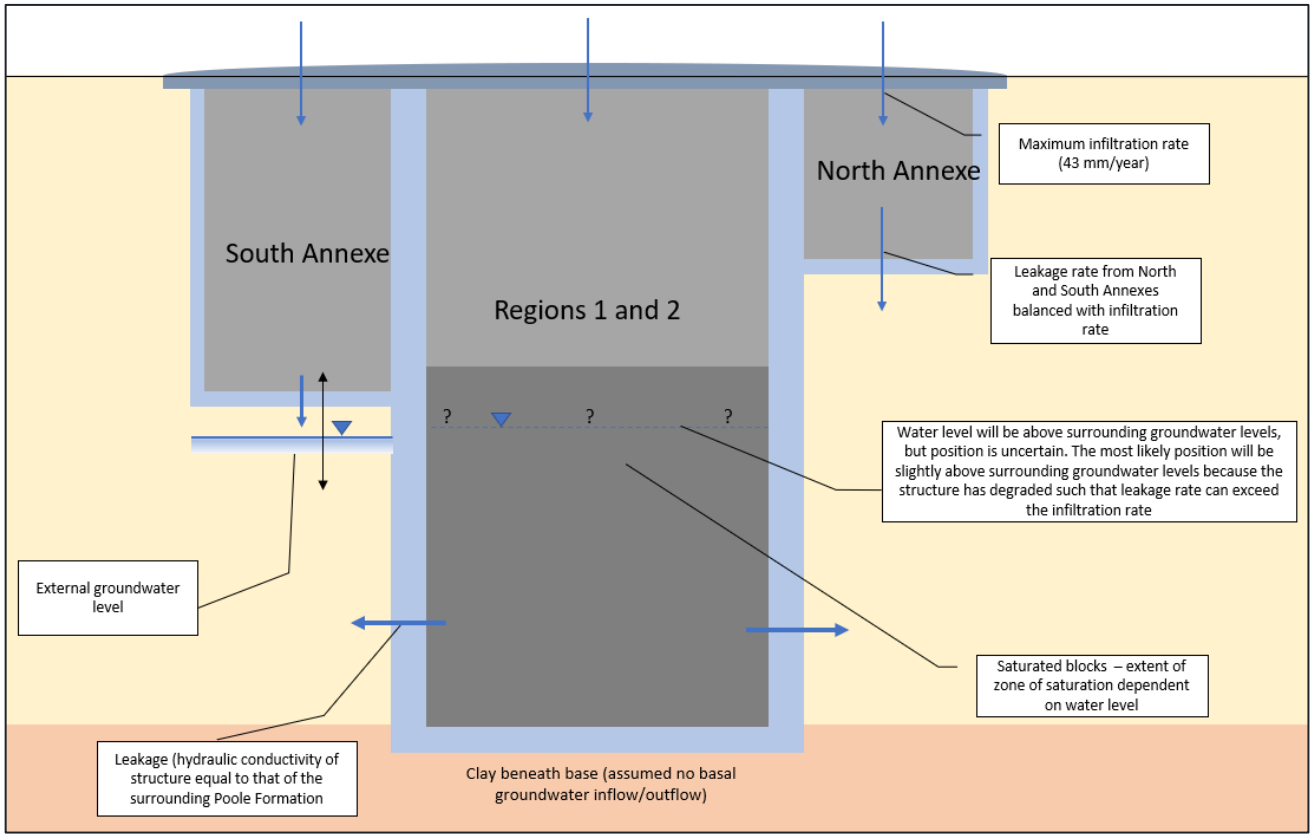

Figure 606/25: SGHWR End State water balance after approximately 1,000 years

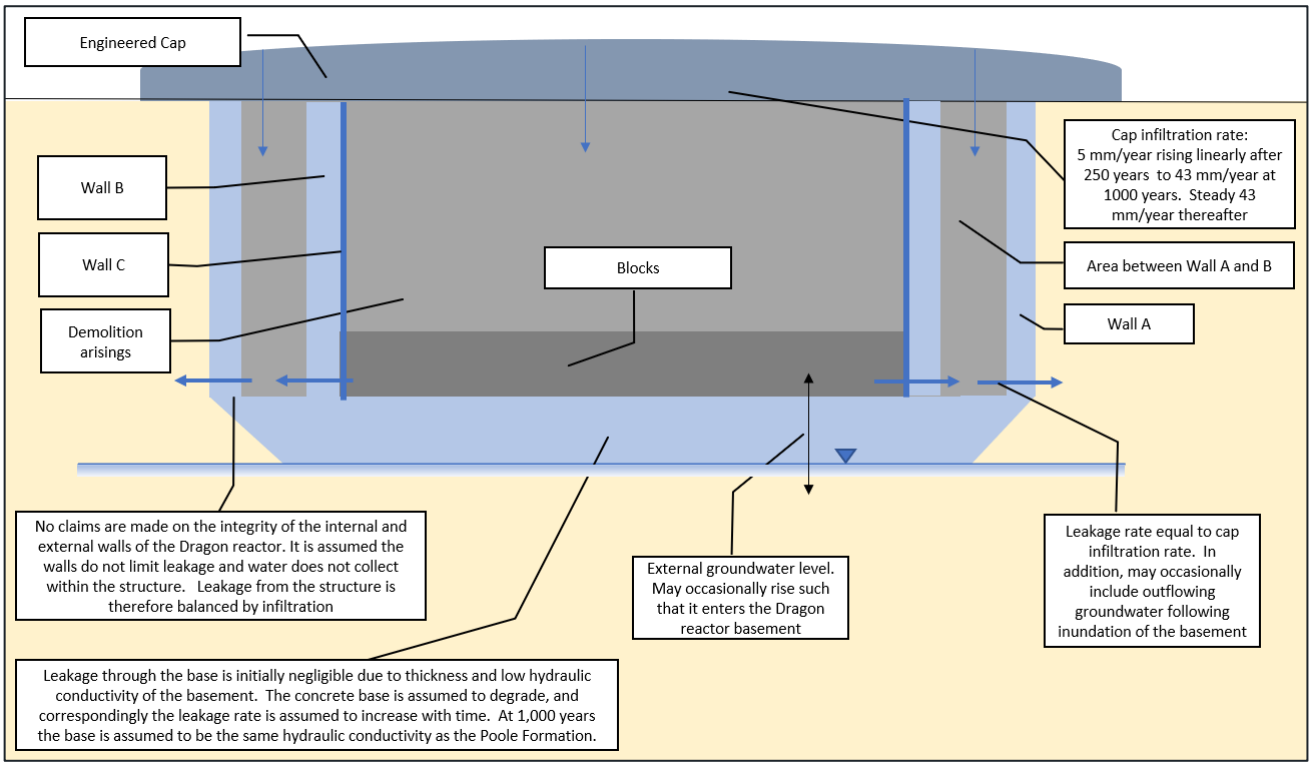

Figure 606/26: Dragon Reactor End State water balance

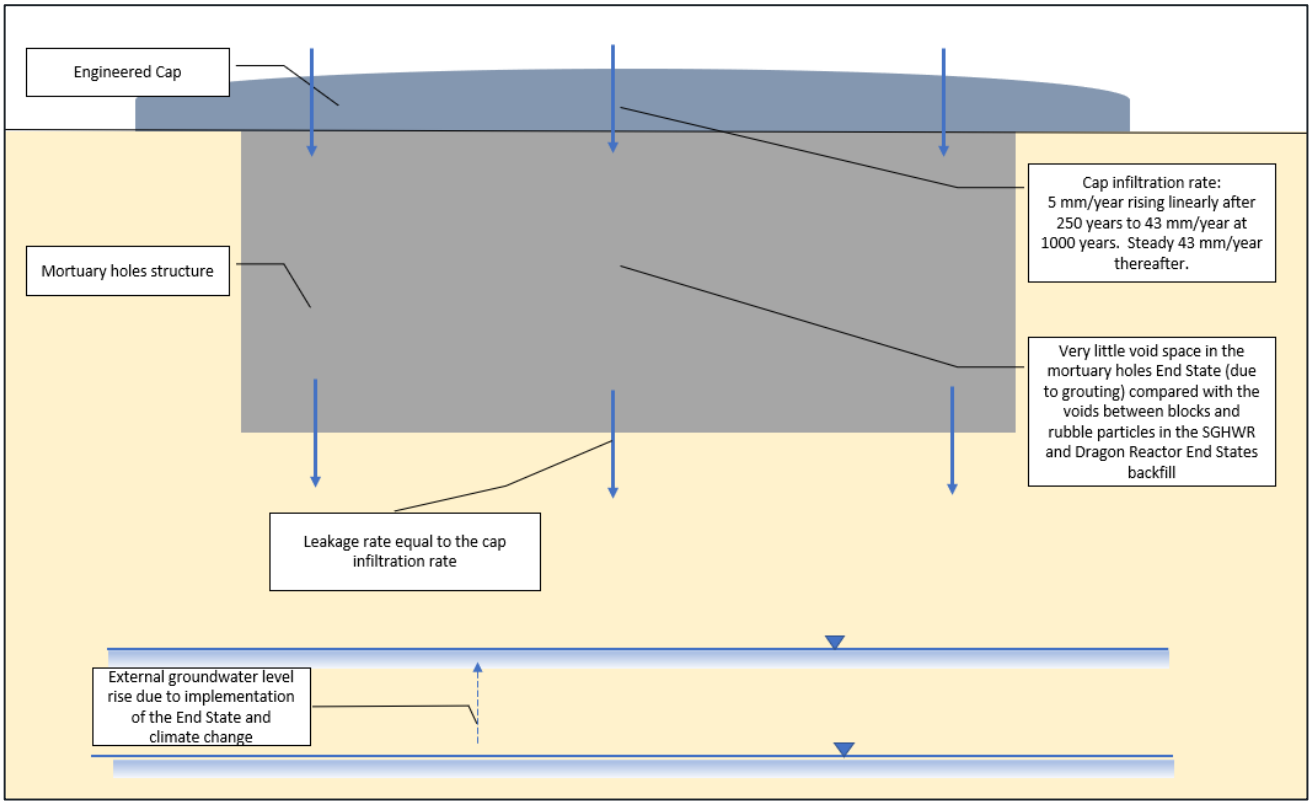

Figure 606/27: Mortuary holes structure End State water balance

5.5 MECHANISMS OF NEAR FIELD RELEASE OF NON-RADIOLOGICAL INVENTORY

Section 3 develops a water available inventory of non-radiological contaminants. Identified are three sources of water available non-radiological contamination:

- Oils in the near surface of the structures;
- Demolition arisings; and
- Structural metals and rebar.

The mechanisms for release of non-radiological contaminants from these three sources are described in the following sub-sections.

5.5.1 RELEASE OF OILS IN THE NEAR SURFACE OF THE STRUCTURES INTO THE DISSOLVED PHASE

Oil in the near surface of the floors and walls is expected to comprise a free phase component and a sorbed phase component.

The free phase component is assumed to be immobile, but it can dissolve directly into water. The sorbed phase component will partition between the water and the concrete and become partially dissolved in the water. Dissolution will be solubility limited. Both these processes require water to be in contact with the oil.

Accumulating water in Regions 1 and 2 (where oil-stained concrete surfaces are found) will saturate the concrete floor and walls and it is conservatively assumed that this results in full contact between water and oil. The dissolved phase oil contamination will migrate from the porewater in the concrete floor and walls to water within the demolition arisings by diffusion according to a concentration gradient. The diffusive flux of a contaminant will be further governed by the porosity and tortuosity of the concrete.

The concept of partitioning, dissolution and diffusion of the oil is illustrated in Figure 606/28.

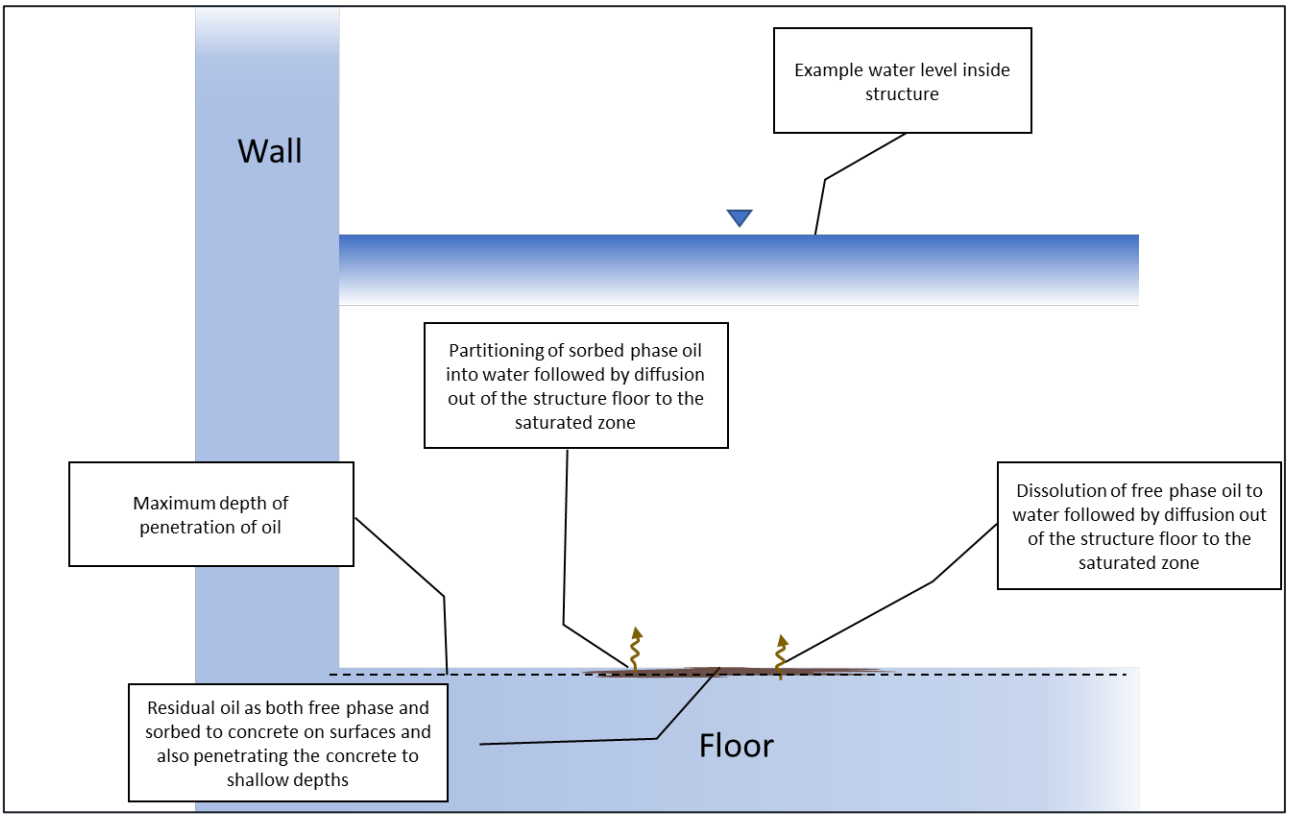

Figure 606/28: Illustration of dissolution, partitioning and diffusion of oil in the near surface of the structure into water (noting there will be wall and floor oil staining)

5.5.2 RELEASE FROM THE DEMOLITION ARISINGS

Inorganic contaminants within the demolition arisings deposited within the SGHWR and Dragon reactor structures will be present in the solid phase in the particles of the arisings.

The assessment inventory of the inorganic contaminants in the demolition arisings is presented in Table 606/25. The inorganic contaminants in the solid phase inventory will partition into water in the pore space within the particles and adjacent to the outer surface of the particles. Inorganic contaminants which have partitioned into the water within the pore space of the concrete particles will migrate by diffusion outwards through the particle to the surrounding water at a rate determined by the concentration gradient. These processes of dissolution, partitioning and diffusion are collectively referred to as leaching.

EA (2003a) states that the concentration of a species at any liquid to solid (LS) ratio, C_{LS}, in the porewater of the deposits because of leaching can be determined from:

$$C_{LS} = C_0 \, e^{-(K * LS)}$$

Where:

C_0 is the initial concentration of the species in leachate, usually determined when LS = 0.1 l/kg (EA, 2003a) (mg/l);

K (kappa) is a parameter specific to the contaminant and the material being leached (kg/l); and

LS is the liquid to solid ratio at time t (l/kg).

The LS ratio is the ratio of the cumulative volume of water that has passed through a fixed mass of material at a chosen point in time. It is therefore time dependent and will increase through time as water enters and leaves the disposals/deposits. The leach test analysis data (Table 606/25) describe the cumulative mass of each inorganic contaminant released from the solid phase into the water at a liquid to solid ratio of 10.

The assessment inventory for organic contamination in the demolition arisings is outlined in Table 606/24. Organic contamination is assumed to exist within the deposits either as free phase (for example, 'foreign material') between particles of concrete or, in the case of PCBs, sorbed onto the concrete particles. The PCB contamination, if it is in the form of staining, may also have penetrated the surfaces of the particles and be present as free phase or sorbed phase. The degree of penetration (if any) is uncertain, and it is assumed that the contamination is on the surface. This is conservative because outward diffusion through the particles is therefore not assumed to have a role in controlling the release of the contamination to the water.

A partition coefficient (K_d value) of a contaminant is the ratio of the concentration of the contaminant on the solid phase (C_s) to the concentration of the contaminant in the liquid phase (C_l) after equilibration:

$$K_d = \frac{C_s}{C_l}$$

A partition coefficient describes the degree of sorption that a substance will undergo to the solid phase assuming aqueous concentrations are not solubility-limited. The concentration of organic contaminants in the porewater will be determined by the degree of partitioning between the demolition arisings and water. Organic substances will sorb to solid organic carbon in the infill. The partition coefficient (K_d value) for an organic substance is the product of its species-specific partition coefficient to organic carbon (K_{oc}) and the fraction of organic carbon (f_{oc}) in the infill:

$$K_d = K_{oc}\, x\, f_{oc}$$

The concentration of all contaminants in water in the near field will be limited by species-specific solubilities.

5.5.3 RELEASE FROM STRUCTURAL METALS AND REBAR

Metal is contained within the structural concrete and concrete blocks as rebar and is also present within the SGHWR and Dragon reactor as components providing structural integrity, which will be retained post-demolition. The primary mechanism by which the constituents of these structural components will be released to water is via corrosion.

LLWR Ltd (2011a) provides corrosion data for mild steel in saturated and unsaturated conditions, allowing for an alkaline environment. Wood (2020) concludes that the range of corrosion rates is insensitive to saturation conditions, with a lower limit corrosion rate of 0.01 microns per year in either saturated or unsaturated conditions and an upper limit of 100 to 200 microns per year for saturated and unsaturated conditions, respectively. The 50th percentile value is around 1 micron per year in either case. These assumptions will be adopted in this assessment.

The I-beams in the SGHWR and structural steel in the Dragon reactor are exposed to water infiltrating the structures and water rising around them, and therefore the corrosion products can enter the water directly. The rebar inventory is encased in concrete, either in the blocks or in the structures' walls and bases. As corrosion of rebar progresses within the structure the amount of

corrosion products will increase. As summarised in section 5.1.2, the corrosion products take up more volume than the metals within the rebar. This increases stress within the concrete causing cracking and increased exposure of the rebar to water (Figure 606/29). I-beams and structural steel can be expected to be protected from corrosion, at least initially, by paint. There is uncertainty about how long it will take for water to fully access the I-beams, structural steel and rebar and initiate corrosion. It is therefore conservatively assumed that corrosion of I-beams, structural steel and rebar throughout the structures and concrete blocks will begin immediately post demolition and corrosion products will be instantaneously available to dissolve into water.

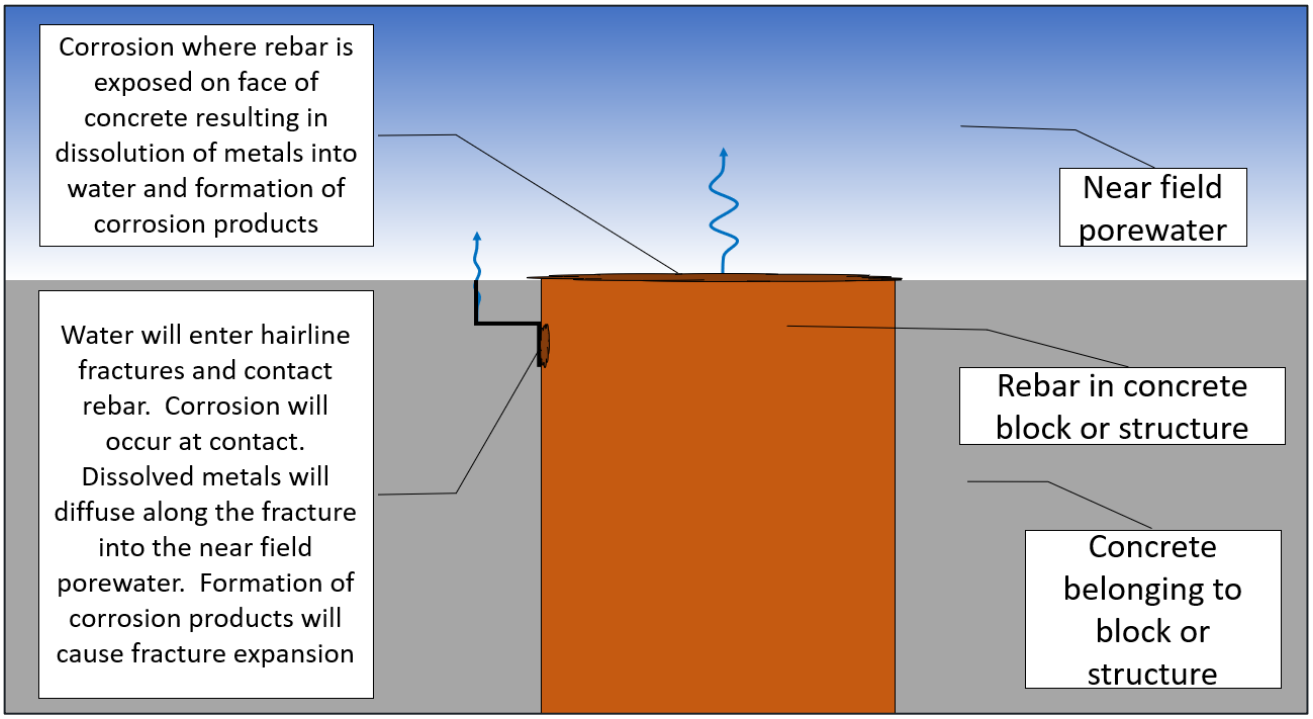

Figure 606/29: Process of corrosion / dissolution of metals in rebar

5.6 MECHANISMS OF NEAR FIELD RELEASE OF RADIOLOGICAL INVENTORY

5.6.1 RELEASE FROM THE DEMOLITION ARISINGS

The processes determining the aqueous concentrations of radiological contaminants (partitioning and diffusion) are the same as for inorganic non-radiological contamination, although the processes are considered individually rather than collectively as a leaching parameter. This difference in approach largely reflects a historical difference between non-radiological risk assessments and radiological PAs and is adopted for Winfrith due to the ready availability of modelling data from the scientific literature.

The demolition arisings are considered as a porous granular concrete material where the contamination is assumed to be homogeneously distributed throughout. Contaminants are released to porewater according to element-specific sorption parameters. Radionuclides are cautiously assumed to be instantaneously available for release from the source material to porewater from the point of implementation of the reactor end state. As the radiological contamination is expected to be predominantly associated with the surface of the demolition rubble, no diffusion is assumed before

contaminants are released into the advective water flow system described in section 6. Radioactive decay of the contamination is included during the time taken for release.

The K_d values are based on those measured for cement and are modified to take account of the proportion of cement to aggregate in the concrete. The cement K_d values are assumed to vary linearly over the 50,000-year period during which the concrete is assumed to chemically degrade from an initial near field value to that of the geosphere (taken to be the same as degraded concrete), as discussed in section 5.1.3.

5.6.2 RELEASE FROM STRUCTURES AND CONCRETE BLOCKS

Unlike for demolition arisings, diffusion of radionuclides through the concrete in-situ structures and emplaced blocks is modelled and the diffusion length reflects the anticipated distance of contamination into the concrete. For example, in the bioshield, most of the contamination has been formed at a significant distance into the concrete by neutron activation. In the pond walls, the contamination is shallower and relates to diffusion of contaminants from pondwater during operations. In the secondary containment, a significant part of the contamination is surface-based only. As for the demolition arisings, sorption to the cement in the concrete structures and blocks is accounted for as part of the release to the porewater and then into the advective flow system.

5.7 INFLUENCE ON NEAR FIELD PH OF THE DEMOLITION ARISINGS AND CONCRETE BLOCKS

5.7.1 MECHANISM OF OH^- RELEASE INTO THE NEAR FIELD POREWATER

pH is a physical measurement (it is equivalent to the negative log activity concentration of the hydrogen ion (H^+) in water) and is not, therefore, measure of a pollutant. Instead, it is the hydroxide (OH^-) ion that gives rise to the high pH of water in contact with freshly broken concrete that is a non-hazardous pollutant. The hydroxide ion concentration in water is related to pH via the equilibrium constant for water dissociation. The pH scale is exponential and a change of 1 pH unit is equal to an order of magnitude change in the OH^- concentration.

As water interacts with the cement within the demolition arisings and blocks either by infiltration or because of groundwater rising into the structure, OH^- ions within the cement will be released from the solid material to the water via dissolution. Dissolution will occur at the interface between water and the surfaces of clasts of demolition arisings and blocks.

Water will also penetrate the fabric of the clasts through interconnected pore space, including fractures. Dissolution of the OH^- ion within the pore spaces will occur, and the dissolved phase OH^- ions will migrate by diffusion into the near field porewater.

The rate of release of hydroxide into the near field porewater will be principally controlled by solubility (of mineral phases described in section 5.7.2) and the surface area available for interaction between the demolition arisings, blocks and water. The presence of fine-grained material within freshly broken concrete may be expected to cause more rapid release due to the increased surface area of the material compared to volume. However, Tompkins et al (2021) carried out a series of leaching tests on material from the D630 stockpiles and found that the eluate pH was lower in the smaller size fractions. This was attributed to enhanced carbonation of the higher surface area particles during storage, and it was concluded long-term stockpiling moderates the leachate pH produced from the weathered cementitious materials. The conclusion suggests there would be little benefit from removing the fines from the existing stockpiled material.

5.7.2 EVOLUTION OF NEAR FIELD PH

Sodium and potassium oxides, which make up around 0.3 and 0.1% by mass of cement, respectively, are highly soluble in water. Sodium and potassium hydroxides can raise the pH of water above 12.5. However, given their relatively low quantity, they are quickly depleted on surfaces exposed to water compared to portlandite and calcium silicate hydroxide (CSH) phases (see below). They are likely to have already been leached from demolition arisings in the D630 stockpiles and aged faces of concrete blocks. Leaching of sodium and potassium hydroxides is therefore disregarded.

The release of hydroxide to water in the near field from the demolition arisings proposed as infill for the SGHWR and Dragon reactor voids will principally occur through the dissolution of the hydrate minerals calcium hydroxide (portlandite) and CSH in the cement. Portlandite and CSH make up around 48.6% and 43.6% of cement by molar concentration, respectively (Amec Foster Wheeler, 2017).

The equation for portlandite dissolution is expressed as:

$Ca(OH)_2 \rightarrow Ca^{2+} + 2OH^-$

The release into water of OH^- increases the pH of the water. Pure cements increase the pH of porewater to ~12.5 (the solubility limit of portlandite). The OH^- that is released then may react with atmospheric CO_2 which results in increased groundwater alkalinity[24], predominantly as the bicarbonate ion (HCO_3^-) at circumneutral pH and carbonate (CO_3^-) at pH values greater than approximately 10. Alternatively, the released OH^- may directly and rapidly react with aquifer solids rather than be converted to bicarbonate in groundwater (described in further detail in section 6.4).

As leaching of portlandite and CSH phases depletes the source of OH^- ions, the pH in near field porewater will reduce from the portlandite equilibrium pH of ~12.5. Eventually all the primary cement minerals will be fully leached and only calcite precipitate will remain. At this point pH in the near field porewater will be controlled by calcite precipitation and dissolution and will be approximately pH 9.9. At this pH dissolved carbonate will dominate the dissolved inorganic carbon speciation.

The effect of carbonation of concrete clasts and secondary mineral formation, which could potentially reduce interaction of water with portlandite and CSH and thereby reduce the release of OH^- ions to the near field porewater, is complex and subject to significant uncertainty. Carbonation of concrete clasts will be conservatively disregarded.

[24] Alkalinity is the capacity of water to resist acidification. An increase of alkalinity, by for instance, an increase in the concentration of bicarbonate in solution does not necessarily cause an increase in pH.

6 AQUEOUS PATHWAYS FOR CONTAMINANTS

Section 6 outlines possible aqueous contaminant transport pathways, once contaminants are released from the near field, through both sub-surface engineered structures and the geosphere, and describes the processes of attenuation that will affect the concentrations of contaminants migrating along the aqueous pathways.

6.1 MIGRATION OF CONTAMINANTS THROUGH THE SGHWR AND DRAGON REACTOR END STATE STRUCTURES

Dissolved contaminants in the near field porewater in the SGHWR and Dragon reactor End States will migrate through the structure to the geosphere by advection through fractures (section 5.1.2) and, in the very long term following cement dissolution, through the matrix of the structure (section 5.1.3).

The way that the evolution of the hydraulic conductivity of structural concrete is represented is explained in section 5.1.4 and the changes in concrete porosity, dry bulk density and tortuosity brought about by cement dissolution are set out in section 5.1.5.

In the period shortly after the disposals are complete there will be no advective leakage from SGHWR Regions 1 and 2, as the hydraulic gradient will be inwards. Given the thickness of the walls and base, the migration of contamination to the geosphere by diffusion is not credible before internal and external water levels equilibrate and an outward hydraulic gradient is established within SGHWR Regions 1 and 2. Contaminants will move by advection through the walls affected to a small degree by mechanical longitudinal dispersion. Once outward advection is established, diffusion is assumed to play no part in contaminant transport through the structure.

For the purposes of non-radiological HRA and radiological PA no claims are made on the integrity of the North Annexe and South Annexe base slabs or the walls of the Dragon reactor (section 5.1.1). Advection from these regions of the SGHWR and Dragon reactor will be dominant from the outset. The effects of dispersion and diffusion are assumed to be negligible.

6.2 SUB-SURFACE PATHWAYS

6.2.1 GEOSPHERE PATHWAYS

Geological and Hydrogeological Summary

The geology and hydrogeology of the Winfrith site is detailed within the Hydrogeological Interpretation Report (NRS, 2024f). A summary of the geological sequence encountered beneath the SGHWR and Dragon reactor follows:

- Superficial Deposits (head, river terrace and alluvial deposits), up to 4 m thick (and locally absent), underlain by, and lithologically indistinguishable from, an up to approximately 30 m thick sequence of interbedded sand and clay of the Poole Formation. The Poole Formation has a high spatial lithological variability;

- The Poole Formation is underlain by sandy clay and sand of the London Clay Formation. The London Clay surface is interpreted to be around 30 m bgl to the northeast of the Winfrith site but has an unconfirmed depth to the southwest of the site (including beneath the SGHWR). The deepest parts of the SGHWR Regions 1 and 2 (i.e., the primary containment) lie within clay which may be the London Clay or may be a laterally extensive clay layer within the Poole Formation (NRS, 2024f). This is illustrated in Figure 606/30; and
- The London Clay is underlain by Chalk of the Portsdown Chalk Formation.

The Superficial Deposits are classified as either Secondary A aquifers (alluvium and river terrace deposits) or Secondary undifferentiated aquifer (head deposits). The Poole Formation is classified as a Secondary A aquifer of medium to high vulnerability. Although the Superficial Deposits and Poole Formation can be locally confined with depth or where extensive clay layers exist, they are assumed to be unconfined for the purposes of the CSM. The London Clay is considered to form a hydraulic base to the Poole Formation aquifer.

Once released from the structure, dissolved contaminants will migrate away from the near field through the unsaturated and saturated zones of the underlying Superficial Deposits and Poole Formation, which will be referred to collectively as the geosphere.

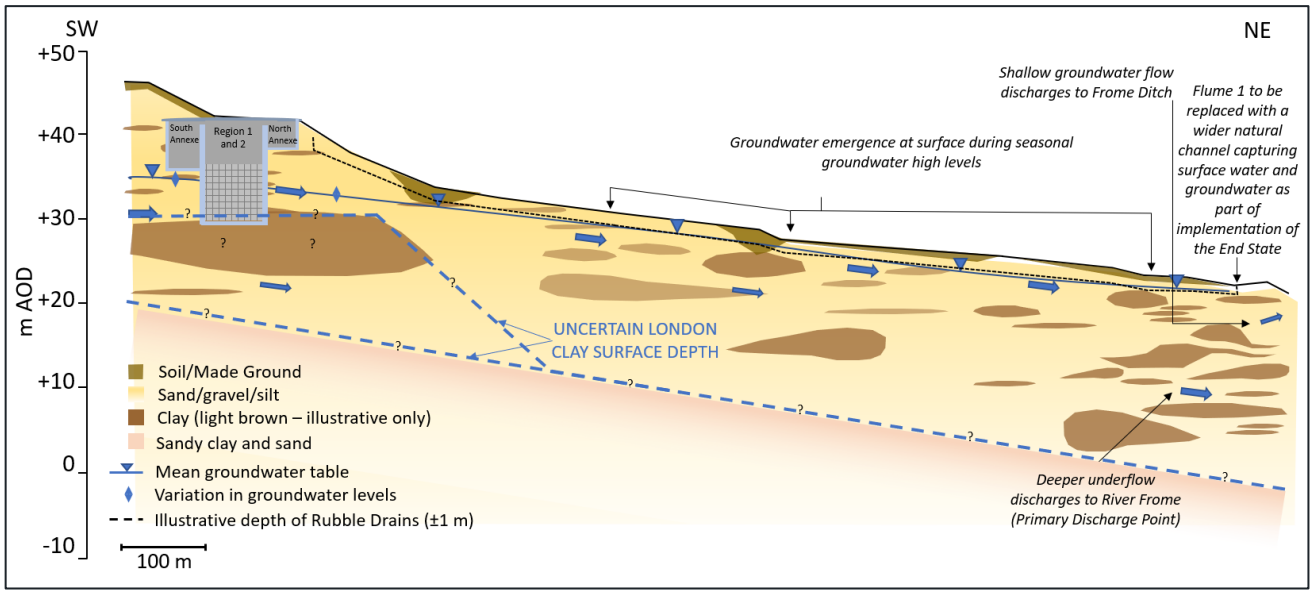

Figure 606/30: Schematic geological and hydrogeological section showing the SGHWR End State and the uncertainty over the London Clay surface elevation

Description of the Unsaturated Pathway

Based upon the difference between ground elevations and groundwater elevations, the unsaturated zone thickness (depth to groundwater) has been estimated for April 2003 when groundwater monitoring was completed for a high number of boreholes over a short period of time. In addition to the borehole data, points of groundwater emergence (zero unsaturated zone thickness) have been applied along the River Win, Frome Ditch and River Frome in Figure 606/31, taken from NRS (2024f).

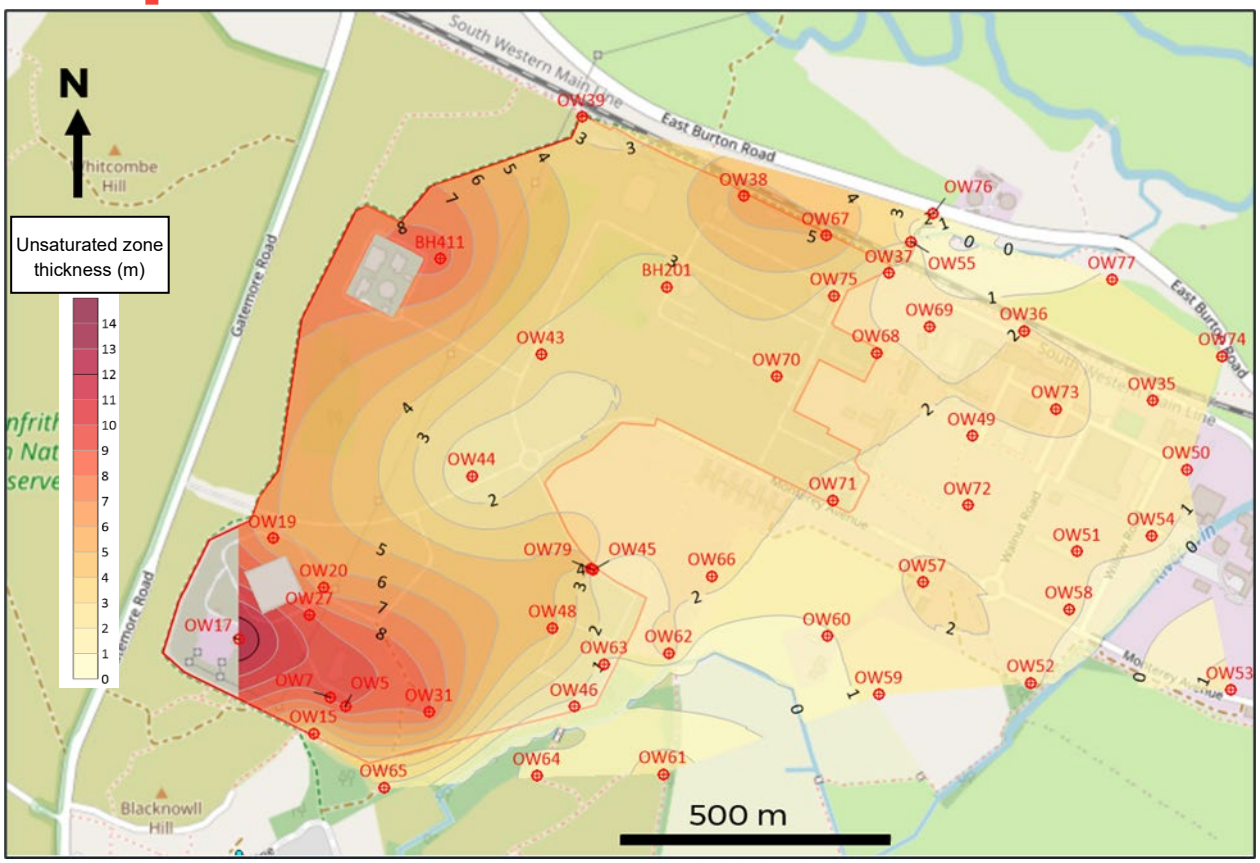

Figure 606/31: Unsaturated zone thickness (depth to groundwater, m) across the Site, 1 April 2003

In the period following site restoration an unsaturated zone will be present beneath the SGHWR North Annexe. Dissolved contaminants will migrate in water by gravity drainage and moisture displacement vertically downwards through the unsaturated zone and into the saturated zone. The width of the unsaturated pathway beneath the SGHWR North Annexe is assumed to be limited to the footprint of the structure above (i.e., there will be no lateral dispersion). The unsaturated zone thickness beneath the North Annexe may reduce over time, as described in sections 5.2 and 7.1, as water levels rise due to the implementation of the End State and the effects of climate change.

The unsaturated zone beneath most of the North Annexe is the Poole Formation. Nevertheless, some of the unsaturated zone consists of voids filled with gravel and zones of mass concrete. These volumetrically smaller parts of the unsaturated zone are ignored for the purposes of the CSM and the unsaturated zone is assumed to comprise the Poole Formation.

There will be no unsaturated zone beneath the deepest parts of SGHWR Regions 1 and 2. It is assumed that the entirety of SGHWR Regions 1 and 2 lies at or below the water table. The deepest parts of SGHWR Regions 1 and 2 rest on clay and Regions 1 and 2 are defined by structures with thick base slabs. Due to both geology and the base slab thickness, contaminants are assumed to migrate only through the sidewalls, and not the base slabs, of SGHWR Regions 1 and 2 structures to the saturated Poole Formation.

Following site restoration an unsaturated zone comprising the Poole Formation will be present beneath the Dragon reactor structure and SGHWR South Annexe for most of the time, but it will be cautiously disregarded. Contaminant migration from the Dragon reactor and the SGHWR South Annexe will be assumed to be directly into the Poole Formation saturated pathway.

Description of the Saturated Pathway

Groundwater flow in the Superficial Deposits/Poole Formation towards the River Frome is expected to dominate in comparison to downwards vertical flow from the Poole Formation through the lower transmissivity basal London Clay and into the underlying Portsdown Chalk Formation. Historically, boreholes have been drilled into the Portsdown Chalk Formation (e.g. Wimpey Laboratories, 1985 and 1991 cited by UKAEA, 1994). NRS will ascertain that these boreholes have been decommissioned or will make reasonable endeavours to locate and decommission them. On this basis, the geosphere saturated pathway for both the SGHWR and Dragon reactor End States is the Superficial Deposits/Poole Formation in which unconfined conditions are assumed. Historical boreholes to the Portsdown Chalk Formation and the London Clay and Portsdown Chalk Formation are disregarded as saturated pathways.

Prior to 2004 groundwater monitoring was undertaken in many boreholes across the Site and in a number of off-site boreholes to the east in the Dorset Innovation Park and to the north and south. Groundwater elevation contours for 1 April 2003, taken from NRS (2024f), are presented in Figure 606/32.

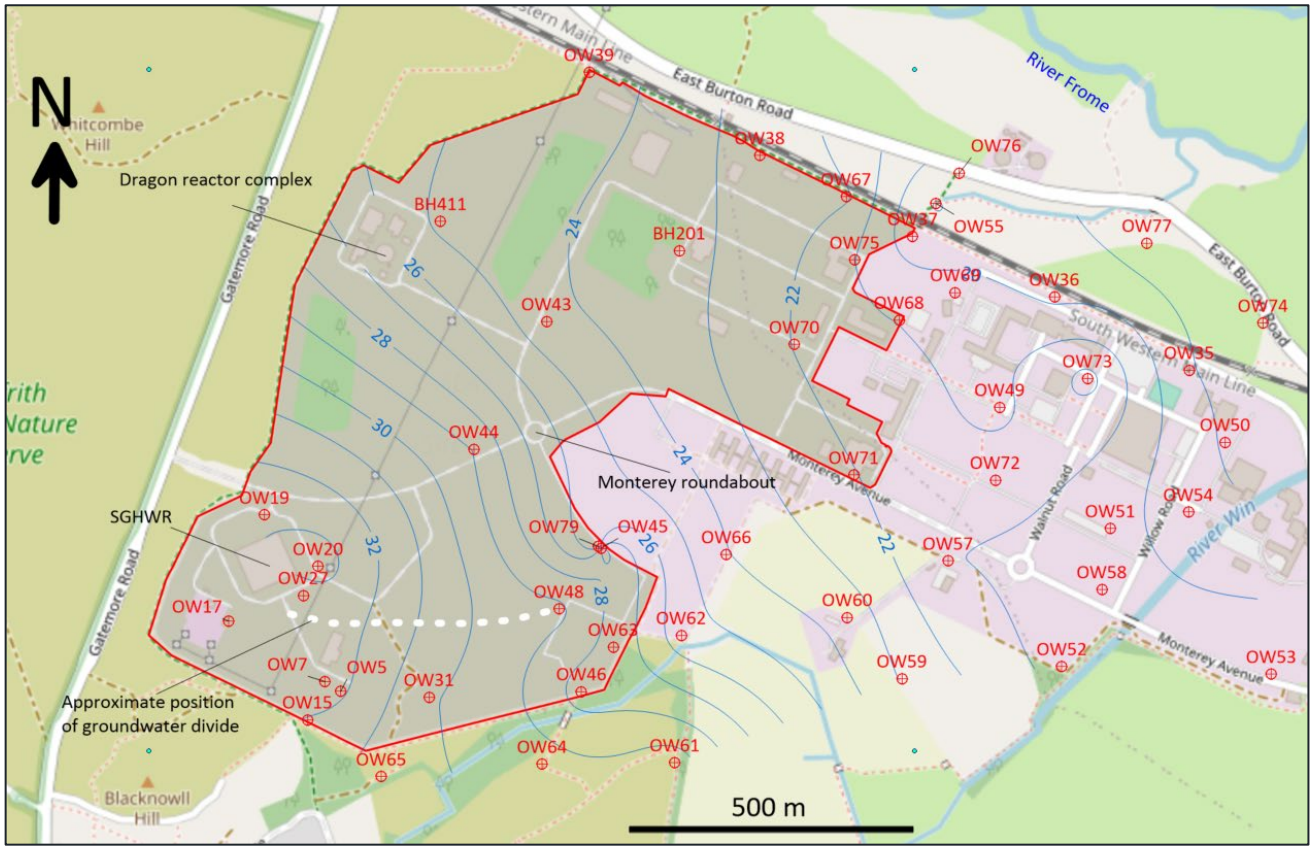

Figure 606/32: Groundwater elevation contours (m AOD) 1 April 2003

The saturated pathways for the SGHWR and Dragon reactor End States are defined as follows:

- The top of the pathway from the SGHWR is the water table and its base is the top of the clay into which the SGHWR Regions 1 and 2 are constructed; and
- The top of the pathway from the Dragon reactor is also the water table. The base of the Poole Formation is interpreted to be much deeper beneath Dragon reactor than beneath the SGHWR and it is judged unlikely that contaminants would disperse and diffuse over the full saturated zone thickness downgradient of Dragon reactor. Non-radiological contaminants migrating from the Dragon reactor are expected to mechanically disperse and diffuse over the upper part of the saturated zone. The vertical extent of this spreading is judged to be 5 m based on vertical dispersivity observations (Gelhar, 1992) and the flow path length. The vertical extent is consistent with Environment Agency guidance (EA, 2003b) that the screen length of groundwater monitoring boreholes should be less than 6 m. Radiological contaminants are assumed to spread over the same vertical thickness, but this thickness increases with rising groundwater levels beyond the IEP because the radiological PA is concerned with a longer saturated pathway than the non-radiological HRA.

The widths of the saturated pathways are equivalent to the widths of the SGHWR and Dragon reactor structures in the direction orthogonal to groundwater flow. The contrast in hydraulic conductivity between the Poole Formation and the parts of SGHWR Regions 1 and 2 below the water table means groundwater flow is deflected around the structure. Concrete degradation will progressively reduce the contrast and progressively more water will flow through the disposals/deposits in Regions 1 and 2.

Groundwater flow and contaminant transport is intergranular through the unconsolidated clay, sand and gravel of the Poole Formation. Whilst some perturbation in flow lines might be expected due to the presence of clay lenses in the Poole Formation, this is ignored. Groundwater at the SGHWR flows approximately north eastwards. A component of groundwater emerges west of the Monterey roundabout typically at a distance of approximately 450 m from the SGHWR although emergence might be closer when groundwater levels are high (section 7.1.3). From the Dragon reactor groundwater flows over 500 m north eastwards to discharge to the River Frome or at the ground surface nearby.

A single groundwater flow line would be unlikely to pass beneath all four regions of the SGHWR. Groundwater flow lines are likely to pass beneath one or two of the four regions only. However, to ensure conservatism in the results, i.e. that account is taken of the potential cumulative effect of leakage from all four regions, it will be assumed that groundwater receives leakage from both the South Annexe and North Annexe as well as from Regions 1 and 2. This is illustrated in Figure 606/34. The groundwater level is expected to rise through time as a result of increased recharge caused by climate change and the rate of groundwater flow along the saturated pathway will be assumed to change accordingly.

6.2.2 SUB-SURFACE DRAINAGE

The “rubble”[25] drains have been identified as potentially important engineered features for contaminant migration at the Winfrith site (NRS, 2024f). Groundwater interaction with “rubble” drains (filled with either rubble or rubble and pipework) is currently restricted to the central, eastern, and north-eastern parts of the Winfrith site. The captured water is ultimately discharged to Flume 1 via the surface water drainage system. The “rubble” drain maximum invert level depth is 3.1 m bgl in the vicinity of the Dragon reactor and 3.0 m bgl in the vicinity of the SGHWR. The water table is too deep to interact with “rubble” drains near the SGHWR and the Dragon reactor End States, both currently (NRS, 2024f, Figure 604/13) and following groundwater level rise under scenarios of intermediate climate change (Magnox, 2021c).

Current (early 2020s) groundwater interaction with other engineered sub-surface drainage features, such as the non-active drains, is understood to be restricted to parts of the drainage system that are structurally degraded.

In preparation for the End State, the functionality of the “rubble” drains will be removed by decommissioning. Some, or all, of the decommissioned “rubble” drains will be left in in situ unless they are radiologically or chemically contaminated in which case they will be removed (Magnox, 2019f). The “rubble” drains are shallow and volumetrically insignificant compared to the geosphere pathway. With time they can be expected to become fouled due to the ingress of surface derived fines. The hydraulic conductivity of the granular material of the “rubble” drains will progressively reduce and assume a bulk hydraulic conductivity equivalent to, or close to, that of the surrounding granular material of the Superficial Deposits and Poole Formation. It is assumed that the “rubble” drains will not become preferential pathways for groundwater movement and contaminant transport, and they are not considered further in the CSM.

6.2.3 SUMMARY OF KEY SUB-SURFACE PATHWAYS

A conceptualisation of the sub-surface pathways for contaminant migration from the SGHWR and Dragon reactor complex End States is presented in Figure 606/33 to Figure 606/36[26].
Figure 606/33 assumes sufficient time has passed beyond the IEP for Regions 1 and 2 internal and external water levels to have equilibrated[27].

[25] Whilst referred to as “rubble” drains, they are both open-channel ditches that are subject to maintenance (periodic dredging and clearance of vegetation); and trenches filled with “rubble”, or “rubble” and pipework. Given construction of the “rubble” drains was an early activity, the “rubble” is likely imported stone and not, as might be suggested by use of the word elsewhere on site, demolition arisings.

[26] Note that, due to their different radiological inventories, Regions 1 and 2 will be modelled as separate components in the radiological PA.

[27] The water inside Region 1 and Region 2 must equilibrate to a level slightly higher than the external groundwater level so the rainfall infiltrating the cap can flow through the walls in response to a head gradient.

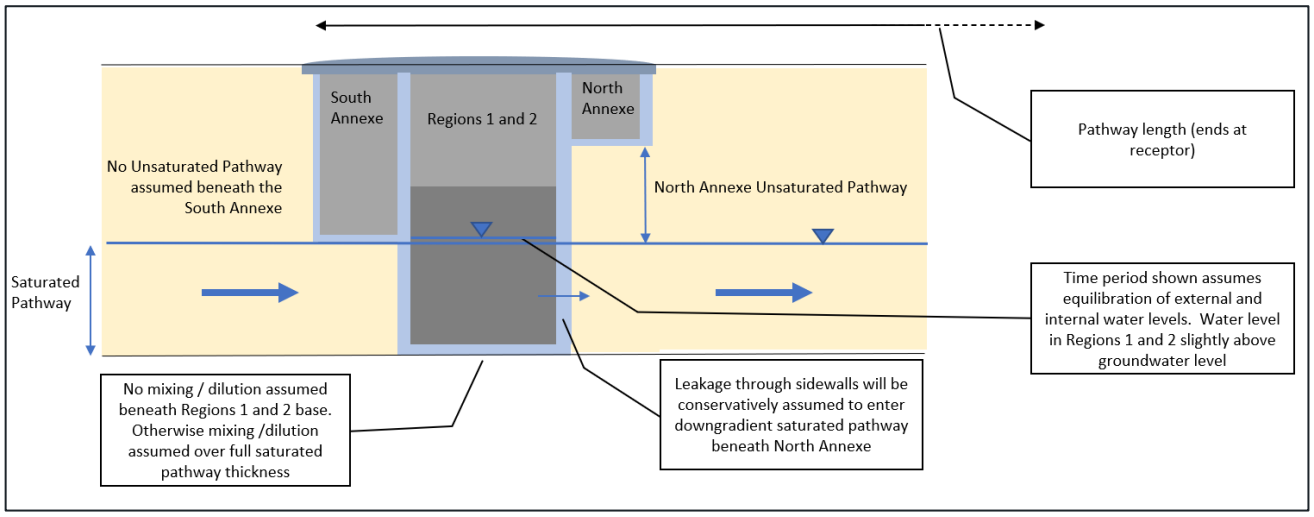

Figure 606/33: SGHWR End State geosphere pathway conceptualisation (cross section).

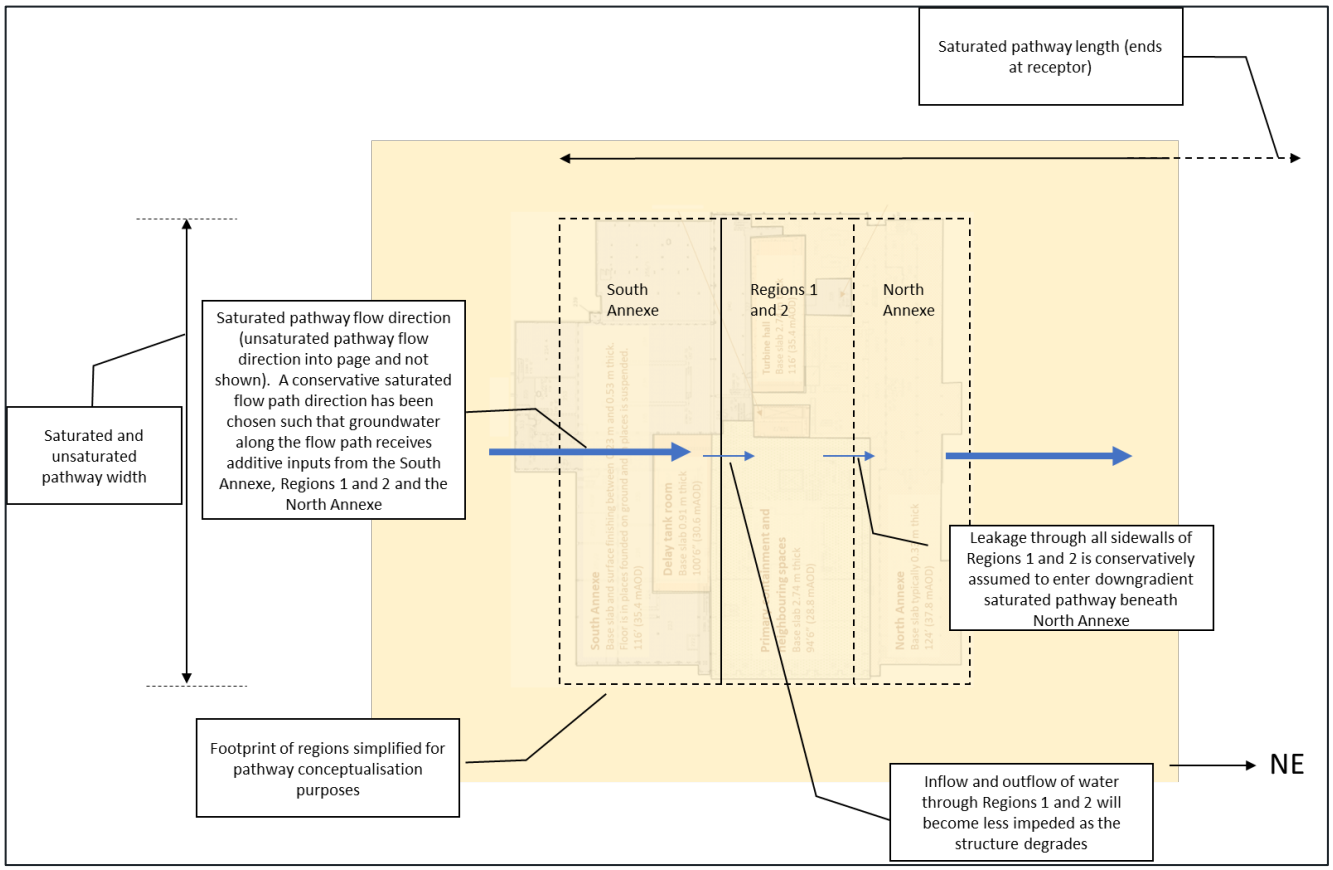

Figure 606/34: SGHWR End State geosphere pathway conceptualisation (plan view).

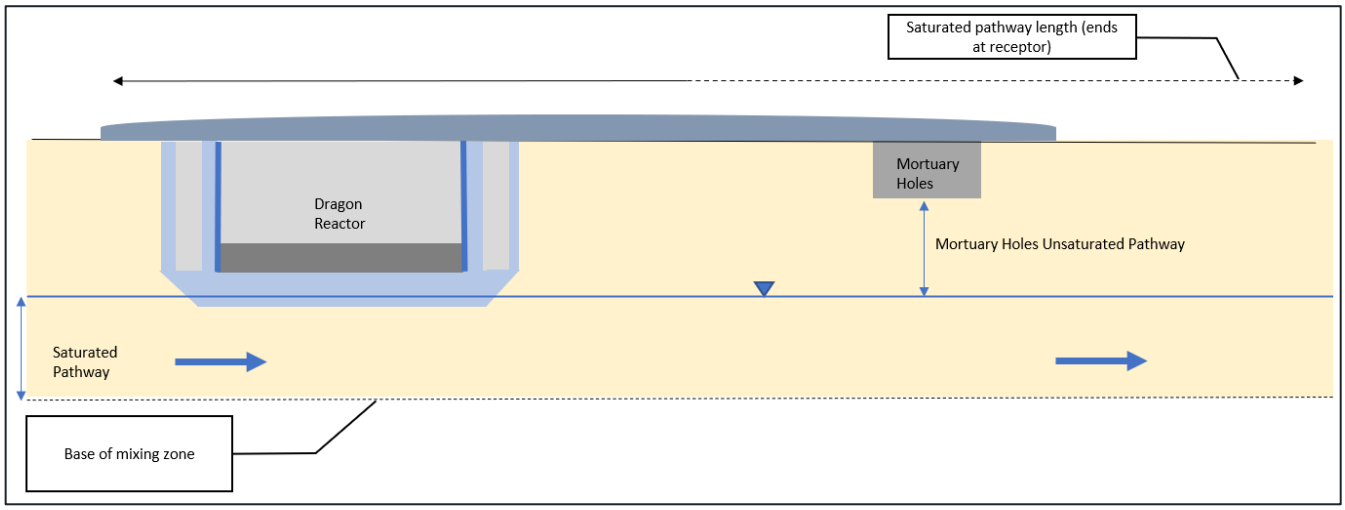

Figure 606/35: Dragon Reactor End State geosphere pathway conceptualisation (cross section)

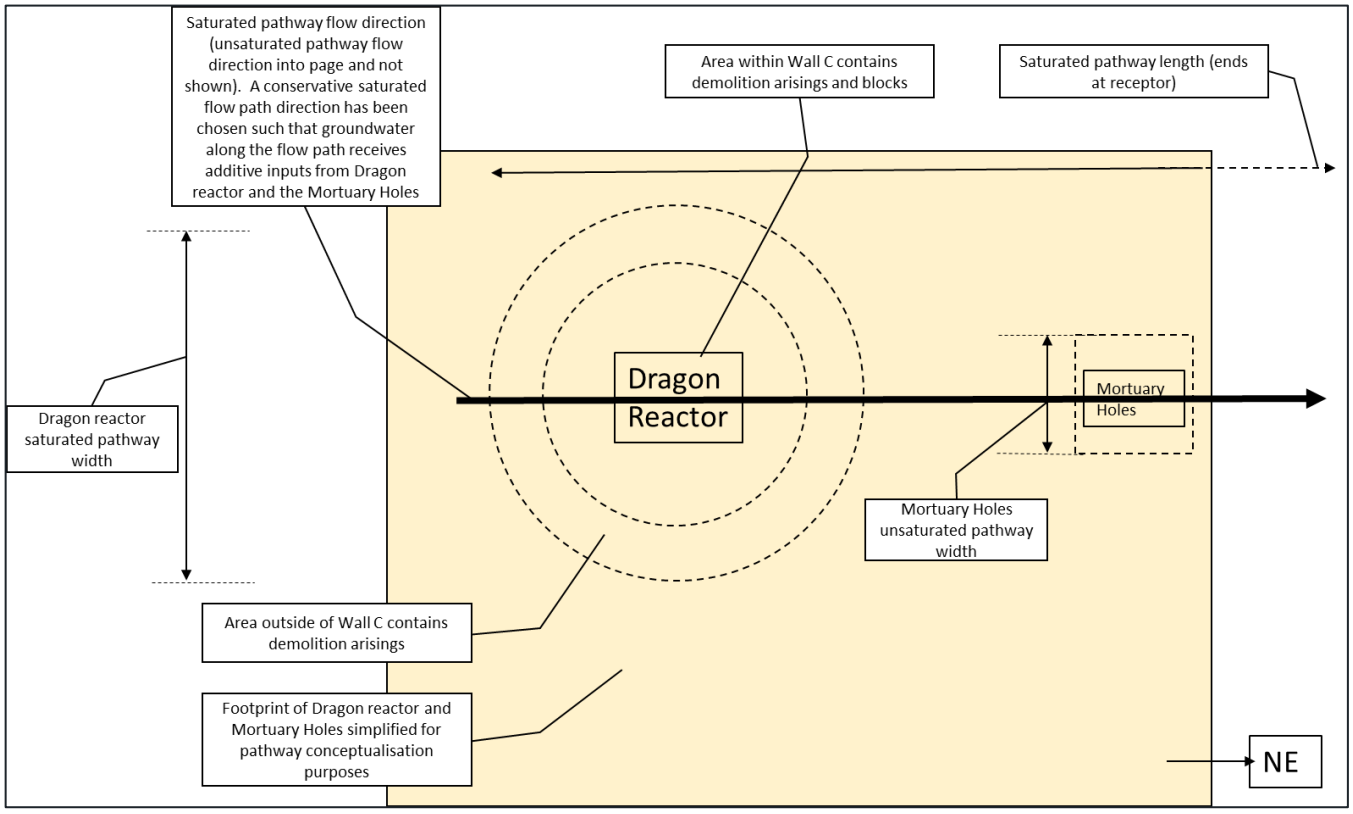

Figure 606/36: Dragon Reactor End State geosphere pathway conceptualisation (plan view)

As described in Figure 606/34 a flow path is assumed that can receive inputs from the SGHWR Regions 1 and 2 (assuming an outward hydraulic gradient exists) and the Annexes. This is a conservative simplification and results in the inputs of contaminants from Regions 1 and 2 and the Annexes being additive along the pathway length.

The ‘mixing zone’ described in Figure 606/35 for the Dragon reactor refers to the thickness of the saturated strata within which mixing and dilution of contaminants entering the groundwater will take place. For the purposes of this CSM the mixing zone is assumed to be 5 m thick at the IEP (section 6.2.1), and this will represent the saturated pathway thickness.

The deflection of groundwater flow caused by the slight penetration of the Dragon reactor End State below the water table is assumed to be insignificant and is disregarded.

6.3 ATTENUATION OF DISSOLVED CONTAMINANTS IN THE SUB-SURFACE (EXCLUDING ALKALINITY)

Processes which attenuate contaminants in the geosphere pathway and reduce contaminant concentration in groundwater include:

- Dilution;
- Dispersion;
- Radioactive decay of radionuclides;
- Biodegradation of organic compounds;
- Sorption; and
- Precipitation and/or coprecipitation.

Dilution

Contaminants from the near field will mix in groundwater and become diluted.

As the flow of water from the near field carrying contaminants increases due to degradation of the near field structures and the caps, the effect of dilution will reduce if there is no change in groundwater flow. Increased groundwater flow due to implementation of the End State and due to climate change will act to increase the dilution of contaminants migrating from the near field.

Dispersion

Mechanical dispersion is mixing caused by local variations in groundwater velocity around a mean advective velocity. Over time, mass becomes gradually more dispersed as water entrained matter (including dissolved contaminants) are transported at slightly different velocities. The main influence on mechanical dispersion is heterogeneity in the geological medium, which directly controls hydraulic conductivity. The greater the variation in hydraulic conductivity in a system, the greater the expected dispersion.

Mechanical dispersion can be assessed over a range of scales from the microscopic scale (at the scale of individual pore throats) to the regional scale (across different geological strata). At Winfrith, due to the high lithological variability across the site (sand and gravel with frequent clay layers), relatively high dispersion can be expected. The dispersivity is not anticipated to change (at least not significantly) with changes in groundwater level as the water bearing geological media have similar lithological characters.

The greatest directional component of dispersion would be expected in the direction of groundwater flow (i.e. in a northeast direction at Winfrith), and less so transverse to it (lateral and vertical). All contaminants will be affected by dispersion. Gelhar et al (1992) reviewed field-scale dispersion in aquifers. Based on this review, a longitudinal (in the direction of groundwater flow) dispersion of 10% of the pathway length is assumed in the saturated and unsaturated pathways. The effect of transverse dispersion is conservatively disregarded.

Radioactive Decay

Radioactive decay is represented using the following equation:

$$N_t = N_0 e^{-\lambda t}$$

where:

N_0: number of atoms at time t=0 (taken as the IEP);

N_t: number of atoms at time t years after the IEP; and

λ: radioactive decay constant (per year).

Radioactive decay can, for some radionuclides, be accompanied by in-growth of daughter products and the degree to which this is expected is explained by the radiological PA.

Biodegradation

Many organic substances undergo biodegradation in the environment. Biodegradation of hydrocarbon compounds is generally fastest under aerobic conditions. Organic biodegradation is typically described by first order decay, similar to the law for radioactive decay given above.

Biodegradation of petroleum hydrocarbons occurs under most subsurface conditions at a rate that means the dissolved phase plumes reach a steady state (the plume stops expanding) within a relatively short distance (typically found to be within about 100 m for a release of a few thousand litres or less from a retail petrol filling station) from the source (CL:AIRE, 2017). Biodegradation of hydrocarbon compounds is favoured by oxygenated conditions such as exist at Winfrith. Nevertheless, hydrocarbon compounds are conservatively assumed to be recalcitrant for the purposes of the CSM.

Literature review drawing on published studies over many years from the US, Finland, the Philippines, China, Pakistan as well as the UK finds that PCBs biodegrade in both anaerobic and aerobic environments. The review is summarised in the box below. The more chlorinated congeners are more recalcitrant and available measurements of half-lives are as long as 38 years. Biodegradation rates of naturally occurring organic compounds in the geosphere vary with changes in environmental conditions. Over the period assessed the degradation rate will not be constant. Factors, such as seasonality, could have an effect on microbial activity. Rather than attempt to quantify the variability of biodegradation rate and to ensure the assessment of PCBs in the Winfrith disposals/deposits is conservative, a half-life for all PCB congeners in the unsaturated zone and saturated zone of 50 years is assumed.

Review of PCB degradation rates

A 1983 review by the US EPA cites a 1980 study by Pal et al that categorises PCB decomposition rates in soils in three groups:

> *"Group 1 is for chlorinated biphenyls with 2 or fewer chlorines per molecule and Baxter et al. (1975) have shown that these degrade rapidly with half-lives of about 8 days. The second group contains the tri- and tetrachloro PCBs which have half-lives of 12 to 30 days. The third group, those with 5 or more chlorines, have half-lives in excess of one year. As with the biodegradation of any chemical in soils, biodegradation rates will vary greatly and depend upon the nature and viability of the microbial populations, the presence of other degradable organic matter, the moisture and oxygen content of the soils, pH, temperature and other environmental variables."*

ATSDR (2000) finds no known abiotic process that significantly degrades PCBs in soil and sediment. ATSDR (2000) reviews literature concerning anaerobic biodegradation of PCBs and cites half-lives up to approximately 5 years. ATSDR (2000) states:

> "*Aerobic degradation rates of PCBs can be highly variable, depending not only on structural characteristics. . . . but also on a number of other factors including previous exposure to PCBs or PCB-like compounds, bioavailability, initial concentration, moisture, temperature, available nutrients such as carbon sources, and the presence of inhibitory compounds. Biodegradation of PCBs in aerobic soil is slow, especially in soils that have a high organic carbon content*."

ATSDR (2000) cites laboratory aerobic sediment/water systems where half-lives up to 82 days were determined.

Borja et al (2003) review literature on the biodegradation of PCBs. They find that there are two biologically mediated PCB degradation processes: anaerobic and aerobic. The anaerobic process removes chlorine atoms of highly chlorinated PCBs, which are then mineralised under aerobic conditions.

The findings of a more recent literature review (Xiang et al, 2020) are little different. It finds that biological transformation of PCBs could take place through anaerobic dechlorination, aerobic microbial degradation, and a combination of anaerobic dichlorination and aerobic microbial degradation. Under anaerobic conditions microbial dichlorination is an important degradation mode for PCBs, especially high-chlorinated congeners. The low-chlorinated compounds could be aerobically degraded and completely mineralised. A contemporaneous literature review by Khalid et al (2021) identifies soil microbes and enzymes responsible for the degradation.

Sinkkonen and Passivirta (2000) report that anaerobic dechlorination has been observed in a large number of sediments. They cite half-lives calculated from monitoring Hudson River sediments and New Bedford Harbour sediments and suggest soil and sediment half-lives from 26,000 hours (3 years) for PCB 28 to 333,000 hours (38 years) for PCB 180 for modelling Baltic sediments. This study is cited by a review in Environment Agency (2007) that is concerned with a nationwide study of PCBs in soil and herbage. The Environment Agency study also describes a 13-year lysimeter study that suggests half-lives for PCB-28 and PCB-52 of 10.9 and 11.2 years, respectively. The mechanism of loss in this study could be volatilisation as well as biodegradation.

The Environment Agency (2007) study reports that UK soil PCB concentrations are declining from a peak in the 1960s of around 1600 µg/kg to 2 µg/kg in 2002. The contribution of the lower congeners to the soil loading has fallen more than that of the higher chlorinated congeners. The report is ambivalent as to whether this is because UK soils may be 'out gassing' lower congener PCBs or whether it reflects differences between the degradation rates in soil of lighter and heavier PCB congeners. Whatever the explanation it points to marked reductions in concentrations and an equivalent PCB half-life of less than 5 years.

Referenced studies:

Agency for Toxic Substances and Disease Registry (ATSDR), 2000. Toxicological profile for polychlorinated biphenyls (PCBs). November 2000.

Baxter, R.A., Gilbert, P.E., Lidgett R.A. et al., 1975. The degradation of polychlorinated biphenyls by micro-organisms. Science of Total Environment 4:53-61.

Borja, J., Taleon, D.M., Auresenia, J. and Gallardo, S., 2005. Polychlorinated biphenyls and their biodegradation. Process Biochemistry 40 (2005) 1999-2013.

Environment Agency, 2007. UK soil and herbage pollutant survey. Environmental concentrations of polychlorinated biphenyls (PCBs) in UK soil and herbage. UKSHS Report No. 8. June 2007

Khalid, F., Hashmi, M.Z., Jamil, N., Qadir, A., and Ali, M.I., 2021. Microbial and enzymatic degradation of PCBs from e-waste-contaminated sites: a review. Environmental Science and Pollution Research (2021) 28:10474-10487.

Pal, D., Weben, J.B. and Overcash, M.R., 1980. Fate of polychlorinated biphenyls (PCBs) in soil-plant systems. Residue Reviews, volume 74, Spring-Verlag New York Inc. pp. 52-69.

Sinkkonen, S. and Paasivirta, J., 2000. Degradation half-life times of PCDDs, PCDFs and PCBs for environmental fate modelling. Chemosphere 40 (2000) 943-949.

US EPA, 1983. Environmental transport and transformation of polychlorinated biphenyls. EPA 560/5-83-025.

Xiang, Y., Xing, Z., Liu, J. Qin, W., and Huang, X., 2020. Recent advances in the biodegradation of polychlorinated biphenyls. World Journal of Microbiology and Biotechnology (2020) 36:145.

Sorption/Desorption

Sorption (and subsequently desorption) involves the partitioning of dissolved contaminants between water (liquid phase) and mineral surfaces (solid phase), increasing the travel time of contaminants along the pathway (retardation).

Many inorganic substances readily sorb to the surface of metal hydroxides and phyllosilicate minerals (for example micas) which are abundant in clay; much more so than to feldspars and quartz which are found in sands and gravels. The chemical interaction between mineral surfaces and some inorganic substances, such as nickel, a heavy metal, is strong (i.e. they have a relatively high K_d value) resulting in contaminant travel times orders of magnitude greater than water molecules. For other inorganic substances, such as chloride, sorption is so weak that they can essentially be considered un-retarded in groundwater by this process.

Organic substances will sorb to solid organic carbon in the pathway. The partition coefficient for an organic substance is the product of its species-specific partition coefficient to organic carbon (K_{oc}) and the fraction of organic carbon (f_{oc}) in the pathway.

Other factors can cause retardation of either sorbing or non-sorbing pollutants (e.g. matrix diffusion) but they have been cautiously disregarded.

Precipitation and/or Coprecipitation

Precipitation is the process of a solid forming from a solution. This occurs when the solubility limit of a substance is exceeded, causing the excess substance to form a solid. Coprecipitation is the process of two or more substances forming a solid together from a solution and can occur when normally soluble compounds are carried out of solution by a precipitate. Changing geochemical conditions can lead to a solid forming from groundwater. For instance, dissolved iron in water precipitates when the water becomes oxygenated. Precipitation and/or coprecipitation are not envisaged to occur in groundwater downgradient of the disposals/deposits.

Table 606/38 presents a summary of the key attenuation processes anticipated to occur for the identified contaminant transport pathways.

Table 606/38: Overview of the Role of Attenuation Processes Over Time for the Main Identified Sub-Surface Contaminant Transport Pathways

Active Process	Below Ground Structures	Unsaturated Pathway	Saturated Pathway
Dilution	**No** – Assume no dilution	**No** – Assume no dilution	**Yes** – Dilution of dissolved contaminants derived from leakage from near field mixing with Poole Formation groundwater flowing from upgradient and with rainwater infiltration to the water table downgradient. Dilution potential will reduce over time as leakage rate increases due to barrier and cap degradation. Dilution potential will increase as groundwater flow increases due to climate change.
Dispersion	**No** – Insignificant within structure walls and base.	**Yes** – Longitudinal (vertical) dispersion. Dispersion is time invariant.	**Yes** – Longitudinal (horizontal) dispersion. Dispersion is time invariant.
Radioactive Decay	**Yes**	**Yes**	**Yes**
Biodegradation	**Yes –** hydrocarbons and PCBs but hydrocarbon compounds are conservatively assumed to be recalcitrant. For reasons of simplicity biodegradation is assumed time invariant.	**Yes -** hydrocarbons and PCBs but hydrocarbon compounds are conservatively assumed to be recalcitrant. For reasons of simplicity biodegradation is assumed time invariant.	**Yes -** hydrocarbons and PCBs but hydrocarbon compounds are conservatively assumed to be recalcitrant. For reasons of simplicity biodegradation is assumed time invariant.
Sorption	**Yes** – Sorption of inorganic substances and organic substances.	**Yes** – Sorption of inorganic substances and organic substances.	**Yes** – Sorption of inorganic substances and organic substances.
Precipitation / Coprecipitation	**No** – Assume geochemical conditions do not favour precipitation or coprecipitation	**No** – Assume geochemical conditions do not favour precipitation or coprecipitation	**No** – Assume geochemical conditions do not favour precipitation or coprecipitation

6.4 ATTENUATION OF ALKALINITY IN THE SUBSURFACE

This section describes attenuation of alkalinity in the unsaturated zone and saturated zone as a consequence of interactions with minerals and with the liquid and gas phases in the geosphere.

6.4.1 NEUTRALISATION

When alkalinity in water (e.g. leachate from infilled voids) mixes with acidic groundwater, attenuation of alkalinity may occur by neutralisation of hydroxide ions (OH^-) by protons (H^+), see equation 1, or by reaction with dissolved metals to form metal-hydroxides (examples are shown in equation 2 and equation 3). The decrease of hydroxide activity in the water leads to a decrease of pH and alkalinity.

$$OH^- + H^+ = H_2O \qquad \text{(equation 1)}$$

$$3\ OH^- + Fe^{3+} = Fe(OH)_3 \qquad \text{(equation 2)}$$

$$2\ OH^- + Mn^{2+} = Mn(OH)_2 \qquad \text{(equation 3)}$$

6.4.2 CARBON DIOXIDE DISSOLUTION AND CALCITE PRECIPITATION

Carbon dioxide dissolves in groundwater to form carbonic acid, as shown in equation 4. Carbonic acid can react with hydroxide ions to form bicarbonate (equation 5), which in turn can react with dissolved metals. The most common reaction is with calcium and precipitates calcite (equation 6). The two latter processes will lead to a decrease of pH and alkalinity.

$$CO_2 + H_2O = H_2CO_3 \qquad \text{(equation 4)}$$

$$H_2CO_3 + OH^- = HCO_3^- + H_2O \qquad \text{(equation 5)}$$

$$Ca^{2+} + 2\ HCO_3^- + 2\ OH^- = CaCO_3 + 2\ H_2O \qquad \text{(equation 6)}$$

6.4.3 REACTION WITH ALUMINOSILICATE MINERALS

The reaction of alkalinity by cation exchange with aluminosilicate minerals, such as feldspars found in the underlying strata leads to precipitation of calcium (aluminium) silicate hydrate (C-A-S-H) gels/solids (e.g., Savage et al., 1992).

The solid products of the interaction of alkalinity in groundwater and silicate rocks can include a wide range of minerals, such as clays, oxides, carbonates, feldspars, and zeolites, depending upon groundwater composition, host rock type, and geological history (Watson et al., 2018). Secondary clay minerals include saponite and montmorillonite (Watson et al., 2018).

These reactions, afforded by the cation exchange capacity provided by aluminosilicate minerals within the subsurface pathway, decrease alkalinity and pH.

6.4.4 SURFACE ADSORPTION AND DESORPTION

Surface adsorption of alkalinity (as carbonate) was initially identified (van Geen et al. 1994) as a result of carbonates blocking the adsorption of metal species on iron oxyhydroxide minerals, commonly referred to as ochre and given the notation HFO for hydrous ferric oxide. Such surface adsorption decreases porewater alkalinity and pH (equation 7 and equation 8). Both iron as HFO and aluminium as gibbsite or $Al(OH)_3$ provide adsorption sites within the subsurface pathway.

Mendez and Hiemstra (2019) find that the adsorption of carbonate on HFO reaches maximum capacity at approximately pH 6.5. As well as pH, surface adsorption of carbonate on HFO is dependent on ionic strength and surface competition. Should groundwater conditions change, carbonate can be released back into groundwater (desorption).

$$HFO\_OH + CO_3^{2-} + H^+ = HFO\_CO_3^- + H_2O \qquad \text{(equation 7)}$$

$$HFO\_OH + CO_3^{2-} + 2H^+ = HFO\_HCO_3 + H_2O \qquad \text{(equation 8)}$$

7 AQUEOUS RECEPTORS FOR CONTAMINANTS

This section describes receptors for contaminants migrating in water from the disposals/deposits: groundwater, water dependent terrestrial ecosystems and surface water. Scenarios by which humans could be exposed to radiological contaminants present in groundwater and surface water are identified and assessed in the radiological PA.

7.1 GROUNDWATER

This sub-section summarises information about groundwater as a receptor presented in NRS (2024f).

7.1.1 GROUNDWATER OCCURRENCE, GROUNDWATER UNITS AND AQUIFER DESIGNATIONS

Groundwater occurs in the Made Ground, Quaternary deposits, Poole Formation, London Clay and Portsdown Chalk.

The similarity in lithology (specifically the high sand content) of the Made Ground, Quaternary deposits and Poole Formation indicates that these formations can be treated as a single hydrogeological unit. Low hydraulic conductivity clay lenses within the Poole Formation may, however, cause a localised effect on the groundwater level and flow. Elsewhere clay lenses may result in water tables at a shallower elevation than the regional water table.

In the London area, the London Clay is traditionally considered, because of its high clay content there, to permit little groundwater flow and it is typically conceptualised as forming the base (or surface) of more transmissive near-surface aquifer units. However, further west, and beneath the Site, the stratum is generally more sandy. Where frequent and persistent clay layers exist, the London Clay can be interpreted to form a vertical barrier to flow. However, it is possible that sand rich zones exist which facilitate the vertical movement of groundwater locally at least through some of the London Clay. Nevertheless, the London Clay is considered to form a hydraulic base to the Poole Formation aquifer.

Although not hydraulically tested beneath the Site, the Portsdown Chalk is understood to be transmissive as evidenced by its use for public water supply between the Winfrith site and the coast (NRS, 2024f). As previously discussed, where clay-rich London Clay layers are laterally persistent, groundwater in the Chalk may be locally confined.

Alluvium and River Terrace Deposits, as well as the Poole Formation, are classified by the EA as Secondary A aquifers (Defra, 2020), which typically comprise permeable layers capable of supporting water supplies at a local rather than strategic scale, and which, in some cases, form an important source of base flow to rivers. The London Clay Formation is classified as an Unproductive Aquifer and has little or no resource potential and the Portsdown Chalk beneath the London Clay is a Principal Aquifer (Defra, 2020).

7.1.2 GROUNDWATER LEVEL AND FLOW AT THE IEP

Figure 606/37 shows the modelled hydrographs in simulated observation wells at the SGHWR and Dragon reactor complex for current conditions and at the IEP. The time shown on the graphs is to 2020. This is because the model has been run with a historical (1990-2014) recharge sequence with the intent of illustrating the effect on current conditions of implementing the End State.

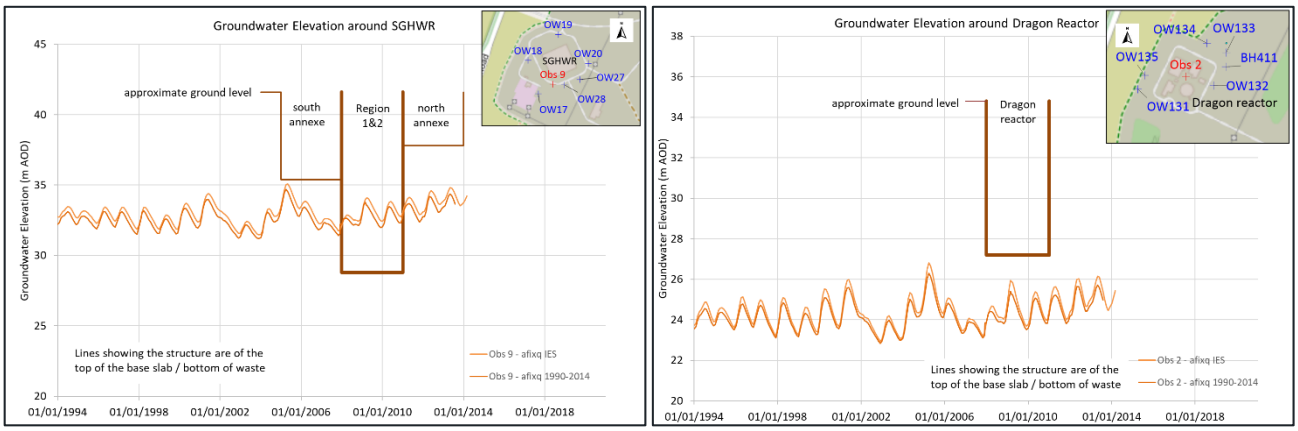

Figure 606/37: Modelled hydrographs at the IEP of the SGHWR and the Dragon reactor

The average groundwater elevation is modelled to rise by approximately 0.4 m at the SGHWR and approximately 0.3 m at the Dragon reactor due to implementation of the End State. Figure 606/37 shows that implementing the End State does not change the range of modelled groundwater levels. Groundwater levels are predicted to remain below the North and South Annexe of the SGHWR and below the Dragon reactor.

Groundwater recharge is on average expected to increase after implementation of the End State leading to an increase in groundwater flow. The decommissioning of “rubble” drains may lengthen groundwater flow pathways, but the general groundwater flow direction (Figure 606/32) is expected to be unchanged from present. Groundwater is expected to continue to discharge where it does at present. The decommissioning of “rubble” drains may mean groundwater locally discharges to the surface in places where this presently does not occur.

WSP (2024) presents the results of modelling of groundwater flow pathlines from the SGHWR and the Dragon reactor complex End States at the IEP. It was carried out to support development of the restoration management plan that includes excavation of ground in the north east part of the Winfrith site to allow a mire to develop. Seeds are released into the transient flow field close to the start of the model run in layer one of the model, i.e. the top 3 m of the saturated zone. This is to represent pathlines from the approximate elevation of the SGHWR and Dragon reactor deposits/disposals. The pathlines of the seeds were obtained with a transient flow field, where the water table is allowed to change during each recharge stress period, to reflect changing groundwater levels and flow directions over seasons.

The pathlines in layer one of the model are plotted in Figure 606/38, for a period starting from three years into the model run (in order to avoid early time modelling artefacts). Seed release sites are represented in Figure 606/38 with yellow dots, and pathlines as blue lines emanating from the release sites.

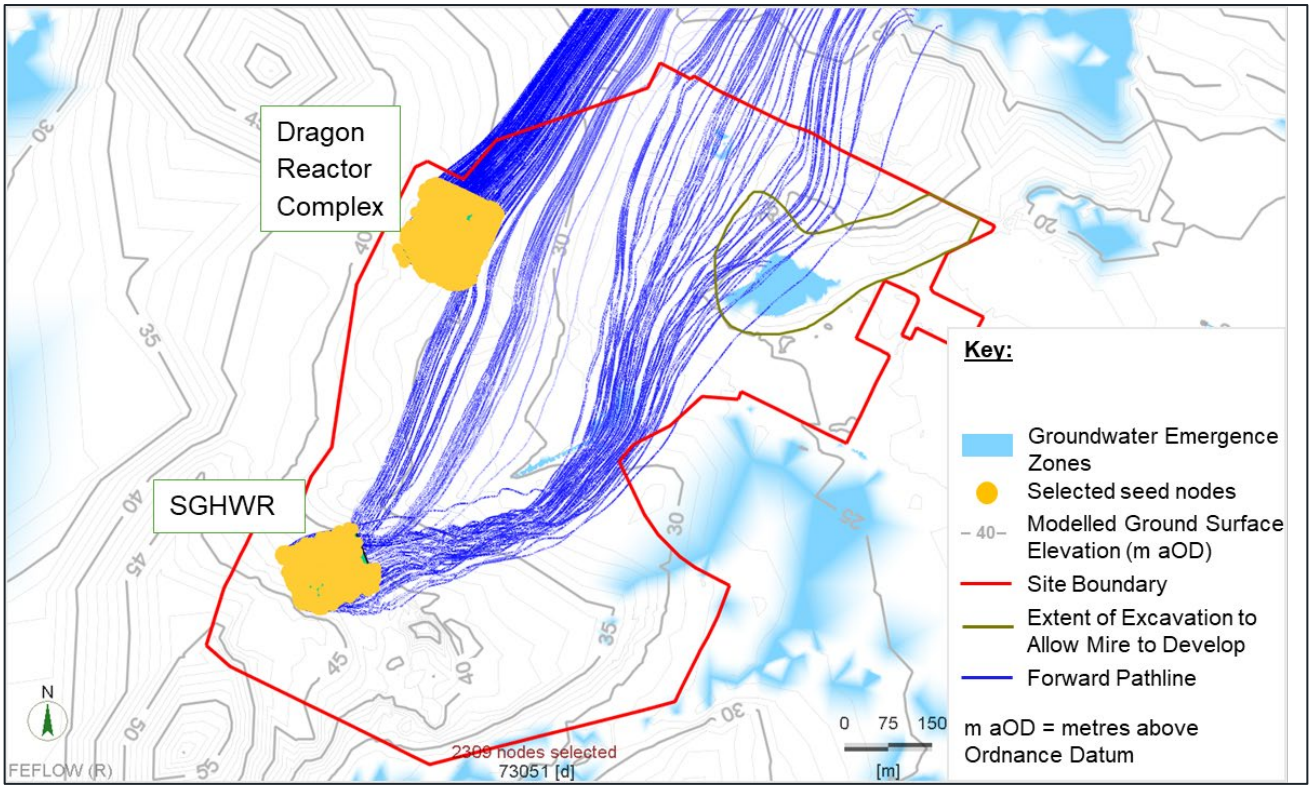

Figure 606/38: Modelled groundwater pathlines at the IEP (WSP, 2024)

Pathlines extend in a north-easterly direction from the Dragon reactor End State and north and north-easterly from the SGHWR End State toward the River Frome. Most of the pathlines indicate groundwater discharge directly into the River Frome. Modelled groundwater beneath the SGHWR flows close to, or emerges in, the proposed mire and groundwater discharges to the central area of the Site, west of Monterey roundabout, can occur.

7.1.3 GROUNDWATER LEVEL AND FLOW UNDER CONDITIONS OF CLIMATE CHANGE (TO 2080S)

Figure 606/39 and Figure 606/40 show the modelled hydrographs at the SGHWR and the Dragon reactor for the late 2050s and for the late 2080s, respectively, using recharge of a CCE model (of an 11-member ensemble of models) of future climate change under a medium greenhouse gas emissions scenario.

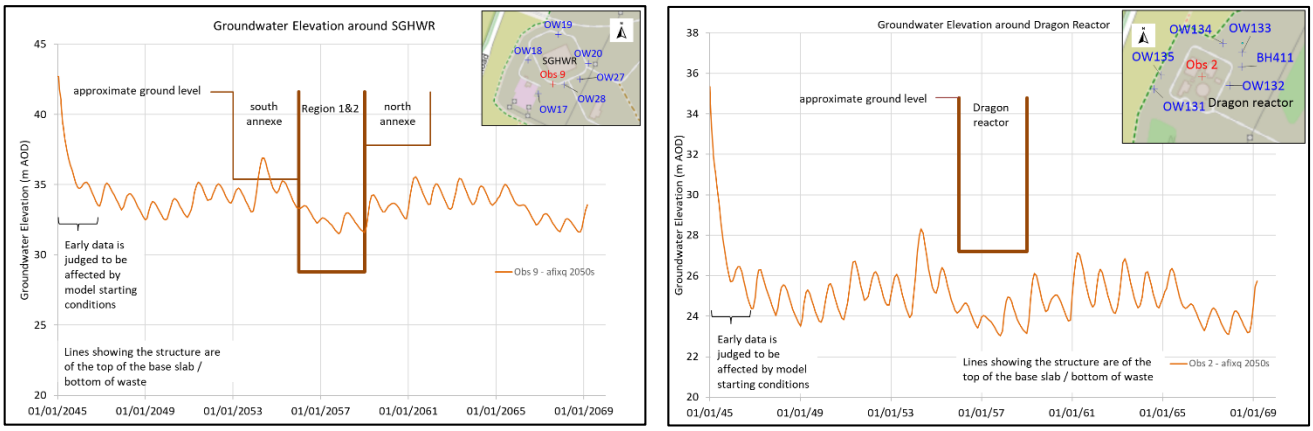

Figure 606/39: Modelled hydrographs for the 2050s at the SGHWR and the Dragon reactor for the CCE

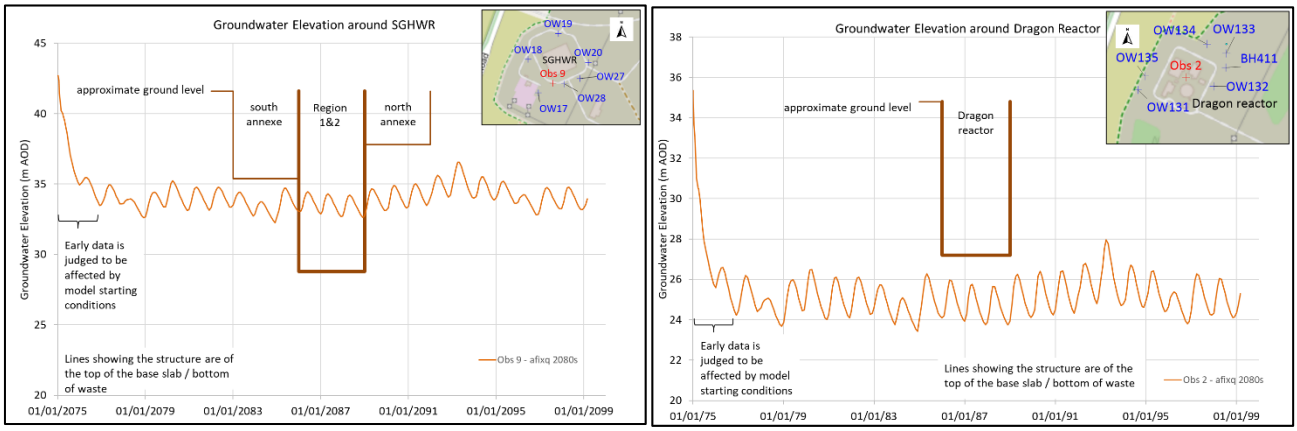

Figure 606/40: Modelled hydrographs for the 2080s at the SGHWR and the Dragon reactor for the CCE

The highest groundwater level in the modelled results at the SGHWR is 1.1 m above the base of the South Annexe and is 0.8 m above the base of the Dragon reactor, indicating that water will periodically enter the south annexe and Dragon reactor basements.

Groundwater elevation contours for the month in the 2080s (defined as 2070 to 2099) in which modelled groundwater levels are highest (May 2093) and locations where groundwater is modelled to emerge at the surface are shown in Figure 606/41.

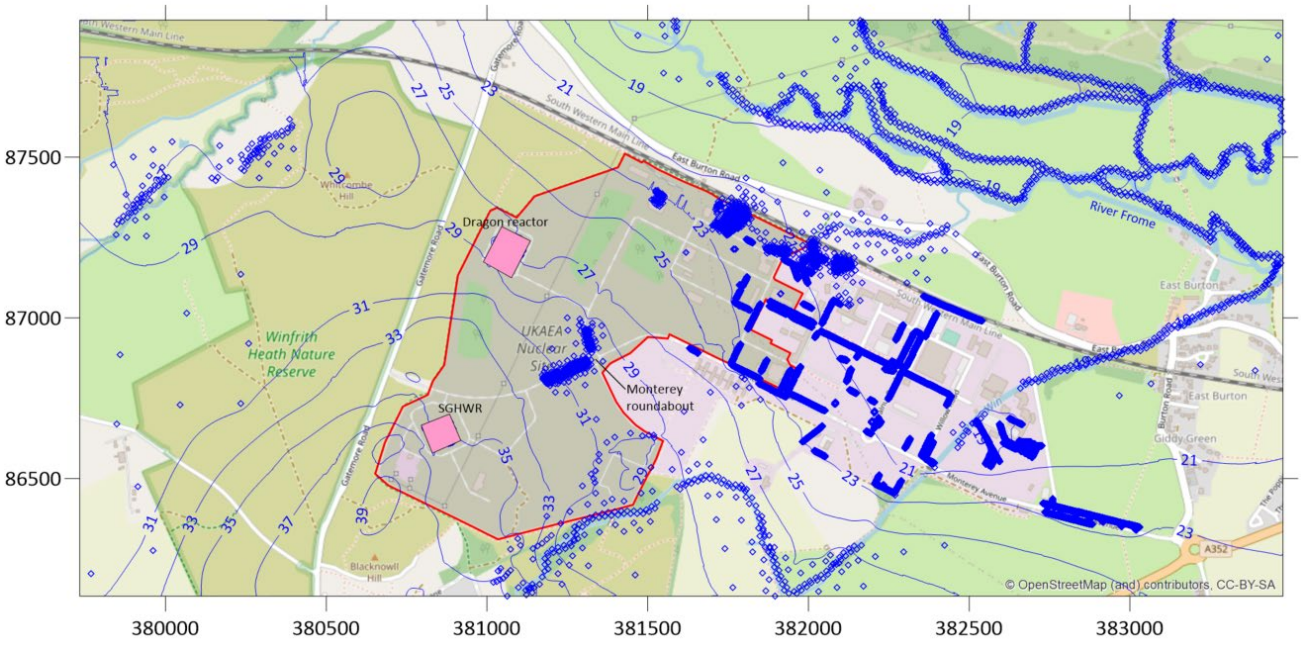

Figure 606/41: Groundwater elevation contours (m AOD) and locations of groundwater emergence (blue diamonds) for the highest modelled groundwater levels of the CCE simulation

Groundwater is modelled to emerge to the west of the roundabout on Monterey Avenue downgradient of SGHWR. Downgradient of the Dragon reactor, groundwater is modelled to emerge in low lying land close to, and in, the River Frome.

When the recharge of a reasonable worst-case model (of an 11-member ensemble of models) of future climate change under a medium greenhouse gas emissions scenario is modelled, the groundwater levels are modelled to be on average a little higher and the frequency with which groundwater rises above the top of the base of the South Annexe and Dragon reactor increases. The highest groundwater level in the modelled results at SGHWR is 1.6 m above the base of the South Annexe and is 1.4 m above the base of Dragon reactor. The locations of groundwater emergence are unchanged from those of the CCE simulation.

The pattern of pathlines from the SGHWR and the Dragon is little different to that shown in Figure 606/38 for the time of implementation of the Interim End State. The general features of the pathlines can be summarised as follows:

- Pathlines from the SGHWR End State emerge into the accessible environment from approximately 300 m north-east of the SGHWR End State when groundwater levels reach the ground surface during the particularly wet winter months.
- A small number of pathlines extend from the SGHWR End State to the River Frome. Other pathlines discharge to the ground surface in the River Frome valley.
- All pathlines from the Dragon reactor End State discharge to the River Frome or to the ground surface in the River Frome valley.

7.1.4 GROUNDWATER LEVEL AND FLOW BEYOND 2080S

IAEA (2020) provides a framework for modelling climate change in the periods 100 to 1,000 years in the future, 1,000 to 10,000 years, 10,000 to 100,000 years, and post 100,000 years.

On timescales of up to about 10,000 years, IAEA (2020) notes that the overall landscape is likely to remain similar in form to that observed at the present day, whereas the climate is likely to be as warm, or somewhat warmer, than at the present day. Thus, the climate-influenced processes of relevance to assessment models are likely to be similar to those of relevance at the present day, though their relative importance may change.

There is considerable uncertainty in the timescale over which the global surface air temperature will remain elevated compared to present and how long into the future it might be until the next glacial period. IAEA (2020) suggests that modelling studies indicate two potential future timings of the next glacial inception (although this is in northern latitudes and not as far south as Winfrith); around 50,000 years after present and around 100,000 years after present.

The EA has explained (Environment Agency, 2021b) that it is possible in the longer term (10,000 to 100,000 years) that aquifer-eustacy will become the dominant response to global orbital forcing cycles rather than glacio-eustacy as the Earth enters a 'warm greenhouse' phase as a result of anthropogenic carbon emissions. The glacio-eustacy model suggests that in a warm greenhouse world, there will be humid phases during which aquifers are recharged and groundwater levels are elevated, whilst eustatic sea levels are low. These will be interspersed with arid periods when aquifers discharge (groundwater levels are low) and eustatic sea levels are high.

Changes in global temperature are expected to persist after 2100 and will, potentially, have a significant impact on eustatic sea level through melting of land-based ice and thermal expansion of the oceans. However, for sites such as Winfrith that are inland and at elevation, changes in sea level will not be important. Therefore, the main impact of climate and temperature change at Winfrith will continue to be the changes in the amount and seasonality of precipitation and the knock-on effects on the water balance, on surface water and groundwater levels, and on flora and fauna.

Given the uncertainties in climate change beyond 2100, the following options have been considered for representing climate change in the long-term assessment modelling for Winfrith:

1) Assume present-day or End State conditions persist into the far future – this option has been adopted for assessments where the impact of climate change is considered low (e.g., East Northants (Eden, 2015); Clifton Marsh (Eden, 2010)).
2) Assume conditions expected at around 2100 persist into the far future – this option was adopted for the assessment for the LLWR where elevated precipitation rates were assumed to remain constant throughout the assessed post-closure timescale (LLWR, 2011b). Sensitivity analyses can consider different conditions based on different CO_2 emission scenarios.
3) Assume conditions evolve from 2100 according to one or more predictions – this option was adopted at Dounreay to consider a reference case and alternative cases with different rates of erosion and durations of elevated sea level and precipitation. The reference case considered that elevated sea level and precipitation persist for 50,000 years (DSRL, 2013).
4) Use a mixture of 1, 2, and 3 to derive one or more bounding analyses – this option was adopted in the Winfrith assessments used to inform the 2020 BAT workshops.

For the non-radiological HRA and radiological PA, it is proposed that assessments of climate evolution until 2100 be adopted and it will be assumed that the conditions at 2100 persist into the far future for each climate scenario considered.

7.1.5 BACKGROUND GROUNDWATER QUALITY

Groundwater beneath the Site is fresh and within potable limits. The electrical conductivity is lowest at the western edge of the site and is higher under the developed parts of the site. There is a tendency for the electrical conductivity to be lower than typical in winter months when groundwater recharge can be expected to have been higher. Samples of groundwater collected from boreholes in heathland areas are typically sodium-chloride type to sodium/calcium-chloride/sulphate type. Samples of groundwater collected from boreholes in the east of the Site are calcium-bicarbonate type. Groundwater flowing from beneath the heathland onto the developed parts of the site transitions between the two water types and this occurs beneath the SGHWR. Under heathland the median pH is typically less than 5.5 (and as low as 4). Under ground cover that is not heathland, including the developed parts of the Site, the pH rises to neutral (pH 7).

7.2 WATER DEPENDENT TERRESTRIAL ECOSYSTEMS

In the area of groundwater emergence west of the Monterey roundabout a water dependent terrestrial ecosystem has developed. The feature lies within the zone of modelled pathlines from the SGHWR End State under assumed conditions at the IEP, as described in section 7.1.2, and also when recharge sequences representative of CCE and reasonable worst-case variants of future climate change are modelled. It should therefore be considered as a potential receptor for contaminants migrating in water from the disposals/deposits.

The feature is a wet heath/acid mire. The National Vegetation Classification (NVC)[28] M16 water dependent terrestrial community currently found within it is characterised by *Sphagnum Compactum*. It is interpreted by Atkins (2024) that the “rubble” drains in this area have played an important role in allowing the *Sphagnum* to develop and persist.

As described in Atkins (2024), *Sphagnum* is intolerant to added or formed bicarbonate (HCO_3^-) such as that of the deeper Ca-HCO_3^- type groundwater of the Poole Formation beneath the central and eastern areas of the Site. NRS (2024f) explains that deeper groundwater is likely intercepted by the “rubble” drains in this area and that the shallow groundwater that currently manifests has likely been locally recharged by rainfall.

The localised recharge water of relatively short flow lengths has significantly lower HCO_3^- than that of the deeper groundwater. Consequently, the layer of shallow, relatively low bicarbonate, water over the deeper groundwater has provided a near/at-surface environment within which *Sphagnum* can develop. The monitored shallow groundwater layer has lower pH than that of the deeper groundwater in the Poole Formation, as demonstrated by well head measurements from shallow hand auger holes (Figure 606/42). The lower pH is an expected consequence of the presence of the *Sphagnum* which acts to engineer a favourable ecosystem for itself firstly, by exchanging hydrogen ions for nutrient cations and secondly, by production of organic acids via decomposition (Atkins, 2024).

[28] The NVC is a comprehensive classification and description of the plant communities of Britain, each systematically named and arranged and with standardised descriptions for each (Rodwell, 2017).

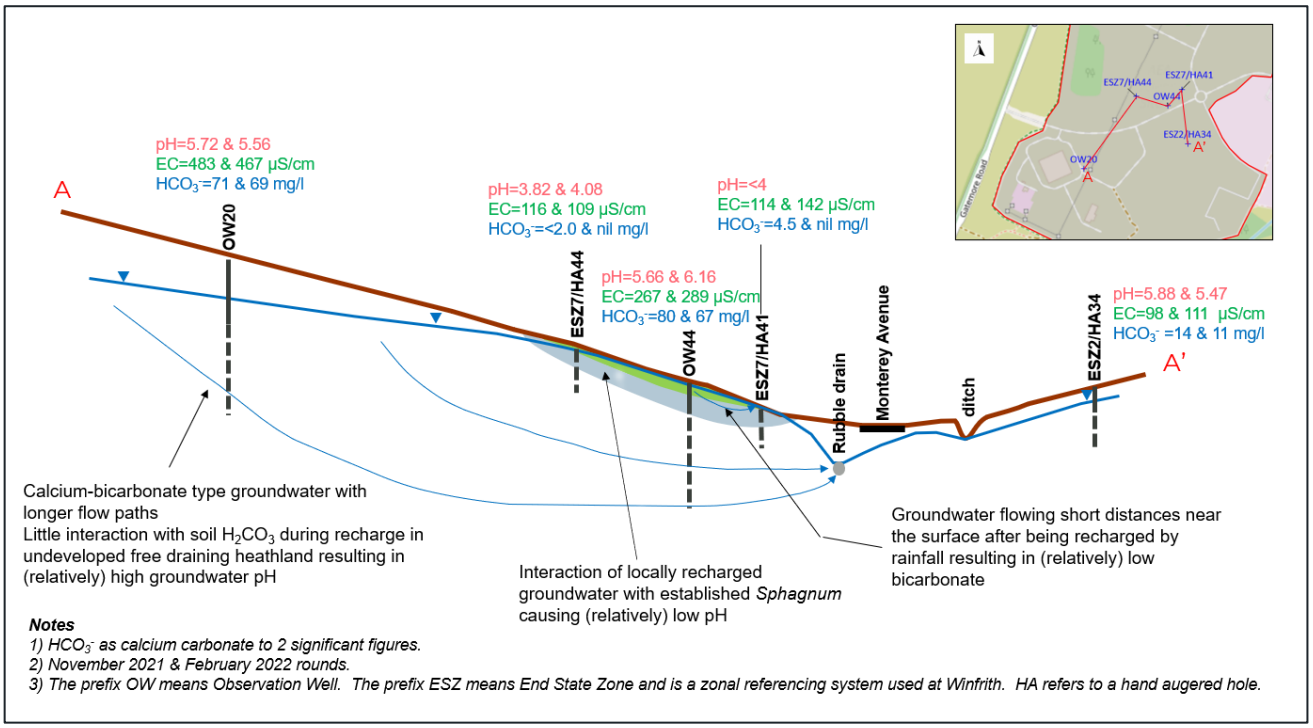

Figure 606/42: Schematic cross section along line A - A' illustrating conditions of groundwater flow and chemistry associated with the establishment of *Sphagnum* currently observed in the area of emergence west of the Monterey Roundabout

It is expected that decommissioning the "rubble" drains in preparation for the End State will allow the deeper Ca-HCO_3^- type groundwater to discharge to the surface in the area west of the Monterey roundabout. Consequently, the shallow layer of relatively low HCO_3^- groundwater will substantially diminish or disappear. Atkins (2024) explains that this probably will cause the existing acid mire M16 community to transition towards a neutral mire (e.g., NVC M10[29]) community better able to tolerate the new conditions.

A schematic conceptual model is presented in Figure 606/43 illustrating a potential flow path between the SGHWR End State and the area of groundwater emergence west of the Monterey roundabout at the IEP and under anticipated future conditions of climate change.

It is concluded that water dependent ecosystems characteristic of a neutral mire should be considered as a potential receptor for non-radiological contaminants migrating in water from the disposals/deposits. It will be assumed for the purposes of this assessment that this will be an M10 NVC community.

[29] Carex dioica – Pinguicula vulgaris mire

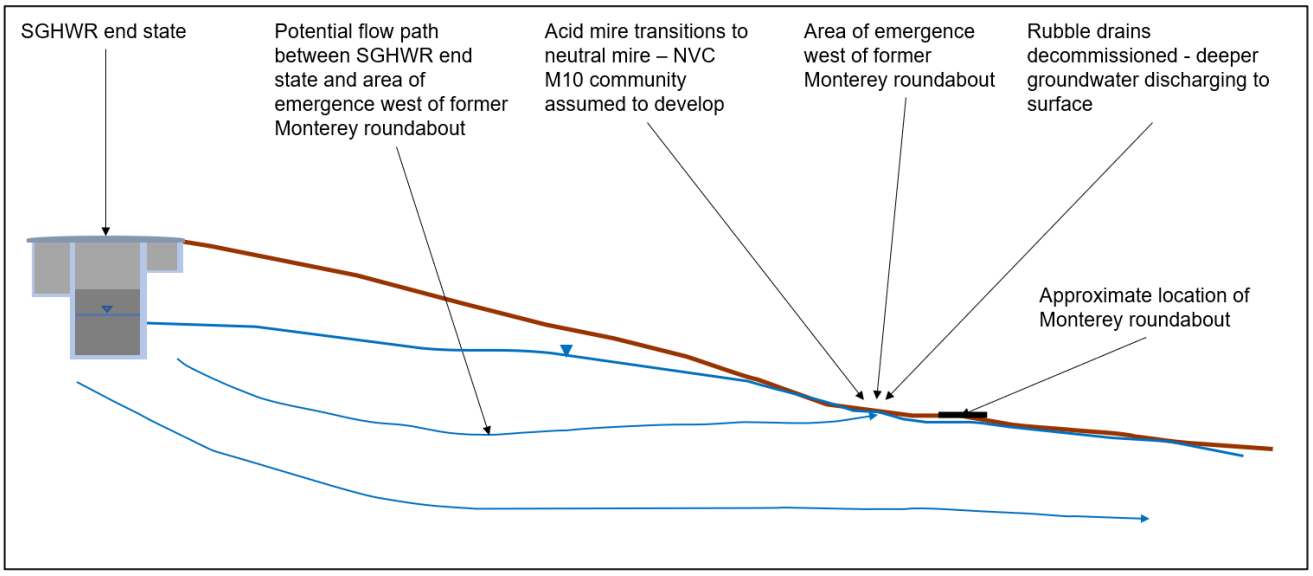

Figure 606/43: Schematic conceptual model demonstrating a potential pathway from the SGHWR End State to the water dependent terrestrial ecosystem receptor west of the Monterey roundabout under conditions representative of the IEP and future climate change

7.3 SURFACE WATER

This section summarises information about surface water as a receptor presented in NRS (2024f).

Whilst drainage has modified the natural drainage catchments, works to implement the End State are expected to restore the natural hydrology. The Site can be split into two natural catchments. The first (Northern Catchment) is approximately 69.75 ha and drains the majority of the Site to the north-east and east towards Flume 1 and the Frome Ditch surface water features. The southern portion of the Site is a smaller catchment (Southern Catchment) of approximately 14.2 ha which drains south and south-east towards the River Win. The two catchments are shown on Figure 606/44.

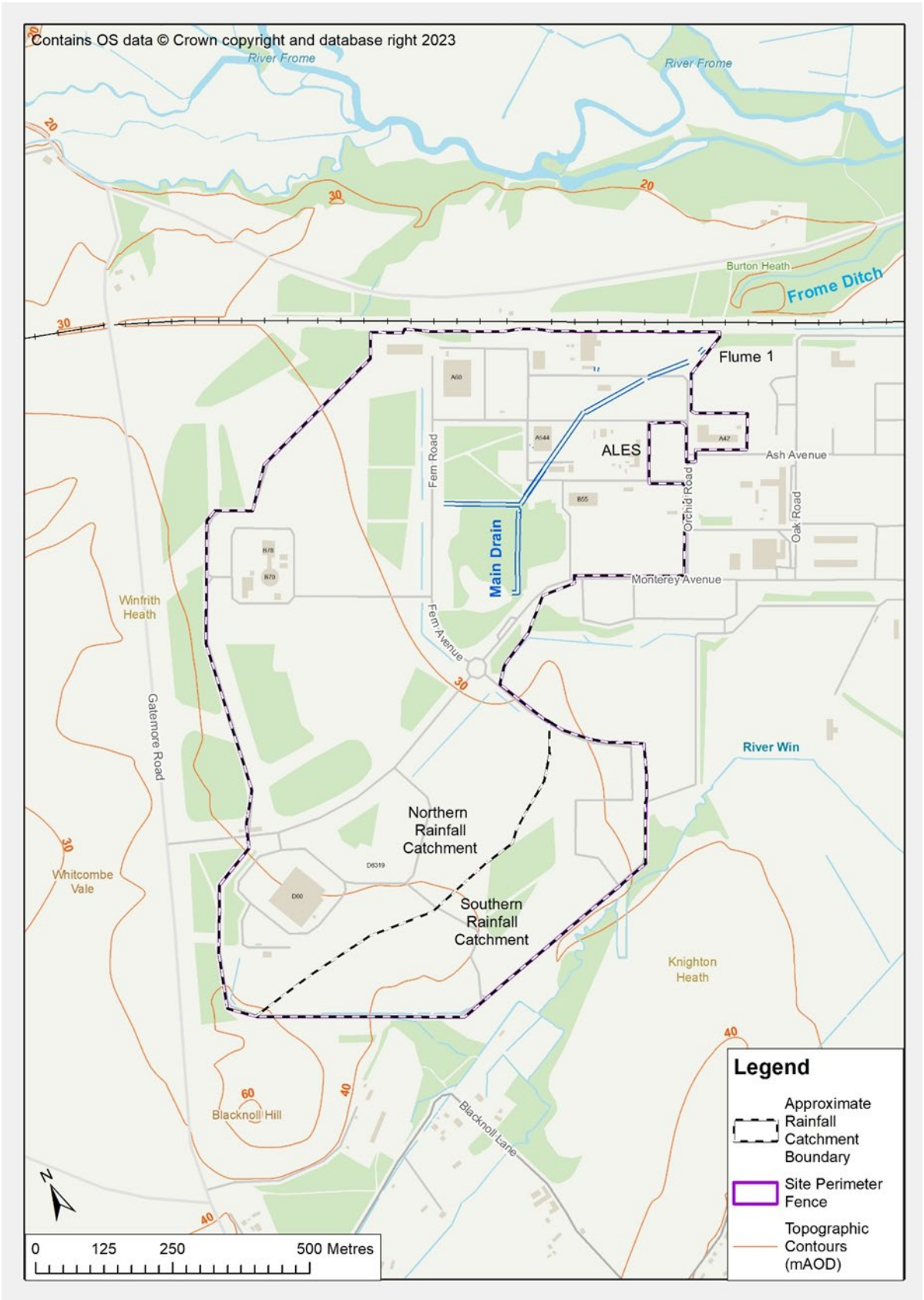

Figure 606/44: Overview of Site Hydrology

Flume 1 (Figure 606/44) receives most of the water from the on-site surface water drainage network. From Flume 1, water flows through the culvert beneath the railway into the Frome Ditch before reaching the River Frome.

Overland flow that is generated on the Site and passed to the Dorset Innovation Park is generally collected by the surface water drainage network and drained to the River Win to the east of the Dorset Innovation Park.

The River Win, located south and east of the Site, is a tributary of the River Frome (Figure 606/44). The River Win, which drains a total catchment area of 27 km^2 (Hyder, 2013) is gauged for flow by the Environment Agency approximately five kilometres upstream of its confluence with the River Frome and approximately two kilometres upstream of the Winfrith Site. The recorded daily mean flow between May 1999 and February 2022 is 0.038 m^3/s[30]. Water entering the river flows approximately northeast, discharging into the River Frome around 1.5 km east-northeast of the Site

The River Frome ultimately discharges into Poole Harbour around 12 km east of the Site. According to the National River Flow Archive (UKCEH, 2020) the catchment area feeding the River Frome at the EA gauging station (EA Station No. 44001, located 4 km east of the Site) is approximately 414 km^2. The Site lies within this catchment area. Flow data available from this gauging station indicates that, based upon the period 1965 to 2021, the mean daily flow rate is 6.72 m^3/s.

The EA has performed a catchment quality assessment of the surface and river quality across England. Surface water quality has been classified in terms of ecological status and chemical status, with the following ecological elements considered:

- Biological quality elements (e.g. fish, invertebrates, macrophytes and phytobenthos). Classified as: High, Good, Moderate, Poor or Bad.
- Physico-chemical quality elements (e.g. pH, dissolved oxygen). Classified as: High, Good or Moderate.
- Specific pollutants (e.g. copper, toluene, tetrachloroethane). Classified as either High or Moderate.
- Hydro-morphological quality elements (hydrological regime, mitigation measures assessment, morphology). Classified as: High, “Support Good” or “Does not support good”.

In 2019, based on these metrics, the reach of the River Frome to the north of the Site from Louds Mill, Dorchester to Poole Harbour was classified as ’moderate’ overall, but noted as ‘high’ for pH. Similarly, the full reach of the River Win was also classified as ’moderate’ overall, but ‘high’ for pH specifically (EA, 2020b). Data available from the EA Water Quality Archive for 2019 within these reaches (EA, 2021a) indicates that the River Frome at sampling point ‘U/S Lytchett Confluence’ approximately 2 km north-east of the Site had a pH of between 8.19 and 8.4 and the River Win at sampling point ‘Seven Stars’ approximately 0.9 km east of the Site had a pH of between 7.52 and 7.87.

[30] Calculated using data downloaded from https://environment.data.gov.uk/hydrology/station/584639e2-90cb-493d-8edc-b66eda95d788

8 SUMMARY

A summary of the CSM is provided in this section, supported by a schematic illustration in Figure 606/44.

8.1 PURPOSE

This report presents a CSM in the form of a narrative, supported by figures, describing the SGHWR and Dragon reactor complex End State characteristics suitable for mathematical model development.

The CSM considers the contamination sources, evolution of the system comprising the deposits/disposals, pathways for migrating contamination and potential receptors for that migrating contamination. It will be used to underpin non-radiological contaminant assessments for the SGHWR and Dragon reactor complex End States; and radiological assessments for on-site disposal at the SGHWR and Dragon reactor complex End States.

8.2 END STATE DISPOSITION

The SGHWR building currently comprises 10 levels, three of which are below the level of the surrounding ground surface (below ground). The reactor has been defueled and ancillary equipment and facilities decommissioned. Above ground, the structure is a steel-clad metal frame with masonry (brick) and concrete internal structures whereas below ground, the structure is mainly reinforced concrete. Although the SGHWR comprises many rooms, for the purpose of describing the End State in a manner suitable for mathematical model development it has been subdivided into the following components:

- Region 1: The reactor bioshield, primary containment and immediate surrounds;
- Region 2: The steam labyrinth to the west of the primary containment, the delay tank room, and turbine hall;
- The South Annexe, including the pump pit to the north of the turbine hall; and
- The North Annexe.

In preparation for the End State, the entire structure of the SGHWR will be demolished to 1 m below ground level (m bgl). Most internal walls in the subsurface structure will remain in-situ unless they need to be removed to gain access for deposition of infill material. The below ground voids in the primary containment area of Region 1 will be part-filled with placed concrete blocks derived from wireline cutting of the primary containment. The remainder of the SGHWR void will be infilled firstly with the material derived from the demolition of the above ground structure, with D630 stockpiled material used to make up any remaining void deficit.

Except for its services duct, the Dragon reactor is circular in plan-view and has four concentric concrete walls. The primary containment is located within the innermost concrete Wall C. The entire structure of the Dragon reactor and accessible non-structural metal elements will be demolished to ground level. As with the SGHWR, most internal walls in the subsurface structure will remain in-situ unless they need to be removed to gain access for deposition of the infill material. The primary containment within the Dragon reactor will be demolished using wireline cutting, and the below ground voids within Wall C will be filled with placed concrete blocks from the cutting. The remainder of the Dragon reactor void will be infilled firstly with the material derived from the demolition of the above ground structure and that of the B78 fuel storage building, with D630 stockpiled material used to make up any remaining void deficit.

The Dragon mortuary holes structure is located within the B78 fuel storage building approximately 30 m north northeast of the Dragon reactor and comprises 50 mortuary holes that were built to store irradiated Dragon fuel elements and 40 holes for fresh fuel. The 50 mortuary holes that were used to store used Dragon fuel elements are planned to be filled with grout and capped. The other 40 holes can be relatively easily removed from their pit and are planned to be disposed of off-site. The fuel storage building will be demolished to ground surface, while its floor slab (into which the mortuary holes structure is set) will be left in-situ.

8.3 ASSESSMENT INVENTORY

A non-radiological assessment inventory representative of the Dragon reactor complex and SGHWR End States has been developed to support hydrogeological risk assessment. A non-radiological assessment inventory has not been developed for the mortuary holes End State because the backfill and sealing materials can be specified and will be defined as being environmentally benign. In the context of hydrogeological risk assessment, the assessment inventory is not described by the total inventory but rather by the 'water available inventory'. The total non-radiological inventory of a substance in solid matter (for example concrete, brick or metal) is defined as the total mass of that substance that is present. The water available inventory of a contaminant is usually less than the total inventory because some of the contaminant is bound inextricably to solid material. The non-radiological assessment inventory for SGHWR and Dragon reactor is derived for the following components (*associated potential contaminants for which an assessment inventory has been quantified are in italics*).

- Demolition arisings generated in-situ and imported from the stockpiles (*hydroxide (pH), sulphate, chloride, fluoride, metals, hydrocarbons and PCBs*)
- Cut concrete blocks (*hydroxide* (*pH*))
- Oil staining of concrete in structures remaining in-situ (*hydrocarbons*)
- Rebar in structures remaining in-situ (*metals*)
- Structural steel remaining in-situ (*metals, sulphate and phosphate*)

A radiological assessment inventory representative of the SGHWR and Dragon End States has been developed to support radiological exposure assessment scenarios for the on-site disposals. The features for which a radiological assessment inventory has been developed are as follows:

SGHWR:	Dragon:
▪ Bioshield; ▪ Mortuary tubes; ▪ Primary containment; ▪ Secondary containment; ▪ Ponds; ▪ Ancillary areas; ▪ SGHWR bulk structure; and ▪ Backfill.	▪ Dragon reactor bioshield; ▪ Dragon reactor building general surface contamination and additional tritium ingress into the structure; ▪ Residual contamination from the PGPC spill; ▪ Dragon fuel storage building general surface contamination and additional tritium ingress into the structure; ▪ Backfill emplaced in the below-ground voids in the Dragon reactor building; and ▪ Primary mortuary holes structure.

8.4 NEAR FIELD EVOLUTION

The various components of the assessment inventory will be released to the water which comes into contact with it, predominantly via partitioning, diffusion and dissolution from the solid phase into the water.

The integrity of the SGHWR and Dragon reactor complex structures influences the rate of ingress and/or leakage of water from the disposals/deposits and therefore the rate at which the assessment inventory is released.

It is assumed that, due to designed penetrations and the damage sustained during demolition and placement of arisings, the North Annexe and South Annexe End States will not retain water from the outset. The works carried out on the SGHWR structure to prepare it for decommissioning are not expected to, and are assumed not to, damage or provide additional reinforcement to the SGHWR Regions 1 and 2 structure. With respect to the Dragon reactor structure, it is assumed that the internal and external walls will offer no barrier to groundwater flow, like the bases of the SGHWR Annexes. Over time the SGHWR Regions 1 and 2 structure will degrade. The effective hydraulic conductivity of the structure will increase through time thereby affecting the rate at which the assessment inventory is released.

Basal elevations and construction details for the SGHWR and Dragon reactor complex structures have been compared with current and potential future groundwater elevations for the purpose of assessing whether there is potential for groundwater to interact with the disposals/deposits and the structures. Historical and current groundwater elevations around the SGHWR are below the top of the base slabs of the Annexes, and there is no potential for saturation of the disposals/deposits by groundwater under current conditions. Under current conditions the deeper parts of SGHWR Regions 1 and 2 are below the water table. Following implementation of the IES and under a CCE of the effect of climate change, more of Regions 1 and 2 will become below the water table, the North Annexe will remain above the water table, as will the South Annexe except for short periods only in extreme conditions totalling 4% of the time in the 2050s and 4% of the time in the 2080s. Conditions beyond the 2080s are assumed to be similar to the 2080s. There is therefore potential for groundwater ingress to Regions 1 and 2 of the SGHWR and, infrequently, for short periods of time into the South Annexe.

Historical and current groundwater elevations around the Dragon reactor structure are below the top of the base slab by at least 1 m. The modelled CCE of groundwater level under conditions of climate change to 2100 is below the top of the base slab of the Dragon reactor. This is except for short periods only in extreme conditions totalling 5% of the time in the 2050s and 2% of the time in the 2080s.

As time progresses the engineered cap placed over the End States will allow the passage of progressively more water such that following the complete degradation of the geomembrane, the infiltration rate into the disposals/deposits is controlled by the GCL.

For those components of the End State which remain above the water table it is assumed the release of the assessment inventory will be controlled by the rate of infiltration through the cap. For those components partly below the water table, the release of the assessment inventory will be controlled by inflows and outflows of water in response to changes in the integrity of the structure and internal and external water levels.

8.5 AQUEOUS PATHWAYS FOR CONTAMINANTS

Dissolved contaminants in the near field porewater in the SGHWR and Dragon reactor End States will migrate through the structure to the geosphere by advection through fractures and, in the very long term, through the matrix of the degraded concrete. Once released from the structure, dissolved contaminants will migrate away from the near field through the unsaturated and saturated zones of the underlying Superficial Deposits and Poole Formation. Processes which attenuate contaminants other than alkalinity in the aqueous (geosphere) pathway and reduce contaminant concentrations in groundwater include:

- Dilution;
- Dispersion;
- Radioactive decay of radionuclides;
- Biodegradation of organic compounds;
- Sorption; and
- Precipitation and/or coprecipitation.

Attenuation of alkalinity in the unsaturated zone and saturated zone is a consequence of interactions with minerals and with the liquid and gas phases in the geosphere and involves processes of neutralisation, carbon dioxide dissolution, reaction with aluminosilicate minerals and surface adsorption and desorption.

8.6 AQUEOUS RECEPTORS FOR CONTAMINANTS

Aqueous receptors contaminants migrating in water from the disposals/deposits are groundwater, water dependent terrestrial ecosystems and surface water**.**

Groundwater occurs in the Made Ground, Quaternary deposits, Poole Formation, London Clay and Portsdown Chalk. Alluvium and River Terrace Deposits, as well as the Poole Formation, are classified by the EA as Secondary A aquifers. The Portsdown Chalk beneath the London Clay is a Principal Aquifer.

In the area of groundwater emergence west of the Monterey roundabout a water dependent terrestrial ecosystem has developed. It is expected that decommissioning the “rubble” drains in preparation for the end state will cause the existing acid mire M16 community to transition towards a neutral mire community better able to tolerate the new conditions. Water dependent ecosystems characteristic of a neutral mire, assumed to comprise a M10 NVC community, should be considered as a potential receptor for non-radiological contaminants migrating in water from the disposals/deposits.

The Site can be split into two natural surface water catchments. The first (Northern Catchment) is approximately 69.75 ha and drains the majority of the Site to the north-east and east towards Flume 1 and the Frome Ditch surface water features. The southern portion of the Site is a smaller catchment (Southern Catchment) of approximately 14.2 ha which drains south and south-east towards the River Win. Flume 1 receives most of the water from the on-site surface water drainage network. From Flume 1, water flows through the culvert beneath the railway into the Frome Ditch before reaching the River Frome. The River Win, located south and east of the Site, is a tributary of the River Frome.

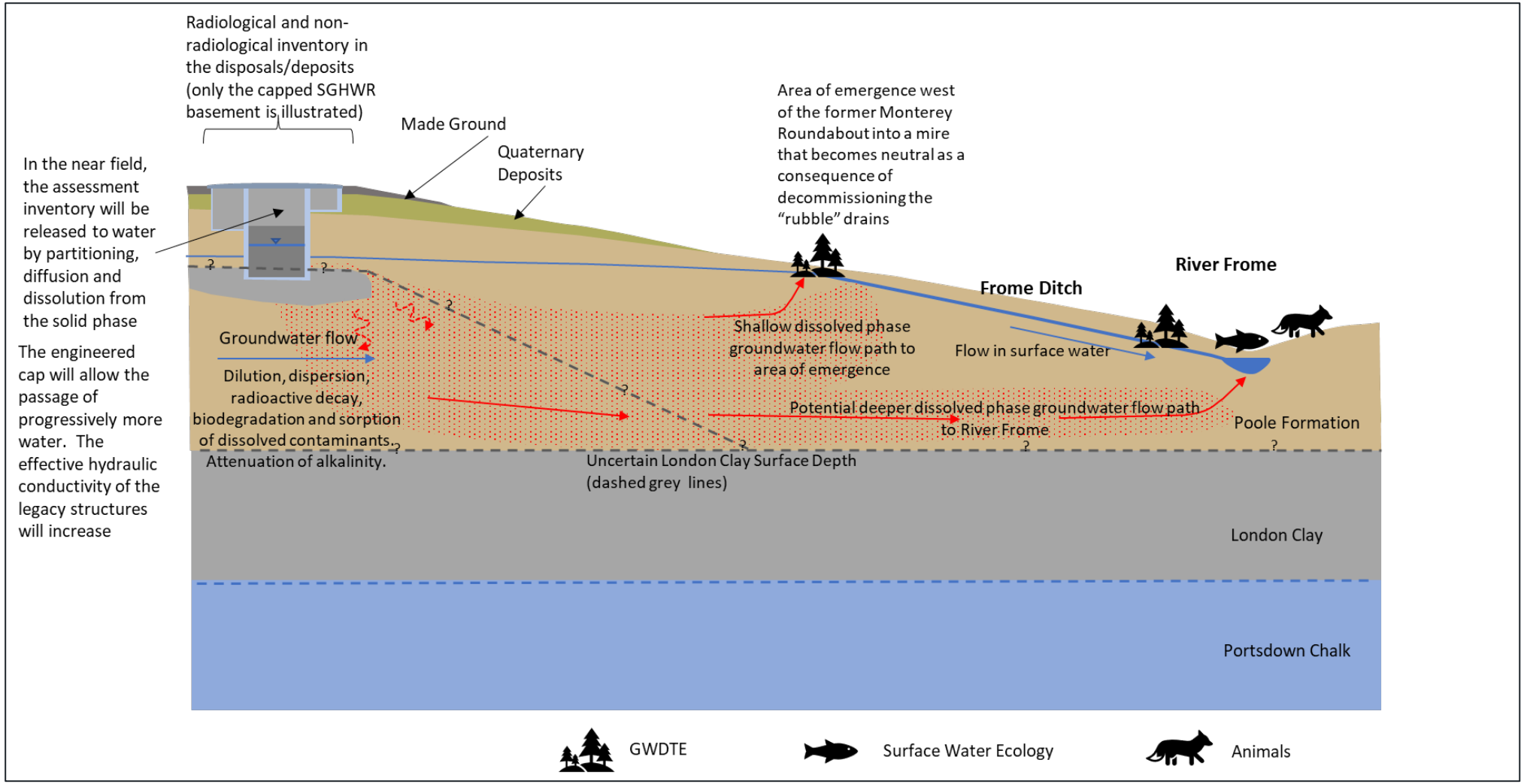

Figure 606/45: Schematic showing a Summary of the Conceptual Site Model

9 UNCERTAINTIES

Magnox (2023) demonstrates how NRS meets the GRR requirements for uncertainty management. Uncertainty is defined in the GRR glossary as a "*Lack of certainty. A state of limited knowledge that precludes an exact or complete description of past, present or future*."

Magnox (2023) explains that the potential significance of uncertainties, assumptions and gaps should be rated as Low, Medium or High defined as follows:

- Low:
  - If the uncertainty is not reduced, additional practical mitigation measure(s) is/are unlikely to be necessary in the near term[31]; and/or
  - The magnitude of uncertainty is currently such that robust demonstration of environmental safety (including optimisation) over the site life-cycle will be straightforward.
- Medium:
  - If the uncertainty is not reduced, additional practical mitigation measure(s)[32] might be necessary in the near term; and/or
  - The magnitude of uncertainty is currently such that robust demonstration of environmental safety (including optimisation) over the site life-cycle could be somewhat difficult.
- High:
  - If the uncertainty is not reduced, additional practical mitigation measure(s) is/are certain or very likely to be necessary in the near term; and/or
  - The magnitude of uncertainty is currently such that robust demonstration of environmental safety (including optimisation) over the site life-cycle is likely to be impossible or very difficult.

Table 606/39 outlines the uncertainties inherent in the CSM.

Winfrith's End State uncertainties are currently managed in an "Uncertainties Management Database" the purpose of which is to capture all uncertainties associated with the end state project. Each uncertainty will be reviewed in accordance with a NRS Uncertainties Management Plan developed in accordance with Magnox (2023), and either closed out because it can be tolerated, or a plan developed for managing it.

[31] In this context, "the near term" covers the timescale for any RSR [Radioactive Substances Regulation] permit variation application for on-site disposal under the GRR that is in progress or planned in the next decade, as well as the timescale for demonstrating that a satisfactory SWESC is in place where no such application is planned.

[32] In this context, "additional practical mitigation measure(s) … necessary in the near term" could include measure(s) required (if the uncertainty cannot be reduced) in order to: comply with extant RSR permit conditions (including conditions on implementing any permitted on-site disposals); make a successful RSR permit variation application; and/or be able to demonstrate a satisfactory SWESC. Such measures are "additional" in the sense that they would be over and above mitigation measure(s) needed regardless of the magnitude of uncertainty.

Table 606/39: CSM Uncertainties

Contractor Reference Number	Feature, Event or Process subject to Uncertainty	Description of Uncertainty	Treatment of Uncertainty / Statement of Assumption	WSP's Rating of Potential Significance (Low, Medium, High)	WSP's Recommended Action
Section 2					
CSM2.1	Voids in the SGHWR building and Dragon reactor structure	Void volumes have been estimated by scaling from drawings and without the benefit of a three-dimensional computer model. These estimates are for the purposes of conceptualisation to support mathematical model development and are not for underpinning detailed design.	The estimated volumes for SGHWR voids are within approximately 5% of those determined using a three-dimensional computer model prior to subdivision of the SGHWR regions. Based on this comparison, the estimated void volumes for both SGHWR and Dragon are deemed sufficiently accurate to support mathematical model development.	Low	Volumes to underpin the detailed design will be calculated during the design phase of works.
CSM2.2	Materials within the Source Area	There is uncertainty associated with the space occupied by internal structures, such as walls and floors, in the SGHWR reactor.	Use UKAEA (2006) to estimate space consumed by internal structures.	Low	Revisit at detailed design.
CSM2.3	Materials within the Source Area	The space occupied by internal structures, such as walls and floors, in the Dragon reactor is unknown.	Use Magnox Waste Recovery Plan (Magnox, 2021a) assumptions.	Low	Revisit at detailed design.
CSM2.4	SGHWR decommissioning strategy	There is uncertainty about the method by which any wall and floor slabs will be removed to allow access to the previously obstructed parts of the SGHWR Region 1 basement void.	All demolition in SGHWR Region 1 will be by wireline cutting.	Low	Revisit at detailed design.

Contractor Reference Number	Feature, Event or Process subject to Uncertainty	Description of Uncertainty	Treatment of Uncertainty / Statement of Assumption	WSP's Rating of Potential Significance (Low, Medium, High)	WSP's Recommended Action
CSM2.5	Materials within the Source Area	The amount of void space between the concrete blocks placed in the SGHWR and Dragon reactor is uncertain.	Assume the void space between the concrete blocks is 10% of the total volume occupied by blocks as stated in Magnox (2020a).	Low	Review as part of detailed design.
CSM2.6	Backfill material properties	The shape of the concrete blocks to be placed in the SGHWR and Dragon reactor is uncertain and will be determined by the wireline cutting design and the part of the structure being demolished.	All concrete blocks are assumed to have a cubic shape.	Low	None.
CSM2.7	Backfill material properties	The porosity of concrete in blocks and in the other demolition arisings in the SGHWR and Dragon reactor is unknown.	Assume the porosity of concrete in blocks and in the other demolition arisings in the SGHWR and Dragon reactor is 15% v/v as determined in a review of the porosity of structural concrete (SKB, 2001a).	Low	Address in sensitivity analysis.
CSM2.8	Backfill material properties	The dry bulk density of the concrete blocks in the SGHWR and Dragon reactor is unknown.	Assume the dry bulk density is 2,400 kg/m^3 that is between the values quoted in SKB (2001a) and SKB (2014) for structural concrete	Low	None.
CSM2.9	SGHWR backfill strategy	The volume of concrete blocks available to be placed in the SGHWR.	The volume of concrete blocks including the void space between the blocks is assumed to be 6,300 m^3 (Magnox, 2020b).	Low	Review during detailed design. Any change to the void space between concrete blocks (CSM2.5) will influence this.

Contractor Reference Number	Feature, Event or Process subject to Uncertainty	Description of Uncertainty	Treatment of Uncertainty / Statement of Assumption	WSP's Rating of Potential Significance (Low, Medium, High)	WSP's Recommended Action
CSM2.10	SGHWR backfill strategy	The location of concrete blocks placed in the SGHWR.	Concrete blocks will be placed in the deepest basal areas of the SGHWR Region 1.	Low	Review during detailed design.
CSM2.1	SGHWR backfill strategy	The location of demolition arisings in the SGHWR.	Demolition arisings will be placed above the concrete blocks in the SGHWR Region 1 and in Region 2, the North Annexe and the South Annexe.	Low	Review during detailed design.
CSM2.12	Backfill material properties	The shape of particles of demolition arisings in the SGHWR and Dragon reactor is unknown.	Assume the particles are spheres.	Low	None.
CSM2.13	Backfill material properties	The porosity of demolition arisings when placed in the SGHWR and Dragon reactor is unknown.	Assume a porosity of demolition arisings based on a bulking/compaction factor and the void space of packed spherical particles.	Medium	Address in sensitivity analysis.
CSM2.14	Backfill material properties	There is variation in the particle size distribution of D630 demolition arisings to be placed in the SGHWR and Dragon reactor. The particle size distribution of demolition arisings generated in situ may be different to that of the D630 stockpiles.	Assume the median particle size is 15 mm and no particles are larger than 150 mm as indicated by the analysis of ten samples of the D630 stockpiles (Magnox, 2019d).	Low	None.
CSM2.15	Dragon backfill strategy	The volume of concrete blocks available to be placed in the Dragon reactor.	The volume of concrete blocks including the void space between the blocks is assumed from the	Low	Review during detailed design. Any change to the void space between concrete blocks

Contractor Reference Number	Feature, Event or Process subject to Uncertainty	Description of Uncertainty	Treatment of Uncertainty / Statement of Assumption	WSP's Rating of Potential Significance (Low, Medium, High)	WSP's Recommended Action
			SWMMP to be 400 m^3 (NRS, 2024i).		(CSM2.5) will influence this.
CSM2.16	Dragon backfill strategy	The location of concrete blocks placed in the Dragon reactor.	Concrete blocks will be placed in the deepest basal areas of the Dragon reactor within Wall C.	Low	Review during detailed design.
CSM2.17	Dragon backfill strategy	The location of demolition arisings in the Dragon reactor.	Demolition arisings will be placed above the concrete blocks in the Dragon reactor.	Low	Review during detailed design.
CSM2.18	Dragon backfill strategy	The source of demolition arisings placed in the Dragon reactor.	The demolition arisings placed in the Dragon reactor are assumed to be derived from the demolition of the Dragon reactor and its ancillary buildings and from the D630 stockpiles.	Low	Review during detailed design.
Section 3					
CSM3.1	D630 stockpiles composition	It is uncertain how results of analysis for contaminants in the D630 stockpiles less than limit of detection should be handled when calculating an assessment inventory.	For the purposes of developing an assessment inventory, concentrations of contaminants <LOD have been assumed to be half the LOD.	Low	None.
CSM3.2	SGHWR rebar	There is uncertainty as to whether the relatively high iron and chromium concentrations in SGHWR concrete core samples S1 to S3 (Wood 2020) are because of rebar in the sample.	It is assumed that samples S1 to S3 contained rebar and the results of analysis of these samples should not be used to determine the composition of structural concrete.	Low	None.

Contractor Reference Number	Feature, Event or Process subject to Uncertainty	Description of Uncertainty	Treatment of Uncertainty / Statement of Assumption	WSP's Rating of Potential Significance (Low, Medium, High)	WSP's Recommended Action
CSM3.3	SGHWR rebar	It is uncertain whether all rebar will be removed from the arisings generated by demolition material.	Assume the rebar will be removed from the above ground demolition material and therefore excluded from metal assessment inventory calculations.	Medium	Assess sensitivity to inventory mass.
CSM3.4	SGHWR oil contamination	The volume per unit area of oil stain used in estimating the mass of surface oil contamination in the SGHWR is uncertain. The depth of oil penetration of the SGHWR structural concrete is uncertain.	Assume a literature value for volume per unit area of oil stain taken from Magnox, 2020c. Assume 10 mm as used by NRS (2024d).	Medium	Assess sensitivity to inventory mass.
CSM3.5	SGHWR oil contamination	The density of oil used in estimating the mass of surface oil contamination in the SGHWR.	Assume literature value taken from Magnox, 2020c.	Medium	Assess sensitivity to inventory mass.
CSM3.6	SGHWR demolition arisings	It is uncertain whether all rebar will be removed from the arisings generated by demolition of the above ground SGHWR.	The SGHWR above ground metal frame and cladding will be removed. All rebar will be removed and will not form part of the disposals/deposits.	Low	Ensure consistency with criteria stipulated in the Emplacement Acceptance Criteria.
CSM3.7	Dragon reactor structure brickwork	The only brickwork present in the Dragon reactor structure is in a few small infill panels that are insignificant in volume compared to the rest of the structure to be demolished.	It is assumed that the demolition material derived from the Dragon above ground structure will be 100% concrete.	Low	Review during detailed design.
CSM3.8	D630 stockpiles composition	The degree to which the concrete and the brick contribute to the metal concentrations reported for the D630 stockpiles is uncertain. It is therefore uncertain how the results of analysis	The concrete alone is assumed to contribute to the metal concentrations reported for the D630 stockpiles.	Medium	Assess sensitivity to inventory mass.

Contractor Reference Number	Feature, Event or Process subject to Uncertainty	Description of Uncertainty	Treatment of Uncertainty / Statement of Assumption	WSP's Rating of Potential Significance (Low, Medium, High)	WSP's Recommended Action
		for metals in the stockpiled material can be used for the concentrations of metals in the demolition arisings that will be generated in-situ.	Because the arisings generated by demolition of the above ground parts of the SGHWR and Dragon reactor will contain a higher proportion of concrete than the stockpiled material, it is conservative to assume the brick in the stockpiles is inert and to increase the reported concentrations of metals in the stockpiled material before they are used to represent the concentrations of metals in the demolition arisings generated in-situ.		
CSM3.9	SGHWR and Dragon backfill strategies	The proportion of the infill of the SGHWR and Dragon reactor that will be D630 stockpiled material is uncertain.	Assume: ▪ all the infill has the proportion of concrete in arisings generated by in-situ demolition; and ▪ the metals content of the D630 stockpiles increased by an amount that assumes brick is inert. All infill will thereby have the maximum possible metals concentrations and the approach is thereby conservative. The need to make an assumption about the	Low	None.

Contractor Reference Number	Feature, Event or Process subject to Uncertainty	Description of Uncertainty	Treatment of Uncertainty / Statement of Assumption	WSP's Rating of Potential Significance (Low, Medium, High)	WSP's Recommended Action
			proportion of the infill of the SGHWR and Dragon reactor that will be comprised D630 stockpiles material is thereby negated.		
CSM3.10	Groundwater quality	The effect of inorganic contaminants in concrete blocks and in the fabric of the concrete structure on groundwater quality is uncertain.	It is assumed an assessment inventory is not required because the inorganic contaminants bound within the concrete blocks and in the fabric of the concrete structure are of sufficiently low mobility and/or they are released so slowly as the cement dissolves over millennia that they do not pose a risk to groundwater quality and do not require an assessment inventory.	Low	Assess the validity of this assumption in the tiered HRA.
CSM3.11	Groundwater quality	The effect of fibreglass on groundwater quality is uncertain.	It is assumed the contaminants bound within the fibreglass have sufficiently low mobility that they do not pose a risk to groundwater quality and do not require an assessment inventory.	Low	Assess the validity of this assumption in the tiered HRA.
CSM3.12	Groundwater quality	The effect of metals in structures on groundwater quality is uncertain.	It is assumed an assessment inventory is not required because the metals bound within the concrete structure are of sufficiently low mobility that they do not pose a risk to groundwater quality and do	Medium	Assess the validity of this assumption in the tiered HRA.

Contractor Reference Number	Feature, Event or Process subject to Uncertainty	Description of Uncertainty	Treatment of Uncertainty / Statement of Assumption	WSP's Rating of Potential Significance (Low, Medium, High)	WSP's Recommended Action
			not require an assessment inventory.		
CSM3.13	Phosphorus and sulphur in structural steel	The state of phosphorus and sulphur in structural steel is uncertain.	Phosphorous and sulphur is assumed to be in the form of phosphate and sulphate in the assessment inventory.	Low	None.
Section 4 (the uncertainties associated with the radiological inventory estimates for the SGHWR and Dragon reactor End States are recorded in the Winfrith End State Radiological Inventory report (NRS, 2024a) and are not repeated here).					
Section 5					
CSM5.1	Integrity of existing structures	The damage to the North Annexe and South Annexe caused by the placement of demolition material is uncertain.	It is assumed that, due to the damage sustained during demolition and placement of arisings, the North Annexe and South Annexe End States will not retain water from the outset.	Low	None.
CSM5.2	Integrity of existing structures	Wall A of the Dragon reactor is a conventional concrete structure, and it is uncertain whether it will suffer loss of integrity during demolition and backfilling.	It is assumed that Wall A will offer no barrier to groundwater flow like the bases of the SGHWR Annexes (Atkins, 2020).	Low	None.
CSM5.3	Integrity of existing structures	Changes to the integrity of the SGHWR structure as a result of works to prepare the SGHWR for decommissioning are uncertain.	The works are not expected to, and are assumed not to, damage or provide additional reinforcement to the SGHWR structure.	Low	Review following works.

Contractor Reference Number	Feature, Event or Process subject to Uncertainty	Description of Uncertainty	Treatment of Uncertainty / Statement of Assumption	WSP's Rating of Potential Significance (Low, Medium, High)	WSP's Recommended Action
CSM5.4	Integrity of existing structures	Magnox (2019b) discusses processes that could affect the integrity of the SGHWR primary containment structure and the effect on gross hydraulic conductivity. It is uncertain whether the discussion is equally applicable to the Dragon reactor structure.	It is assumed the processes and effects discussed in Magnox (2019b) are applicable to other parts of Regions 1 and 2 and to Wall B of the Dragon reactor (as described in Atkins, 2020).	Low	None.
CSM5.5	Degradation of existing structures	The initial effective hydraulic conductivity of the structures of the SGHWR Regions 1 and 2 is uncertain.	The initial effective hydraulic conductivity of the structures of the SGHWR Regions 1 and 2 is assumed to be $4.4x10^{-11}$ m/s.	Medium	Assess sensitivity to the assumption with a variant evolution of the effective hydraulic conductivity.
CSM5.6	Degradation of existing structures	The effective hydraulic conductivity of the SGHWR Regions 1 and 2 structures when loss in integrity of the structure leads to no further increase in effective hydraulic conductivity is uncertain.	The effective hydraulic conductivity of the SGHWR Regions 1 and 2 structures when loss in integrity of the structure leads to no further increase in effective hydraulic conductivity is that of the Poole Formation ($2.7x10^{-4}$ m/s).	Medium	Assess sensitivity to the assumption with a variant evolution of the effective hydraulic conductivity.
CSM5.7	Degradation of existing structures	The point in time when loss in integrity of the SGHWR Regions 1 and 2 structure leads to no further increase in effective hydraulic conductivity is uncertain. NRS (2024e) concludes that the basements are robust structures that will maintain their structural integrity both during demolition and backfilling operations and in their End State configurations. In contrast, modelling of the	The point in time when loss in integrity of the SGHWR Regions 1 and 2 structure leads to no further increase in effective hydraulic conductivity is assumed to be 1,000 years after the IEP.	Medium	Assess sensitivity to the assumption with a variant evolution of the effective hydraulic conductivity.

Contractor Reference Number	Feature, Event or Process subject to Uncertainty	Description of Uncertainty	Treatment of Uncertainty / Statement of Assumption	WSP's Rating of Potential Significance (Low, Medium, High)	WSP's Recommended Action
		durability of steel reinforced concrete radioactive waste containers (AMEC Foster Wheeler, 2016) indicates that rebar corrosion and concrete degradation could take place within tens to hundreds of years depending on environmental conditions.			
CSM5.8	Cap design	The disposals/deposits at the SGHWR and the Dragon reactor will be covered by an engineered cap. The current concept cap design will be subject to future optimisation.	It is assumed for the purpose of developing a time variant profile of infiltration through the capping system for mathematical model development that the optimised cap design will include a composite FML/clay layer overlain by drainage. It is assumed the cap will be designed to include a layer or layers that, in the unlikely event that the disposals/deposits became saturated, would divert water from within the disposals/deposits into the unsaturated zone thereby preventing water from breaking out at the surface	Low	Review following cap optimisation.
CSM5.9	Cap performance	The design infiltration rate for the cap is uncertain.	A conservative initial infiltration rate of 5 mm/year is assumed.	Low	None.
CSM5.10	Cap performance	The time to onset, and rate of, FML degradation within the cap is uncertain.	The time to onset of degradation is assumed to be 250 years. A linear	Medium	Assess sensitivity to the assumption by

Contractor Reference Number	Feature, Event or Process subject to Uncertainty	Description of Uncertainty	Treatment of Uncertainty / Statement of Assumption	WSP's Rating of Potential Significance (Low, Medium, High)	WSP's Recommended Action
			increase in infiltration rate between the initial infiltration rate and the long-term infiltration rate is assumed for the period of 250 years to 1,000 years.		shortening the timescale to onset of degradation at 125 years and shortening the time period to the long-term infiltration rate to 500 years.
CSM5.11	Cap performance	The long-term cap infiltration rate is uncertain.	A conservative long-term infiltration rate is assumed of 43 mm/year.	Medium	None – conservative value assumed.
CSM5.12	Hydraulic head distribution with depth	The distribution of hydraulic head with depth of water which accumulates in the SGHWR Regions 1 and 2 is uncertain.	Any variation with depth of hydraulic head within the saturated zone of the disposals/deposits will be neglected.	Low	None.
CSM5.13	Oil contamination	The degree of, and timescales for, contact between water and oil in the SGHWR and Dragon reactor End States following demolition is uncertain.	It is conservatively assumed that there is full contact between water and oil immediately post demolition.	Low	None.
CSM5.14	Oil contamination	Oil in the near surface of the floors is expected to comprise a free phase component and a sorbed phase component. There is uncertainty whether the free phase component is mobile.	Attempts to clean the floors are likely to have removed mobile free phase oil. The free phase component is therefore assumed to be immobile, but it can dissolve directly into water.	Low	None.
CSM5.15	PCB contamination	The PCB contamination may have penetrated the surfaces of the particles and be present as	It is conservatively assumed that the contamination is on the surface.	Low	None.

Contractor Reference Number	Feature, Event or Process subject to Uncertainty	Description of Uncertainty	Treatment of Uncertainty / Statement of Assumption	WSP's Rating of Potential Significance (Low, Medium, High)	WSP's Recommended Action
		free phase or sorbed phase. The degree of penetration is uncertain.			
CSM5.16	Corrosion of metals	The corrosion rates for metals in rebar and structural steel are uncertain.	Assume a lower limit corrosion rate of 0.01 microns per year in either saturated or unsaturated conditions and an upper limit of 100 to 200 microns per year for saturated and unsaturated conditions, respectively. A 50th percentile value of around 1 micron per year in either case is assumed.	Low	None.
CSM5.17	Corrosion of metals	The time of onset of corrosion of metals in rebar and structural steel by water entering the End States is uncertain.	Assume that corrosion of I-beams, structural steel and rebar throughout the structures and concrete blocks will begin immediately post demolition.	Low	None.
CSM5.18	Corrosion of metals	The timescales over which corrosion products of metals in rebar and structural steel can dissolve into water are uncertain.	Assume that corrosion products of I-beams, structural steel and rebar throughout the structures and concrete blocks will be instantaneously available to dissolve into water.	Low	None.
CSM5.19	Near field alkalinity	The effects of secondary mineral formation in the demolition material which could potentially reduce the concentration of OH^- ions in the near field porewater are complex and subject to significant uncertainty.	The effects of secondary mineral formation will be conservatively disregarded.	Low	None.

Contractor Reference Number	Feature, Event or Process subject to Uncertainty	Description of Uncertainty	Treatment of Uncertainty / Statement of Assumption	WSP's Rating of Potential Significance (Low, Medium, High)	WSP's Recommended Action
CSM5.20	Near field alkalinity	The effects of carbonation in the demolition material which could potentially reduce the concentration of OH^- ions in the near field porewater are complex and subject to significant uncertainty.	The effects of carbonation will be conservatively disregarded.	Low	None.
Section 6					
CSM6.1	Degradation of existing structures	There is uncertainty over the rate of increase of effective porosity from fracture porosity to matrix porosity of the wall and base of the SGHWR and Dragon reactor End States as they degrade.	It is assumed that this increase will be linear.	Low	None.
CSM6.2	Contamination transport through engineering	There is uncertainty over the role of diffusion of contaminants through the walls and bases of the SGHWR and Dragon reactor End States.	It is assumed that advective transport of contaminants through the structures will dominate and the effects of diffusion are assumed negligible.	Low	None.
CSM6.3	Saturated pathway	The Poole Formation can be locally confined with depth or where extensive clay layers exist.	Although the Superficial Deposits and Poole Formation can be locally confined with depth or where extensive clay layers exist, they are assumed to be unconfined for the purposes of the CSM.	Low	None.
	Saturated pathway	It is uncertain whether historical boreholes drilled to the Portsdown Chalk Formation could be a saturated pathway.	Historical boreholes to the Portsdown Chalk Formation are disregarded as a saturated	Low	NRS to ascertain that historical boreholes drilled to the Portsdown

Contractor Reference Number	Feature, Event or Process subject to Uncertainty	Description of Uncertainty	Treatment of Uncertainty / Statement of Assumption	WSP's Rating of Potential Significance (Low, Medium, High)	WSP's Recommended Action
			pathway because NRS will ascertain that they have been decommissioned or will make reasonable endeavours to locate and decommission them.		Chalk Formation have been decommissioned or will make reasonable endeavours to locate and decommission them.
CSM6.4	Unsaturated pathway contaminant transport	Lateral dispersion of contaminants may occur as they migrate through the unsaturated zone to the water table.	The width of the unsaturated pathway beneath the SGHWR annexes and the Dragon reactor is assumed to be limited to the footprint of the structure above.	Low	None.
CSM6.5	Saturated pathway	The deepest parts of SGHWR Regions 1 and 2 lie beneath the water table at the IEP. Other parts will be above the water table for at least some of the time.	It is assumed that the entire footprint of SGHWR Regions 1 and 2 lies at or below the water table at the IEP.	Low	None.
CSM6.6	Saturated pathway	The deepest parts of SGHWR Regions 1 and 2 rest on clay and Regions 1 and 2 are defined by structures with thick base slabs. There is uncertainty about how much water can move through the base slabs and into the clay.	Due to both geology and the base slab thickness contaminants are assumed to migrate only through the sidewalls, and not the base slabs, of SGHWR Regions 1 and 2 structures to the saturated Poole Formation.	Low	None.
CSM6.7	Unsaturated pathway contaminant transport	The unsaturated zone beneath most of the plan area of the SGHWR annexes is Poole Formation. Nevertheless, some of the unsaturated zone consists of voids filled with gravel and zones of mass concrete.	The volumetrically smaller parts of the unsaturated zone comprised of voids filled with gravel and zones of mass concrete are ignored for the purposes of the CSM and the	Low	None.

Contractor Reference Number	Feature, Event or Process subject to Uncertainty	Description of Uncertainty	Treatment of Uncertainty / Statement of Assumption	WSP's Rating of Potential Significance (Low, Medium, High)	WSP's Recommended Action
			unsaturated zone is assumed to comprise the Poole Formation.		
CSM6.8	Saturated pathway	The potential for groundwater to flow beneath or around all four regions of the SGHWR is uncertain.	Groundwater flow lines are likely to pass beneath one or two of the three regions of the SGHWR only. However, to ensure account is taken of the potential cumulative effect of leakage from all four regions, it will be assumed that there is a groundwater flow line that can pass beneath both the South Annexe and North Annexe as well as around or through Regions 1 and 2.	Low	None.
CSM6.9	Saturated pathway	There is uncertainty over the role of the "rubble" drains as preferential pathways for groundwater movement and contaminant transport.	It is assumed the "rubble" drains will not become preferential pathways for groundwater movement and contaminant transport.	Low	None.
CSM6.10	Saturated pathway	There is uncertainty regarding the mixing zone thickness of the saturated pathway beneath the Dragon reactor End State.	The mixing zone is the vertical saturated thickness below the water table over which contaminants are assumed to mechanically disperse and diffuse. It is assumed to be 5 m thick at the IEP, and this will represent the saturated pathway thickness.	Low	None.

Contractor Reference Number	Feature, Event or Process subject to Uncertainty	Description of Uncertainty	Treatment of Uncertainty / Statement of Assumption	WSP's Rating of Potential Significance (Low, Medium, High)	WSP's Recommended Action
CSM6.11	Saturated pathway	There is uncertainty regarding the effect the Dragon reactor End State penetrating the water table will have on groundwater flow.	The deflection of groundwater flow caused by the slight penetration of the Dragon reactor End State below the water table is assumed to be insignificant and is disregarded.	Low	None.
CSM6.12	Unsaturated pathway contaminant transport and saturated pathway contaminant transport	There is uncertainty regarding the degree of longitudinal dispersion along the saturated and unsaturated pathways.	In the saturated and unsaturated pathways a longitudinal dispersivity of 10% of the pathway length is assumed based on Gelhar et al (1992).	Low	None.
CSM6.13	Unsaturated pathway contaminant transport and saturated pathway contaminant transport	There is uncertainty regarding the degree of transverse dispersion along the saturated and unsaturated pathways.	The effects of transverse dispersion are conservatively disregarded.	Low	None.
CSM6.14	Unsaturated pathway contaminant transport and saturated	There is uncertainty regarding the degree of biodegradation PCBs will undergo along the saturated and unsaturated pathways.	PCB congeners are conservatively assumed biodegrade with a half-life of 50 years based on literature review.	Medium	Assess with sensitivity analysis.

Contractor Reference Number	Feature, Event or Process subject to Uncertainty	Description of Uncertainty	Treatment of Uncertainty / Statement of Assumption	WSP's Rating of Potential Significance (Low, Medium, High)	WSP's Recommended Action
	pathway contaminant transport				
Section 7					
CSM7.1	Hydrogeological conditions	There is uncertainty associated with interpretation of present and future hydrogeological conditions as described in NRS (2024f).	Assumptions have been made and are listed in NRS (2024f).	Low	As set out in NRS (2024f).
CSM7.2	Water dependent terrestrial ecosystems	It is expected that decommissioning the "rubble" drains in preparation for the end state will allow bicarbonate rich water to discharge to the surface west of the Monterey roundabout. The consequence for the existing acid mire M16 community is uncertain.	It is assumed that the existing acid mire M16 community will transition towards a neutral mire.	Low	None.

10 REFERENCES

- Amec Foster Wheeler, 2016. Modelling the Expansion and Cracking of Grouted Wasteforms Containing Mild Steel or Magnox. AMEC/002053/001 Issue 2. 26 May 2016.
- Amec Foster Wheeler, 2017. Winfrith SGHWR End State Options: Assessment of Alkalinity in the Environment. 205412/01 Issue B, 26 May 2017.
- Atkins, 2020. Technical Note: Applicability of SGHWR Engineering Solutions to Dragon. Revision 1, February 2020.
- Atkins, 2024. Winfrith End State. Wetland investigation and assessment. 5201813-v6.1, 28 June 2024. NRS reference ES(24)P400 Issue 1.
- British Nuclear Fuels Ltd, 2002. Drigg Post-Closure Safety Case, Overview Report, September 2002.
- CL:AIRE, 2017. Petroleum Hydrocarbons In Groundwater: Guidance On Assessing Petroleum Hydrocarbons Using Existing Hydrogeological Risk Assessment Methodologies. Version 1.1. 29 March 2017.
- Crawley, D.B., 1960. Dragon Project Report: Preliminary Shielding Report for the Dragon Reactor Experiment, A.E.E. Winfrith, Report 6 (DPR0006), November 1960.
- Defra, 2020. MAGIC website. MAGIC (defra.gov.uk). Accessed on 1 December 2020.
- DSRL, 2010. Dounreay New Low Level Waste Facility Run 3 Performance Assessment, NLLWF/3/REP/GAL/0315/A/01, Issue 1, December 2010.
- DSRL, 2013. New Low Level Waste Facilities – Run 4 Performance Assessment. DSRL Report No. NLLWF/3/REP/GAL/0927/IS/01.
- DSRL, 2021. D3100 LLW Disposal Facilities: Run 5 Performance Assessment. D3100/4/REP/GAL/40134, Issue 1, 26 February 2021.
- Eden, L., 2010. Radiological Risk Assessment and Capacity Calculation for the Clifton Marsh Landfill Site. Nuvia, Report 89290/IN/RA/002, Issue 2, May 2010.
- Eden Nuclear and Environment, 2015. Environmental Safety Case: Disposal of Low Activity Low Level Radioactive Waste at East Northants Resource Management Facility, Report ENE-154/001, Version 02, 23 July 2015.
- Element Materials Technology, 2022. D630 Rubble Store, Test Report 22/5668 Batch 1, Winfrith, Final Report, Issue 1, 22nd April, 2022.
- Environment Agencies, 2018. Management of radioactive waste from decommissioning of nuclear sites: Guidance on the Requirements for Release from Radioactive Substances Regulation. Version 1.0 July 2018.
- Environment Agency, 2003a. The Development of LandSim 2.5. The National Groundwater and Contaminated Land Centre.
- Environment Agency, 2003b. Guidance on monitoring of landfill leachate, groundwater and surface water. LFTGN02.
- Environment Agency, 2010. Landfill operators: environmental permits. What to include in your environmental setting and site design report. https://www.gov.uk/guidance/landfill-operators-environmental-permits/what-to-include-in-your-environmental-setting-and-site-design-report. Accessed February 2024.
- Environment Agency, 2020a. Land contamination: risk management guidance on .gov.uk. (https://www.gov.uk/government/publications/land-contamination-risk-management-lcrm).

- Environment Agency, 2020b. https://environment.data.gov.uk/catchment-planning/WaterBody/GB108044009692 and https://environment.data.gov.uk/catchment-planning/WaterBody/GB108044009650. Accessed on 7 December 2020.
- Environment Agency, 2021a. Water Quality Archive. https://environment.data.gov.uk/water-quality/view/landing. Accessed on 10 March 2021.
- Environment Agency, 2021b. Comments on "Magnox Ltd, 2021. Decommissioning Site Restoration. Winfrith End State: Assessment of the effect of climate change on groundwater levels. ES(20)P333. Draft 2, 24 February 2021". 15 June 2021."
- GAU, 2013. Analysis of one smear, three paint, eight bulked concrete chippings and twelve concrete core samples. (Sample ID's: D60/SEC/ ….). GAU2938/GAU2955. 6 December 2013.
- GAU, 2022. Analysis of 1 paint and 1 shot blast sample. Sample IDs: D60/SC/PNT (1&2) & D60/PC/Shot Blast. GAU4324 (Issue 1). 21 February 2022.
- Gelhar, LW, Welty, C and Rehfeldt, KR, 1992. A critical review of data on field-scale dispersion in aquifers. Water Resources Research, Volume 28, No. 7, pages 1955-1974. July 1992.
- Giroud, J. P., 1997. Equations for Calculating the Rate of Liquid Migration Through Composite Liners Due to Geomembrane Defects. Geosynthetics International, Volume 4, pp. pp. 335-348.
- Golder Associates (UK) Limited, 2021. Winfrith Site: Historical Groundwater Level Measurements Judged 'Erroneous'. 19123012.619/B.0. 9 March 2021.
- Golder, member of WSP, 2022. Winfrith End State – Further Assessment of the Effect of Climate Change on Groundwater Levels. 20146580.614/A.1. 28 February 2022.
- Gronow, JR., 1986. Mechanisms of particle movement in porous media. Clay Minerals (1986) 21, 753-767.
- Hyder, 2013. Winfrith End State Project: Water Management and Ecological Appraisal, Hyder Report 5001-UA006471-UP31R-R01. November 2013.
- IAEA, 2020. Development of a Common Framework for Addressing Climate and Environmental Change in Post-closure Radiological Assessment of Solid Radioactive Waste Disposal. IAEA-TECDOC-1904.
- Jacques, D., Perko, J., Seetharam, S., Mallants, D., Govaerts, J., 2013. Modelling Long-Term Evolution of Cementitious Materials Used in Waste Disposal. Belgium: International Atomic Energy Agency. Chapter in book: Behaviours of Cementitious Materials in Long Term Storage and Disposal (pp.26) Edition: TECDOC-1701.
- LLWR Ltd, 2011a. Elicitation of Uncertainties for the LLWR 2011 ESC. Serco Report SERCO/TAS/E003796/001 Issue 2, April 2011.
- LLWR Ltd, 2011b. The 2011 Environmental Safety Case: Assessment of Long-term Radiological Impacts. Report LLWR/ESC/R(11)10028, May 2011.
- LLWR Ltd, 2011c. LLWR Environmental Safety Case, Radiological Assessment Calculation for the Groundwater Pathway for the LLWR 2011 ESC. SERCO/TCS/E003796/011, Issue 6, April 2011.
- Magnox, 2017. Optimising the End State of the Dragon Facility. ES(17)P170 Issue 3. August 2017.
- Magnox, 2018. Winfrith Site: BAT Analysis for SGHWR Fibreglass Pond Liners. ES(17)P177 Issue 1. January 2018.
- Magnox, 2019a. Approved end state and interim state terminology for Magnox Ltd sites. DD/EAN/0021/18 Issue 2. September 2019.
- Magnox, 2019b. Winfrith End State Technical Note: Hydraulic conductivity and long-term degradation of the SGHWR RC structures. ES(19)P303. Issue 4, December 2019.

- Magnox, 2019c. Decommissioning: Site Restoration: Decommissioning. Winfrith End State Technical Note: Cap Concept Design and Performance. ES(19)P304. Issue 3, December 2019.
- Magnox, 2019d. Summary of 2018 Characterisation of the D630 Rubble Stockpile. Reference Number: ES/18/NFR/035. Issue 1, February 2019.
- Magnox, 2019e. Winfrith Site: BAT Analysis for SGHWR Residual Asbestos. ES(19)P267. Issue 1. April 2019.
- Magnox, 2019f. Winfrith Drains Strategy. ES(18)P239. Issue 2. February 2019.
- Magnox, 2020a. SGHWR & Dragon End State: Engineering Concept Designs Workshop Briefing Note. ES(20)P321, Issue 1. 12 March 2020.
- Magnox, 2020b, Site Void Volume and Backfill Estimates, ES (18) 213 Issue 2, 28 January, 2020.
- Magnox, 2020c. Winfrith Site: BAT Analysis for SGHWR Residual Oil Contamination. Issue 1. 28 May 2020.
- Magnox, 2021a. Site Restoration Programme: Winfrith End State Project. Waste Recovery Plan. ES(19)P285. Formal Draft 3. March 2021.
- Magnox, 2021b. Note for the Record. Dragon Oil Spill Survey. Project Reference Number: DRA WST 21 08341, Issue 2, 24 May 2021.
- Magnox, 2021c. Decommissioning Site Restoration. Winfrith End State: Assessment of the effect of climate change on groundwater levels. ES(20)P333. Issue 1, 24 February 2021.
- Magnox, 2023. Methodology for Managing Magnox Sites' GRR Uncertainties (and Guidance on the Use of the Associated Database). DD/REP/0030/19 Issue 3.
- Mendez, J.C. and Hiemstra, T., 2019. Carbonate adsorption to ferrihydrite: Competitive interaction with phosphate for use in soil systems. ACS Earth and Space Chemistry, 3(1), pp.129-141.
- Mindat, 2021. Baryte. https://www.mindat.org/min-549.html. Accessed March 2021.
- Mindat, 2023. Portlandite. https://www.mindat.org/min-3264.html. Accessed July 2023.
- NRS, 2024a. Site Restoration: Winfrith Site: End State Radiological Inventory, NRS Report ES(19)P281, GSL Report 1624-10, Version 2, December 2024.
- NRS, 2024b. Site Restoration: Winfrith Site: End State Radiological Performance Assessment 2024, NRS Report ES(23)P388, GSL Report 2242-01, Issue 1, December 2024.
- NRS, 2024c. Winfrith End State: Design Substantiation Report (Concept Stage) – SGHWR and the Dragon Reactor. ES(23)P387, Issue 1, October 2024.
- NRS, 2024d. Description of the SGHWR oil-stained concrete sampling and analysis performed in 2022. ES(23)NFR/054, Issue 2, September 2024.
- NRS, 2024e. Winfrith End State: SGHWR and Dragon Reactor – Structural Integrity Assessment. ES(24)P398, Issue 1, November 2024.
- NRS, 2024f. Winfrith Site. Interpretation of present and future hydrogeological conditions. ES(21)P331, Issue 2, December 2024.
- NRS, 2024g. Winfrith End State Project. Overview of the Non-Radiological Inventory of Winfrith site end state. ES(22)P366, Issue 4, May 2024.
- NRS, 2024h. Site Restoration Programme: Winfrith End State Project: Accompanying report to the Non-radiological Inventory of SGHWR, Dragon Reactor Complex and Backfill. ES(21)P335, Issue 4, May 2024. This report appends spreadsheets: ES(21)SS09 SGHWR NRI Issue 4 and ES(21)SS10 Dragon NRI Issue 4.
- NRS, 2024i. Site Restoration Programme: Winfrith End State Project: Site Wide Materials Management Plan. ES(19)P324, Issue 4, August 2024.
- NRS, 2024j. Winfrith Site: Winfrith Site Description. ES(18)P196, Issue 1, December 2024.

- ONDRAF/NIRAS, 2011. Selection of near field parameters for the Dessel near surface repository. ONDRAF/NIRAS Report NIROND-TR 2010-07 E, Version 1, Revision 9, December 2011.
- Posiva, 2012. Safety Case for the Disposal of Spent Nuclear Fuel at Olkiluoto – Complementary Considerations 2012. December 2012.
- Rodwell, J.S., 2017. The UK National Vegetation Classification. Phytocoenologia 48(2), December 2017.
- RSRL, 2012a. Assessment of Analytical Data for the SGHWR Cooling Tower Base Slab (D63). WPC/NFTR/12/08, Issue 1.
- RSRL, 2012b. Assessment of Analytical Data for the SGHWR Cooling Tower Base Slab (D64). WPC/NFTR/12/10, Issue 1.
- Savage, D., Bateman, K., Hill, P., Hughes, C., Milodowski, A., Pearce, J., Rae, E., Rochelle, C., 1992. Rate and mechanism of the reaction of silicates with cement pore fluids. Appl. Clay Sci. 7, 33–45.
- SKB, 2001a. Project SAFE. Compilation of data for radionuclide transport analysis. R-01-14. November 2001.
- SKB, 2001b. Modelling of future hydrogeological conditions at SFR, R-01-02, March 2001.
- SKB, 2001c. Project SAFE. Modelling of long-term concrete degradation processes in the Swedish SFR repository, R-01-08, April 2001.
- SKB, 2014. The impact of concrete degradation on the BMA barrier functions. R-13-40. August 2014.
- SKB, 2023. Post-closure safety for SFR, the final repository for short-lived radioactive waste at Forsmark. Main report, PSAR version. Technical report TR-23-01. March 2023.
- Tompkins, C.D., Stewart, I.D., Graham, T.J., Burke, T.I., 2021. In situ disposal of crushed concrete waste as void fill material at UK nuclear sites: Leaching behaviour and effect of pH on trace element release, School of Earth and Environment Thesis, University of Leeds, Leeds.
- UK Centre for Ecology and Hydrology (UKCEH), 2020. https://nrfa.ceh.ac.uk/data/station/info/44001. Accessed 7 December 2020.
- UKAEA, 1962. Drawing AE133370 Mod M dated 16 May 1962.
- UKAEA, 1994. A hydrogeological investigation of the area around the SGHWR Active Sludge Tanks, AEA Winfrith. AEA-ESD-0045. June 1994.
- UKAEA, 2006. Concrete Volume Calculations, WSCP 2221. Issue 1. 19 October 2006.
- Van Geen, A., Robertson, A.P. and Leckie, J.O., 1994. Complexation of carbonate species at the goethite surface: Implications for adsorption of metal ions in natural waters. Geochimica et Cosmochimica Acta, 58(9), pp.2073-2086.
- Watson, C., Wilson, J., Savage, D., Norris, S., 2018. Coupled reactive transport modelling of the international Long-Term Cement Studies project experiment and implications for radioactive waste disposal, Applied Geochemistry, 97, pp. 134-146, https://doi.org/10.1016/j.apgeochem.2018.08.014.
- Wexham Developments Limited, 1985. An examination of concrete samples from the SGHWR reactor at Winfrith. December 1985.
- WHO, 2017. Guidelines for drinking-water quality. Fourth edition incorporating the first addendum.
- Wilson, E., construction era document. Construction of the Steam Generated Heavy Water Reactor, Winfrith Heath, Dorset.

- Wimpey Laboratories, 1985. Site investigation for possible power station at United Kingdon Atomic Energy Establishment Site (1983), Winfrith, Dorset, Volume 7, Hydrogeological and Dewatering Report, Report reference S/20657, 1985.
- Wimpey Laboratories, 1991. Site investigation at Winfrith Heath – Stage 2, Report reference S/18165/G394, 1991.
- Wood, 2020. Non-radiological Hydrogeological Risk Assessment for Disposals at the SGHWR and Dragon Reactors at the Winfrith Site, Report 208530/012 Issue 2. 30 April 2020.
- WSP, 2023a. Technical Memorandum. Description of the performance of the caps over the SGHWR and Dragon reactor disposals/deposits. 20146580.615/A.0. 11 April 2023.
- WSP, 2023b. Technical Note. Winfrith Site: Below Ground Void Volumes and Volumes of Waste Anticipated to be Emplaced at the SGHWR and Dragon Reactor. 20146580.612/A.5. 12 October 2023.
- WSP, 2024. Winfrith Site. Annex 2 Restoration Management Plan – Groundwater Modelling. 70089718.600. November 2024.

WSP House
70 Chancery Lane
London
WC2A 1AF

wsp.com